Determination of the change in Hydraulic Capacity in Pipelines

Report to the
Water Research Commission

by

Stefanus Johannes van Vuuren & Marco van Dijk
Department of Civil Engineering
University of Pretoria

WRC Report No. 1820/1/12
ISBN 978-1-4312-0290-4

July 2012

WATER RESEARCH COMMISSION

UNIVERSITEIT VAN PRETORIA
UNIVERSITY OF PRETORIA
YUNIBESITHI YA PRETORIA
Denkleiers • Leading Minds • Dikgopolo tša Dihlalefi

Obtainable from

Water Research Commission
Private Bag X03
Gezina, 0031

orders@wrc.org.za or download from www.wrc.org.za

The User Manual and supporting software Hydraulic Performance DBV1 mentioned in this report can be obtained at www.wrc.org.za/software/.

Determination of the change in Hydraulic Capacity in Pipelines

Executive Summary

During the design stage of any water transporting pipeline, it is essential to predict the anticipated future hydraulic behaviour of the system. This requires an understanding of the relative influences of water quality, pipe material aging and operational variation on the expected change in the hydraulic performance of the system. Future expected hydraulic performance can be predicted if the influence of these factors on the expected absolute roughness of pipelines can be quantified. This study aimed to obtain as much as possible operational field data of a number of pipelines in order to:

- Determine the current roughness and derive the roughness variation and roughness decay;
- Compare the calculated roughness obtained from the field tests with the available literature;
- Compile a database to be used as a guide in selecting the appropriate expected future roughness required in the design and optimisation of the water system components.

In the design of new pipelines or the refurbishment, upgrade or replacement of existing components of the water supply system the cost of energy as well as the influence of biofilm growth in the pipeline should also be reviewed. These aspects were also included in this research project.

Influence of energy cost on the optimization of system components

The contribution of energy cost during the life cycle outweighs the capital cost of most pumping systems, requiring thorough analyses of the optimal component design. A recent review (Van Wyk, 2010) of 11 pump stations in the Tshwane Metropolitan Council's water distribution systems reflected that the electricity tariff structure as agreed upon by the Energy Regulator (NERSA) and Eskom requires larger diameters to provide an optimized pumping system in the majority of these cases for a number of possible energy cost scenarios which were identified.

Influence of biofilm growth on the hydraulic capacity of pipelines

The assessment of the hydraulic performance of the main supply pipeline in the Lower Blyde River Irrigation Systems reflected that the presence of the biofilm significantly reduced the hydraulic capacity of pipeline. Biofilm, which is present in all water carrying pipelines, will however not only reduce the hydraulic capacity of pipelines but could also lead to a loss of operational control due to the blockage of the communication pipes of the pilot control valves.

To be able to measure the thickness of the biofilm in a pipeline, a Biofilm Thickness Measuring Apparatus (BTMA) was developed (see **Figure 1**). The apparatus provided biofilm thicknesses in the pipelines investigated varying from 2 mm to 10 mm.

Figure 1: The Biofilm Thickness Measuring Apparatus

Figure 2 reflects the Biofilm (MOB) residue, which has been accumulated to a thickness of about 8-10 mm in the Lower Blyde River Irrigation System over a period of about 10 years. Field experimental setups were deployed in the Lower Blyde River Irrigation System to monitor the rate of biofilm growth for different constant flow rates.

The results obtained from the Energy-dispersive X-ray spectroscopy (EDS) reflected the composition of the residue of the biofilm, which was harvested from the pipe wall. The mass distribution reflected a high presence of Carbon (C), Oxygen (O) and Manganese (Mn). It was further established that the Biofilm represents the characteristics of the Manganese Oxidising Bacteria (MOB). In the case of the upper pipe section of the Lower Blyde River Irrigation System where the MOB was identified, the absolute roughness was calculated to be 1,76 mm.

Figure 2: Biofilm growth in the Lower Blyde River Irrigation Pipeline (Area of the section that was scraped was about 300 x 400 mm and had a volume of about 1000 ml).

Roughness assessment of existing pipelines

A number of pipelines were hydraulically assessed in South Africa and Namibia. Based on the recorded field data, the roughness in the pipeline segments was calculated. Accurate pressure recordings and flow measurements are essential to be able to calculate the roughness in the pipeline.

Table 1 provides a comparison between the referenced roughness and the calculated roughness based on the recorded field data, reflecting that the reference roughness for different pipe materials are not always representative. Hence, the need to compile sufficient data to be used in future designs is essential to ensure optimal design components for cost effective water supply system.

Table 1: Comparison of the recorded and reference roughness for different pipe material and liner systems

Country	Pipe ID	Pipe diameter (mm)/ Installation date	Pipe material/ Liner	Water quality #	Roughness parameter				
					Reference roughness new pipe			Calculated roughness	
					smooth (mm)	rough (mm)	Reference	Barr (mm)	Colebrook-White (mm)
	Bloemwater: De Hoek to Uitkijk	1168/1971	PCP/none	T	0,06	0,6	Wallingford and Barr (2006)	0,167	0,176
	Bloemwater: Uitkijk to Brandkop							0,091	0,098
South-Africa	Hendrina-Duvha *	1400/1974	Steel/Bitumen	R	0,04	1	Mecaflux (2009)	0,292	0,302
	Kuthala Kendal **	650/1986	Steel/Bitumen	R	0,06	1	Bhave (1991)	0,624 to 1,599	0,622 to 1,597
	Morgenstond Dam to Jericho Dam M1-J	1500/2003	Steel/CML	R	0,06	1,5	Bhave (1991) & Barr et al. (2006)	0,533	Not determined
	Morgenstond Dam to Jericho Dam M2-J	1500/1964 (relined 2008)	Steel/CML (replaced)	R	0,06	1,5	EDSTech & Bhave (1991)	0,963	Not determined
	Lower Blyde Irrigation System Pipeline	1500/2000	Steel/Copon	R	0,02	Not defined	EDSTech	1,76	
	Baviaanspoort-Kameelfontein	250/Unknown	Steel/Bitumen	T	0,015	0,3	Bhave (1991)	Not determined	1,327
Namibia	Rössing Pipeline	600/1979	Ductile Iron/CML	T	0,02	Not defined	EDSTech	0,080	0,079
	Langer Heinrigh Mine	325/2004	Steel/CML	T	0,06	1,5	EDSTech & Bhave (1991)	0,088	0,086

Notes: # "R" reflects raw water and "T" reflects treated water;

* In this case it was established that the secondary losses at the couplings are significant;

** The profile allows sections of the pipeline to drain, resulting in the variance of the absolute roughness values.

Some pipelines such as the raw water supply line from the Hendrina Power station to the Duvha power station which is a continuous welded steel pipeline indicated significant secondary losses at the field joints (every 12 m). **Figure 3** reflects the increase in absolute roughness at a typical field joint in the Hendrina-Duvha Gravity Main. These losses should be included in the determination of the assessment of the hydraulic capacity of pipelines.

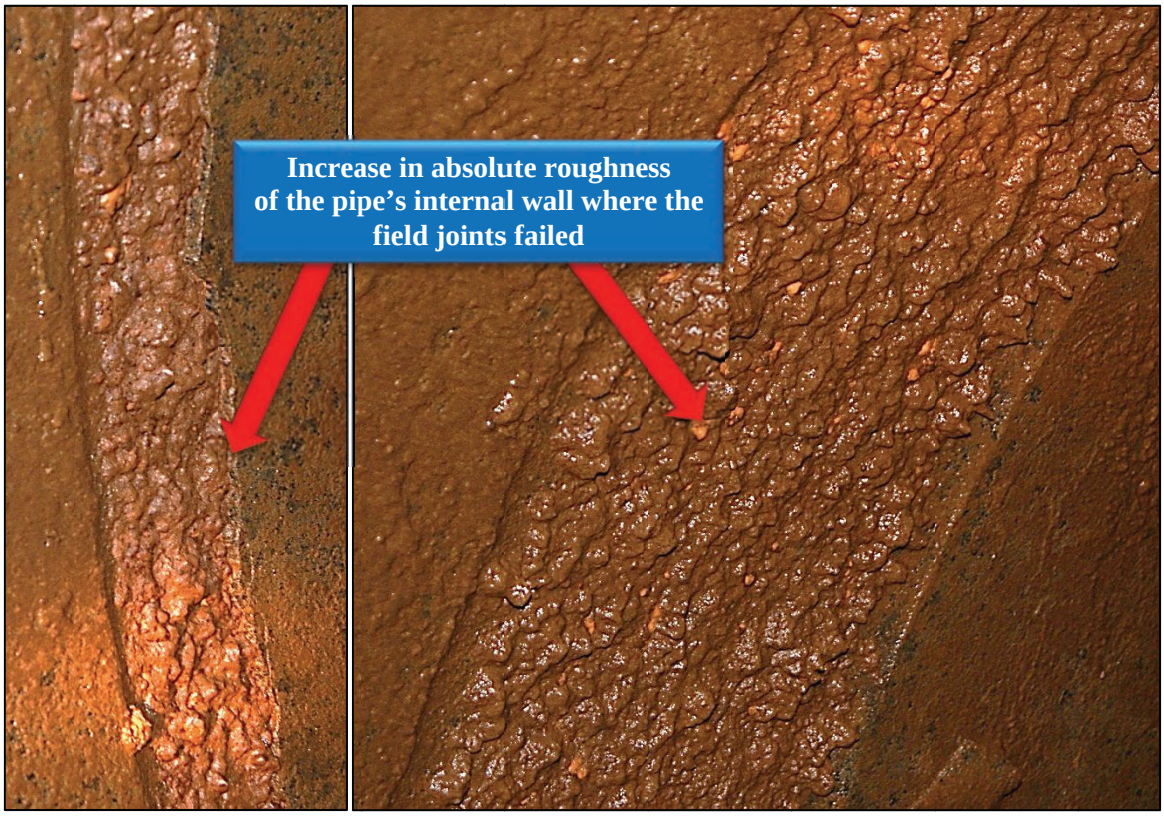

Figure 3: Increase in absolute roughness of the pipe's internal diameter at field joints

The roughness were recalculated with the incorporation of the losses at the couplings, air valves, access holes, bulk off takes and farmer supply lines. **This case demonstrated the severity of the secondary losses associated with the failure of the field joints.**

Common expectations that pipelines operate within the full-turbulent flow regime region rendering to the Moody-diagram was also investigated. According to the recorded data measurements of the Hendrina-Duvha Gravity Main it was found that operation of the pipeline in all cases are within the transition flow regime which necessitates the use of relationships which include the influence of the liquid's inherent resistance (Moody, Barr, and Colebrook-White) different to the renowned Karman-Prandtl relationship. Reference to these recorded measurements that fall within the transition flow regime reflected graphically on the Moody-diagram, is reflected in **Figure 4.**

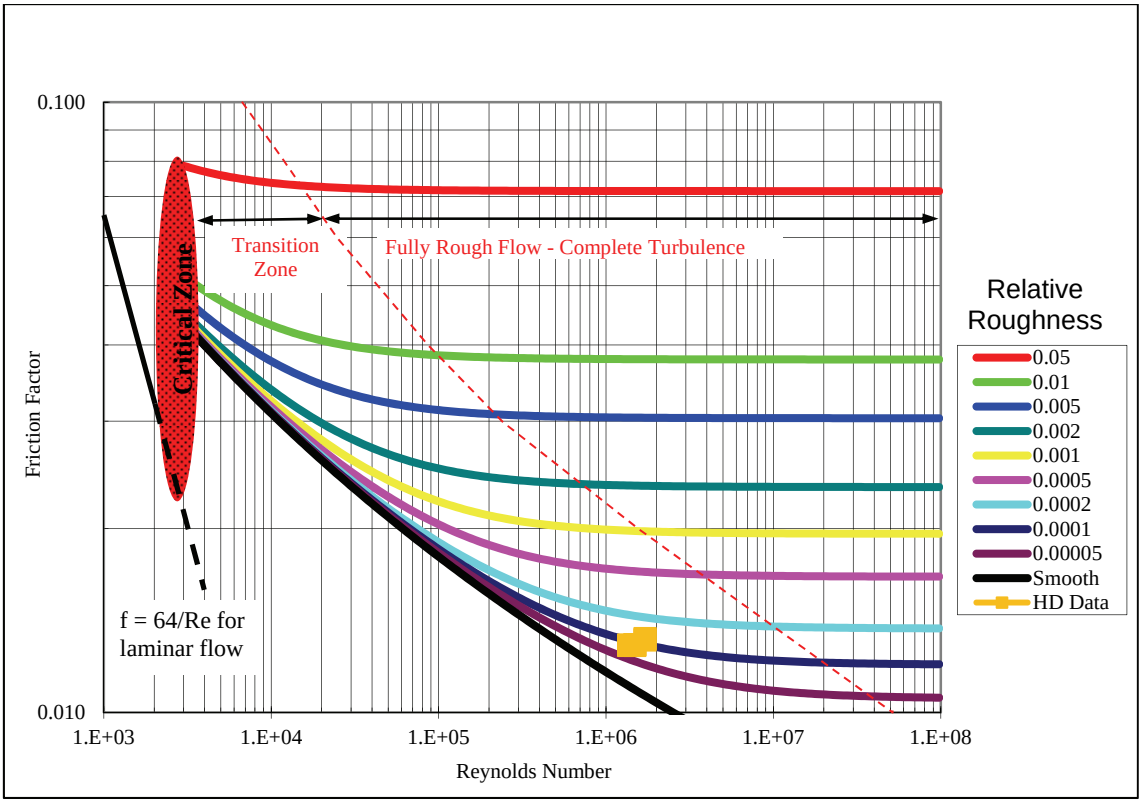

Figure 4: Recorded data observed for Hendrina-Duvha Gravity Main fall within the transition flow regime

Development of an information system (IS) for water infrastructure

An information system (IS) was developed with the objective to capture sufficient data on current systems to be used in future designs and to have the ability to conduct continuous assessments of pipelines in South Africa. The IS will allow designers and managers of pipelines to study the performance of different types of pipelines in varying areas under different operating conditions. The information is essential to improve the design of future pipeline systems and to optimize the maintenance on existing pipelines. The accurate prediction of expected future capacities will enhance the planning and management of the infrastructure ensuring a timeous implementation of augmentation schemes.

The database was developed in Microsoft Access 2007. An access protocol was developed to control and protect the database against tampering and unauthorised alterations. The software can be used to view reports linked to the database, to recall operational data and to update the database.

Conclusions & recommendations

This study highlighted the general lack of hydraulic performance history and hence little information is available to be considered for the hydraulic assessment and future planning of extensions or improvements to system components. Monitoring the performance of infrastructure provide

knowledge to make informed decisions on the limitations and decay of the system and to optimally determine the required upgrade and extensions to the system.

The expected high energy cost in South Africa highlighted the importance to re-assess the energy efficiency of pumping systems. In this regard a decision diagram has been developed to guide the decision whether to upgrade replace or rebuild section of the pipeline system.

The influence of biofilm on the hydraulic capacity and the energy losses occurring at the field joints of pipelines has to be researched in more details.

Based on the findings of this research it is recommended that:

- The database of recorded hydraulic pipeline performance for different water qualities, pipe material and operational conditions needs to be extended;
- During the design and construction of water conveyance systems, provision should be made for the incorporation of flow and pressure recording positions. These pressure recording positions should be surveyed to an accuracy of at least 10 mm vertically and horizontally to 200 mm; and
- The hydraulic performance of pipelines should be reviewed frequently (every 3 to 5 years). Such investigations will confirm the change in the hydraulic capacity of the pipeline and provide directives to the required investment and time scales to replace, refurbish or upgrade components of the water infrastructure in South Africa.

Determination of the change in Hydraulic Capacity in Pipelines

Acknowledgements

The research findings presented in this report emanated from a study funded by the Water Research Commission (WRC), whose support is acknowledged with gratitude.

The Steering Committee made an important contribution in steering and guiding this study to obtain the format and results reflected in this report. The support of the Chairman and Manager of this study, Mr Jay Bhagwan, as well as the staff of WRC, is greatly appreciated. The Steering Committee and Project Team responsible for this study consisted of the following persons:

Mr JN Bhagwan	Water Research Commission – Chairman
Mr PJ le Roux	GMKS/SASTT
Prof GGS Pegram	University of KwaZulu-Natal
Mr N Trebicki	Rand Water
Mr Andre Dyer	Amatola Water
Dr Mike Shand	Aurecon
Mr Stephan Burke	Umgeni Water
Mr Edwin Varkevisser	Rand Water
Mr Roelf le Roux	Magalies Water
Mr Walter van der Westhuizen	DWA
Prof SJ van Vuuren (Project leader)	University of Pretoria
Mr M van Dijk	University of Pretoria
Mr A de Klerk	University of Pretoria

The contribution the following students from the University of Pretoria, Civil Engineering Department are acknowledged:

Mr Louis Coetzee,
Mr Pierre Victor Lynch and
Ms Cara van Wyk.

Determination of the change in Hydraulic Capacity in Pipelines

Table of Contents

Determination of the change in Hydraulic Capacity in Pipelines

Table of Figures

List of Tables

Determination of the change in Hydraulic Capacity in Pipelines

1 Introduction

1.1 Background

During the optimization and design of a water distribution system it is essential to know the initial roughness of the pipe material and how the roughness will change during the operational life of the system

With limited available capital the funding of new water projects with the option to renovate, replace or the upgrade of existing infrastructure.

Long term performance data of water infrastructure is essential for the assessment of the performance and expected future hydraulic behaviour of pipelines.

The objective to determine the change in the hydraulic capacity for the selected candidate pipelines requires that the following parameters should be assessed:

- Pressure variance along the pipeline;
- Flow rate;
- Water quality;
- Operational history and record of remedial work;
- Pipe material;
- Installation date;
- Liner systems, and
- Required future expected flow demand to be supplied.

The compilation of the findings in a “roughness database” will be valuable in the design of new pipelines as well as assist in the operation and refurbishment of existing pipelines.

The database will have to reflect the calculated absolute roughness, the roughness used in the design of the system and the rate at which the roughness changed.

1.2 Methodology

In this research a number of pipelines were reviewed. Assessments of the hydraulic performance were conducted based on the recorded pressure drop at a specific flow rate in the pipeline.

The pressure recordings were obtained at a minimum of at least three positions along the pipeline where pressure transducers and the data acquisition system were recording the pressures and capturing the data at a frequency of 1 Hz. The pressure recordings were conducted at different flow rates.

The drop in the hydraulic grade line between two measuring points along the pipeline reflects the total energy loss between the measuring points. The contribution of secondary losses was assessed based on the available system details. The friction loss was used to calculate the absolute roughness in the system.

The results are reflected in a tabular format which will in future be included in a database to be updated and populated as the details of different pipeline reviews become available.

1.3 Objective of the research

The research aims to determine:

- Determine the current roughness and derive the roughness variation and roughness decay;
- Compare the calculated roughness obtained from the field tests with the available literature, reflecting the expected future hydraulic capacity;
- Compile a database to be used as a guide in selecting the appropriate expected future roughness required in the design and optimisation of the water system components; and
- Indicate the influence of high power cost on the determination of the optimum pipe diameter.

1.4 Layout of report

The report consists of the following chapters and annexures:

Chapter 1:	Introduction (This chapter)
Chapter 2:	Literature review on energy losses due to friction, secondary losses and biofilm in conduit systems
Chapter 3:	Development of a database to capture the field data
Chapter 4:	Field work
Chapter 5	Hydraulic analysis
Chapter 6	Influence of high energy cost on the optimal diameter of pumping mains
Chapter 7	Conclusions and Recommendations
Chapter 8	References

APPENDIX A – Supporting CD at back of report

2 Literature review on energy losses due to friction, secondary losses and biofilm in conduit systems

2.1 Introduction

A pipeline is a conduit that transports a fluid (in this case potable water) from one point to another. In order to transport the fluid effectively the pipeline system also requires valves, bends, couplings, etc. In a pipeline system, the total head loss is a summation of the following loss components:

- The friction loss in the pipe itself (h_{fs});
- the entrance loss (h_{Le});
- the loss in bends (h_{Lb});
- the loss at discontinuities (h_{Ld});
- the loss at couplings (h_{Lc});
- the loss due to biofilm growth (h_{fBio});
- the loss associated with transitions where the diameter changes (h_{Lt});
- the loss across valves (h_{Lv}), and
- the exit loss (h_{Lx}).

The contribution of the losses related to the growth of biofilm (h_{fBio}) has not been fully quantified and is currently not assessed in the design of pipelines.

The well-known friction factor and friction loss equation such as Colebrook White and Darcy-Weisbach makes provision to quantify the energy loss due to surface roughness and viscosity. The other losses in the system are defined as local or secondary losses and are caused by disruption in the boundary of the pipeline leading to eddy losses at these positions.

The inclusion of a brief overview of the development of the relationships to determine energy losses in pipelines provides insight in the current understanding of the hydraulic performance of pipeline systems.

2.2 The history of the friction formulae

Since the 1930s various researchers contributed to the identification and development of factors and relationships to quantify the energy loss in pipelines, which led by 1958 to the development of pressures, head losses and discharge relationships (Chadwick, Morfett and Borthwick, 2004) for the design and evaluation of pipes and pipe systems. **Table 2.1** reflects the contribution of the researchers who contributed to the current understanding of pipe flow.

Table 2.1: The chronological development of pipe flow theories (Chadwick et al., 2004)

Date	Contributor	Contribution
1839-1841	Hagen & Poiseuille	Laminar flow equation
1850	Darcy & Weisbach	Turbulent flow equation
1884	Reynolds	Distinction between laminar and turbulent flow – Reynolds' number
1913	Blasius	Friction factor equation for smooth pipes
1914	Stanton & Pannell	Experimental values of the friction factor for smooth pipes
1930	Nikuradse	Experimental values of the friction factor for artificially roughened pipes
1930s	Prandtl & von Kármán	Equations for rough and smooth friction factors
1937-1939	Colebrook & White	Experimental values of the friction factors for commercial pipes and the transition formula
1944	Moody	The Moody diagram for commercial pipes
1958	Ackers	The Hydraulic Research Station Charts and Tables for the design of pipes and channels
1975	Barr	Direct solution for the Colebrook-White equation

2.3 Friction losses in conduit flow systems

It was establish that the two main contributing factors to energy losses are:

- Inherent resistance against flow exerted by the fluid (viscosity); and
- The friction losses and secondary losses resulting from the inter-phase (shear) between the fluid and the stationary conduit boundary.

The distinction between **Laminar** and **Turbulent** flow is based on the value of the Reynolds Number which is a dimensionless parameter and is defined by:

$$\mathrm{Re} = \frac{DV}{\upsilon} \qquad \ldots (2.1)$$

where: Re = Reynolds' number (dimensionless)
D = Diameter (m)
V = Velocity (m/s)
υ = Kinematic viscosity (1,14 x 10^{-6} m²/s for water at 20°C)

For *Re* less than ± 2 000 the flow is **always laminar**, and for *Re* **greater than ± 4 000 the flow is almost always fully turbulent**. The transition between 2 000 and 4 000 is either laminar or turbulent flow.

For turbulent flow in pipes which is the flow regime normally prevailing in pipelines, several relationships for the determination of the energy losses, h_f, could be used. For conduit flow, the well-known **Darcy-Weisbach equation** (Equation 2.2) is commonly used to determine the energy loss.

$$h_f = \frac{\lambda L V^2}{2gD} \qquad \ldots (2.2)$$

where: h_f = Friction head loss in conduit (m)
λ = Pipe friction factor (dimensionless)
L = Length of conduit (m)
V = Flow velocity of fluid inside conduit (m/s)
g = Gravitational acceleration (m/s²)
D = Internal diameter of conduit (m)

There is a change in the friction factor, (λ), as the Reynolds number varies. Equations relating lambda (*λ*) to both the Reynolds' number and the pipe roughness were developed (see **Table** 2.2).

Table 2.2: Formulae for calculation of the friction factor (λ)

…(2.3-2.10)

Eq nr	Name	Equation
2.3	Kármán & Prandtl	$\frac{1}{\sqrt{\lambda}} = 2\log\left(\frac{Re\sqrt{\lambda}}{2,51}\right)$ for smooth pipes
2.4	Kármán & Prandtl	$\frac{1}{\sqrt{\lambda}} = 2\log\left(\frac{3,7D}{k_s}\right)$ for rough pipes
2.5	Colebrook-White transition	$\frac{1}{\sqrt{\lambda}} = -2\log\left(\frac{k_s}{3,7D} + \frac{2,51}{Re\sqrt{\lambda}}\right)$
2.6	Barr	$\frac{1}{\sqrt{\lambda}} = -2\log\left(\frac{k_s}{3,7D} + \frac{5,1286}{Re^{0,89}}\right)$ with $k_s/D < 0,01$ and $Re > 4*10^4$
2.7	The Moody diagram	$\lambda = 0,0055\left[1 + \left(\frac{20000k_s}{D} + \frac{10^6}{Re}\right)^{1/3}\right]$
2.8	Darcy-Weisbach Colebrook-White combination	$V = -2\sqrt{2gDS_f}\log\left[\frac{k_s}{3,7D} + \frac{2,51\nu}{D\sqrt{2gDS_f}}\right]$ and $S_f = \frac{h_f}{L}$
2.9	Manning	$Q = \frac{1}{n}\frac{A^{5/3}}{P^{2/3}}\sqrt{S_f}$ and $S_f = \frac{h_f}{L}$
2.10	Hazen-Williams	$h_f = \frac{10,69LQ^{1,852}}{C^{1,852}D^{4,87}}$

Where:

Q = flow rate (m³/s)

V = flow velocity (m/s)

D = inside diameter (m)

g = gravitational acceleration (m/s²)

L = pipe length (m)

P = wetted perimeter of inside pipe (m)

A = internal area of pipe (m^2)

h_f = friction loss (m)

h_l = secondary losses (m)

S_f = friction slope (m/m)

H = available energy (m)

k_s = absolute pipe roughness (m)

C = Hazen-Williams roughness coefficient

n = Manning roughness value

λ = friction factor – lambda

ν = kinematic viscosity ($1{,}14 \times 10^{-6}$ m^2/s)

Table 2.3 provides recommended absolute roughness values for concrete pipes (Wallingford and Barr, 2006).

Table 2.3 Typical recommended absolute roughness for concrete pipes

Material	**Suitable values for k_s (mm)**		
	Good	**Normal**	**Poor**
Prestressed	0,03	0,06	0,15
Precast concrete pipes with “O” ring joints	0,06	0,15	0,6
Spun precast concrete pipes with “O” ring joints	0,06	0,15	0,3
Monolithic construction against steel forms	0,3	0,6	1,5
Monolithic construction against rough forms	0,6	1,5	-

The determination of the absolute roughness from recorded head losses in pipelines provides a snapshot operational capacity of the pipeline.

2.4 Relationship between the energy loss and age of the infrastructure

In the planning and design of water supply systems, it is important to know their hydraulic behaviour not only when the pipes are new, but also as the system ages during its design life. With ageing, the hydraulic capacity of the pipe reduces due to the increase in the roughness parameter of the pipe wall. This results in an increase in friction loss and in some cases a decrease of the pipe cross sectional area as shown in **Figure 2.1**.

Figure 2.1: Decrease of hydraulic capacity of pipe due to scaling (reduction in cross sectional area – an extreme case of calcium precipitation from an artesian ground water source)

Although the effect of pipe ageing has attracted the attention of several investigators, there is little quantitative information available on commercial pipes. The following linear increment of the absolute roughness is usually proposed:

$$k = k_0 + \alpha t \qquad \ldots (2.11)$$

where: k = Absolute roughness at time t (mm)

k_0 = Absolute roughness of the new material (mm)

α = Growth rate (mm/year), varies considerably with water conditions

2.5 The influences of biofilm on the hydraulic characteristics of pipe flow

2.5.1 Introduction

In addition to the normal wall roughness in pipelines the influences of biofilm on the roughness should also be addressed. To understand the response of biofilm to various flow velocities and how it may influence the flow conditions in the distribution system the basic principles of pipe flow should be considered.

Biofilm is defined as an assemblage of microscopic animals; plants and bacteria attached to a surface, also known as “slime”, “biological deposits”, “ microbial mat”. Most water systems become covered by biofilms that consist of very complex microbial populations, see **Figure 2.2**. In a potable water system, the occurrence of biofilms often has the **undesired consequence of increased friction, which causes higher energy consumption.**

Figure 2.2: Example of biofilm growth (MOB) in large diameter pipeline (Blyde River Irrigation System)

A biofilm is a natural accumulation of micro-organisms at an interface such as between a liquid and a fixed boundary. Biofilm formation is the result of a number of processes, which either increase (adhesion, attachment, growth) or decrease (detachment, death, grazing) the amount of accumulated biomass. Biofilm plays a key role in ecosystems and nutrient cycle, but could also cause economic damage and health risks.

Biofilms are so common that they are not really noticed. They are known as “slime”, “biological deposits”, “microbial mat”, and “organic glue” or by many other descriptive names. Biofilms do not enjoy special attention, although they represent a unique form of life and play a key role in production and degradation of organic matter and in the cycle of phosphorus, nitrogen and sulphur.

Biofilms consist mainly of water (79-95%), which is held by the highly hydrated extracellular polymer substances (EPS). The EPS contribute 70-95% of the organic matter of the biofilm and the micro-organisms represent only a minor part of mass and volume.

Physical properties (rheology) of biofilms determine the shape and mechanical stability of the biofilm structure and affect both mass transfer and detachment processes. Knowledge of biofilm rheology is

crucial to fully interpret the behaviour of biofilms, particularly those growing in flowing fluids subjected to shear stresses (τ) that vary in magnitude and frequency.

The small dimensions and pliability of biofilms makes sample handling extremely difficult and removal from the substratum radically changes the integrity of the sample. Various methods have been developed to conduct simple stress-strain and creep experiments on culture biofilms in situ by observing the structural deformations caused by changes in hydrodynamic shear stresses (τ_w).

Biofilms behave like elastic and viscoelastic solids below τ_w, but behave like viscoelastic fluids at shear stresses elevated above τ_w. Vieira, Melo and Punheiro (1993) found that the biofilms that are grown at the elevated shear stresses were more cohesive than those at the low shear stresses.

The yield point of biofilms growing in steady dimensional flow is a function of the magnitude of the hydrodynamic shear stress (τ_w) acting upon them during development. An increase in τ_w may result in thinning of the material and finally detachment of the biofilm structures.

Reduction in thickness of the biofilm will effectively increase biofilm density and decrease porosity. Since it had been demonstrated that water could flow through biofilm channels (Stoodley, De Beer and Lewandowski, 1994) and increase the supply of nutrients to the biofilm cells, a reduction of thickness can thus have a significant impact on the mass transfer processes.

Additional to reducing the porosity of the biofilm, flattening of the individual structures squeezes water out of the EPS matrix, reducing the micro-porosity and solute diffusivity. Dehydration increases the stiffness and viscosity and the rate of diffusion of water back into the biofilm will determine the rate of recovery of the shape.

The surface on which a biofilm develops is called a substratum. Biofilm accumulation is the net result of a number of physical, chemical and biological processes, each leading to either an increase or decrease of the amount of biomass accumulated at the substratum.

All the processes involved in biofilm development are influenced by hydrodynamic conditions in the bulk liquid. Micro-organisms are transported to the substratum by diffusion and gravitational settling. In the turbulent flow regime, a higher bulk flow rate will reduce the thickness of the liquid boundary layer and thereby decrease the distance that needs to be overcome.

Although the higher flow enhances the transport of cells to the substratum, there is only a fraction that is able to establish irreversible adsorption to the surface. Rougher substrata offer protected sites where the cells are shielded from flow, in a way that enables the cell to absorb.

2.6 Detrimental effects of biofilm

- Biofilm promote the possible growth of pathogenic bacteria in drinking water pipes, bio corrosion and may sustain the colonisation of undesirable organisms.

- Biofilm increase the friction resistance, as they are viscoelastic and consume kinetic energy of water. This is the case in water lines and leads to an increased energy demand (Characklis, 1990).

- Biofilm layers contribute to the formulation of corrosion tubicles, encrustation of organic and inorganic matter and extra-cellular polymers. These substances produce adverse impact on the quality of distributed water and endanger public health and welfare. Understanding microbial behaviour is essential for environmental concerns.

2.7 Secondary/Local head losses in closed conduit flow

Energy losses, according to Chadwick et al. (2004), are always encountered at junctions, valves; pipe bends etc. in addition to those due to friction. Eddy formation generated in the fluid at the fitting causes these local head losses. The local losses may be insignificant in the case of long pipelines (e.g. several kilometers), but may be greater than the frictional losses in short pipelines.

Entrance losses are usually expressed as follows:

$$h_{Le} = \frac{k_e V^2}{2g} \qquad \ldots (2.12)$$

where: h_L = The local head loss (m)

k_e = Coefficient of entrance loss which is a function of the shape of the entrance to the pipe

V = Velocity (m/s)

g = Gravitational acceleration (m/s²)

Wherever there is a **bend** in a pipeline, an increase in head loss will occur due to the additional turbulence. The magnitude of this loss is expressed as follows:

$$h_{Lb} = \frac{k_b V^2}{2g} \quad \ldots (2.13)$$

where: h_{Lb} = The local head loss at the bend (m)

k_b = A function of deviation at the bend

The head loss in a **valve** depends on the type of valve, while the manufacturer generally provides the head loss coefficient. The actual head loss is then calculated using the local head loss equation.

$$h_{Lv} = \frac{k_v V^2}{2g} \quad \ldots (2.14)$$

where: h_{Lv} = The local head loss at the valve (m)

k_v = dependent on the valve type and obstruction caused

Exit losses are expressed as:

$$h_{Lx} = \frac{k_x V^2}{2g} \quad \ldots (2.15)$$

where: h_{Lx} = The local head loss at the exit (m)

k_x = Coefficient of 1,0 for a pipe discharging water from the system

The total secondary loss in a pipe system is calculated by the summation of all these local head losses due to bends, valves etcetera as shown in Equation 2.16 with typical loss coefficients shown in **Table 2.4**.

$$h_L = \sum \frac{k_i V_i^2}{2g} \quad \ldots (2.16)$$

where: h_L = The total local head loss (m)

k_i = Secondary loss coefficient at position *i*

V_i = Velocity at position *i* (m/s)

g = Gravitational acceleration (m/s²)

Table 2.4: Typical local head loss coefficients

Fitting	**Loss Coefficients**				
	Type	**k**			
Entrance	*Projecting*	*0,80*			
(Stephenson, 1979)	*Sharp cornered*	*0,50*			
	Slightly rounded	*0,25*			
	Bellmouth	*0,05*			
Exit	Projecting	1,0			
(Stephenson, 1979)	Sharp	1,0			
	Slightly rounded	0,5			
	Bellmouth	0,2			
Bends (Bureau of Reclamation, 1987)	**k_b for Angles**				
	$\frac{R_b}{D}$	**22,5°**	**45°**	**67,5°**	**90°**
R_b = bend radius	1	0,09	0,15	0,19	0,20
d = pipe diameter	2	0,05	0,09	0,11	0,13
	3	0,04	0,07	0,09	0,10
	4	0,03	0,06	0,07	0,08
	6	0,03	0,05	0,06	0,07
	8	0,03	0,05	0,06	0,07
Contractions (King, 1954)	**d_1/d_2**		**k_a**		
Use the velocity in	1,1		0,05		
smaller pipe	1,2		0,11		
diameter	1,4		0,20		
	1,6		0,26		
	1,8		0,34		
	2,0		0,38		
	2,5		0,42		
	3,0		0,44		
	4,0		0,47		

Valves	k_v for openings			
	1/4	1/2	3/4	Full
Gate	10	1,8	0,7	0,2
Butterfly	160	14	1,5	0,3
Y-pattern control (Globe):				
Disc	14	5,1	3,3	5,5
V-Port	7 300	225	25	9,0
Sleeve	22	4,8	1,5	0,5
Needle	5,0	1,2	0,7	0,6
Ball	80	10	0,9	0,0

Check valves	k_v
Swing depending on design	0,8 to 2,5
Recoil (Globe)	12
Swing	1,5 to 2,5
Multi-disc	2,3 to 2,5
Tilting disc	0,7 to 1,0

3 Development of a database to capture the field data

3.1 Introduction

It is acknowledged that a large database of representative operational data from industry pertaining the status of water infrastructure is required to ensure a sustainable water supply and to be proactive in identifying the shortcomings leading to the refurbishment, extension or replacement of system components.

In this chapter a number of aspects are discussed in defining the parameters of a database, protocols, and interrelationships of the interested and effective parties and the development of an Access Database.

The focus of this development is to create the platform for the acquiring of historical operational data to determine a pipeline's expected operational lifespan and to perform economic analyses for upgrading or refurbishing the pipeline or to define the essential maintenance and upgrades that needs to be performed on the pipeline systems over the design life thereof. Pipelines decay over time, resulting in a reduction of the hydraulic capacity and hence a regular update of the performance data is required to be able to determine the change in the hydraulic capacity.

3.2 Requirements of an information system

The objective of the "hydraulic performance information system" (HPIS) is to gather and record all the necessary data and perform the required hydraulic and economic analysis, informing managers and owners of these systems to manage proactively.

The hydraulic performance information system (HPIS) will further allow planners and designers of pipelines to study the operational and performance relationships for different operating conditions, pipe material, liner performance, roughness parameter and the effect of water quality. This will be valuable for the planning of future schemes and will underline the need for maintenance, refurbishment or replacement of existing pipeline systems. On a longer time span the HPIS will contribute to ensure an optimal capital expenditure and operational costs.

Based on the key parameters of the HPIS: performance, information, economy, control, efficiency and services the following (PIECES) table has been compiled to reflect the minimum or non-functional requirements to create a HPIS (**Table 3.1**).

Table 3.1: Minimum requirements to ensure a useful HPIS (PIECES diagram)

Requirement Type	Requirements/Explanation
Performance	The system must be able to process the data and convert it into value adding information at defined intervals – fast throughput rate. Throughput speed of incoming data being screened must be on a real time basis preventing the back-up of incoming data. The response time of feedback alarms must be short in notifying possible problems on the pipelines (e.g. out of range pressures, flows, etc.).
Information	The system must receive hydraulic data packages from the field via a wireless network or allow manual input. All the data must be verified. The accompanying information on the pipeline systems must be as current as possible. Back-ups of data and calculated information must be made. Data must be well organized and easily traced to a pipeline section. The hydraulic information must be well organized and easily traced to a pipeline section. The data and hydraulic information must be protected from vandalism (e.g. read only). Information from other databases should be shared.
Economy	This project reflects the development of an information system which could potentially be used to retrieve field data and review hydraulic features of the pipeline. Further development and refinement of the proposed information system will be required prior to the development of a general implementable information system.
Control (& Security)	Security must be put into place so that only the research team can access the information system and make relevant changes to it. Information on the pipeline systems may be of a sensitive nature and therefore privacy requirements must be put in place to only allow authorized personnel to see information. Back-ups of the data and reports will be made on a regular basis.
Efficiency	This is a new system without any benchmark, but it is envisioned that the system must be user-friendly and focus on gathering hydraulic data and calculating pipe roughness. Later versions of the system will broaden the functionality of the system.
Service	The system should require minimum training (brief user manual) be user friendly

Requirement Type	Requirements/Explanation
	and easily understood. The system must be flexible to change (e.g. upgrades of existing versions). System must produce accurate and reliable reports for the stakeholders.

3.3 System components of a typical water supply system

Pipelines are utilized to transport water over long distances to supply domestic, agricultural and industry demand. **Figure 3.1** reflects the typically components of a pipeline system starting at a reservoir, flowing through a pump station and ending at reservoir. The section under focus is the pipeline (section A to B).

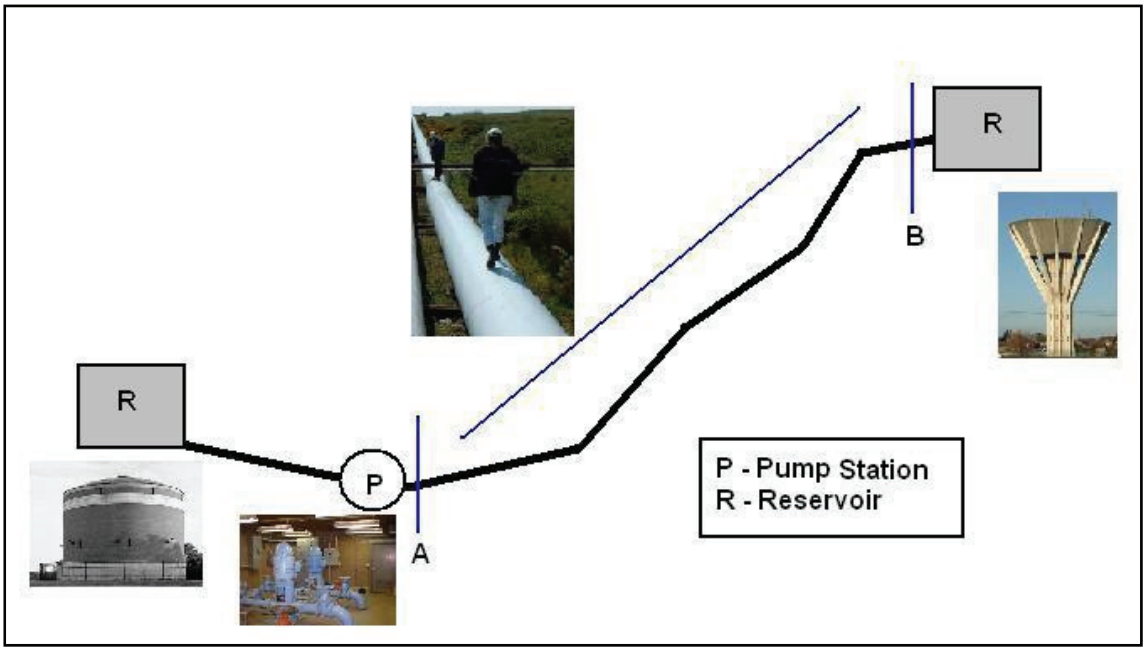

Figure 3.1: Typical components of a pipeline system

The HPIS must typically collect the following information:

- pressures,
- flow rate,
- operational data (water quality, temperature, repair of failures, ect)
- pipe material,
- age,

Furthermore it would be ideal and it is recommended that if it could interface with other information systems. The information system must be able to transform the data into reports (graphs and hydraulic calculations) detailing the hydraulic performance of the pipeline system, and must be able to asses and verify the input data. The HPIS must ultimately allow designers and managers of pipelines to obtain operational data and perform the required analyses.

3.4 An overview of commercially available information systems

3.4.1 Introduction

The following commercially available information software is discussed:

- UPTIME – http://www.uptimesoftware.com
- PipeCraft – http://www.greenpipe.com/Software_Products/PipeCraft/default.htm

Some features of these packages are briefly discussed in the following paragraphs.

3.4.2 UPTIME

Uptime combines powerful decision support tools with a data management system to address pipeline risk and integrity management (Advantica, 2008).

The software package offers the following applicable applications:

- Data management
- Planning
- Integrity analysis and risk assessment
- Consequence of failure analysis

- Corrosion management
- Inspection and maintenance strategies
- Plan outlining and development
- Database planning and development
- Threat assessment
- Data analysis

This package allows one to monitor an operating pipeline as well as the accompanying infrastructure on a real time basis. The software also allows for future planning of pipelines as well as upgrading of existing ones.

3.4.3 PipeCraft

PipeCraft pipeline software is a set of pipeline integrity management tools that helps pipeline owners and operators to design, operate and maintain their pipelines (PipeCraft, 2008).
The following features of the software package are relevant to the water pipeline environment and related to the project.

- Develop integrity plans and track on-going integrity activities.
- Corrosion monitoring
- Inspection and repair work tracking in the field by data loggers
- Assess pipeline risk
- Optimize pipeline performance and troubleshoot operating problems
- New routing and optimization for the construction of new pipelines
- Maintenance history of every asset in your pipeline system
- Scheduling maintenance activities using a risk-based maintenance program generator
- View your pipelines and facilities through the fully integrated Geographic Information System (GIS)

These three mentioned software packages have features that are relevant and important in the monitoring and analyses of pipelines. One critical short-coming of all three software packages is that they do not have the capacity to conduct any analyses on the data.

3.5 System Design requirements

3.5.1 Introduction

In order to design, construct and eventually implement an information system, one must first identify, analyse, and understand the stakeholders and user requirements (Bentley and Whitten, 2007). This is crucial as the gathering of wrong or insufficient requirements will lead to a suboptimal or completely ineffective information system being developed.

The following system models were constructed in order to clarify the functional requirements of the proposed information system:

- Context diagram – holistic overview of the system components;
- Process Flow diagrams- reflect the interrelationships and detail of the different processes;
- Use-Case diagrams and narratives – defines the relationships between the different stakeholder;
- Entity Relationship Diagrams (ERD) – reflects the requirements and details of the data to be captured; and
- Decomposition review – indicating the different subsystems of the HPIS.

3.5.2 Context Diagram

A context diagram (**Figure 3.2**) was set-up in order to obtain a holistic view of the IS and all the type of inputs and outputs to the system. The context diagram allows one to better understand the problem domain (Bentley and Whitten 2007).

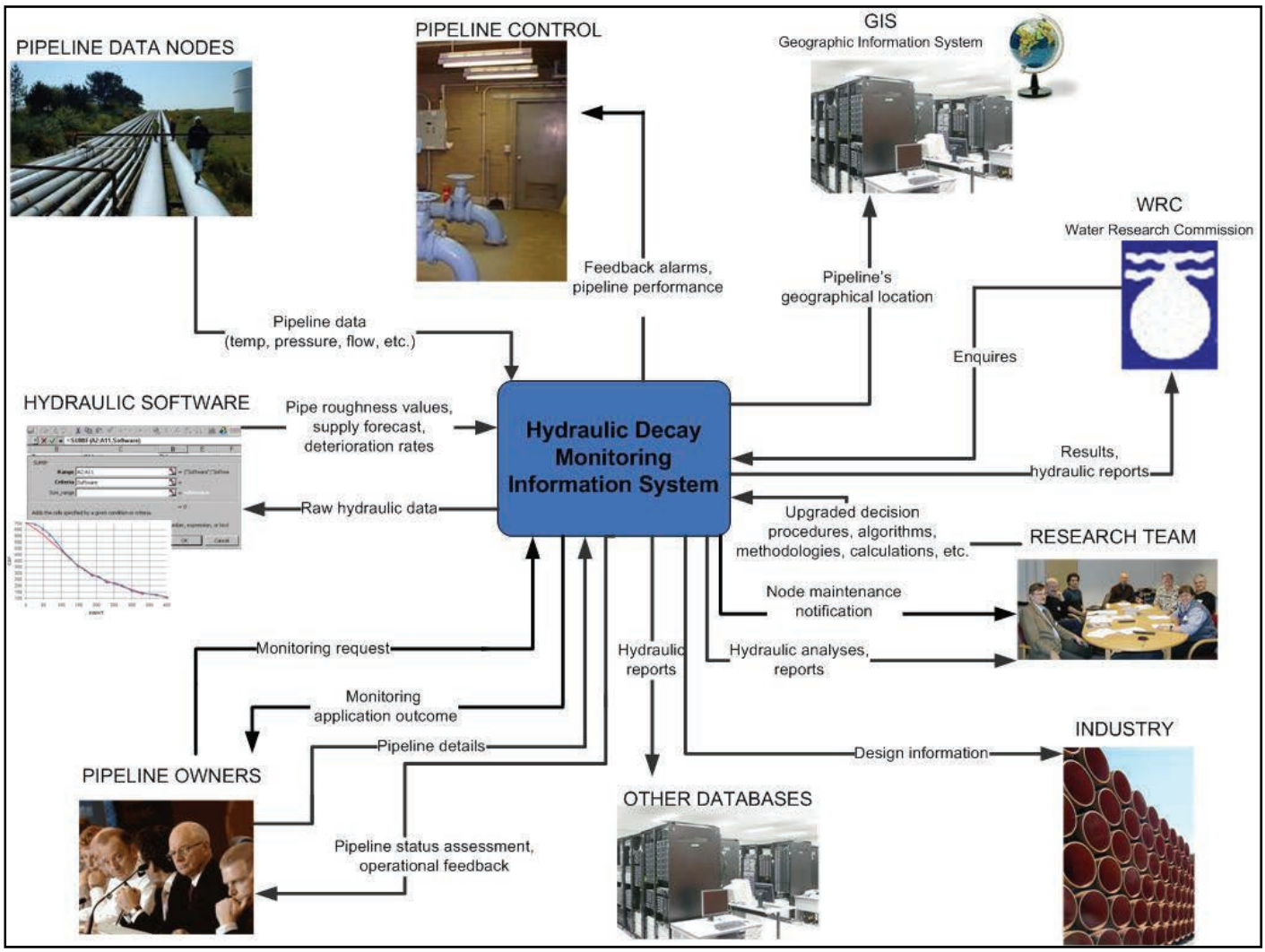

Figure 3.2: Schematic presentation of the inter relationship of the interested and affected parties

3.5.3 Process Flow Diagrams

Process Flow diagrams were constructed in order to better understand the processes and procedures relating to the information system's operation and the information system's supporting functions. The entire system, once operational, could consist of more than just the centralised information system.

The following process flow diagrams were compiled, reflecting different aspects with regards to system security, system installation, integrity and operation:

- Installation of the database
- Normal System Operation of the Database
- Input Data Problems
- System Maintenance

3.5.3.1 Installation

All information systems aim to include the maximum economical extend of available data. In this research the aim was however to create an information system and populate the system with data of a selected scheme, verifying the functionality of the information system and to highlight possible shortcomings. If the information system had to be implemented, the system will have to be reviewed and the database extended.

Figure 3.3 outlines the procedure (process) that needs to be followed to add a new pipeline or new sections of an existing pipeline (upgrade).

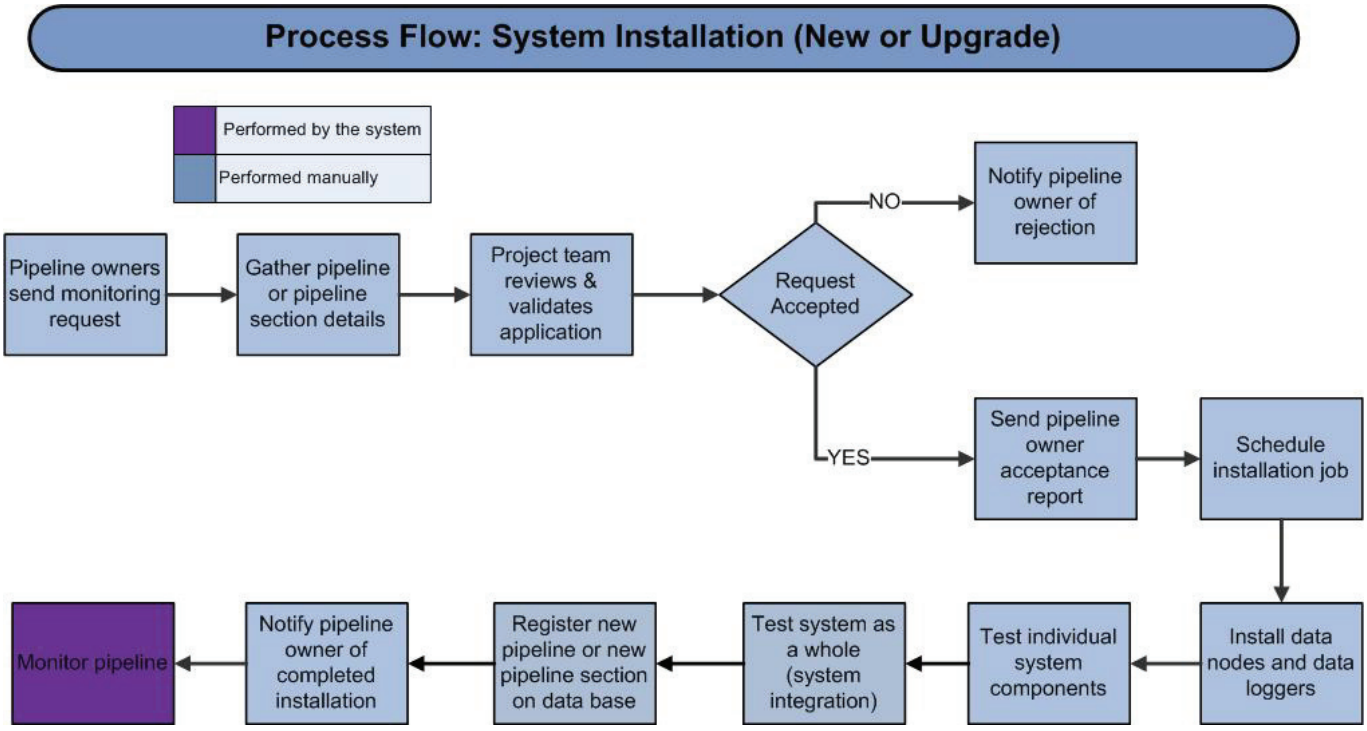

Figure 3.3: Process Flow Diagram of System Installation

3.5.3.2 System Operation

Figure 3.4 portrays the intended data flow of the system once the entire system is operational, reflecting the distinct phases of:

- Data input and integrity evaluation;
- Data assimilation; and
- Query handling.

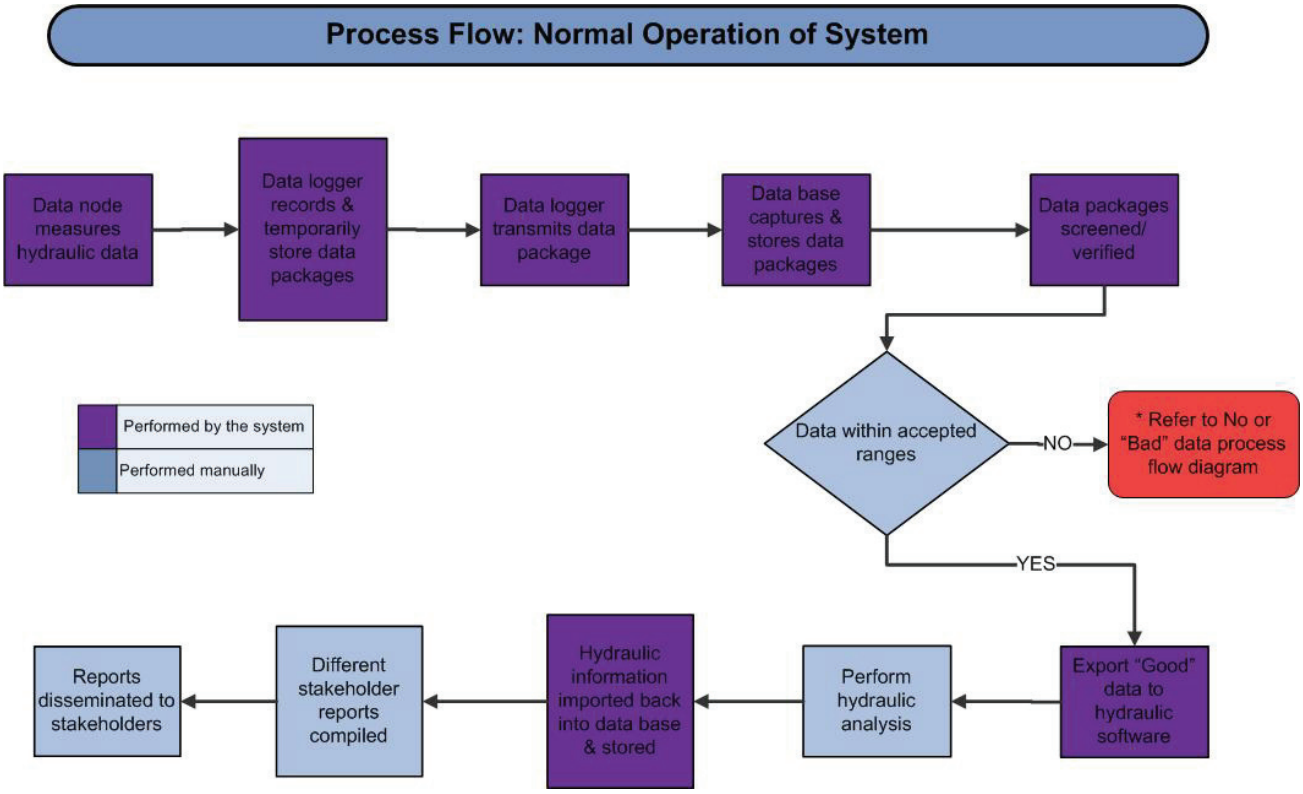

Figure 3.4: Process Flow Diagram of Normal Operation

3.5.3.3 Data verification

All data received at the define intervals or submitted manually should be verified prior to the addition to the database. **Figure 3.5** depicts a verification process.

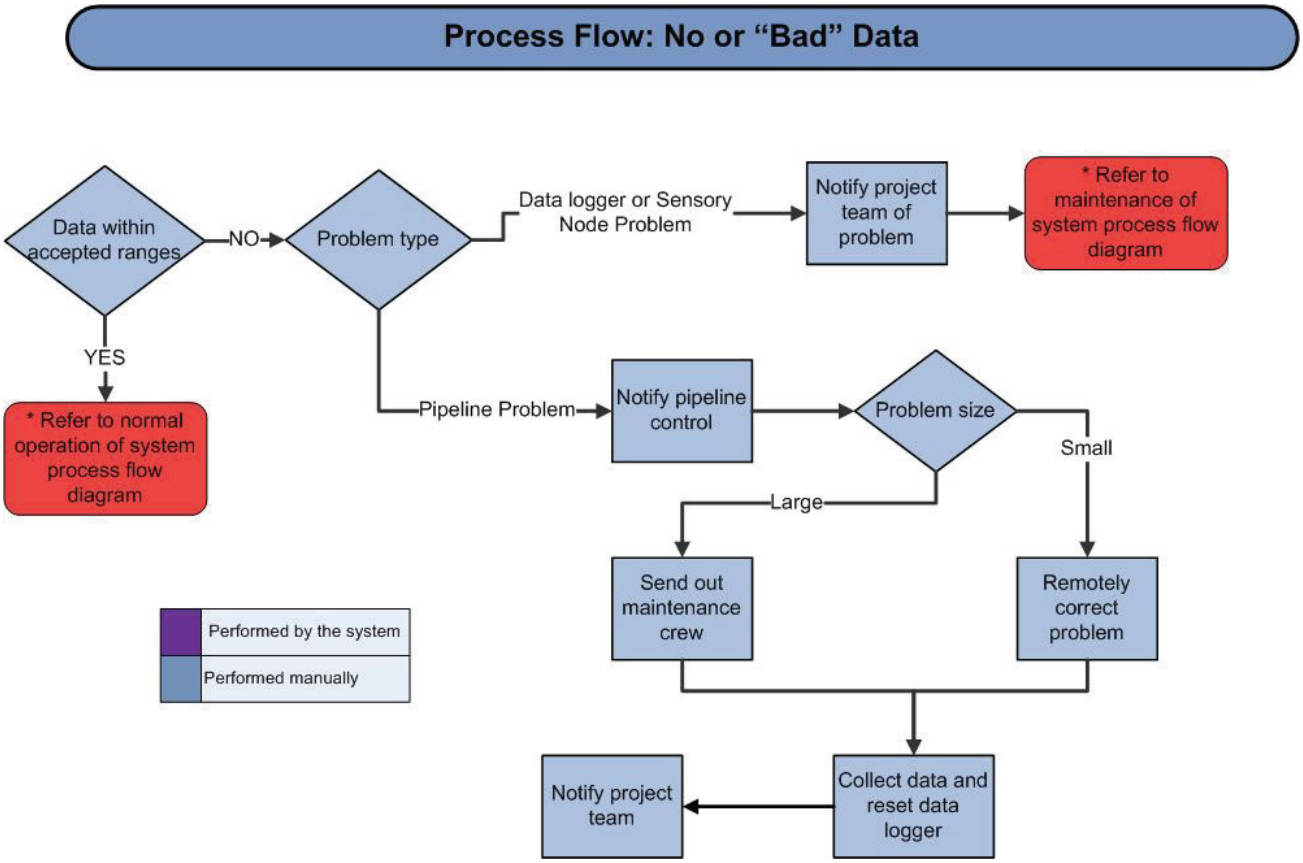

Figure 3.5: Process Flow Diagram of Input Data Problem

3.5.3.4 System Maintenance

As for all system, maintenance remains an important aspect ensuring an operational system. A general maintenance process has been outlined in **Figure 3.6**. The process also includes unscheduled maintenance that must be performed as break-downs arise in normal operation of the system. The scheduled maintenance tasks are recorded in the database to notify the team that a component needs to be serviced.

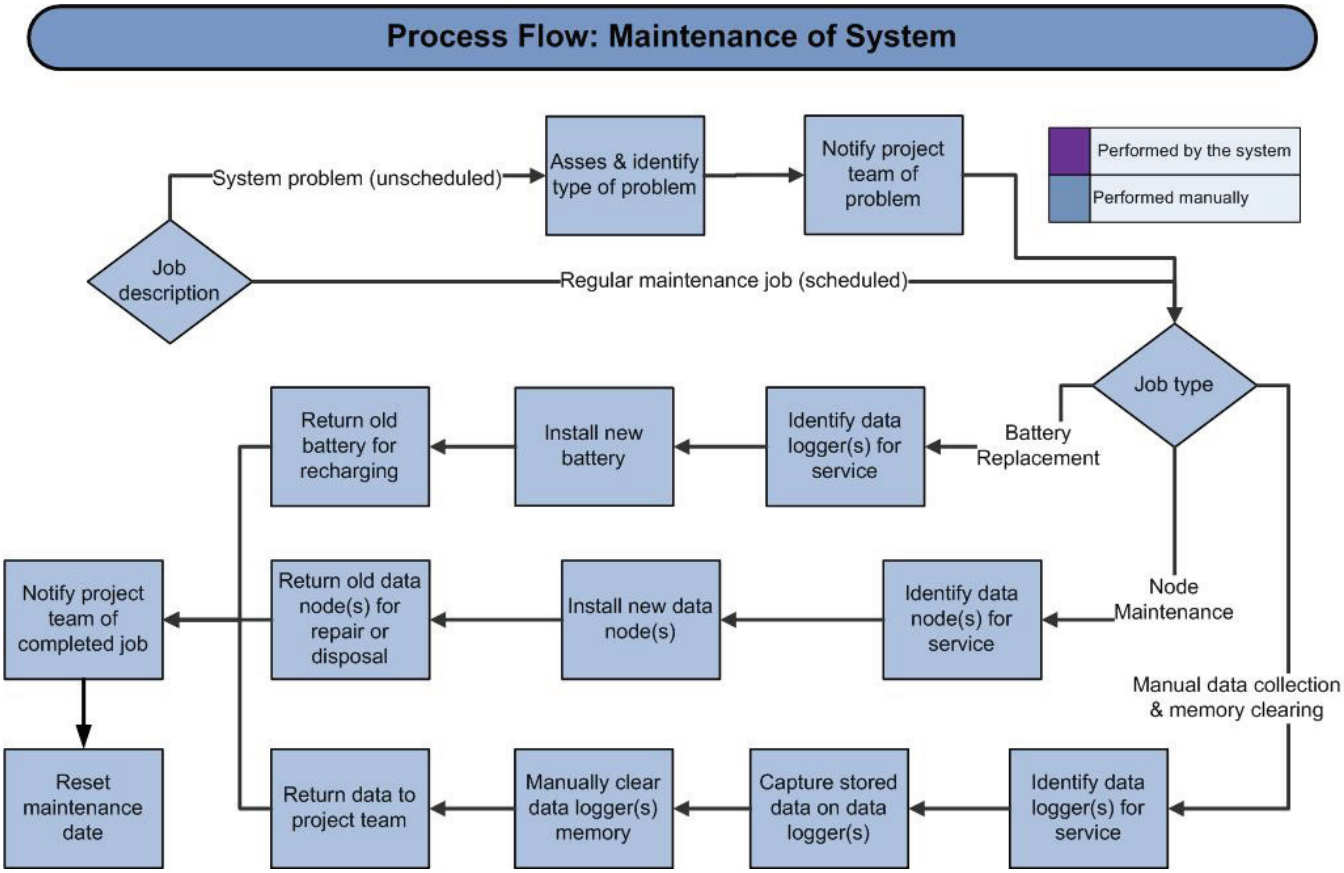

Figure 3.6: Process Flow Diagram of System Maintenance

3.6 Use-Case Diagrams

Use-case diagrams (UCD) formulate the relationships between the stakeholders or interested parties (pipeline owners, operational staff, database operators and managers) and define the query and response lines and reflect the data and reporting formats and procedures. This aspect will require further development prior to the development of the information system.

3.7 Entity Relationship Diagrams

The ERD contains a number of history entities (e.g. Pipeline Section History, Pump Station History and Reservoir History), allowing for a timeline function.

The database will record large volumes of hydraulic data and store hydraulic results (back calculated pipe roughness results) over the years. This data and results need to be archived from time to time in order to prevent cluttering of the database as well as back-up the valuable historic information in the event of a database failure. The two entities; Hydraulic Data Package and Hydraulic Results therefore have archive tables. These archive tables will eventually be in a separate database.

A pipeline system is broken into pipeline sections, defined by locations where the diameters change, the pipeline bifurcation, or material change. A section of pipeline can contain a number of pipeline components such as bends, valves, etc. A pipeline section may split into different sections or sections might merge into one section. To keep track of these changes two entities were created, Pipeline Section Split and Pipeline Section Merge respectively.

Entities were created to keep details on accompanying pipeline system changes such as leak identification, pipe bursts, pipeline replacements, new consumers added and extensions to the system.

Figure 3.7 represents the Hydraulic Performance Information System's data requirements.
\

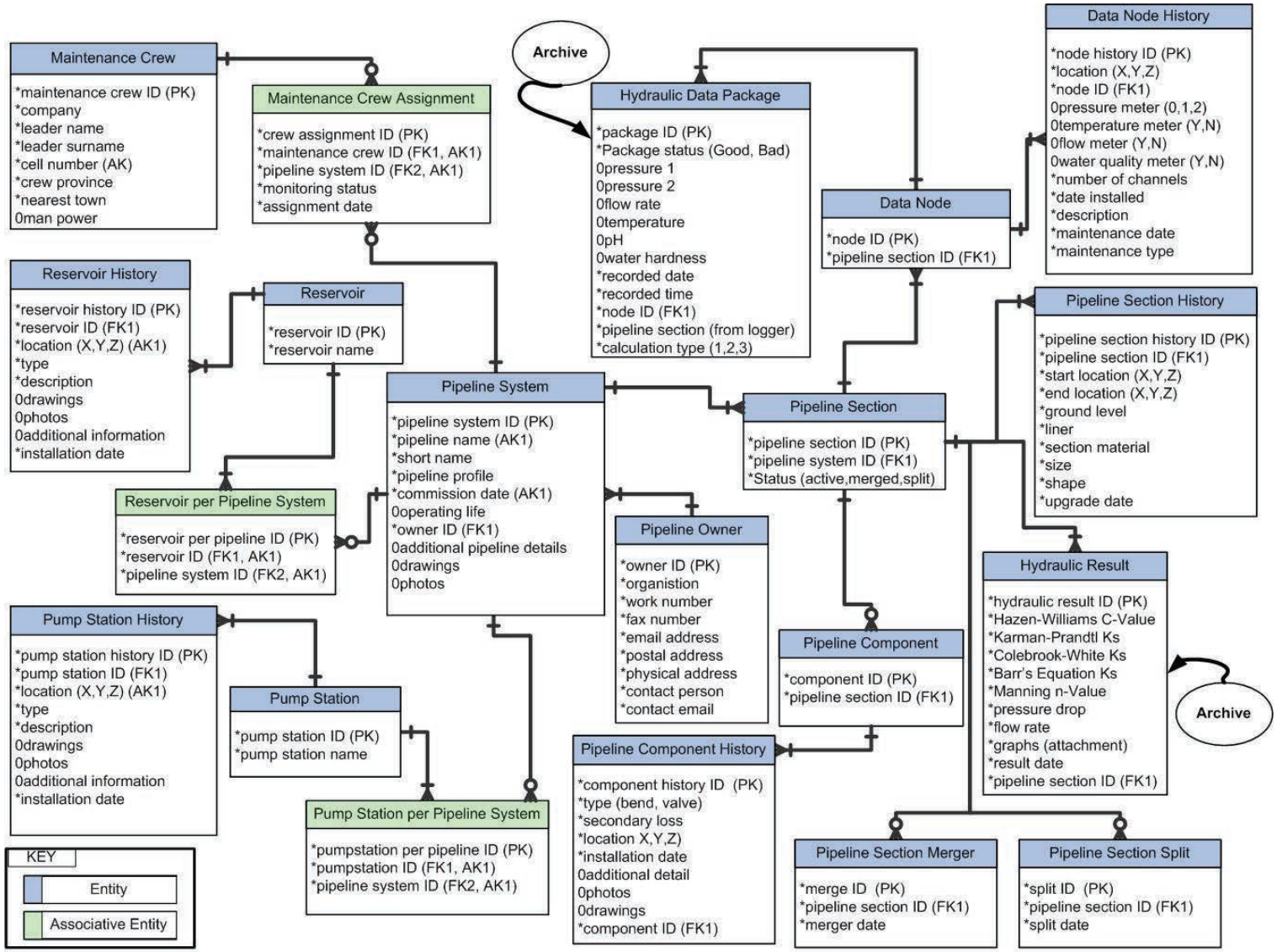

Figure 3.7: System ERD

The system requires a certain amount of user level security. There are three main roles that a user can engage in; namely System Administrator, System Editor and System Viewer. Each user will have a user name, password and a Role (e.g. System Administrator, Full Access or Read-Only). This solution was designed to overcome the problem that MS Access 2007 does not have user level security like past versions (MS Access, 2008).

3.8 Decomposition review

A decomposition review was done to quantify the structure of the proposed system and divide it into logical subsystems and functions. The subsystems which have been identified are:

- Feedback;
- Supporting functions;
- Other features;
- Pipeline functions; and
- Reporting.

It is envisaged that further changes and improvements will be required for the prototype.

3.9 Software architecture – Prototype analysis decision

Microsoft Access is suitable to handle the required data and it was motivated on the following facts:

- The Microsoft Office Suite is widely used;
- It offers a database creation and maintenance features as well as form (interface) capabilities; and
- The package is user friendly.

The following summary (Table 3.2) shows the applicable features and limitations of Microsoft Access. The package is relatively easy to use compared to Oracle or Microsoft SQL as one does not require advanced database knowledge.

Table 3.2: MS Access Limitations (adapted from Microsoft website)

Attribute	Maximum (limitation)
Microsoft Access database (.mdb) file size	2 gigabytes minus the space needed for system objects.
Number of objects in a database	32,768
Number of characters in an object name	64
Number of characters in a password	14
Number of characters in a user name or group name	20
Number of concurrent users	255
Number of objects in a database	32,768
Number of tables in a query	32
Number of levels of nested forms or reports	7
Number of fields or expressions you can sort or group on in a report	10

Some of the limitations of Microsoft Access are:

- The number of concurrent users actually depends on the size of the database and Microsoft's own recommendation, states that the Microsoft Jet engine's practical limit on concurrent users is only 20 (AccessDB.info, 2008);
- The number of MS Access records that can be stored in a table is limited. The total database file must not exceed two gigabytes. Experts suggest that anything over 100 000 or 250 000 records, depending on the number of attributes in a table, become too much for Access to handle (MS Access 07 Thinkcentre, 2008);
- The amount of data traffic that the final information system might handle, will be too much for Access as numerous data loggers will be sending data on a regular basis; and
- The overall security of MS Access is limited which restricts the application of this software for the final database.

Based on these limitations, the prototype will only be built in Microsoft Access in order to convey the functionality required in the final development which might use different software architecture.

Microsoft Access 2007 can handle attachments to records and can create multiple views for a report for different users can be handled. It also allows forms to be created in HTML format in order to be emailed (any email software, e.g. online email, Outlook, GroupWise, etc.) negating that tables have to

be retyped. It was decided that Microsoft Access 2007 will be used for building the prototype and that user level security will be developed separately.

3.10 Physical Design

The Hydraulic Performance Information System (HPIS) will be to populate data which has been collected during the execution of this research project. This data will then be used to back-calculate valuable information regarding hydraulic decay over time and how this influences the performance and functioning of the pipeline systems.

The database allows the project team to collect information regarding the following elements:

- Pipeline Owners;
- Pipeline Systems and Pipeline Sections;
- Pump Stations and Reservoirs;
- Pipeline Components;
- Data Nodes;
- The information system's maintenance crews; and
- Pipeline alterations.

The HPIS allows for password protection, preventing unauthorized people from accessing the database. The system then further differentiates between security levels with user level security. These levels range from administration, full access and read-only. This feature was added as MS Access 2007 did away with user level security (MS Access, 2008).

The information system was designed to be user-friendly, making use of logical layouts and using a similar layout for similar actions performed on different elements (e.g. adding a pipeline component screen layout is similar to adding a pipeline data node screen). The User Manual is available on the supporting CD.

Lists where records are shown were refined using queries so that only the essential information is displayed. This prevented cluttering of records. A feature of MS Access 2007 was utilized called multi-field records. This feature allows a field to store more than one record, such as all the pipeline sections fused in a merged section.

As mentioned earlier in this document the constructed system is only a prototype and therefore does not have all the functionality the final system will be desired to perform. Research was done on how information can be retrieved from the data loggers, via a wireless network, to the database. This data will then be exported to the hydraulic software in order to back-calculate hydraulic performance. The information must then be imported back into the database to be linked and stored with the relevant pipeline sections. It was found that databases are designed for this purpose and can easily accompany these desired actions. In MS Access 2007 the tab "External Data" allows one to save, import and export actions. These actions can then be called up repeatedly.

The final system must be able to validate incoming data against predetermined acceptable ranges. This can be achieved by adding high and low level range values to the data records for each value. (e.g. pressure high and pressure low). The incoming data can then be verified against the high and low values be means of a formula and can be flagged (highlighted) if it falls out of the ranges. Reports of out of range data can then be produced. This feature was not incorporated in this research.

3.11 Limitations and Constraints

As with any project or system there are always limitations or constraints that will make a solution sub-optimal. The following areas were of concern:

- MS Access knowledge: Lack of absolute MS Access knowledge altered certain design aspects.

- MS Access limitations – Some form designs were changed to less desirable layouts due to limitations of MS Access. For example some forms were split up into separate forms due to the list box becoming inactive with the record being displayed.

- Limited Data – As the large project is still in the development phase, little or in some circumstances no data was present. The project team provided realistic test data in order to validate the information system. This data was used to determine characteristic such as text box size, number fields specified as double or integer, and other design aspects.

- Time – Limited time was present to refine and change features of the information system.

The User Manual is available on the supporting CD and contains more detailed information regarding the physical design of the information system. Recommendations for future design of certain screens were included in the manual.

3.12 Towards the Final HPIS

A programmer will be contracted in order to build the final information system in a more industrious Relational Database Management System (RDBMS). The reason for this decision is the following:

- The information system must be able to handle large volumes of data (records).
- Future versions may require simultaneous user login.
- The information system must handle large traffic volumes in the form of data coming in from data loggers.
- More reliable security is required (including user level security).
- As newer versions are required, a dedicated company/programmer can use the existing versions to upgrade to newer versions.
- The Company/programmer can provide database support.

As there was no such a database, it had to be designed. The system extends from the measuring instruments in the field, capturing data by the data loggers, sending data from the data loggers via a wireless network to the database and capturing the data on the database. The database exports this data to hydraulic software to back-calculate pipe roughness. Therefore, information is imported back into the database where it is combined with other details collected by the information system. Consequently, value adding information is provided to the project team and various reports can be produced for the stakeholders. Commercial software packages were looked at, but nothing met the objectives of the project, thus a system was designed and a prototype built.

To keep track of changes to the records in the information system, the details of the user that logs onto the system could be recorded using the global variable function. This will then be recorded if a record is altered, added or deleted. For this the main entities in the ERD will require another two attributes, “last updated person” and “last updated date” which will be filled in automatically by the global variable and current date.

3.13 Development of the database utility

3.13.1 Introduction

The data capturing software titled "**Hydraulic Performance DB V.1**" is included on the accompanying CD can be used to create a database with valuable information of the historical performance and current status of the system. The structure which was discussed above was incorporated in the software which was compiled in Microsoft Access. The system is easy to use and a User Manual for "**Hydraulic Performance DB V.1**" is included on the supporting CD.

3.13.2 Installation of the HPIS

To run the HPIS, copy the database file (Hydraulic Performance DB V.1) from the CD and then run the utility which is a MS Access version 2007 file.

3.13.3 Viewing the database

Step 1: Double click on the file Hydraulic Performance DB V.1, which was stored to the hard drive, to open the file. The following screens will popup.

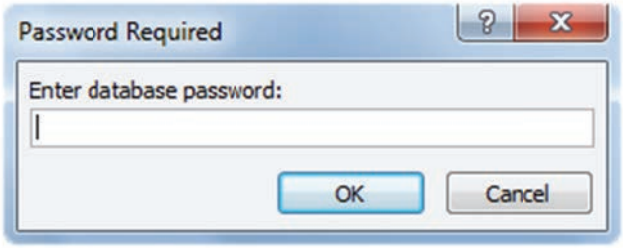

Step 2: Provide the security access by using the following password: "hydraulic".

Step 3: Select the user name from the drop box.

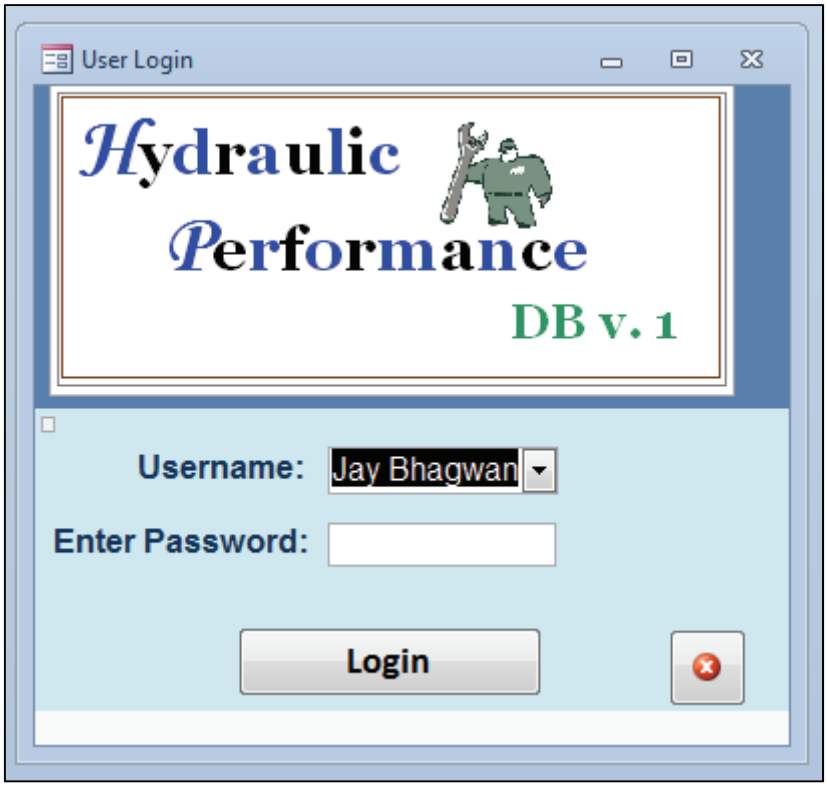

Step 4: Enter the password: “wrc1”.

Step 5: Full access will be available to all material.

4 Fieldwork

4.1 Introduction

Most pipelines in South Africa have not been hydraulically reviewed since their installation, hence the current hydraulic characteristics is unknown. The hydraulic capacity can be determined by establishing a relationship between the energy losses and the flow rate, which requires the recording of pressure and flow rate for the system.

In the following paragraphs the criteria for suitable pressure and flow recordings positions are reflected. Some details of suitable instrumentation for pressure and flow recordings are reflected followed by the details of the pipelines which were reviewed.

4.2 Data recording positions for the hydraulic performance review

4.2.1 Pressure recording positions

Pressure recordings must be conducted at locations on the pipeline where the following criteria are satisfied:

- Pressure gauging positions had to be accessible (close to roads).
- The location should be dry;
- It should be possible to secure the access to the instrumentation;
- A tapping position with a cock to isolate the connection point should be available;
- The flow rate between the pressure tapping locations should be controllable and hence no large abstractions or inflows should be present;
- The pipe material and dimensions should be the same between the pressure gauging locations;
- All the secondary loss elements should be identifiable; and
- At least 3 pressure recording positions should be used to determine the roughness in a specific section of the pipeline.

4.2.2 Flow measurement positions

Flow recordings must be conducted at locations on the pipeline where the following criteria should be adhered to:

- Flow gauging positions had to be accessible (close to roads).
- The location should be dry;
- It should be possible to secure the access to the instrumentation;

- A straight section of the pipeline with a length of at least 20 diameters should be accessible up to the shoulder of the pipeline;
- The flow rate at the flow recording position should represent the flow in the pipeline between the pressure recording positions, hence no large abstractions or inflows should be present;
- The pipe material, diameter, wall thickness, liner type and liner thickness should be known;
- The operational control should be able to control the flow at a constant rate for a long enough time to ensure a stationary flow condition; and
- The operational flow rate should represent at least 3 different flow rates (low, intermediate and high).

4.3 Typical instrumentation which could be used to review the hydraulic capacity of pipelines

4.3.1 Introduction

In the following paragraphs details of pressure transducers, data recording system and the flow recording instrumentation are discussed.

4.3.2 Pressure transducers

Different pressure transducers with varying pressure ranges were used to measure the pressure (**Figure 4.1**). These were either GEMS or Endress & Hauser make pressure transducers (4 barA, 10 bar, 16 bar and 16 barA).

Figure 4.1: Pressure transducer

4.3.3 Data recording devices

Pressures were captured using HOBO U-12 Industrial loggers (**Figure 4.2**) with a resolution. These loggers are externally excited by a 12 Volt battery.

The data loggers accommodate the input from the pressure transducers (Maximum of 4 channels) which gives an output signal of between 4-20 mA. The recorded output (4 to 20 mA) is converted to a pressure or head related to the rating of the transducer. The recording accuracy is defined by the discreet outcomes which is 2^{12} for a 12bid system. This relates to an accuracy of pressure of 1/4096 of the full scale of the pressure transducer. In the case of a 10 Bar transducer this will equate to an accuracy of 10*100/9,81*1/4096 = 0,0249 m.

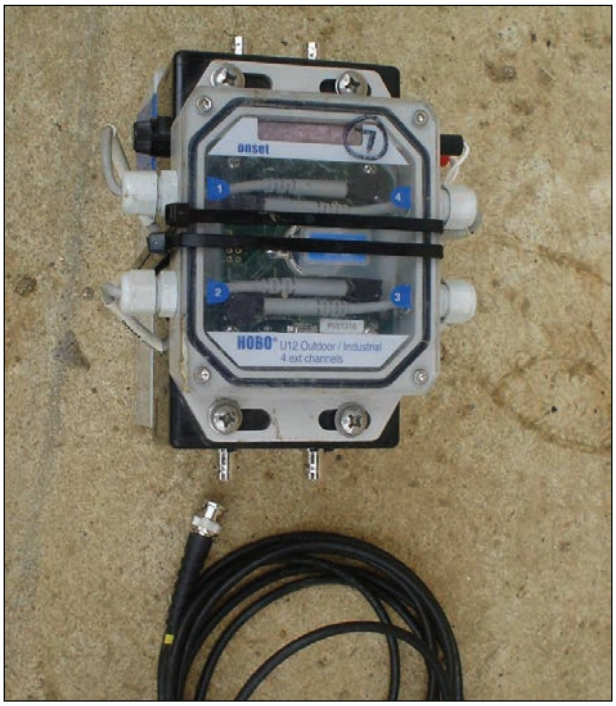

Figure 4.2: HOBO U-12 Industrial Logger

4.3.4 Flow measurement instrumentation

The flow rate was normally measure with the PORTAFLOW (Fuji Electric) Serial number Q1A5441T, Ultrasonic Flow Meter shown in **Figure 4.3** which indicates the V-type installation of the FLD51 sensors.

Figure 4.4 reflects a typical installation of a magnetic flow meter. In cases where the flow data were recorded from an installed instrument, the flow data were compared.

Figure 4.3: Typical installation of the PORTAFLOW meter

Figure 4.4: Typical installation of a Magflow meter

4.4 Locations of the pressure recording position

The locations of the pressure recording positions were either sourced from:

- As-Build drawings;
- Surveyed data; or defined from
- GPS coordinates.

The accuracy of the elevations of the pressure gauging positions is crucial for the accurate assessment of the hydraulic roughness of the pipeline. Although the surveying technology has expanded the best typical vertical accuracy varied between 0,08 m and 0,15 m.

4.5 Pipelines which were reviewed

4.5.1 Introduction

Pipelines conveying raw- and treated water were reviewed. The following pipelines conveying treated water were reviewed:

- De Hoek to Uitkijk pipeline (BloemWater);
- Uitkijk to Brandkop pipeline (BloemWater);
- Swakopmund to Rossing Pipeline (Namwater); and
- Swakopmund to Langer Heinrich Pipeline (Namwater).

The following raw water pipelines were reviewed:

- Morgestond Dam to Jericho Dam;
- Jericho Dam to Onverwacht reservoir;
- Hendrina to Duvha Power Station; and
- Lower Blyde River Irrigation System.

In the following paragraphs details of the recording positions and the instrumentation used are discussed, followed by the description of the different schemes. Results from the Baviaanspoort-Kameeldrift Pipeline and the Kuthala-Kendel Pipeline were included, although these two pipelines are not discussed in detail in the following sections.

4.6 Pressure recording positions on the De Hoek to Uitkijk pipeline (BloemWater)

4.6.1 Introduction

The De Hoek to Uitkijk pipeline has not been hydraulically reviewed since the installation of the pipeline in 1975. The current hydraulic characteristics of the pipeline were obtained during field measurements conducted during July 2010.

4.6.2 Recording positions on the De-Hoek to Uitkijk Pipeline

Table 4.1 reflects details of the pressure recordings locations which were selected based on the criteria in paragraph 4.4. All the measuring points were surveyed to obtain an accurate vertical level for each of these points.

Table 4.1: Pressure recording positions on the De Hoek-Uitkijk pipeline

Pressure recording position	Chamber ID number	Maximum pressure (m)[#]	Chainage (m)[##]	Elevation at measuring point (m)*	Coordinates*	
DU1	TAV1	23,1	338,02	1 635,994	S29° 53,168'	E26° 48,254'
DU2a	TAV17	111,3	10 926,95	1 540,156	S29° 48,514'	E26° 44,438'
DU2b	TAV18	111,3	10 926,95	1 540,053	S29° 48,519'	E26° 44,443'
DU3	TAV31	123,6	20 066,13	1 528,013	S29° 44,601'	E26° 41,044'
DU4	TAV46	81,6	29 490,01	1 569,083	S29° 40,508'	E26° 37,525'
DU5	TAV56	74,5	34 504,75	1 576,593	S29° 38,495'	E26° 35,482'
DU6	TAV69	105,1	41 673,41	1 546,060	S29° 35,598'	E26° 32,543'
DU7	UITKIJK	80,7	47 005,95	1 576,547	S29° 33,627'	E26° 30,123'

Notes: [#] Maximum static pressure was used to select pressure transducer range

[##] Chainages were obtained from the Tender Drawings

* A detailed survey of the measuring points were conducted by YMAX Engineering

The locations of these measuring points are shown in Figure 4.5.

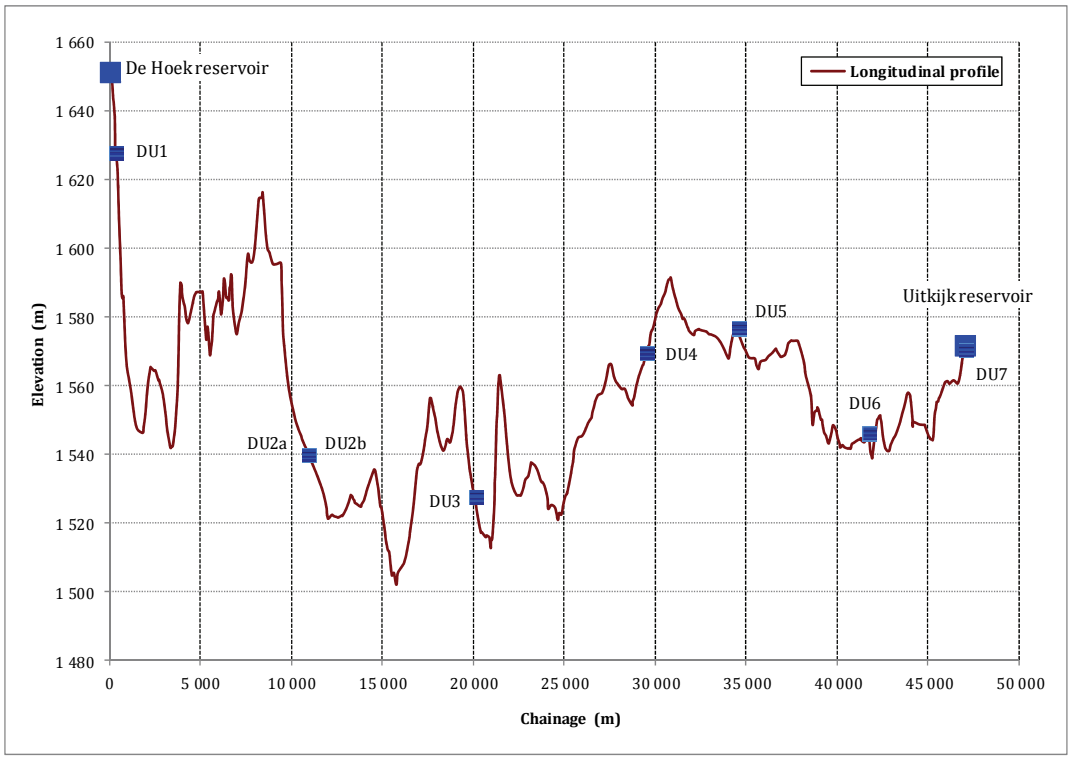

Figure 4.5: Location of the pressure recording positions

The average horizontal precision obtained in the survey was 26 mm and the average vertical precision was 38 mm. Detail of the pressure recording equipment and the pressure transducers are shown in **Table 4.2**.

Table 4.2: Details of the pressure transducers and data loggers used on the De Hoek to Uitkijk Pipeline

Measuring point	Chamber ID number	Pressure transducer		Recording accuracy (m)*	Recording frequency (Hz)	Data logger
		Channel 1	Channel 2			
DU1	TAV1	4 bar A	4 bar A	0,010	2	784501
DU2a	TAV17	16 bar A	16 bar A	0,040	2	2044486
DU2b	TAV18	16 bar	16 bar A	0,040		
DU3	TAV31	16 bar	-	0,040	2	951316
DU4	TAV46	10 bar A	10 bar A	0,025	2	784505
DU5	TAV56	10 bar A	-	0,025	2	784502
DU6	TAV69	16 bar A	16 bar A	0,040	2	784504
DU7	UITKIJK	10 bar	10 bar	0,025	2	2010102

Note: *The data logger is a 12 bit logger

4.7 Pressure recording positions on the Uitkijk to Brandkop (Bloemfontein) pipeline (BloemWater)

4.7.1 Introduction

The hydraulic characteristics of this pipeline were obtained during a site visit in June 2010. Similar to the instrumentation which was discussed in paragraph 4.4 were used here to measure flow and pressure and record the data.

4.7.2 Location of the pressure recording positions

Table 4.3 reflects the selected locations where recordings of pressures at different flow rates.

Table 4.3: Details of the pressure transducers and data loggers used on the Uitkijk-Brandkop pipeline

Measuring point	Chamber ID number	Maximum pressure (m)[#]	Chainage (m)[##]	Elevation at measuring point (m)*	Coordinates*	
UB1	TAV1	11,39	294,4	1 565,272	S29° 33,475'	E26° 30,059'
UB2a	TAV12	41,19	5875,1	1 533,718	S29° 30,594'	E26° 28,941'
UB2b	TAV13	41,19	5895,1	1 533,830	S29° 30,587'	E26° 28,938'
UB3	TAV35	76,89	19626,6	1 498,801	S29° 23,842'	E26° 25,360'
UB4	LIEUWKOP LCV	128,00	25610,1	1 452,639	S29° 21,262'	E26° 23,510'
UB5	TAV69	157,39	39862,4	1 418,646	S29° 15,448'	E26° 17,494'
UB6	TAV86	159,37	50226,0	1 417,665	S29° 12,116'	E26° 12,303'
UB7	AIR VALVE AT BRANDKOP	83,19	58753,9	1 492,737	S29° 08,695'	E26° 09,305'
UB8	LCV10	83,19	58756,9	1 492,919	S29° 08,679'	E26° 09,318'

Notes: [#] Maximum static pressure was used to select pressure transducer range.

[##] Chainages were obtained from the Tender Drawings.

* A detailed survey of the measuring points was conducted by YMAX Engineering. The average horizontal precision obtained in the survey was 8 mm and the average vertical precision was 13 mm.

The locations of these measuring points are shown on the longitudinal profile, **Figure 4.6**.

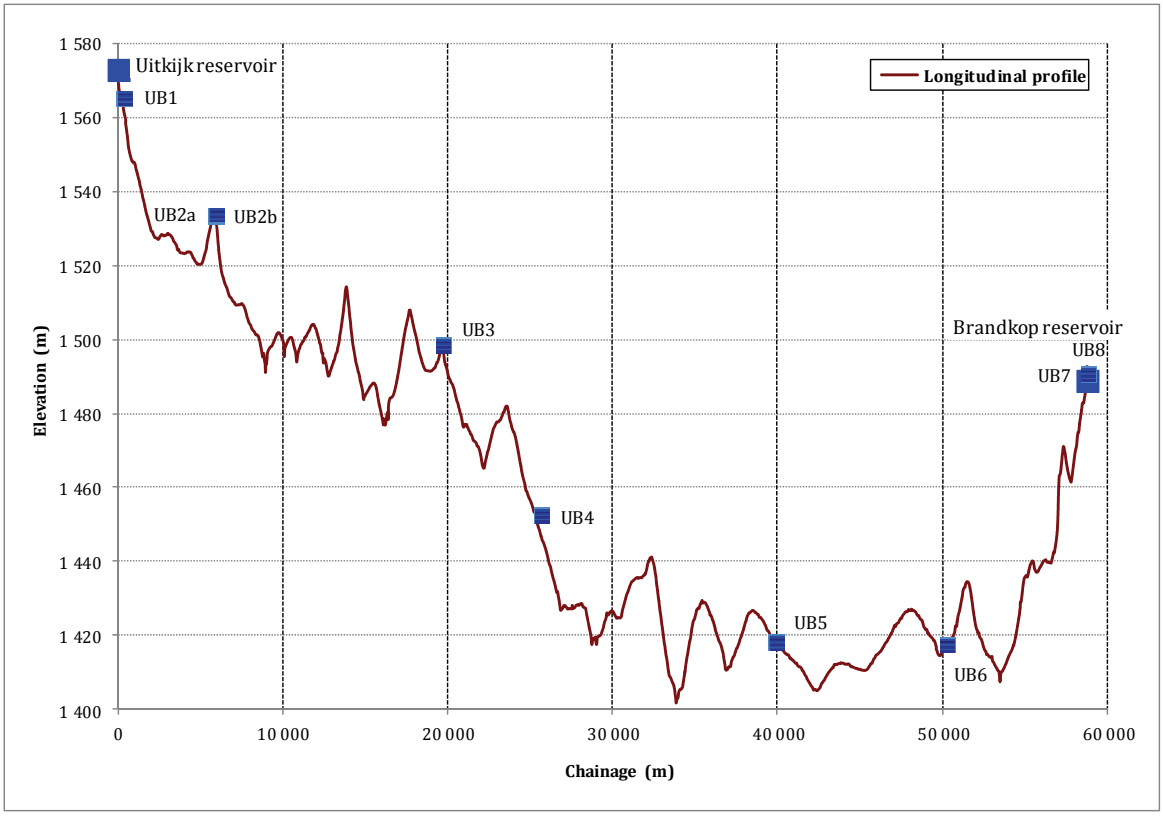

Figure 4.6: Location of pressure recording positions

Figure 4.7 reflects a typical installation of a pressure transducer on the Uitkijk to Brandkop pipeline.

Figure 4.7: Setup of the pressure transducers at UB1 (TAV1) on the Uitkijk to Brandkop pipeline

Table 4.4 reflects the details of the instrumentation used to capture the pressures in the Uitkijk to Brandkop Pipeline.

Table 4.4: Details of the pressure transducers and data loggers used on the Uitkijk to Brandkop Pipeline

Measuring point	Chamber ID number	Pressure transducer		Recording accuracy (m)*	Recording frequency (Hz)	Data logger
		Channel 1	Channel 2			
UB1	TAV1	4 bar A	4 bar A	0,010	2	2044485
UB2a	TAV12	10 bar	10 bar	0,025	2	2010102
UB2b	TAV13	10 bar	-	0,025		
UB3	TAV35	16 bar A	16 bar A	0,040	2	784505
UB4	LIEUWKOP LCV	16 bar A	-	0,040	2	2044486
UB5	TAV69	25 bar	25 bar	0,062	2	951316
UB6	TAV86	25 bar	-	0,062	2	684504
UB7	AIR VALVE AT BRANDKOP	16 bar A	16 bar	0,040	2	784501
UB8	LCV10	16 bar	16 bar	0,040	1	784502

Note: *All the data loggers are 12 bit loggers.

During the testing the flow will be controlled by opening and closing of the Bermad control valves at Brandkop Reservoir.

4.8 Pressure recording positions on the Rössing Pipeline (Namwater)

4.8.1 Introduction

The water supply to the Rössing Mine on the West Coast of Namibia consists of an above ground pipeline installation over a distance of 54,1 km. Water is pumped from the Base Pump Station (Chainage 0, km) towards the Rössing Mine. Except for the Base Pump Station near Swakopmund, two booster pump stations are used to overcome the friction and secondary losses as well as the static head difference of about 583,8 m.

Figure 4.7, **Figure 4.8** and **Figure 4.9** indicate some typical details of the installation, while the main features of the Rössing Pipeline are summarized in **Table 4.5**.

Figure 4.8: Above ground installation with profile following the topography – Rössing Pipeline

Figure 4.9: Typical support for the Rössing Pipeline (R reflects that the footing has to be replaced)

Figure 4.10: Replacement of the pipeline support under construction

Table 4.5: General details of the Rössing Pipeline

Parameter	Value	Units
Total length (Three pump sections)	54 100	m
Elevation difference	583,8	m
Pipe material	Steel	
Material yield strength	420	MPa
Coupling system	Viking Johnson	-
Pipe manufacturer	Unknown	-
Unit pipe length	9,2	m
Outside diameter (mm)	713,5	mm
Wall thickness	6	mm
Internal Copon coating thickness	250	μm
Internal diameter (calculated)	701,5	mm
Number of pumps in the Base station	3	
Number of booster stations	**3 (Base station included)**	

4.8.2 Longitudinal detail of the Rössing pipeline sections

Figure 4.11 and **Figure 4.12** respectively indicate the total longitudinal profile of the Rössing Pipeline and the section between the Booster 2 and Booster 3.

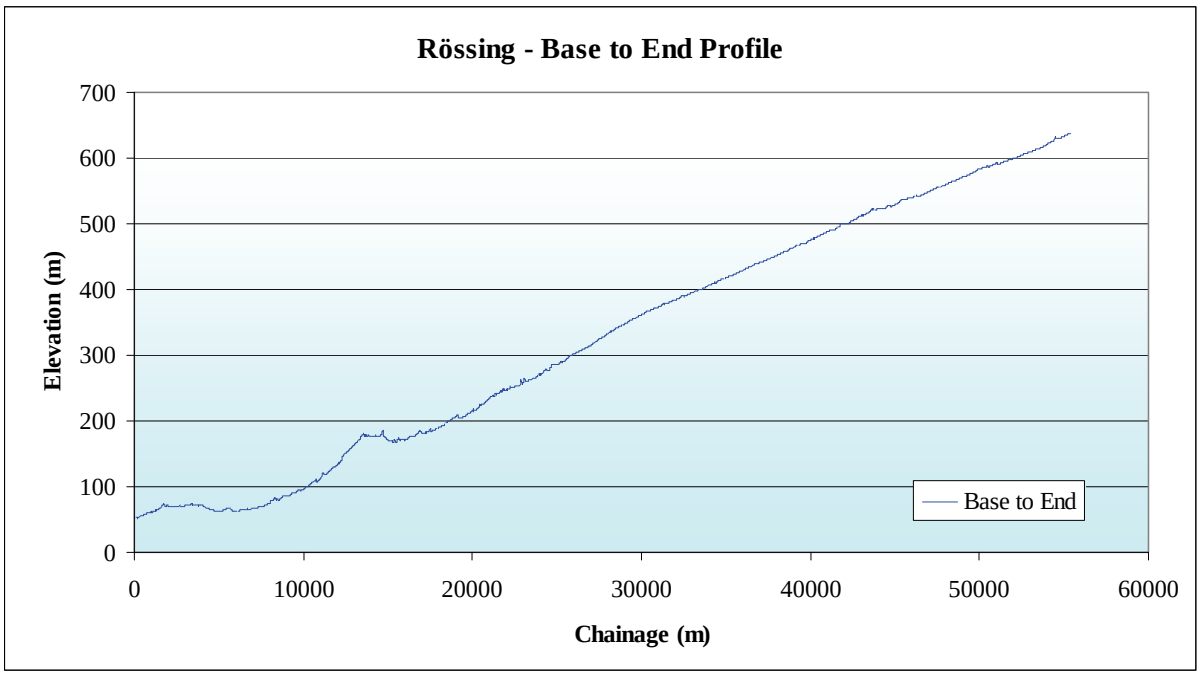

Figure 4.11: Longitudinal profile of the Rössing Pipeline (Base Pump Station to End)

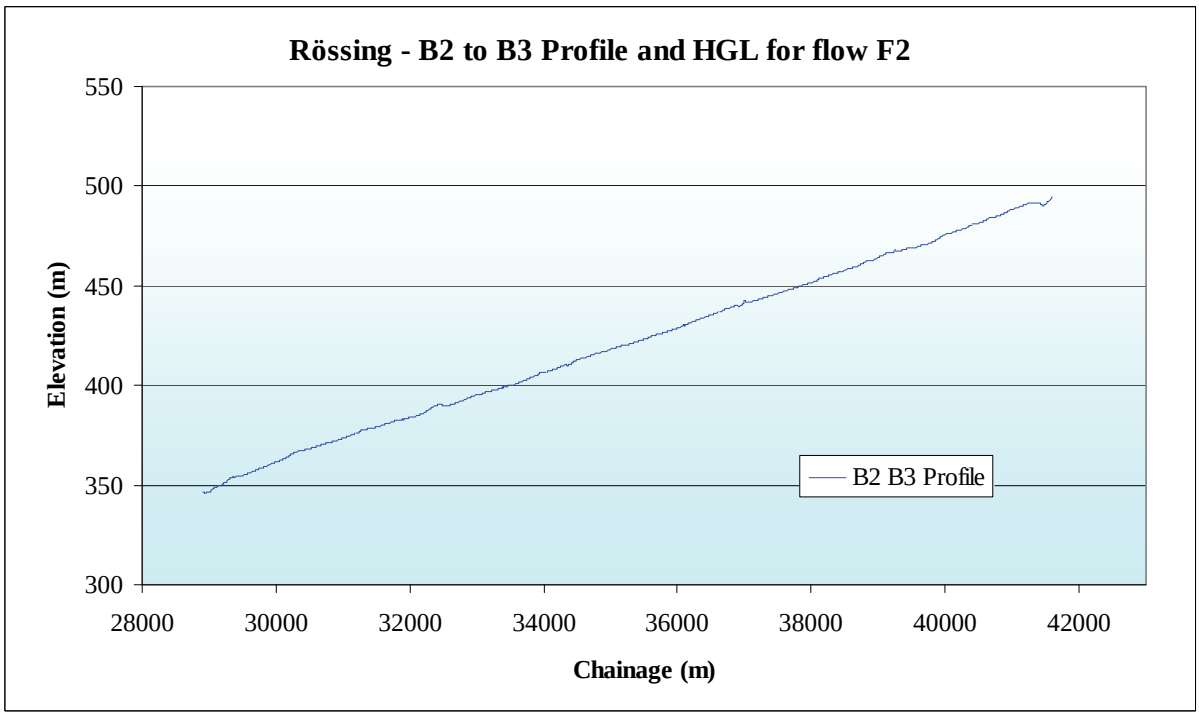

Figure 4.12: Longitudinal profile of the first section of the Rössing Pipeline (Booster 2 to Booster 3)

Figure 4.13 reflects some details of the pump layout in the Booster Station 2.

Figure 4.13: Pumps in the Booster Station 2 – water supply to Rössing Mine

4.8.3 Details of the pressure recording positions

Table 4.6 provides details of the surveyed details at the gauging positions. Both sides of the air valve chamber were surveyed. It is assumed that these levels refer to the crown of the pipeline [(1)]. The elevation at the air valve was then assumed to be the average values of the surveyed levels on the crown of the pipeline, taken on the upstream and downstream side of the valve chambers/rooms.

Table 4.6: Locations of the pressure recording positions

Surveyed point ID	Reference ID	Elevation (masl)	Chainage (m)
bs3-455-1 and 457-2	R1	396,485	33 031,982
bs3-1134-2 and 1135-2	R2	468,958	39 255,434
bs3-1258-2 and 1259-2	R3	481,738	40 392,709

From the data provided in **Table 4.6**, the elevation of the recording position was assumed to be level on the crown of the pipe at the air valve.

Figure 4.14 illustrates a typical installation of the pressure transducers.

Figure 4.14: Pressure recording position R1 (Chainage 33 031,98 m)

Table 4.7 reflects more details of the recording positions.

Table 4.7: Details of the recording positions on the Rössing Pipeline

Coordinates		Recording position	Reference positions	Elevation (m)	Chainage (m)	Installation above pipe crown (m)
South	East					
22º 43' 075"	14º 37' 323"	R1	bs3-455-1 and 457-2	396,485	33 031,982	0,924
22º 44' 673"	14º 40' 662"	R2	bs3-1134-2 and 1135-2	468,958	39 255,434	0,966
22º 46' 016"	14º 44' 332"	R3	bs3-1258-2 and 1259-2	481,738	40 392,709	0,914

Figure 4.15 indicates the positions of the recording positions on the longitudinal profile between Booster 2 and Booster 3.

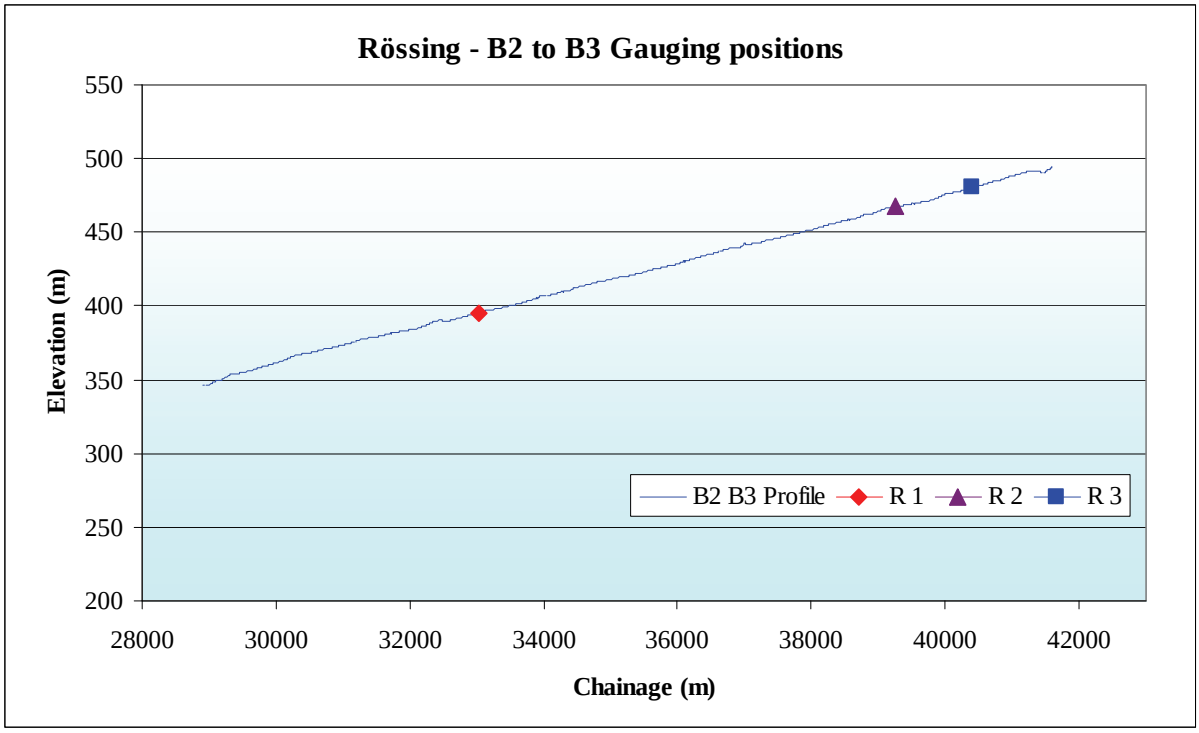

Figure 4.15: Positions of the recording positions along the Rossing Pipeline – Booster 2 to Booster 3

4.8.4 Position of the flow recording

The flow rate from the Base Pump Station and the flow rate into the terminal Reservoir at Rössing Mine is recorded and displayed in the Control Room in the Base Pump Station (Swakopmund). The flow rate between Booster 2 and Booster 3 was measured using the Fuji Clamp-on Ultrasonic Flow Meter as illustrated in **Figure 4.16**.

Figure 4.16: The flow measurement on the Rössing Pipeline using a Fuji clamp-on Ultrasonic Flow Meter

4.9 Pressure recording positions on the Langer Heinrich Pipeline Pipeline (Namwater)

4.9.1 Introduction

The water supply to the Langer Heinrich Mine on the West Coast of Namibia consists of an above ground pipeline installation over a distance of 82,4 km. Water is pumped from the Base Pump Station (Chainage 0, km) towards the Langer Heinrich Mine. Except for the Base Pump Station near Swakopmund, two booster pump stations are used to overcome the friction – and secondary losses as well as the static head difference of about 570 m.

Figure 4.17 indicates typical details of the installation, while the main features of the Langer Heinrich Pipeline are summarized in **Table 4.8**.

Figure 4.17: Above ground installation with profile following the topography – Langer Heinrich Pipeline

Table 4.8: General details of the Langer Heinrich Pipeline

Parameter	Value	Units
Total length	82 500	m
Elevation difference	588,8	m
Pipe Material	Ductile Iron	
Material yield strength	420	MPa
Pipe Class	K9	
Coupling System	Spigot and sock	
Unit pipe length	6	m
Outside Diameter (mm)	325	mm
Wall thickness	7,2	mm
Liner (CML) thickness	3,5	mm
Internal Diameter (calculated)	303,6	mm
Number of pumps in the Base Station	5	
Number of booster stations	2	

4.9.2 Longitudinal details of the Langer Heinrich Pipeline

Figure 4.18 and **Figure 4.19** respectively indicate the total longitudinal profile of the Langer Heinrich Pipeline and the section between the Base Station and Booster 1.

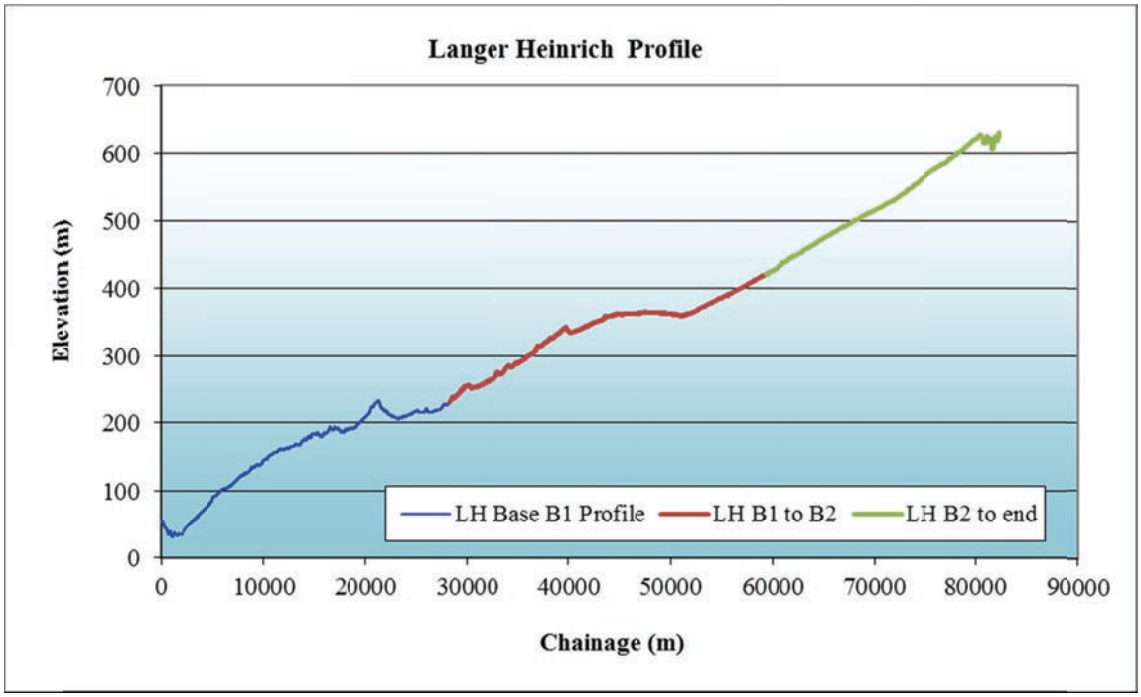

Figure 4.18: Longitudinal profile of the Langer Heinrich Pipeline

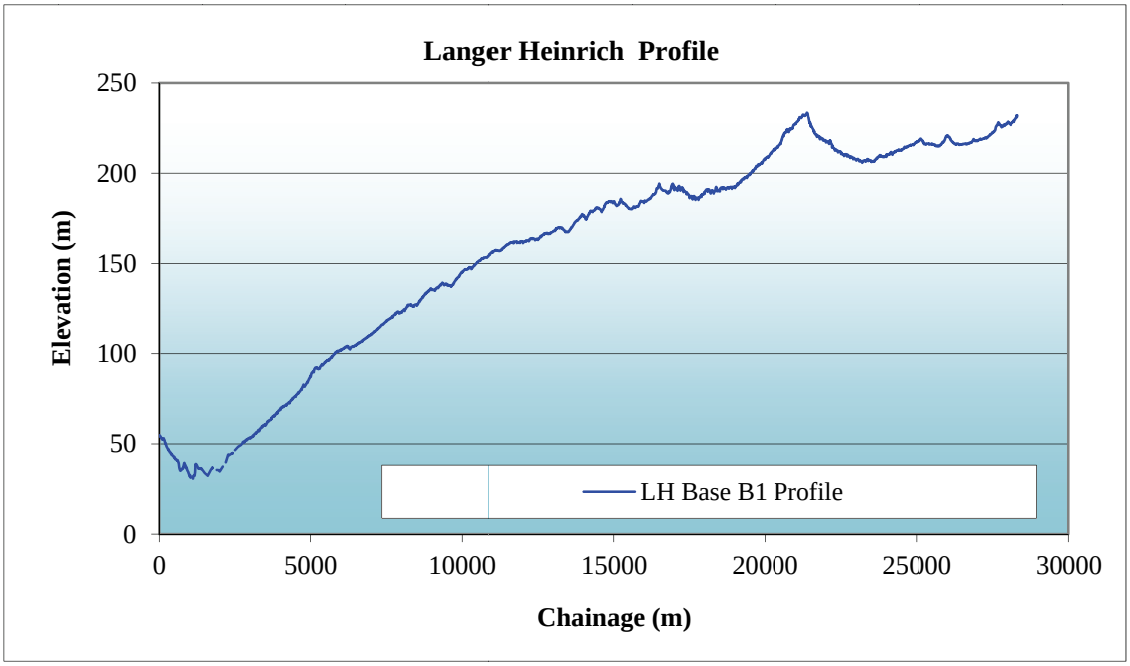

Figure 4.19: Longitudinal profile of the first section of the Langer Heinrich Pipeline (Base Pump Station to Booster 1)

Figure 4.20 and **Figure 4.21** provide information of the pump layout in the Base Station and a general view of the Booster 1 Station.

Figure 4.20: Pumps in the Base Pump Station delivering to Langer Heinrich Mine

Figure 4.21: General layout view at Booster 1 – Langer Heinrich Pipeline

4.9.3 Details of pressure recording positions

The purpose of the pressure recordings is to obtain the characteristic behaviour of the Langer Heinrich Pipeline under different steady state operating conditions. A selection of the pressure recording positions was made and the access points were installed by NamWater. The steady state pressures were recorded at these gauging positions.

Table 4.9 reflects details of the recording positions.

Table 4.9: Details of the recording positions on the Langer Heinrich Pipeline

Coordinates		Recording position	Junction	Chainage (km)	Elevation (m)	Installation above pipe CL (m)
South	East					
22º 43' 075"	14º 37' 323"	L1	AV-16	7491,605	118,189	0,856
22º 44' 673"	14º 40' 662"	L2	AV-27	13961,09	177,255	0,910
22º 46' 016"	14º 44' 332"	L3	AV-41	20716,45	224,3525	0,905

The flow rate was recorded on the display in the Base Pump Station (Swakopmund) by the Operator because the external unevenness on the Ductile Iron Pipe is not ideal to accommodate a clamp-on ultrasonic flow meter. The recorded flow was not verified and it is assumed that the flow data is accurate.

Table 4.10 reflects the details of the flow rates for the different operating conditions (Base Station to Booster 1).

Table 4.10: Flow rates from the Base Station to Langer Heinrich Mine for different operating conditions

Flow rate ID	Flow rate (l/s) #	Number of Pumps operational in the Base Station	Date of the test	Time when the flow occurred
F1	16,1	1	28 September 2009	11:47
F2	30,6	2		11:55
F3	43,9	3		12:47

Note:

Instability in the flow rate was experienced

4.9.4 Pressure transducers used during the field tests

The range of the pressure transducers needs to be selected as close as possible to the expected maximum (and minimum) pressures that could be experienced during the field tests. This improves the accuracy of the data recordings.

Table 4.11 reflects details of the pressure transducers that were selected for the different recording positions.

Table 4.11: Summary of the pressure transducers and data recorders that were used during the field measurements

Recording positions ID	Pressure transducer, ID	Range (Bar)	Recording position ID	Accuracy for 12-Bit recording (mm)	Zero reading (mAmp)
L1	3-1	25	L1-1	61,04	3,97
	3-2		L1-2		3,935
L2	A031787/8	16 A	L2-1	36,62	5,058
	6-1	10	L2-2	24,41	3,985
L3	PT2	4	L3-1	9,77	3.925
	PT23		L3-2		3.925

Table 4.12 reflects the details of the data recorders used to conduct the recordings.

Table 4.12: Details of the data recording equipment and installation position of the transducers

Recording positions ID	Air valve ID	Chainage (m)	Elevation (masl)	Recorder position ID	Recorder Type	Accuracy for 12-Bit recording (mm)	Zero reading (mAmp)	Transducer distance above the pipe Centre Line (m)	Elevation of the pressure transducers (masl)
L1	AV-16	7491,605	118,189	L1-1	HOBO	61,04	3,970	0,856	119,045
				L1-2			3,935		
L2	AV-27	13961,09	177,255	L2-1		36,62	5,058	0,910	178,165
				L2-2		24,41	3,985		
L3	AV-41	20716,45	224,3525	L3-1		9,77	3.925	0,905	225,2575
				L3-2			3.925		

4.10 Pressure recording positions on the pipeline from Morgestond Dam to Jericho Dam and the pipeline from Jericho Dam to Onverwaght Reservoir – Usutu State Water (DWA)

4.10.1 Introduction

Two of the pipelines of the Usutu State Water Scheme were reviewed. The pipeline between the Morgenstond Dam and the Jericho Dam (M-J) (**Figure 4.22**) and the pipelines from Jericho Dam, bypassing Kliphoek Booster Pump Station, to Onverwacht break pressure reservoir (J-O) (**Figure 4.23**).

Figure 4.22: Transfer routes of the pipelines from Morgenstond Dam to Jericho Dam (not to scale)

Figure 4.23: Jericho Dam to Onverwacht Reservoir

Pressure recordings were conducted on both the pipelines at three locations along the pipeline. At these positions the appropriate pressure transducers and the data acquisition system were installed to record the pressure data at a frequency of 1 Hz.

Different flow rates were introduced during the recording of the pressures by operating different pump sets or by the partial closure of the pump control valves.

To simplify the reference to the different sections of the pipelines that were included in this investigation, identifications (IDs) were allocated to the pipelines as reflected in **Table 5.2**.

Table 4.13: Identification of the Usuthu State Water Scheme which were reviewed

Pipeline characteristics and identification (ID)						
Start #	**End ##**	**Length (m)**	**Diameter (m)**	**Constructed**	**Refurbished**	**ID**
Morgenstond PS	Jericho Dam	8679.4	884	2003	-	M1-J
		8679.4	888	1964	CML – 1999	M2-J
Jericho Dam PS	Bypass Kliphoek BPS to Onverwacht Reservoir	25146	841.6	1966	CML – 1991	J1-O (Northern)
		25146	850.6	2001	CML – 2007	J2-O (Southern)

Notes:

*PS refers to a Pump Station*

*BPS refers to a Booster Pump Station*

4.10.2 Pressure recordings

Low frequency recordings (1 Hz) of the pressure are sufficient to establish the pressure drop between two measuring points along the pipeline, as long as the flow rate is kept constant during the time of the recording. The pressure data has been recorded at a rate of 1 Hz with HOBO U12 Outdoor 4 channel recorders that were connected to an appropriate pressure transducer.

Table 4.14 and

Table 4.15 respectively provides a summary of the data recording equipment (Boxes) and the pressure transducers that were used to capture data of the Morgenstond to Jericho and the Jericho to Onverwacht pipelines.

Table 4.14: Summary of the data acquisition boxes that were used during the field survey of the Usutu Government Water Scheme (January 2008)

Box	HOBO Serial no	Channel
1	1025537	2,3
2	951316	1,2,3
3	1025536	1
4	893415	1,2

Table 4.15: Summary of the pressure transducers that were used during the field survey of the Usutu Government Water Scheme (January 2008)

Pressure transducer			Filename used to capture the data
Type	**Range(Bar)**	**Serial no**	
Gems	4	PT 2	B2 M2 P2
Gems	4	PT 3	B3 M2 P3
Gems	50	PT 5	J1 J2 P1
Gems	50	PT 19	
Gems	25	Y113023	B2 J1 J2 P3
Gems	25	Y096798	
Gems	5	Y125090	B2 M1 P2
Gems	5	Y125091	
Gems	4	Y1021082	B3 M1 P3
Gems	10	Y125088	B1 M2 P2
Gems	40	Y111336	B1 J1 J2 P2
Gems	40	Y111338	

Details of the positions along the pipelines where the pressure recordings were taken are indicated in **Table 4.16** for the Morgenstond to Jericho pipelines and

Table 4.17 for the Jericho to Onverwacht pipelines.

Table 4.16 Details of the locations where the pressure data was recorded on the Morgenstond-Jericho pipelines

Pipe ID	Position	Box	Chainage (m) #	Transducer gauging elevation (m) ##
M1-J	P1	1	447	1414,80
	P2	2	2749	1448,33
	P3	3	7498	1450,74
M2-J	P1	1	941	1433
	P2	2	4831	1453
	P3	3	7493	1450,74 ###

Note: **#** *The chainage is the horizontal chainage.*

*The elevation was determined from the profile data.*

*The level was assumed to be similar to the invert of M1-J.*

Table 4.17 Details of the locations where the pressure data was recorded on the Jericho-Onverwacht pipelines

Pipe ID	Position	Box	Chainage (m) #	Transducer gauging elevation (m)
J1-O	P1	4	640	1473,76
	P2	1	11000	1537,55
	P3	2	20523	1513,73
J2-O	P1	4	640	1474,03
	P2	1	11000	1538,07
	P3	2	20523	1514,09

Note: # The chainage is the horizontal chainage.

The pressure transducers were all installed on bleed valve situated on the body of the air valve or on the connector piece below the air valve (**Figure 4.24)**.

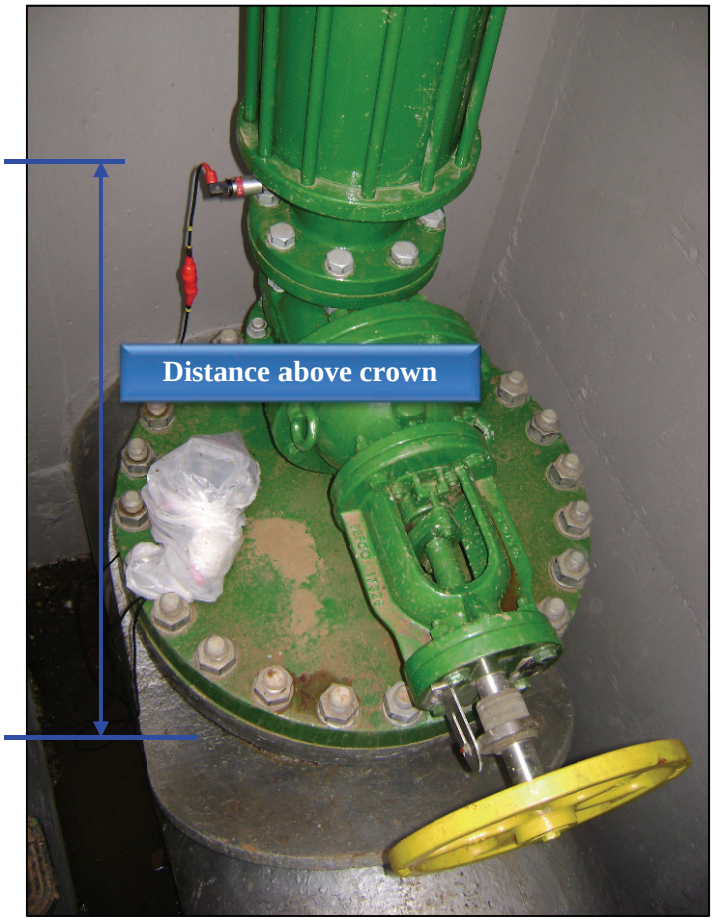

Figure 4.24: Installation of the pressure transducers on the riser underneath the air valve

The relative position of these pressure tapings with regard to the crown of the pipeline differs, necessitating the documentation of the locations of each pressure transducer.

Table 4.18 and

Table 4.19 reflect the installation details relative to the crown of the pipeline for the recordings on the Morgenstond pipelines, while **Table 4.20** reflects the similar details on the Jericho pipelines.

Table 4.18: Installation details of the pressure transducers on the new Morgenstond-Jericho pipeline, M1-J

Variable	**Box 1**	**Box 2**		**Box 3**
Recording channel	2	1	2	1
Launch time	9h02:26	9h06:03		9h10:15
Recording starting time	11h55	12h38		13h00
Recording end time	17h16	17h54	17h54	18h10
Serial no of the transducers	Y096798	Y125090	Y125091	Y1021082
Transducer capacity	25 Bar G	5 Bar G	5 Bar G	4 Bar G
Zero reading at the gauging point	3,98	4,088	3,998	5,703
Data recorder ID	1025537	951316		1025536
Distance above crown of pipe (mm)	890	890		620
Transducer level (masl)	1414,794	1448,334		1450,744
Horizontal Chainage (m)	447,1	2749		7498
Air valve size	200	200		200
Accuracy (m) #	0,061	0,012	0,012	0,0098

Note: # The HOBO system is a 12-bit system resulting in the accuracy that is indicated above.

Table 4.19: Installation details of the pressure transducers on the old Morgenstond-Jericho pipeline, M2-J

Variable	Box 1	Box 2	Box 3
Recording channel	2	1	1
Launch time	6h58:00	7h01:00	7h02:00
Recording starting time	9h20:55	13h16:20	10h48:54
Recording end time	16h30	16h45	16h58
Serial no of the transducers	125088	PT 2	PT 3
Transducer capacity	10 Bar G	4 Bar G	4 Bar G
Zero reading at the gauging point	4,093	4,547	4,228
Data recorder ID	1025537	951316	1025536
Distance above crown of pipe (mm)	570	570	570
Transducer level (masl)	1433	1453	1450,74 ##
Horizontal Chainage (m)	947	4831	7500
Air valve size	400	300	400
Accuracy (m) #	0,024	0,0098	0,0098

Note: # The HOBO system is a 12-bit system resulting in the accuracy that is indicated above.

The level was assumed to be similar to the invert of M1-J.

Table 4.20: Installation details of the pressure transducers on the Jericho Dam to Onverwacht pipelines, J1-O and J2-O

Variable	Box 4		Box 1		Box 2	
Recording channel	1	2	2	3	2	3
Pipeline ID	J1-O	J2-O	J1-O	J2-O	J1-O	J2-O
Launch time	12h16:15 (17/1)		7h37:09		7h39:06	
Recording starting time	12h40:25		9h36:59		10h51:41	
Recording end time	15h05	15h05	15h38	15h38	16h18	16h18
Serial no of the transducers	PT 5	PT 19	Y111336	Y111338	Y113023	Y096798
Transducer capacity	50 Bar G	50 Bar G	40 Bar G	40 Bar G	25 Bar G	25 Bar G
Zero reading at the gauging point	4,429	4,078	3,984	3,989	3,998	3,975
Data recorder ID	893415		1025537		951316	
Distance above crown of pipe (mm)	745	1030	545	1070	730	1090
Transducer level (masl)	1473,745	1474,03	1537,545	1538,07	1513,73	1514,09
Horizontal Chainage (m)	640		11000		20523	
Air valve size	200		200		200	
Accuracy (m) #	0,122	0,122	0,0978	0,098	0,061	0,061

Note: # The HOBO system is a 12-bit system resulting in the accuracy that is indicated above.

4.11 Pressure recording positions on the Hendrina to Duvha Power Station (Eskom/DWA)

4.11.1 Introduction

The Hendrina-Duvha Gravity Main (indicated in red in **Figure 4.25**) is part of the Komati-Usutu GWS which was constructed during 1977/79. The pipeline gravitates water over a distance of about 31,6 km between the Hendrina- and Duvha power stations with an elevation difference of about 33,4 m. The 1397 mm diameter steel pipe is lined with bitumen and coated with bitumen/fibre glass wrapping.

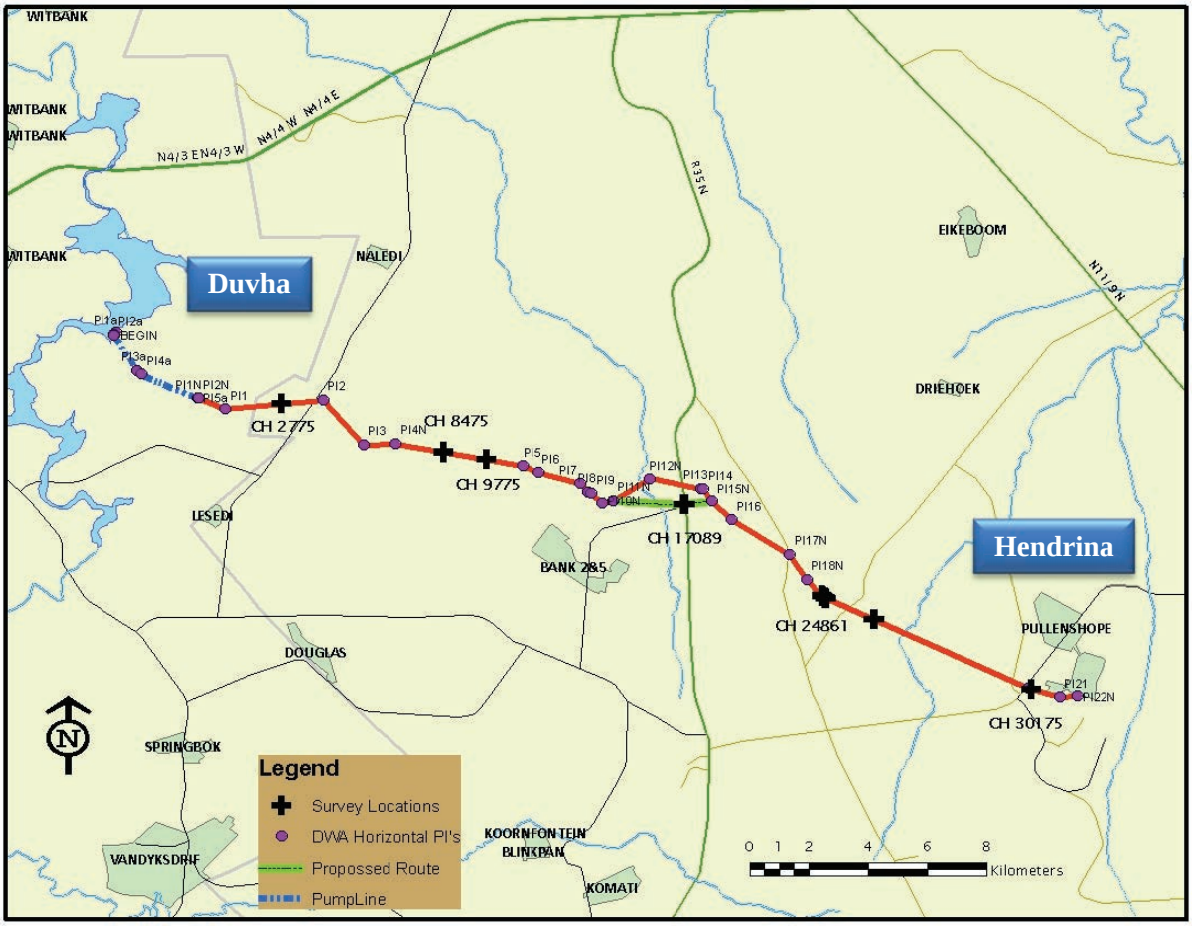

Figure 4.25: Location Map, Hendrina-Duvha Gravity Main X1

The energy head on the Hendrina-Duvha pipeline is regulated at the "distribution box" at the Hendrina power station. Water is fed into the "distribution box" from one or both of the pipelines which flows under gravity from Arnot power station.

Figure 4.26 provides a schematic layout of the gravity supply to the Duvha power station as obtained from Eskom.

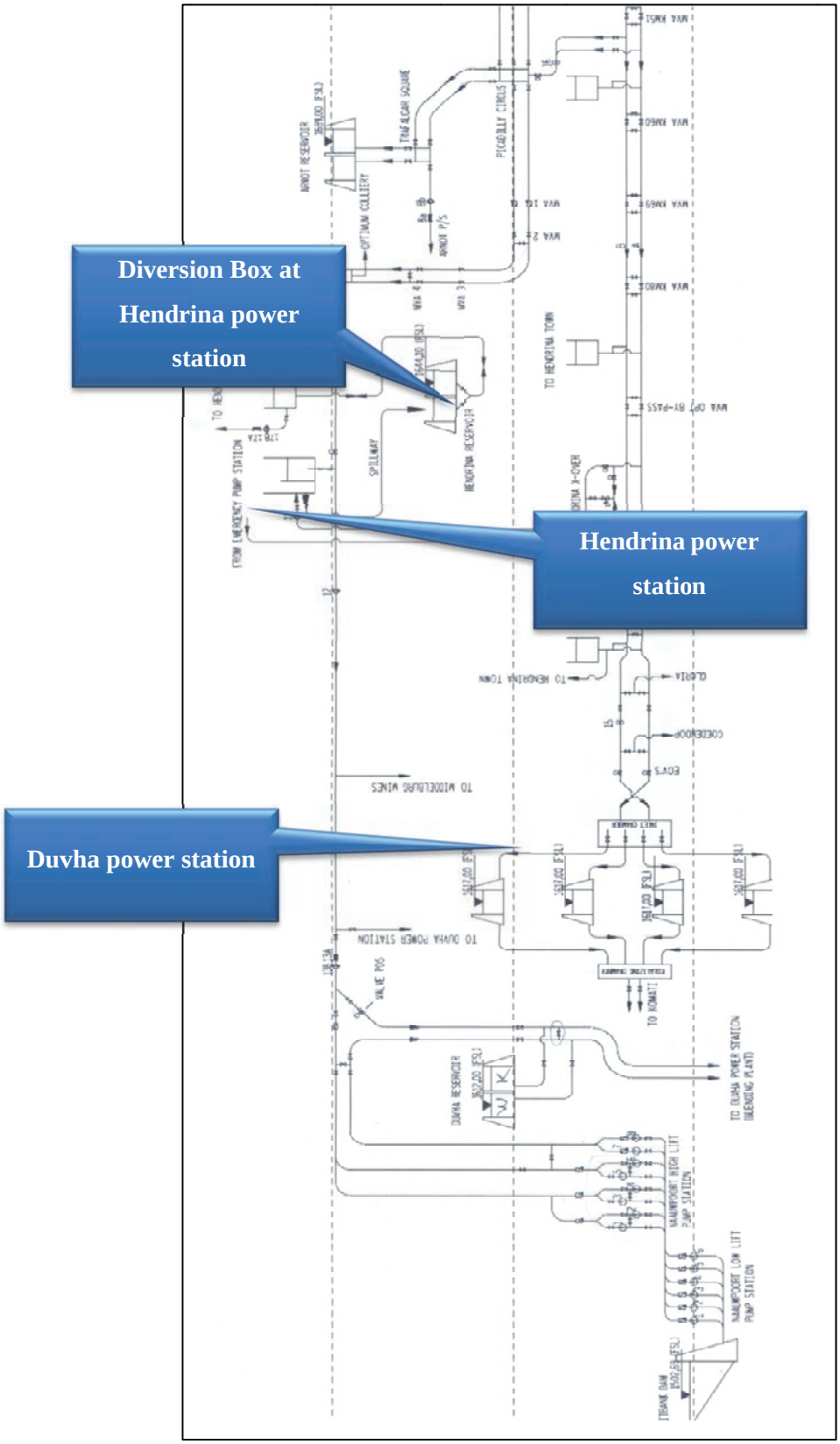

Figure 4.26: Schematic layout of the gravity water supply to Duvha power station

The entire length of 30 963 m of the Hendrina-Duvha Gravity Main consist of a Bitumen coated and lined steel pipeline, with an outside diameter of either 1397 mm or 1420 mm and a wall thickness of either 10 or 12 mm. Different steel grades have been used, ranging from Grade A to Grade C steel. **Although the chainage on a longitudinal profile normally increase along the flow path, the convention used here is that the chainages actually runs from Duvha (Chainage = 0 m) to Hendrina (Chainage 30 963 m).** This could probably be described to the fact that the pipeline was originally designed as a pump line to transfer water from Duvha to Hendrina Power Station.

Information of the pipeline was obtained from the design drawings titled "Komati-Usutu Rivers Link System Government Water Scheme" with Registration numbers 63870/76 to 63880/76. **These drawings were certified during April 1979 as the "As Build Drawings"**.

The Hendrina-Duvha Gravity Main pipeline has apparently not been hydraulically reviewed since the installation of this pipeline in 1979. The current hydraulic characteristics of the pipeline were obtained during field measurements during February and March 2011.

Due to the discrepancy between the elevations (chainage 7 925 m to chainage 11 209 m) obtained from DWA, and Google Earth's version of the elevations it was decided to survey the locations of the pressure recording positions. **Figure 4.27** reflects details of the elevation as recorded by the surveyor on the air valve chamber at chainage 23 291 m from which the surveyed data was obtained. All the pressure measuring points (HD 1 to HD 6) were surveyed. The actual elevations of the pressure recording positions are reflected in **Table 4.21.**

Figure 4.27: Survey equipment and enlargement of the marking on top of air valve chamber, marked by green paint

Table 4.21: Locations where pressure recordings were conducted on the Hendrina-Duvha Gravity Main Pipeline

Measuring point	Maximum pressure (m)[#]	Chainage (m)[##]	Elevation at measuring point (m)*	Coordinates*	
				Latitude	Longitude
HD 1	18,779	30170	1625,321	26° 2'12,13"S	29°35'5,65"E
HD 2	13,415	23620	1630,685	26° 0'32,70"S	29°31'21,99"E
HD 3.1	51,545	17089	1592,555	25°58'49,45"S	29°28'45,26"E
HD 3.2	51,623	17078	1592,477	25°58'49,84"S	29°28'44,74"E
HD 4	32,725	8475	1611,375	25°57'52,78"S	29°24'23,31"E
HD 5	66,012	2775	1578,088	25°57'0,18"S	29°21'25,22"E
HD 6	62,548	1750	1581,552	25°57'3,74"S	29°20'48,10"E

Notes: [#] Maximum static pressure was used to select pressure transducer range

[##] Chainages were obtained from the As Build Drawings

* A detailed survey of the measuring points were conducted by Ian McIlrae Surveyors

4.11.2 Locations where the pressures were recorded on the Hendrina-Duvha Pipeline

Table 4.22 indicates locations (reference chainages) where recording of pressure heads were conducted at different flow rates. All the measuring points were surveyed to obtain an accurate vertical level for each of these pressure recording points (**Table 4.22**). A schematic presentation of the air valve chamber reflecting where height measurements have been measured is illustrated in **Figure 4.28**.

Table 4.22: Calculation of the elevation at measuring points

	Measuring Points						
	HD 1	**HD 2**	**HD 3.1**	**HD 3.2**	**HD 4**	**HD 5**	**HD 6**
Elevation top of chamber(m)	1626,24	1631,92	1593,75	1593,39	1612,66	1579,06	1583,02
Flange to pressure transducers (m)	0,421	0,385	0,385	0,422	0,385	0,423	0,422
Chamber bottom to flange (m)	0,29	0,37	0,42	0,285	0,33	0,245	0,26
Chamber top to bottom (m)	1,63	1,99	2	1,62	2	1,64	2,15
Measuring point elevation (m)	**1625,321**	**1630,685**	**1592,555**	**1592,477**	**1611,375**	**1578,088**	**1581,552**

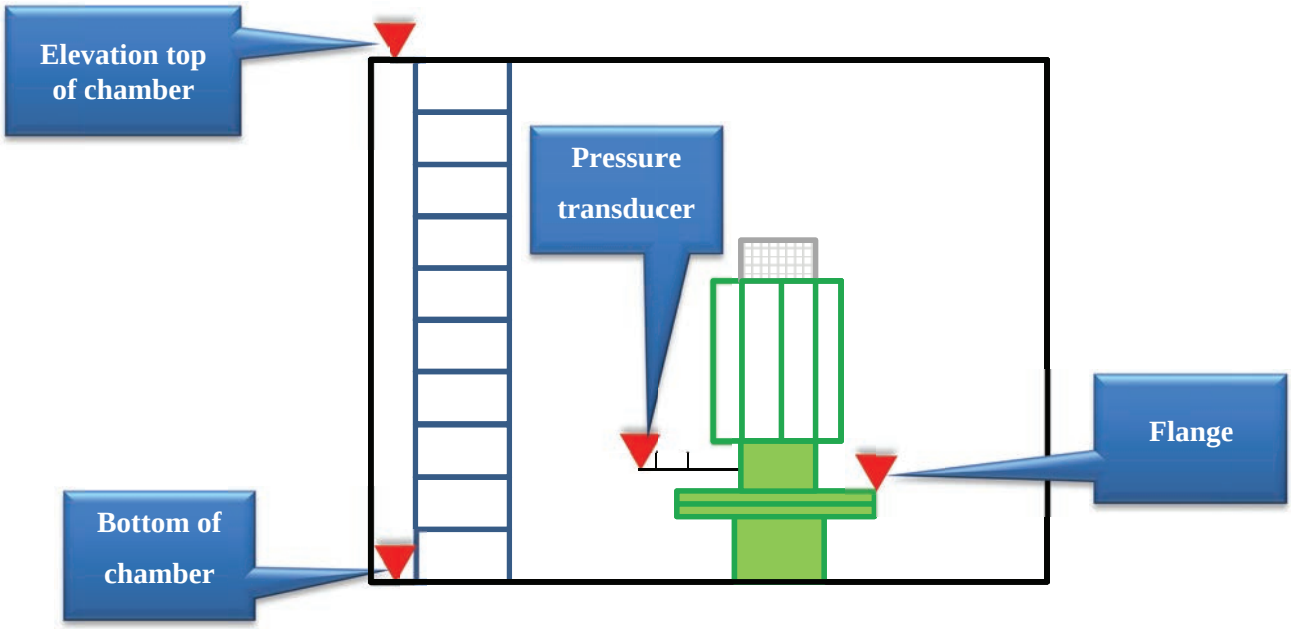

Figure 4.28: Schematic of air valve chamber layout with locations where the elevations were recorded

The locations of these measuring points are shown in **Figure 4.29**.

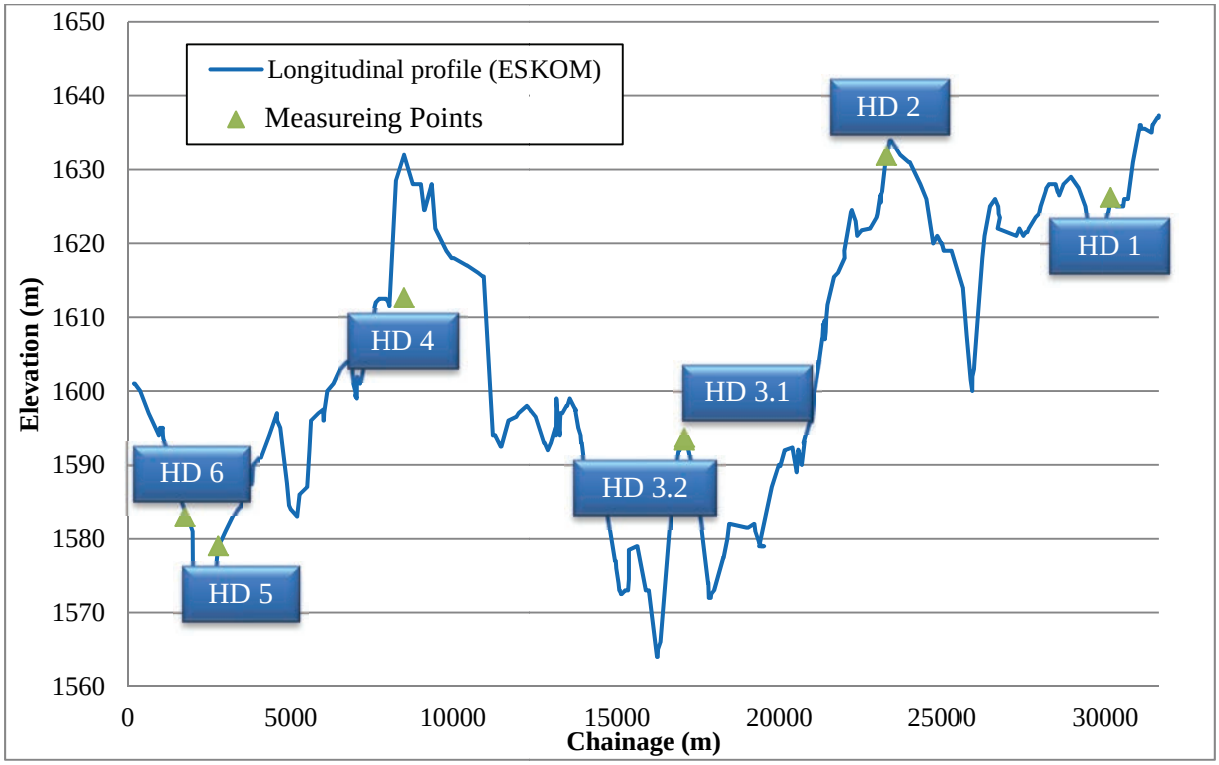

Figure 4.29: Location of measuring points on the Hendrina-Duvha Pipeline

The average horizontal precision obtained in the survey conducted by Mr Ian McIlrae was ±0,03 m and the average vertical precision was ±0,15 m.

4.11.3 Details of the Data recorders used during the assessment of the Hendrina-Duvha Pipeline

The data logger capture the data from the pressure transducer which gives an output signal of between 4-20 mA, which was converted into pressure (measured in bar). The accuracy of recorded pressure measurements at each pressure measuring point is indicated in **Table 4.23** for 8 February 2011 and **Table 4.24** for 3 March 2011.

Table 4.23: Instrumentation detail for the recording of pressures

Pressure recordings conducted on 8 February 2011							
Reference	**Chainage (m)**	**Measuring point elevation (m)**	**Channel 1: Transducer Rating (Bar)**	**Channel 2: Transducer Rating (Bar)**	**Frequency (Hz)**	**Accuracy of recorded pressures (m)**	**Data logger serial number***
HD 1	30170	1625.32	4 A	4 A	0.5	0.01	1025537
HD 2	23620	1630.69	4 A	4 A	0.5	0.01	951316
HD 3.1	17089	1592.56	10 G	10 G	0.5	0.025	784501
HD 3.2	17078	1592.48	10 A	10 A	0.5	0.025	2044486
HD 4	8475	1611.38	4 G	4 G	0.2	0.01	2044485
HD 5	2775	1578.09	16 G	10 A	0.5	0.025	784505
HD 6	1750	1581.55	10 A	10 A	0.5	0.025	784504

Note: *The data loggers are all 12 bit loggers

Table 4.24: Instrumentation detail for the recording of pressures

Pressure recordings conducted on 3 March 2011							
Reference	**Chainage (m)**	**Measuring point elevation (m)**	**Channel 1: Transducer Rating (Bar)**	**Channel 2: Transducer Rating (Bar)**	**Frequency (Hz)**	**Accuracy of recorded pressures (m)**	**Data logger serial number***
HD 1	30170	1625.32	10 A	4 A	0.5	0.01	1025537
HD 2	23620	1630.69	10 A	4 A	0.5	0.01	784505
HD 3.1	17089	1592.56	10 G	40 G	0.5	0.025	784502
HD 3.2	17078	1592.48	40 G	10 G	0.5	0.025	784501
HD 4	8475	1611.38	10 A	4 A	0.5	0.01	2044486
HD 5	2775	1578.09	25 G	10 A	0.5	0.025	784504
HD 6	1750	1581.55	16 A		1	0.04	2044485

Note: *The data loggers are all 12 bit loggers

4.11.4 Flow measurement on the Hendrina-Duvha Pipeline

The flow was measured in the culvert of the R35 road crossing ± at chainage 17 210 m, just upstream of measuring point HD 3.1. The ultra-sonic flow meter setup was installed on the pipeline in the culvert as indicated in **Figure 4.31**, the setup and flow metering was conducted by ATLANTA INSTRUMENTS.

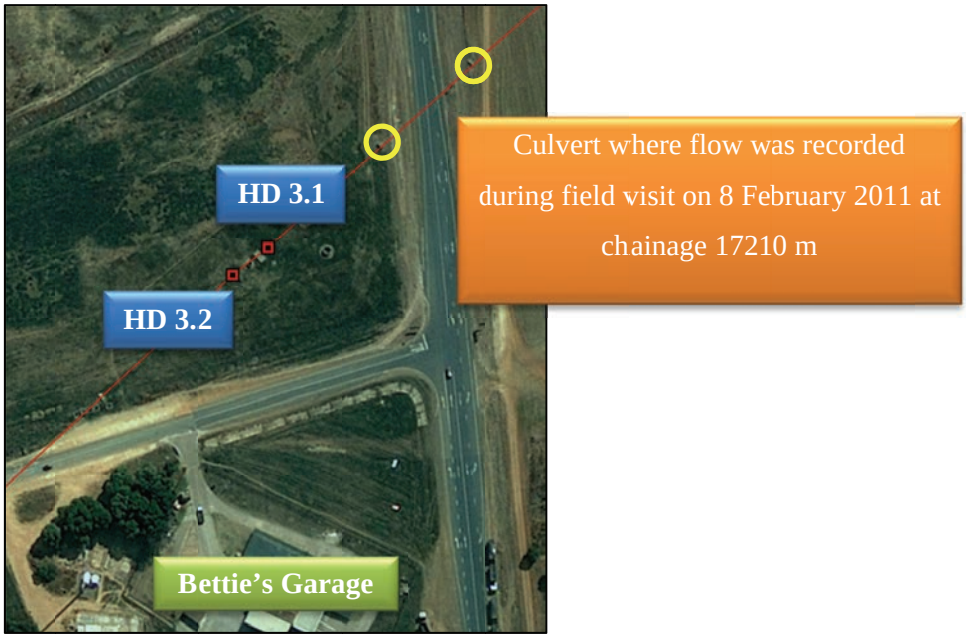

Figure 4.30: Culvert at chainage 17210 m where flow measurements were recorded

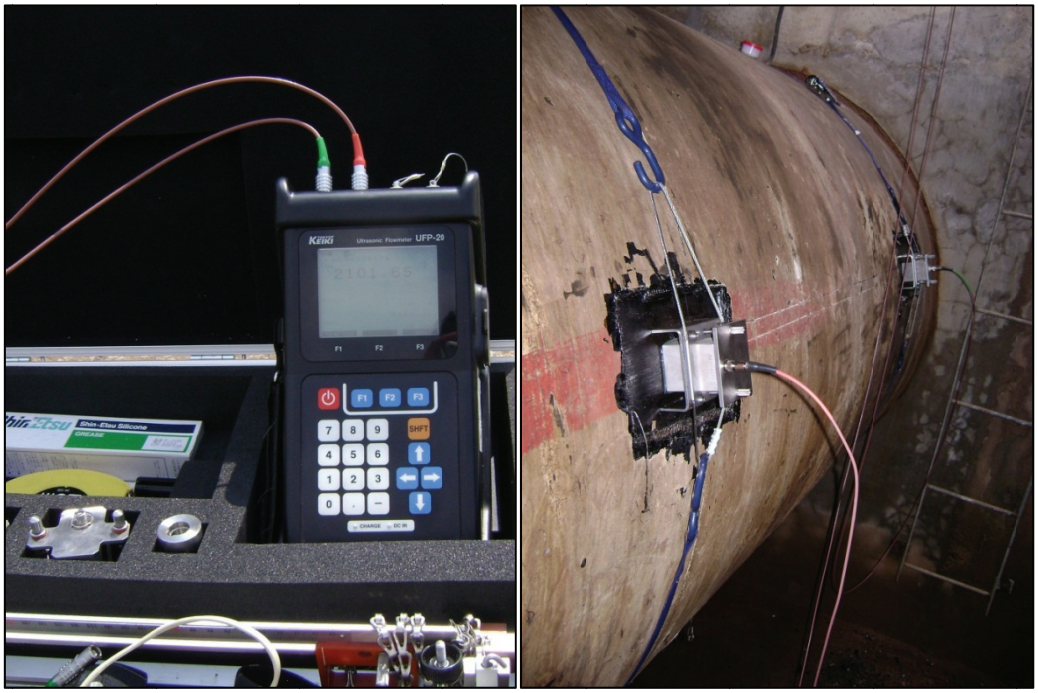

Figure 4.31: Ultrasonic flow meter installation at chainage 17 210 m

Flow recordings were also obtained from the operation staff of ESKOM and compared with the ultra-sonic flow meter's measurements. Head loss calculations were based on the recorded flow measurements from ATLANTA INSTRUMENTS (ultra-sonic flow meter) at times when the flow corresponds to the recorded pressure measurements captured by the HOBO U-12 Data Loggers.

During field visits in February and March 2011, the flow was the controlled by opening and closing of the needle valve situated at the Duvha Power Station.

4.12 Lower Blyde River Irrigation System (Rand Merchant Bank)

4.12.1 Introduction

The Blyderivierspoortdam is the source of water for the Lower Blyde Irrigation System (LBIS). A locality map of the dam is shown in **Figure 4.32**. The LBIS was developed with the following objectives:

- Use the limited water resources optimally by reducing the amount of losses and by following a demand specific control;
- Provide a convenient supply to the consumers;
- Manage the water allocation; and
- Provide a pressurised supply to the consumers (reduction in energy consumption)

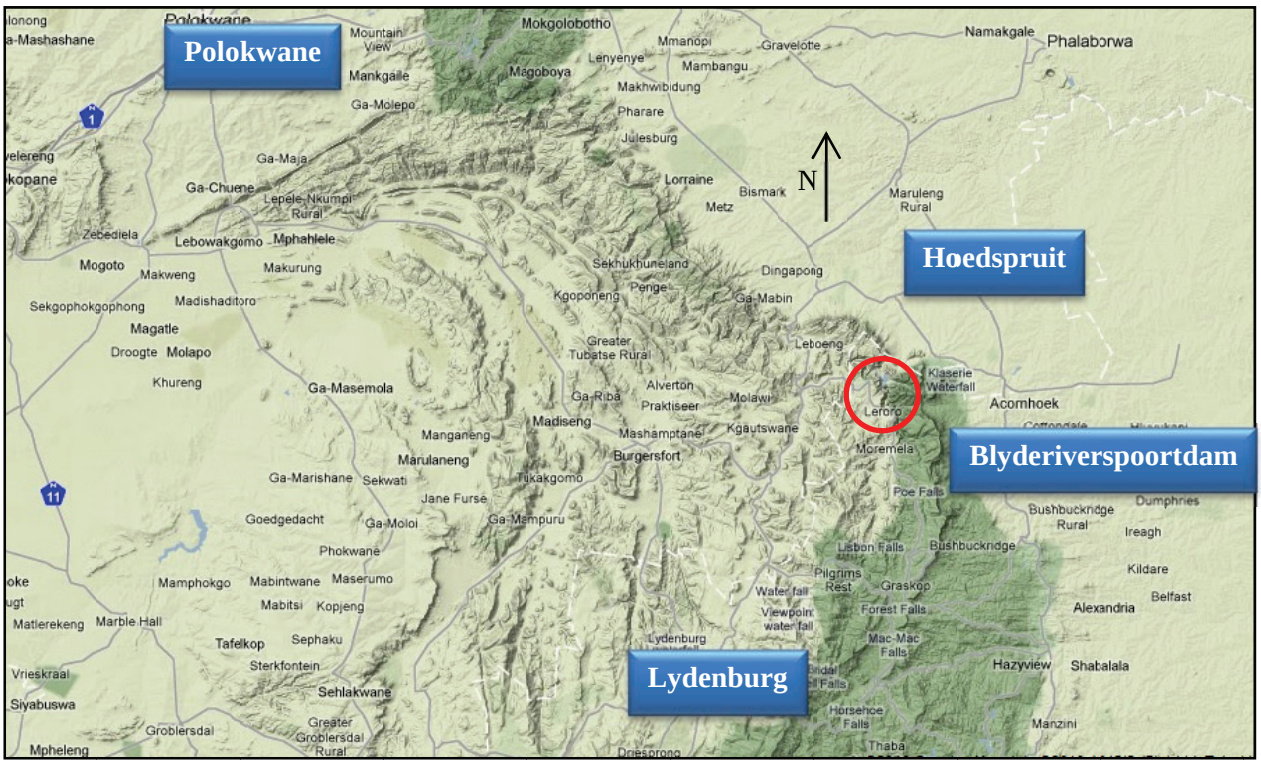

Figure 4.32: Location Map of Blyde River Dam area

The project was financed by Rand Merchant Bank (RMB), who currently owns and manages the system. The scheme consists of about 150 km pipelines, varying in diameter from 1,5 m to 250 mm (some branch lines are 250 mm diameter). The total demand used in the design of the system was based on the crop water requirements and it was estimated to be the peak summer demand would be 4,24 m^3/s.

The capital cost optimization of the distribution network, required the inclusion of pressure zones, generated by control valves to produce the four pressure zones. **Figure 4.33** provides a schematic layout of the Lower Blyde River Irrigation System and the four pressure zones. The total static head across the pressure zones is reduced by 85 m.

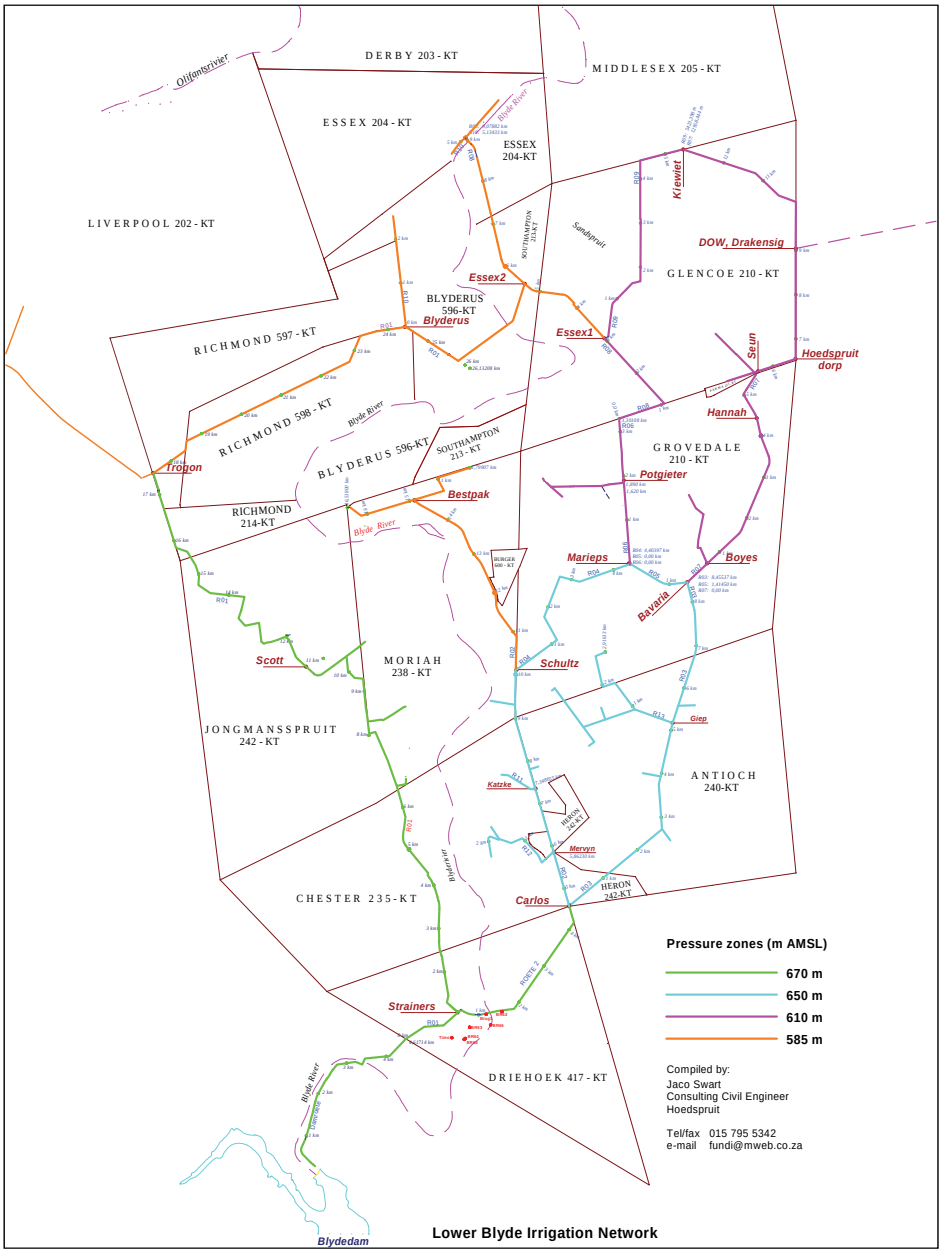

Figure 4.33: Layout of the Lower Blyde River Irrigation Network (Courtesy: Mr Jaco Swart)

Construction commenced in November 1998 and the irrigation network was practically completed by September 2003. The project was never officially commissioned but supply to the consumers commenced towards the end of 2003.

Recently the operator (MBB Consulting Services (Pty) Ltd) (MBB) and end users experienced more-and-more low pressure heads in various locations on the network, but it was specifically notable at the strainers some 6,4 km downstream from the dam release. Currently it is estimated that the maximum instantaneous demand could be as high as 5,6 m^3/s.

Some initial estimates of the pressure drop in the pipe section between the Blyderivierspoort Dam and the Strainers indicated that the loss in pressure (effective roughness) is much more than what would have been expected. **Figure 4.34** reflects these findings graphically.

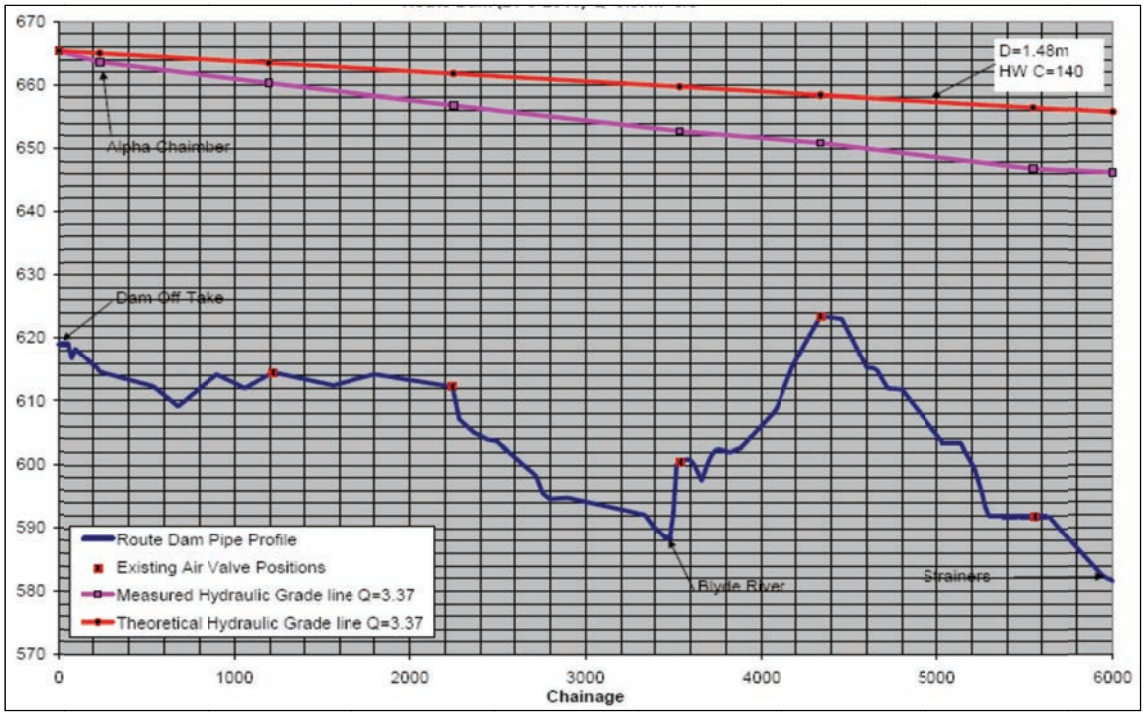

Figure 4.34: Initial findings of the assessment of the hydraulic capacity by MBB

4.12.2 Objectives of the field work conducted on a section of the LBIS

Based on the operational experience it was agreed that the field investigation would have to assess the hydraulic characteristics of the pipeline between Blyderivierspoort Dam and the Strainers, and secondly to review the fouling status of the pipeline.

The objective of the field work was therefor to:

- Conduct the required pressure and flow gauging to be able to determine the current effective roughness of the system between chainage 242 m and 6300 m;
- Conduct an internal inspection to review the status of the pipeline; and
- Measure the thickness of the biofilm.

4.12.3 Location of the pressure recordings on the pipeline between the Blyderivierspoort Dam and the Strainers

In order to establish the change in the hydraulic capacity of the pipeline the current hydraulic capacity must be established and compared with the commissioned hydraulic capacity of 2003. Hydraulic capacity assessment requires the compilation of an energy balance along the pipeline. The pipeline elevation, pressure head, flow velocity and energy losses are quantified to give a complete picture of the hydraulic status of the pipeline. A longitudinal section of the pipeline is used as the basis for quantifying the *elevation* along the pipeline. *Pressure head* were recorded at four locations along the pipeline in the pipeline, reflected in **Figure 4.24.** Details of the recording equipment are also shown in **Figure 4.24**.

Table 4.25: Details of pressure recording positions and recording equipment

Gauging point	Chainage (m)	Elevation (m)	Hobo data logger, ID	Transducers installed on the Hobo logger					
				Channel 1			Channel 2		
				Number	Range (Bar)	Zero reading	Number	Range (Bar)	Zero reading
B1	239/242	619.579	2044485	B064666	10 A	5.56	B064667	10 A	5.624
B2	1197	619.441	784501	None			A031788	16Bar A	4.944
B3	3536	605.841	951316	B064668	10 A	5.52	None		
B4	6000	586.181	2044486	A031786	10 A	5.432			

The field tests were conducted on the 24 and 25 July 2010 during which time the Blyderivierpoort Dam spilling, (**Figure 4.35**).

Figure 4.35: Spilling Blyde River dam

4.12.4 Flow recording during the field tests conducted on the pipeline between the Blydepoortpoort Dam and the Stariners

The LBIS pipeline is equipped with a flow meter. It was however agreed that during the field work the flow rate will also be recorded by the Research Team. The flow meter was installed on a rocker pipe just downstream from the Dam at chainage 120 m. The flow rate was recorded with a PORTAFLOW (Fuji Electric) Serial number Q1A5441T, Ultrasonic Flow Meter. The flow data was recorded every 5 seconds.

Table 4.26 reflects the details of the flow meter installation.

Table 4.26: Dimensional parameters of the LBIS Pipeline, PORTAFLOW pipe parameters

Variable	Rocker pipe
Pipe material	Steel (Spiral welded)
Outside diameter (mm)	1480
Wall thickness (mm)	11
External coating	Bitumen Fiber wrapping
Internal liner	Epoxy paint (300 micron)
PORTAFLOW sensor spacing (mm)	1244,5
Sensor Type	FLD51/FLW51

Figure 4.36 shows the V-type installation for PORTAFLOW Ultrasonic Flow Meter a typical installation of one of the sensors.

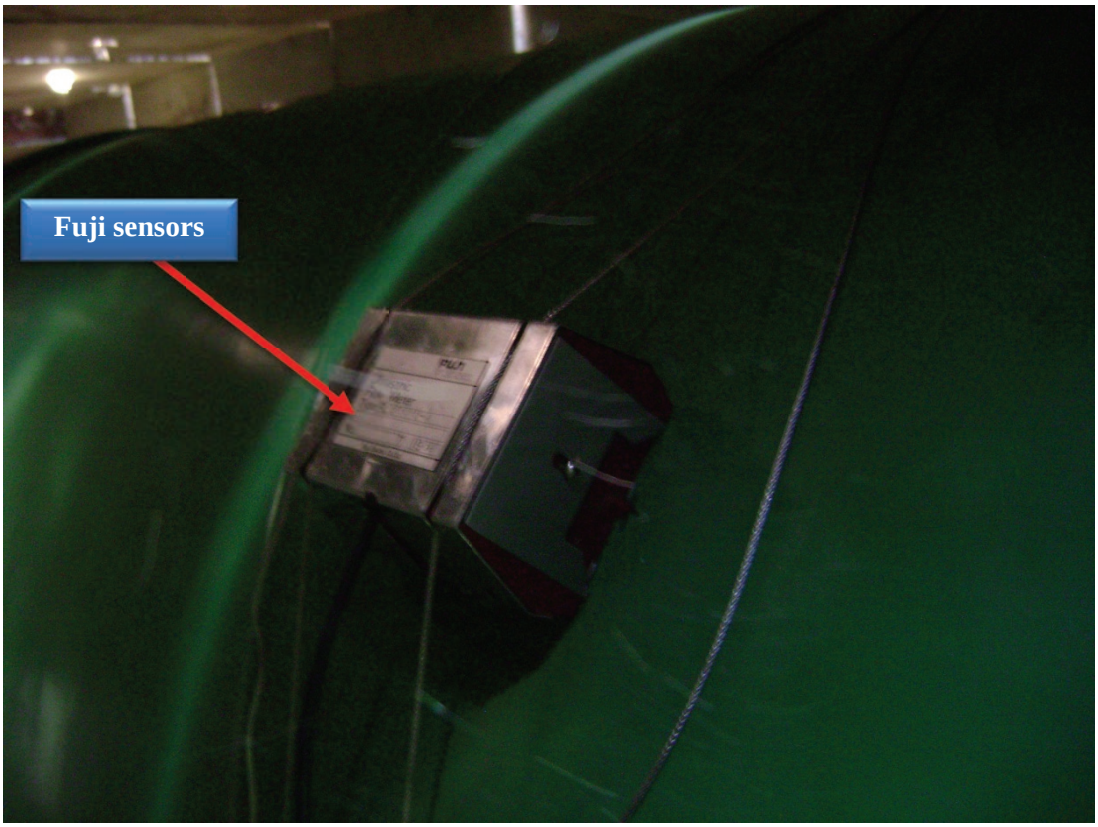

Figure 4.36: Typical details of the Fuji sensor installation

The flow rate data reflected in **Table 4.27** was also recorded by the SCADA system which correlated well with the recorded data obtained by the Research Team.

Table 4.27: Flow rate data by LBIS SCADA system

Status	Q (m^3/s)	Pressure at Strainers (US gauge) (m)
Scour + 1 Strainer Open	2.85	66
Scour + 2 Strainers Open	4.1	54
Scour + 3 Strainers Open	5.1	41
Scour + 3.5 Strainers Open	5.45	35.5

The system was isolated at the Strainers (chainage 6300 m) and flow was introduced in the pipeline section between the dam and the strainers by opening the scour valves on the strainers. **Figure 4.37** reflects the discharge through 3 of the strainers.

Figure 4.37: Three scour valves at the strainer open

4.12.5 Reviewing the fouling status in the Lower Blyde River Irrigation System

Access to the pipeline at chainage 4340 m was possible after the pipeline was isolated and drained slowly, **Figure 4.38**.

Figure 4.38: Air valve removed to obtain access at chainage 4340 m

5 Hydraulic analysis

5.1 Introduction

In the following sections the roughness in the pipelines which were identified in Chapter 4 are reviewed.

5.2 De Hoek to Uitkijk Pipeline

5.2.1 Recorded pressure data in the De Hoek to Uitkijk Pipeline

Recordings from both these pressure transducers were captured on a data logger, which measured the pressure as milliamps. These values of the current were converted into pressure based on the specific pressure transducers' range installed at the measuring point. As was discussed in paragraph 4.6 pressures were recorded at a number of positions along the De Hoek to Uitkijk Pipeline. At all these pressure tappings positions two pressure transducers were installed on the De Hoek to Uitkijk Pipeline.

The recorded difference in pressure between these two pressure transducers were determined as well as the maximum difference and this is shown in **Table 5.1**.

Table 5.1: Pressure transducer comparisons on the De Hoek to Uitkijk Pipeline

Measuring point	Chamber ID number	Average pressure difference (m)	Maximum pressure difference (m)
DU1	TAV1	0,053	0,100
DU2a	TAV17	0,075	0,190
DU2b	TAV18	0,040	0,651[#]
DU3*	TAV31	-	-
DU4	TAV46	0,082	0,209
DU5*	TAV56	-	-
DU6	TAV69	0,010	0,394
DU7	UITKIJK	0,029	0,395

Notes: * Only a single pressure transducer was connected at this measuring point

[#] Turbulence experienced downstream of the line control valve.

Table 5.2 and **Table 5.3** graphically reflect the calculated hydraulic grade lines (HGL) for the measuring points for the recording period. The HGL is the sum of the recorded pressure at the measuring point plus the measuring point elevation as measured by YMAX Consulting Engineers. These recording periods varies based on the time when the connection point was activated on 16 July 2010.

Each of the graphs, in **Table 5.2** and **Table 5.3** depicting the HGL is the average of the two pressure transducer recordings except for measuring points DU3 and DU5 where only one pressure transducer could be installed.

Table 5.2: Graphical presentation of the HGL at positions DU1, Du2a, Du2b and DU3 on the De Hoek to Uitkijk Pipeline

Recording position	Description		Graphical presentation of recorded data
DU1	Chainage (m)	338,0	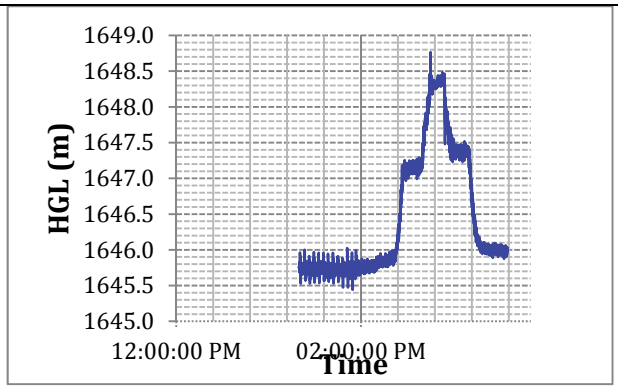
	Elevation (m)	1 635,994	
DU2a	Chainage (m)	10 926,95	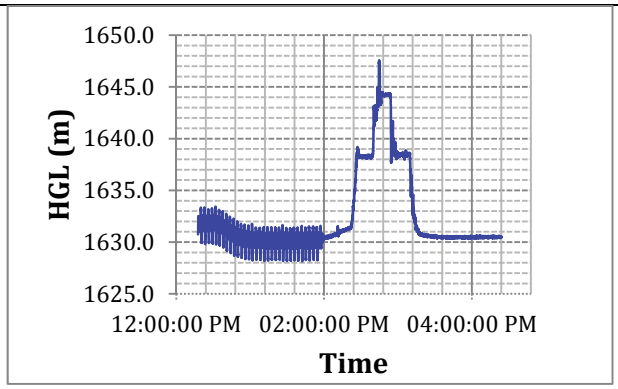
	Elevation (m)	1 540,156	
DU2b	Chainage (m)	10 926,95	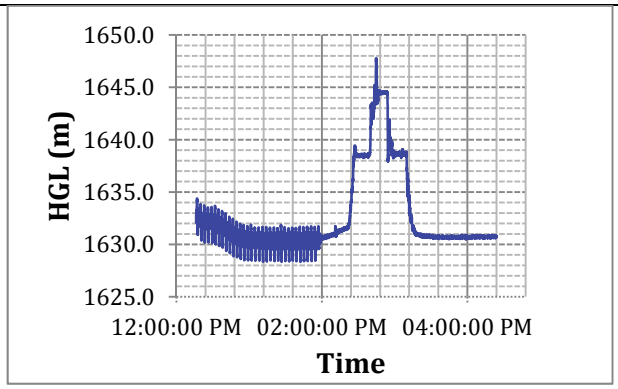
	Elevation (m)	1540,053	
DU3	Chainage (m)	20 066,13	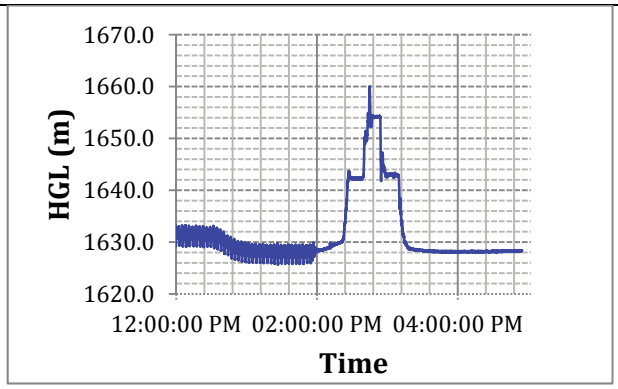
	Elevation (m)	1 528,013	

Table 5.3: Graphical presentation of the HGL at positions DU4, DU5, DU6 and DU7 on the De Hoek to Uitkijk Pipeline

Recording position	Description		Graphical presentation of recorded data
DU4	Chainage (m)	29 490,01	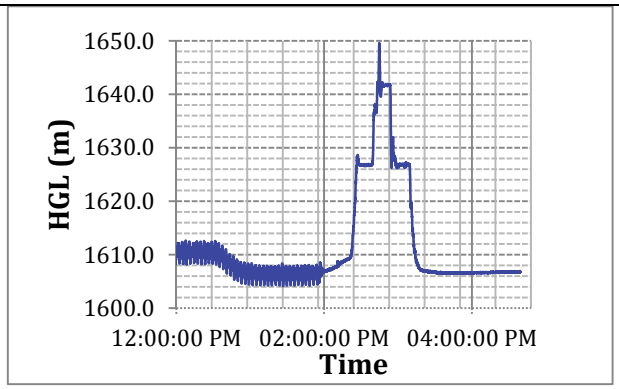
	Elevation (m)	1 569,083	
DU5	Chainage (m)	34 504,75	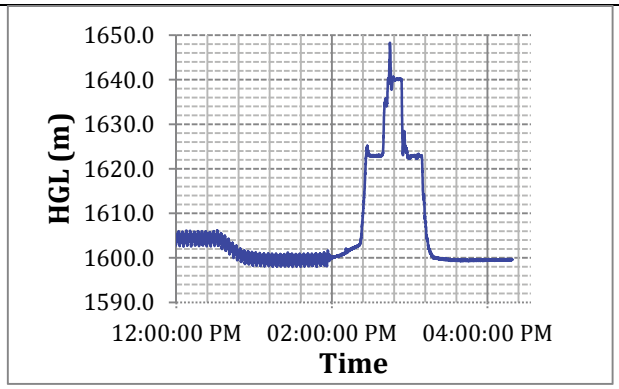
	Elevation (m)	1 576,593	
DU6	Chainage (m)	41 673,41	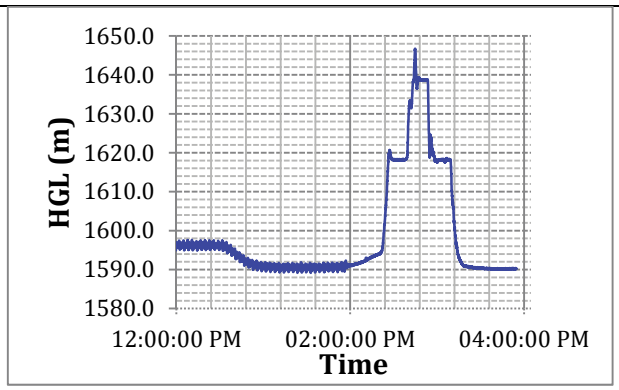
	Elevation (m)	1 546,060	
DU7	Chainage (m)	47 005,95	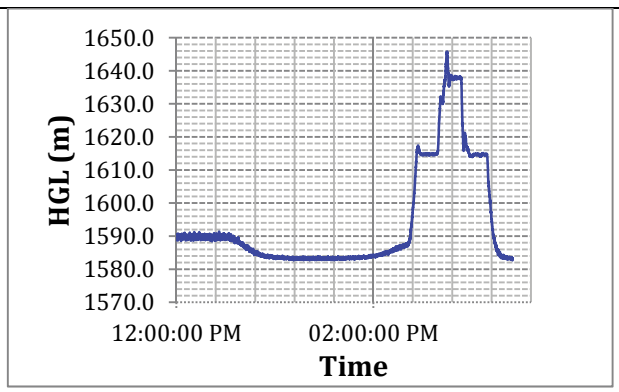
	Elevation (m)	1 576,547	

5.2.2 Flow recordings on the De Hoek to Uitkijk Pipeline

Flow was recorded at a frequency of 0,5 Hz (every 2 seconds) by the project team. The flow data from the MagFlow was electronically recorded by Bloemwater's operational staff at a frequency of 1 per hour. **Figure 5.1** reflects the recorded flow rates in the De Hoek to Uitkijk Pipeline.

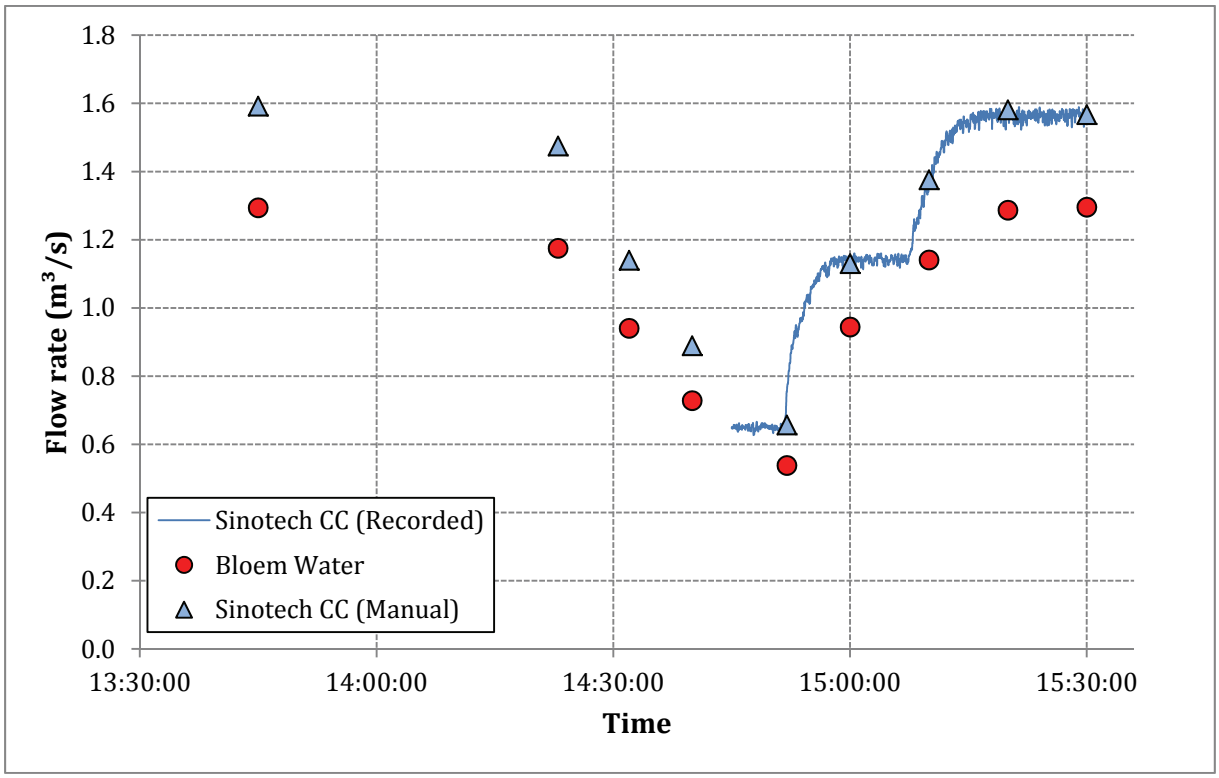

Figure 5.1: Flow data recorded on 16 July 2010

Figure 5.1 reflects that he recorded flow measurements by the Research Team were approximately 20% higher than that measured by Bloemwater.

At DU4 the pressure variation is approximately 4 m as is reflected in **Table 5.3**. Closer to the start and ends of the pipeline these pressure fluctuations are however less. It seems as if this is caused by a disturbance between DU3 (chainage 20 066,13 m) and DU4 (chainage 29 490,01). The disturbance could be for instance a loose butterfly disc or a pressure control valve that "hunts" at one of the off takes (De Wets Dorp off take).

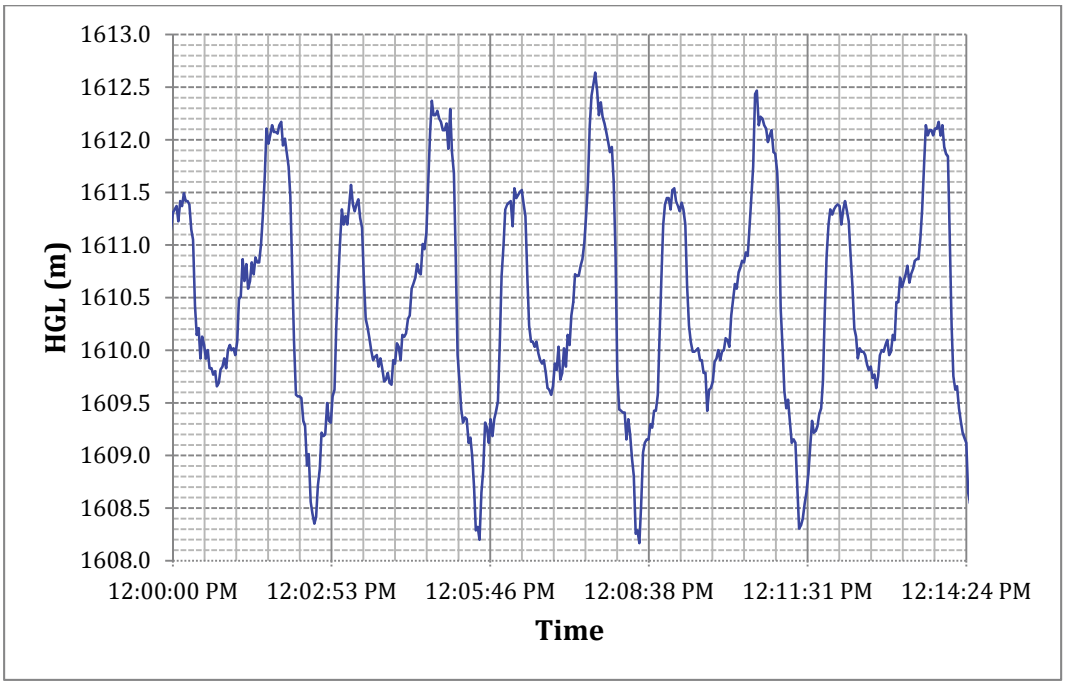

Figure 5.2: Instability in pressure measurements (DU4)

5.2.3 Selection of periods to calculate the roughness in the De Hoek to Uitkijk Pipeline

From the recorded flow and pressure recordings, 5 distinct time periods were selected where pressures and flow could be compared between all the measuring points. These 5 periods are at times 14:00, 14:30, 14:50, 15:05 and 15:30 where stable flow and pressure conditions prevailed as shown in **Figure 5.3**.

Table 5.4 provides a summary of the recorded pressures and flows at the selected time periods. The pressure and flow values shown in **Table 5.4** were obtained by calculating an average pressure or flow where possible over at least a 2 minute period.

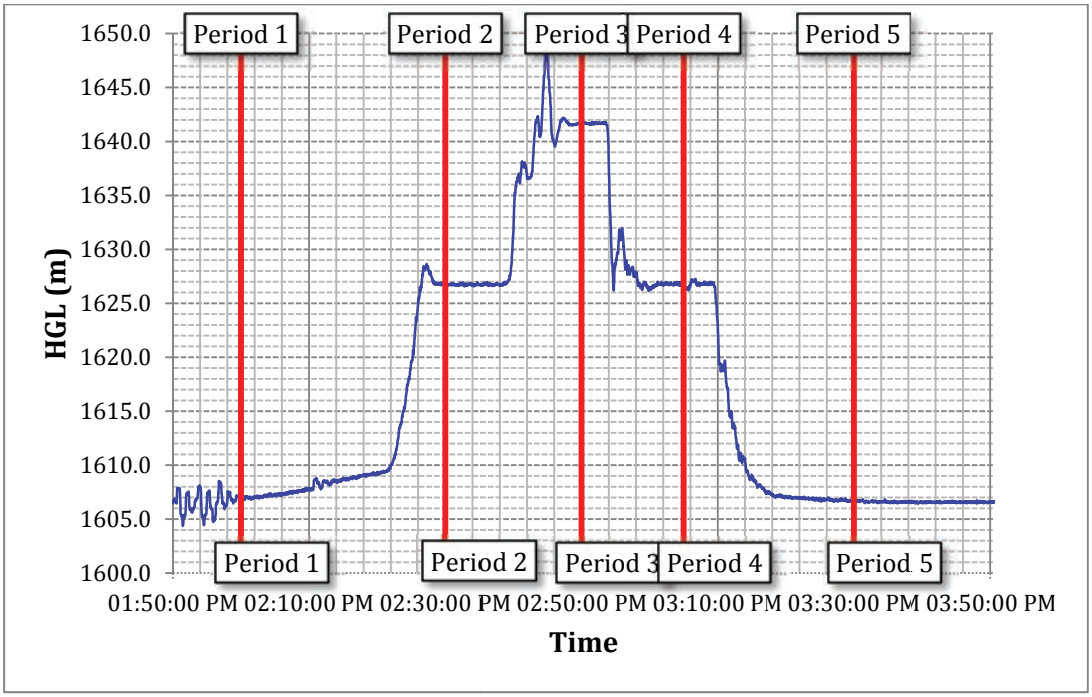

Figure 5.3: Selected time periods (shown at DU4)

Table 5.4: Summary of recorded hydraulic grade lines at the pressure recording positions on the De Hoek to Uitkijk Pipeline

		Period 1	**Period 2**	**Period 3**	**Period 4**	**Period 5**
		16 July 2010 ±14:00	**16 July 2010 ±14:30**	**16 July 2010 ±14:50**	**16 July 2010 ±15:05**	**16 July 2010 ±15:30**
Measuring point	**Chainage (m)[##]**	**Hydraulic grade line level (m)**				
		Flow rate (l/s)				
		1 592,0	**1 140,0**	**649,8**	**1 142,1**	**1 564,4**
		Velocity (m/s)				
		1,485	**1,063**	**0,606**	**1,065**	**1,459**
DU1	**338,02**	1645,759	1647,133	1648,317	1647,368	1645,995
DU2a	**10 926,95**	1630,428	1638,184	1644,145	1638,352	1630,524
DU2b	**10 926,95**	1629,995	1637,773	1643,758	1637,935	1630,093
DU3[#]	**20 066,13**	*1628,349*	*1642,254*	*1654,220*	*1642,906*	*1628,336*
DU4	**29 490,01**	1606,955	1626,724	1641,764	1626,798	1606,626
DU5	**34 504,75**	1600,129	1622,911	1640,078	1622,891	1599,566
DU6	**41 673,41**	1591,114	1618,198	1638,906	1618,287	1590,348
DU7	**47 005,95**	1584,005	1614,700	1638,010	1614,581	1583,271

Notes: # This measuring point had only one pressure transducer connected to it. There seems to be an error in the data set with all the pressures being ±9,7 m too high. This data set was discarded.

Chainages were obtained from the Tender Drawings

The data in **Table 5.4** is graphically represented in **Figure 5.4**.

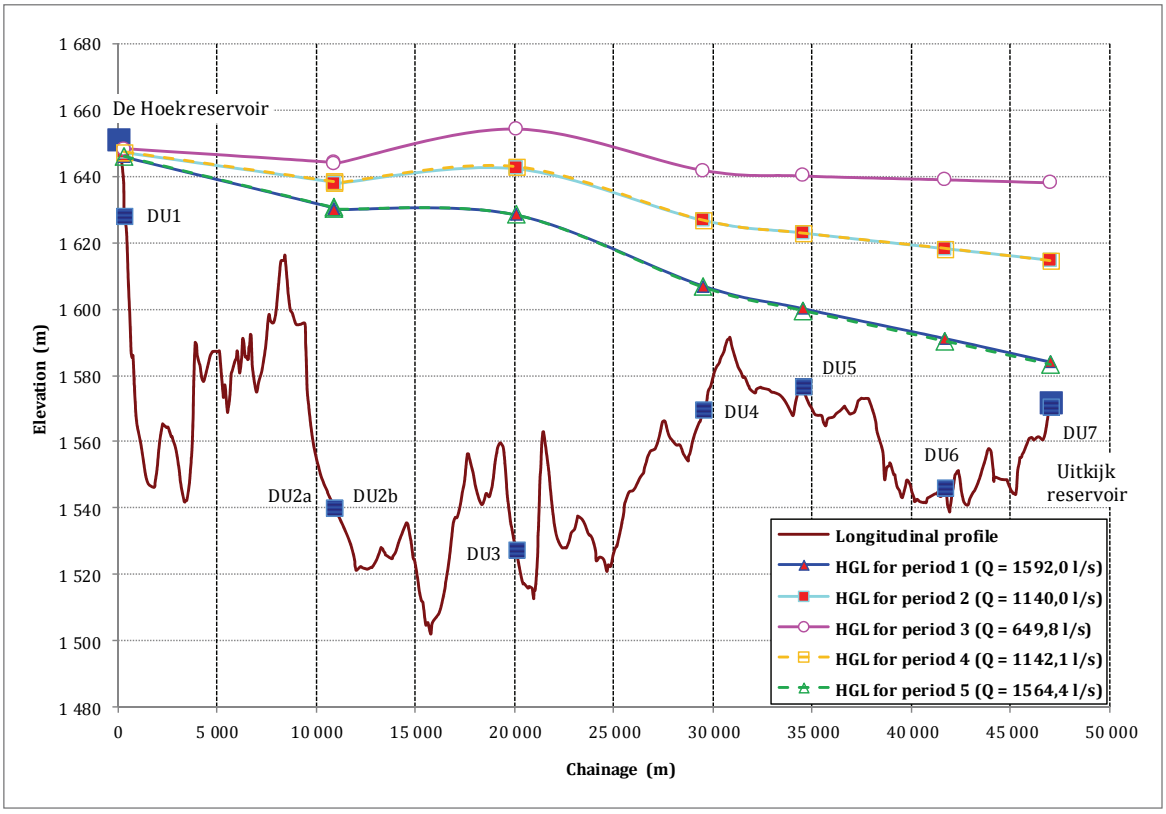

Figure 5.4: Combined graph with hydraulic grade lines

Figure 5.4 depicts the HGLs for different flow rates. Although the HGL values (**Table 10**) were simply connected with straight lines in **Figure 5.4,** it is acknowledged that local losses occurring at the isolating valves are not reflected in **Figure 5.4.** These secondary losses are however incorporated in the recorded HGL values at each of the measuring points.

As indicated in **Table 5.4** the recorded pressures at DU3 were too high and unrealistic and hence this data set was discarded. Without the recorded pressures at DU3, the lines between all the remaining measuring points, as shown in **Figure 5.5** reflected straight hydraulic grade lines.

Pressures recordings at UB2a and UB2b were used to calculate the typical the secondary loss caused by the butterfly (isolating) valve (LCV2). **Table 5.5** indicates the losses from UB2a to UB2b, i.e. across the line control valve 2.

Table 5.5: Secondary losses through line control valve (LCV2)

Period	Period 1	Period 2	Period 3	Period 4	Period 5
Flow rate (m^3/s)	1,592	1,140	0,650	1,142	1,564
Velocity through valve (m/s)	2,426	1,737	0,990	1,741	2,384
Pressure drop (m)	0,433	0,411	0,387	0,417	0,431

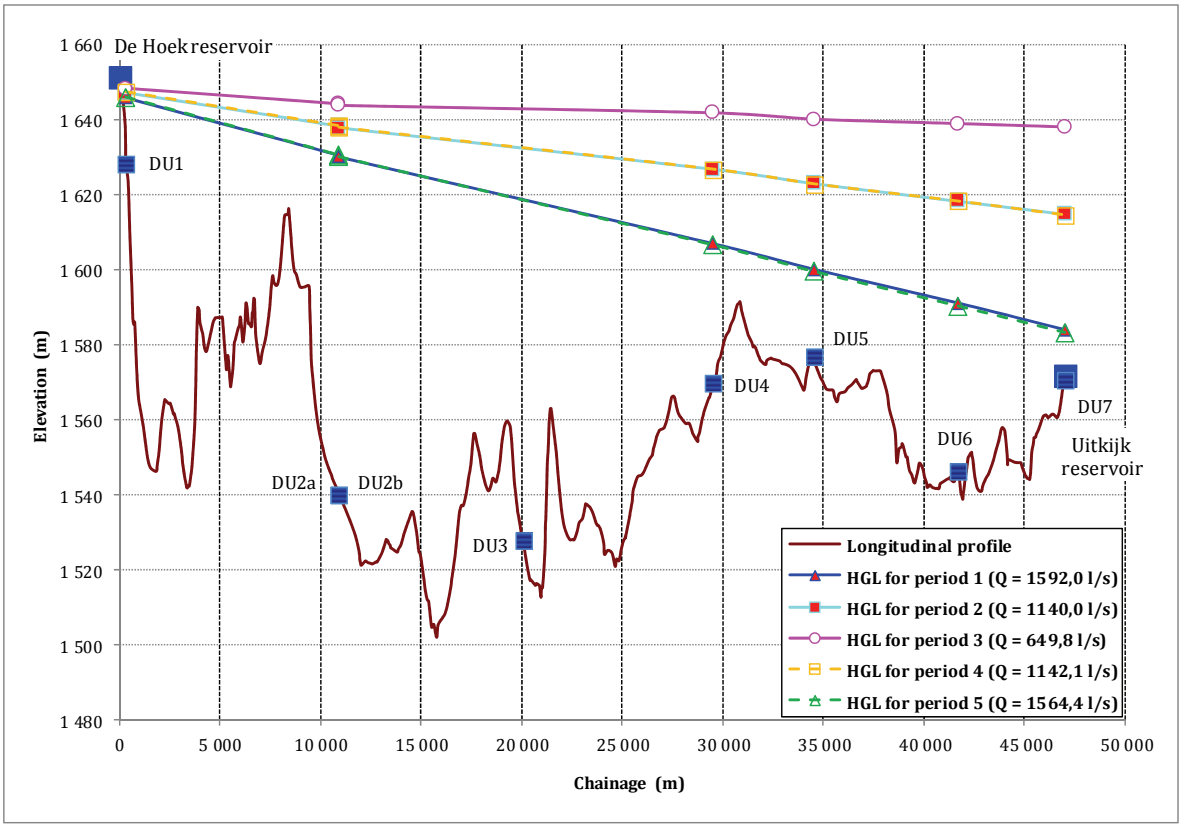

Figure 5.5: Hydraulic grade lines (discarding DU3)

5.2.4 Calculated roughness parameters in the De Hoek to Uitkijk Pipeline

Between measuring point DU1 and DU7 there are 7 isolating valves which cause secondary losses. It was assumed that the secondary losses at the other line control valves will be similar to the loss that was measured across LCV2 (**Table 5.5**). The sum of the secondary losses at all the line control valves were subtracted from the total recorded energy loss between DU1 and DU7 (46 667,9 m). The roughness was then calculated for the different discharge rates without including any additional secondary losses at the directional changes, off takes or air valves (**Table 5.6**).

Table 5.6: Calculated roughness parameters between DU1 and DU7 with provision of secondary losses at the isolating valves

Parameter		Period 1	Period 2	Period 4	Period 5
Measured flow (l/s)		1592,0	1140,0	1142,1	1564,4
Calculated velocity (m/s)		1,485	1,063	1,065	1,459
Re		1 521 797	1 089 729	1 091 737	1 495 414
ΔH (m) – Between DU1 and DU7		61,755	32,433	32,787	62,724
H_L(m) – Total secondary losses		3,033	2,878	2,917	3,016
H_f (m)		58,722	29,555	29,870	59,708
S_f (m/m)		0,00126	0,00063	0,00064	0,00128
Friction factor (λ)		0,01308	0,01284	0,01293	0,01378
Absolute roughness – k_s(mm)	**Kármán& Prandtl**	0,184	0,167	0,173	0,238
	Colebrook-White transition	0,122	0,079	0,086	0,176
	Barr	0,114	0,073	0,080	0,167
	The Moody diagram	0,114	0,085	0,091	0,160
Manning – n ($s/m^{1/3}$)		0,0105	0,0104	0,0105	0,0108
Hazen-Williams – C		139,6	144,9	144,3	136,0

The velocity for Period 3 was low, resulting in friction losses of only 7,6 m. This result in an extremely flat hydraulic grade line and it is subsequently difficult to accurately determine the roughness parameters from the recorded data.

5.3 Uitkijk to Brandkop Pipeline

5.3.1 Introduction

The data loggers, pressure transducers and flow meter were installed on the day of testing. Once all the recording equipment was in place the instruction was given to Bloemwater's operational staff to change the flow rate. The flow remained fairly constant from approximately 12:30 on 14 July 2010. By this time all the equipment has been installed and all the control valves, branches 1 to 5, at Brandkop were open. This resulted in a maximum flow of 1430 l/s. At 16h45 the valves (branches 1 and 2 and then later 3) at Brandkop control station were being closed reducing the flow to approximately 700 l/s. At approximately 17:30 the next branch was closed resulting in a further reduction in the flow. These variations are clearly visible in the recorded data set.

5.3.2 Recorded pressure data of the Uitkijk to Brandkop Pipeline

As described earlier each measuring point was equipped with two pressure transducers. Both these were connected to the same data logger. The logged data, measured as milliamps, were converted into pressure based on the pressure transducers' range.

The recorded difference in pressure between these two pressure transducers were determined as well as the maximum difference and this is shown in **Table 5.7**.

Table 5.7: Pressure transducer comparisons of the Uitkijk to Brandkop Pipeline

Measuring point	Chamber ID number	Average pressure difference (m)	Maximum pressure difference (m)
UB1	TAV1	0,026	0,046
UB2a	TAV12	0,010	0,094
UB2b*	TAV13	-	-
UB3	TAV35	0,025	0,238
UB4*	LIEUWKOP LCV	-	-
UB5	TAV69	0,256	0,969
UB6*	TAV86	-	-
UB7	AIR VALVE AT BRANDKOP	0,012	0,379
UB8	LCV10	0,122	0,700[#]

Notes: * Only a single pressure transducer was connected at this measuring point

\# Measuring point is situated downstream of two 90° bends and on a butterfly valve which causes turbulence resulting in larger pressure differences.

In **Table 5.8**, **5.9** and **5.10** the hydraulic grade lines (HGL) for the measuring points are depicted over the recording period. These recording periods varies and were based on when the connection point was activated during the hydraulic testing on 14 July 2010.

Each of the graphs, in **Table 5.8** depicting the HGL is the average of the two pressure transducer recordings except for measuring points UB2b, UB4 and UB6 where only one pressure transducer could be installed. The recording time starting points at the different measuring points vary due to the fact that the data logging was activated once the installation was completed.

Table 5.8: Graphical presentation of the recorded pressures at UB1, UB2a, UB2b and UB3 on the Uitkijk to Brandkop Pipeline

Recording position	Description		Graphical presentation of recorded data
UB1	Chainage (m)	294,4	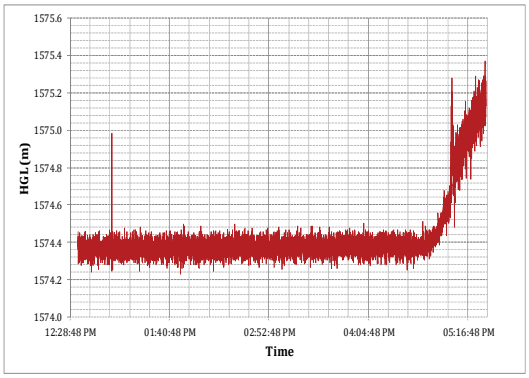
	Elevation (m)	1565,272	
UB2a	Chainage (m)	5875,1	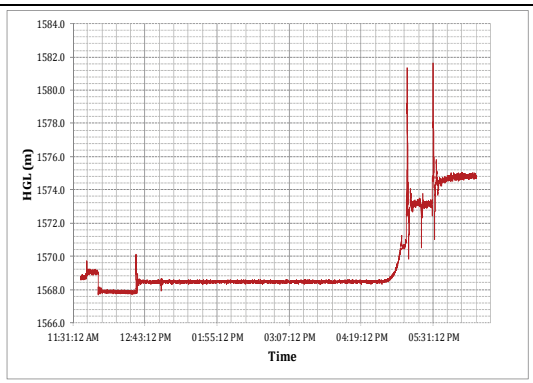
	Elevation (m)	1 533,718	
UB2b	Chainage (m)	5895,1	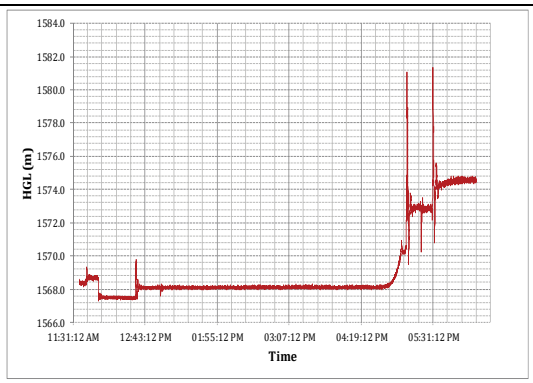
	Elevation (m)	1533,830	
UB3	Chainage (m)	19 626,6	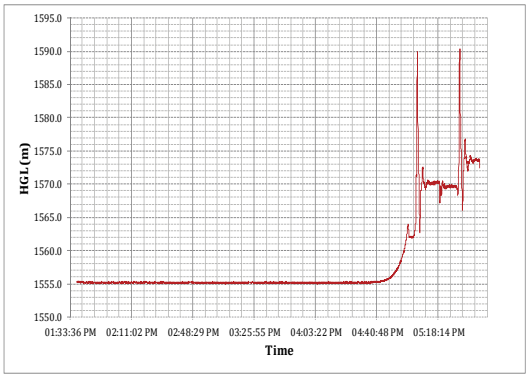
	Elevation (m)	1 498,801	

Recording position	Description		Graphical presentation of recorded data
UB4	Chainage (m)	25 610,1	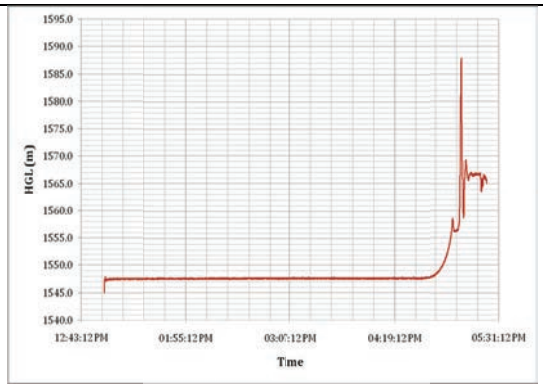
	Elevation (m)	1 452,639	
UB5	Chainage (m)	39 862,4	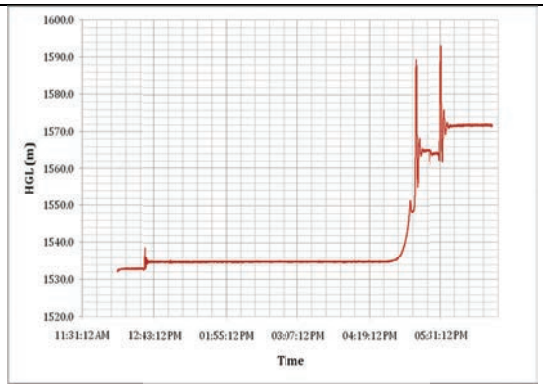
	Elevation (m)	1 418,646	
UB6	Chainage (m)	50 226,0	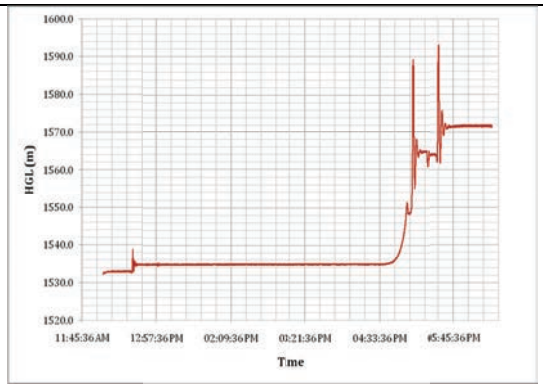
	Elevation (m)	1 417,665	
UB7	Chainage (m)	58 753,9	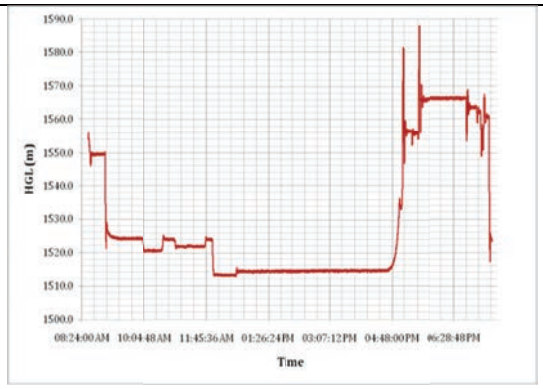
	Elevation (m)	1 492,737	

Recording position	Description		Graphical presentation of recorded data
UB8	Chainage (m)	58 756,9	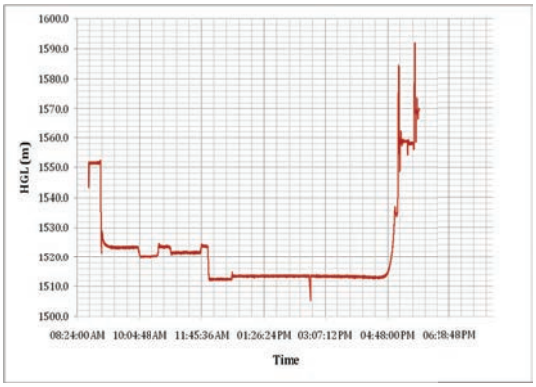
	Elevation (m)	1 493,067	

5.3.3 Flow recordings of the Uitkijk to Brandkop Pipeline

Flow was recorded at a frequency of 0,5 Hz (every 2 seconds) by the project team. The flow data recorded by Bloemwater's operational staff at a frequency of 1 per hour was also obtained as shown on **Figure 5.6**.

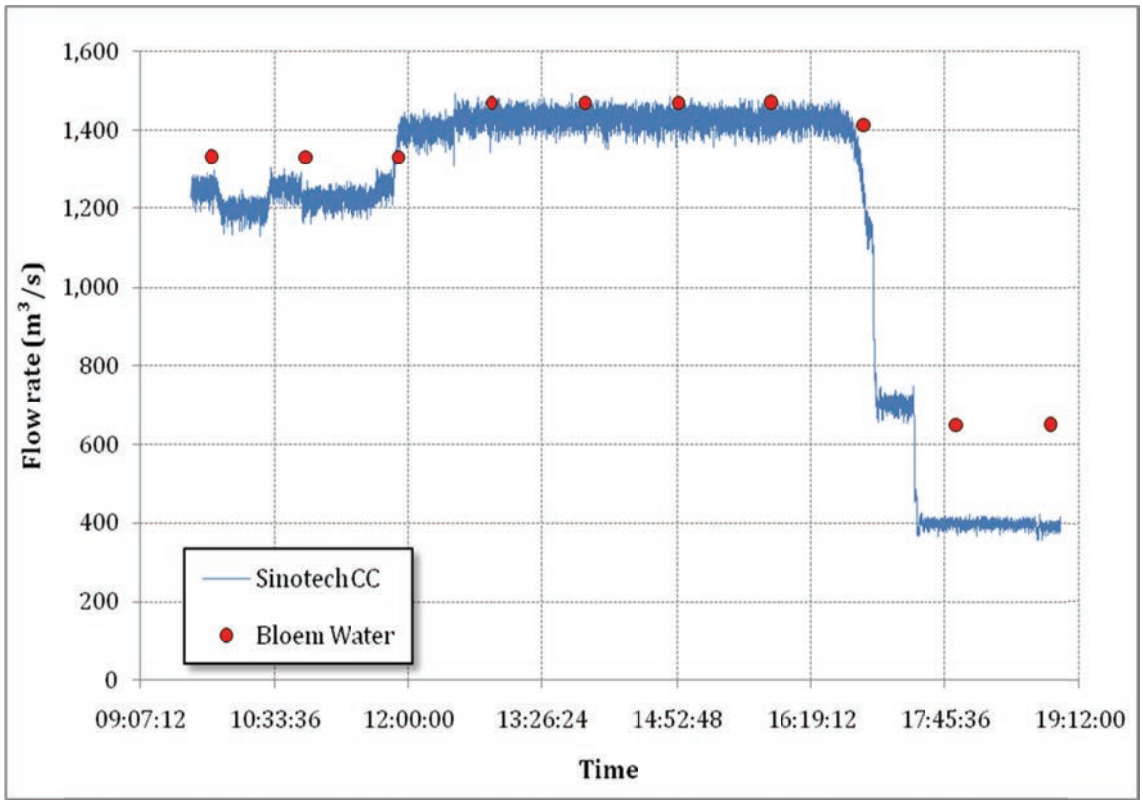

Figure 5.6: Flow data recorded on 14 July 2010

Figure 5.6 reflects that at high flows the recorded flows by the Research Team closely correlate with that recorded by Bloemwater (1432 l/s versus 1470 l/s) but at lower flow rates the values recorded by Bloemwater are however significantly higher (650 l/s versus 402 l/s).

From the recorded flow and pressure recordings 5 distinct time periods were selected where pressures and flow could be compared between all the measuring points. These 5 periods are at times 16:00, 17:02, 17:15, 17:25 and 17:45 where stable flow and pressure conditions prevailed as shown in **Figure 5.7**.

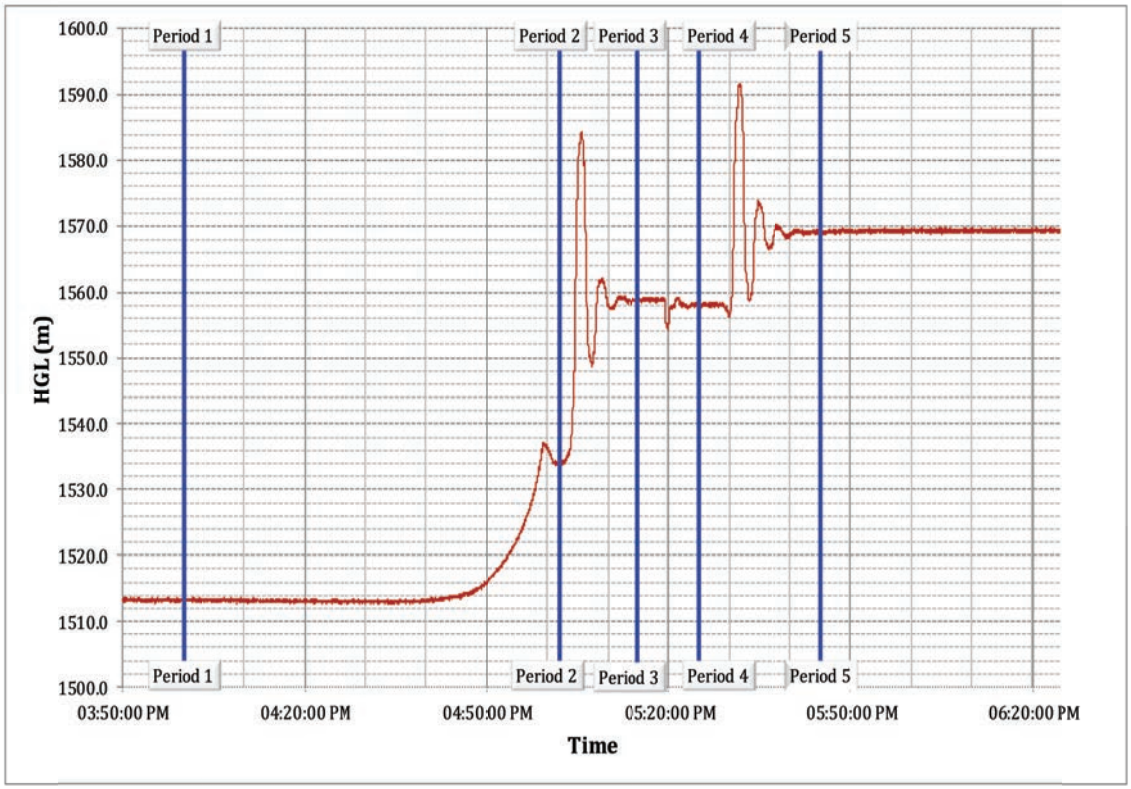

Figure 5.7: Selected time periods (shown at UB8)

Table 5.9 provides a summary of the recorded pressures and flows at the selected time periods. The pressure and flow values shown in **Table 5.9** were obtained by calculating an average pressure or flow over at least a 2 minute period.

Table 5.9: Summary of recorded hydraulic grade lines at each measuring point

		Period 1	**Period 2**	**Period 3**	**Period 4**	**Period 5**
		14 July 2010 ±16:00	**14 July 2010 ±17:02**	**14 July 2010 ±17:15**	**14 July 2010 ±17:25**	**14 July 2010 ±17:45**
Measuring point	**Chainage (m)[##]**	**Hydraulic grade line level (m)**				
		Flow rate in l/s				
		1 423,7	**1 143,3**	**698,9**	**705,1**	**395,0**
		Velocity in m/s				
		1,328	**1,066**	**0,652**	**0,658**	**395,0**
UB1	294,4	1574,376	1574,586	1574,929	1575,083	1575,181
UB2a	5875,1	1568,465	1570,548	1573,153	1573,123	1574,710
UB2b	5895,1	1568,116	1570,233	1572,873	1572,839	1574,455
UB3	19626,6	1555,150	1562,063	1570,147	1569,638	1573,613
UB4[#]	25610,1	1547,581	1556,306	1566,619	1565,737	-
UB5	39862,4	1534,832	1548,638	1564,703	1563,995	1571,600
UB6	50226,0	1523,721	1540,957	1561,057	1560,434	1569,681
UB7*	58753,9	1514,428	*1533,490*	*1556,345*	*1555,697*	*1566,221*
UB8	58756,9	1513,426	1534,343	1558,878	1558,209	1569,265

Notes: [#] Measuring point was disconnected before the data could be recorded for Period 4

[##] Chainages were obtained from the Tender Drawings

* Periods 2 to 5 had suspect data

The data in **Table 5.9** is graphically represented in **Figure 5.8**.

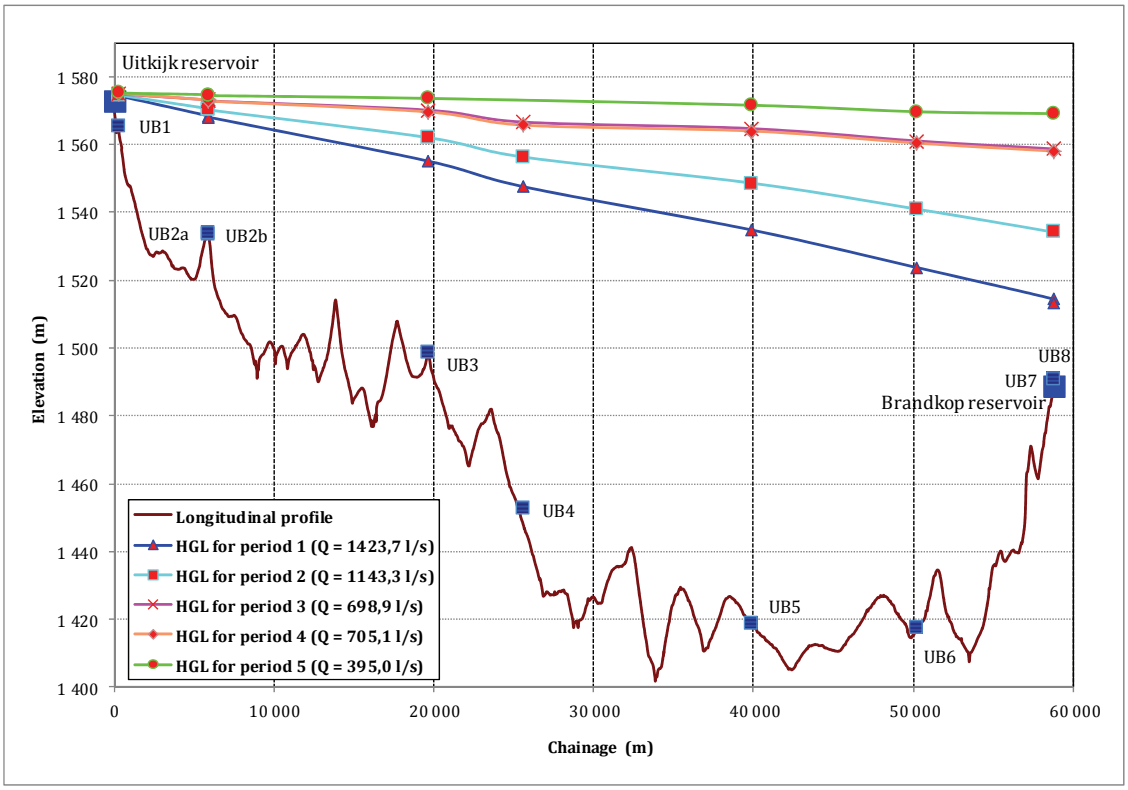

Figure 5.8: Combined graph with hydraulic grade lines

Figure 5.8 depicts the HGLs for different flows. Although the HGL values (**Table 5.9**) were simply connected with straight lines in **Figure 5.8,** it is acknowledged that local losses occurring at the isolating valves which are not reflected in **Figure 5.8.** These losses are however incorporated in the recorded HGL values at each of the measuring points.

Pressures were recorded at UB2a and UB2b to enable the calculation of the secondary loss caused by the butterfly (isolating) valve (LCV1). **Table 5.10** summarizes the losses from UB2a to UB2b, i.e. from the upstream to the downstream side of line control valve, LCV 1.

Table 5.10: Secondary losses through line control valve (LCV1)

Period	**Period 1**	**Period 2**	**Period 3**	**Period 4**	**Period 5**
Flow rate (m^3/s)	1,424	1,143	0,699	0,705	0,395
Velocity through valve (m/s)	2,170	1,743	1,065	1,075	0,602
Pressure drop (m)	0,3488	0,3146	0,2798	0,2837	0,2551

5.3.4 Calculated roughness parameters of the Uitkijk to Brandkop Pipeline

Between measuring point UB1 and UB8 there are 10 isolating valves which cause secondary losses. At LCV5 the butterfly was temporarily removed and replaced with a distance piece (Sinotech CC, 2010a).The calculation of the secondary loss was thus based on the 9 line control valves assuming the similar pressure drops as determined at LCV1 (**Table 5.10**). The distance from measuring point UB1 to measuring point UB8 is 58 462,5 m. The calculated roughness parameters are shown in **Table 5.11**.

Table 5.11: Calculated roughness parameters of the Uitkijk to Brandkop Pipeline

		Period 1	**Period 2**
Flow (l/s)		1423,7	1 143,3
Velocity (m/s)		1,328	1,066
Re		1360919	1 092 884
ΔH (m)		60,950	40,243
H_L(m)		3,139	2,831
H_f (m)		57,811	37,412
S_f (m/m)		0,00099	0,00064
Friction factor (λ)		0,0129	0,0129
Absolute roughness – k_s(mm)	**Kármán & Prandtl**	0,168	0,171
	Colebrook-White transition	0,098	0,084
	Barr	0,091	0,078
	The Moody diagram	0,097	0,089
Manning – n ($s/m^{1/3}$)		0,0104	0,0105
Hazen-Williams – C		142,2	144,5

The velocities for Periods 3, 4 and 5 are low resulting in friction losses of only 13,681 m, 14,469 m and 3,768 m respectively. This result in extremely flat hydraulic grade lines and it is subsequently difficult to accurately determine the roughness parameters.

The results in Table 5.11 contradict the previous tests results from 2003 (WRC, K5/1269, 2005). During the study of 2003 it was only possible to setup two points (one downstream of Uitkijk at TAV8 and one at Brandkop). A review of the 2003 data utilizing the updated survey information indicated that a very similar HGL was obtained to what was obtained during this study; see **Figure** 5.9. The calculation of the roughness parameters is sensitive for any change in energy consumption

(ΔH). A 10% change in energy results in a ±50% change in roughness parameter (Colebrook White equation).

The roughness parameter was also recalculated and this is provided in **Table 5.12**.

The pressures at the beginning of the pipeline and end of the pipelines for Period 1 (2010) and the 2003 tests are very similar. This indicates typically that all 5 branches were open at Brandkop Reservoir. The recorded flow rate of 2003 was however significantly less (193 l/s), resulting that the back calculated roughness parameter was over estimated. Unfortunately during the tests in 2003, no intermediate pressure recordings were obtained along the pipeline route.

A large secondary loss, for instance a half closed line control valve, could be the reason for the large difference in obtained flow rates. The relatively straight HGL obtained during the 2010 tests indicates that nowhere on the pipeline were there any major secondary losses which would result in a drop in the pressure and subsequently the flow rate. Another reason for the lesser flow during the 2003 tests could be that one of the major off takes was not isolated and the flow rate was only measured at Brandkop reservoir.

The project team have confidence in the latest tests results since the flow rate correlates with that measured by Bloemwater (see **Figure 5.6**).

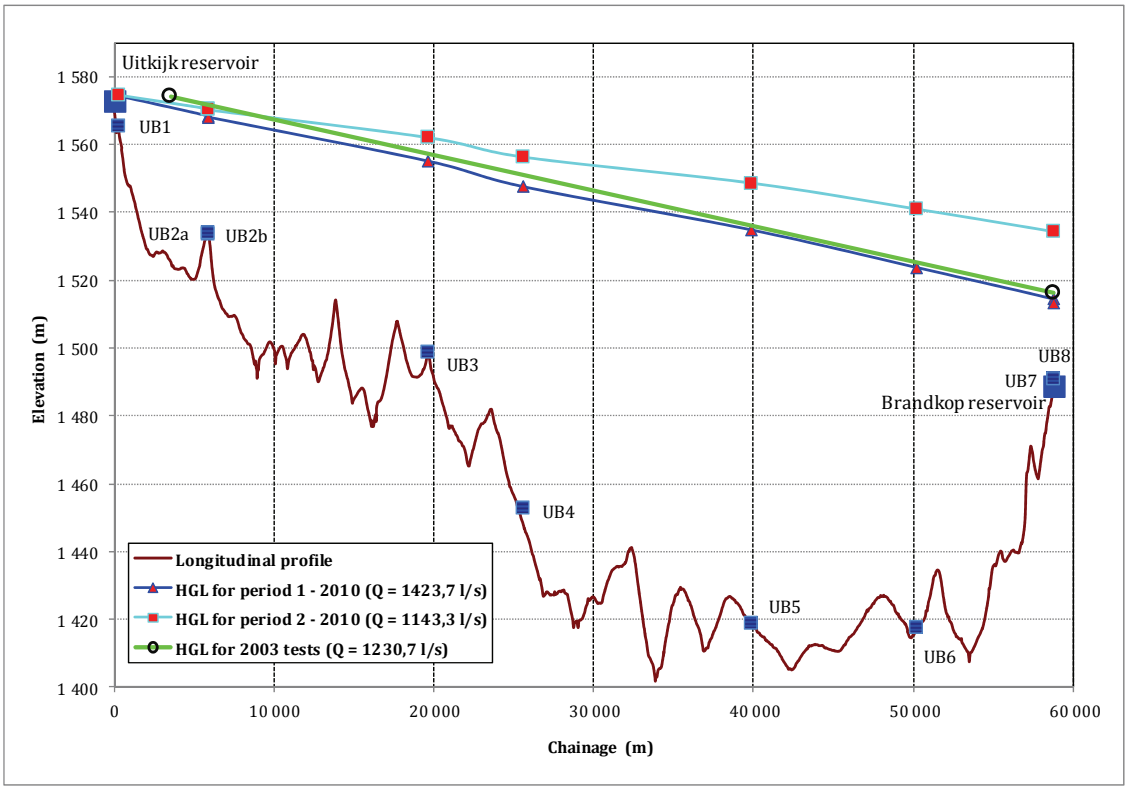

Figure 5.9: Comparison of hydraulic grade lines of the Uitkijk to Brandkop Pipeline

Table 5.12: Recalculated roughness parameter from the 2003 recorded data of the Uitkijk to Brandkop Pipeline

Flow (l/s)		1 230,7
Velocity (m/s)		1,148
Re		1 176 340
ΔH (m)		57,851
H_L(m)		2,640
H_f (m)		55,211
S_f (m/m)		0,00094
Friction factor (λ)		0,0164
Absolute roughness – k_s(mm)	**Kármán & Prandtl**	0,544
	Colebrook-White transition	0,472
	Barr	0,456
	The Moody diagram	0,409
Manning – n (s/$m^{1/3}$)		0,0118
Hazen-Williams – C		126,0

5.4 Swakopmund to Rossing Pipeline

5.4.1 Recorded data on the Swakopmund to Rossing Pipeline

On 29 September 2009 the pressure recordings were conducted on the Rössing Pipeline for a number of steady state conditions. **Figure 5.10** reflects the recorded incidences where steady state occurred. These steady state conditions are related to the number of pumps operational and reference to these have been made in **Table 5.16**. The same reference is reflected in **Figure 5.10** to show the different steady state conditions at R1 (sk33.8km-2, Chainage 33 031,982). **Figure 5.10** also reflects the discrete positions where the recorded data will be used to represent the pressures for the flow rate at that point in time.

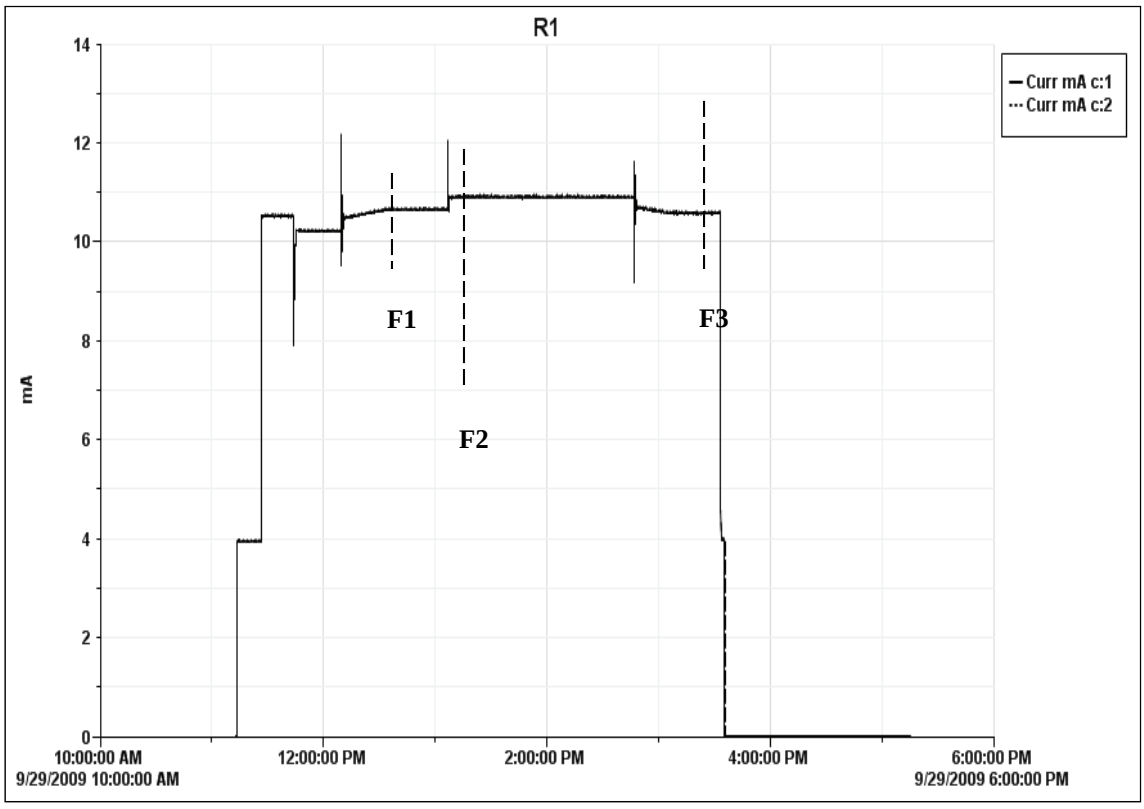

Figure 5.10: Pressure – time plot of the recorded pressures (in mAmp) at Station R1 for the different flow scenarios

Table 5.14 reflects some of the recorded heads, in milliamp, respectively at the two of the three recording positions for the different operating conditions/flow rates. The head is calculated by converting the milli-ampere recording to a head.

Table 5.13 reflects the recorded flow rates that were used to determine the hydraulic behaviour of a section of the Rossing Pipeline.

Table 5.13: Recorded flow rates used for the assessment of the hydraulic characteristics of a section of the Rossing Pipeline

Flow rate ID	Flow rate (m^3/h) #	Number of Pumps operational in the Base Station	Date of the test	Time when the flow occurred
F1	**512**	**1**	**29 September 2009**	**12:45**
F2	**986**	**2**		**13:11**
F3	**524**	**1**		**15:20**

Note:

 # Flow instability was experienced

Table 5.14: Recorded heads at the three recording positions for a flow F2 of a section of the Rossing Pipeline

Recording position	Flow details	Graphical presentation of recorded data
R1	Flow Id F2 represented a flow arte of 986 l/s	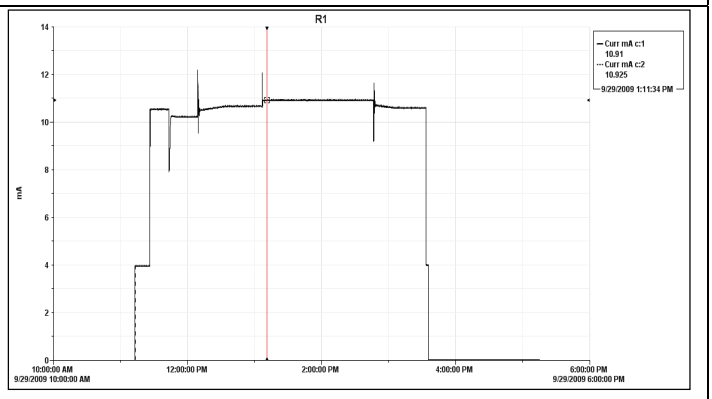
R2		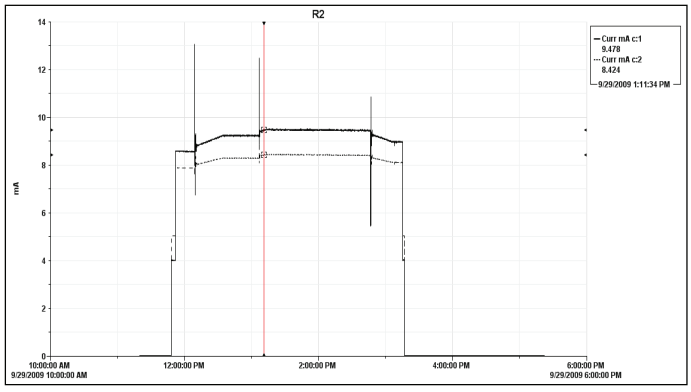

Recording position	Flow details	Graphical presentation of recorded data
R3		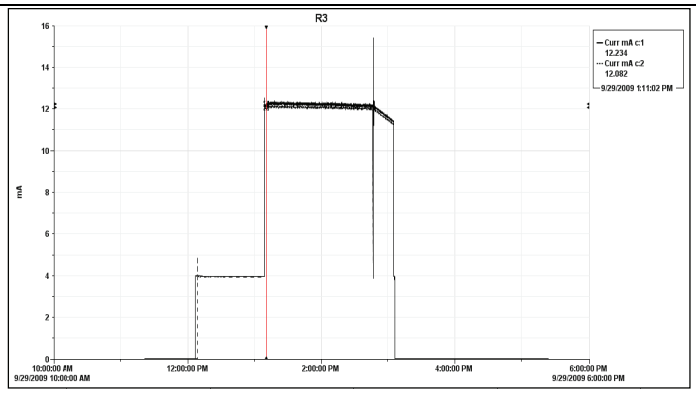

Figure 5.11 reflects the dynamic pressures at R1 in the system if the pump status is varied.

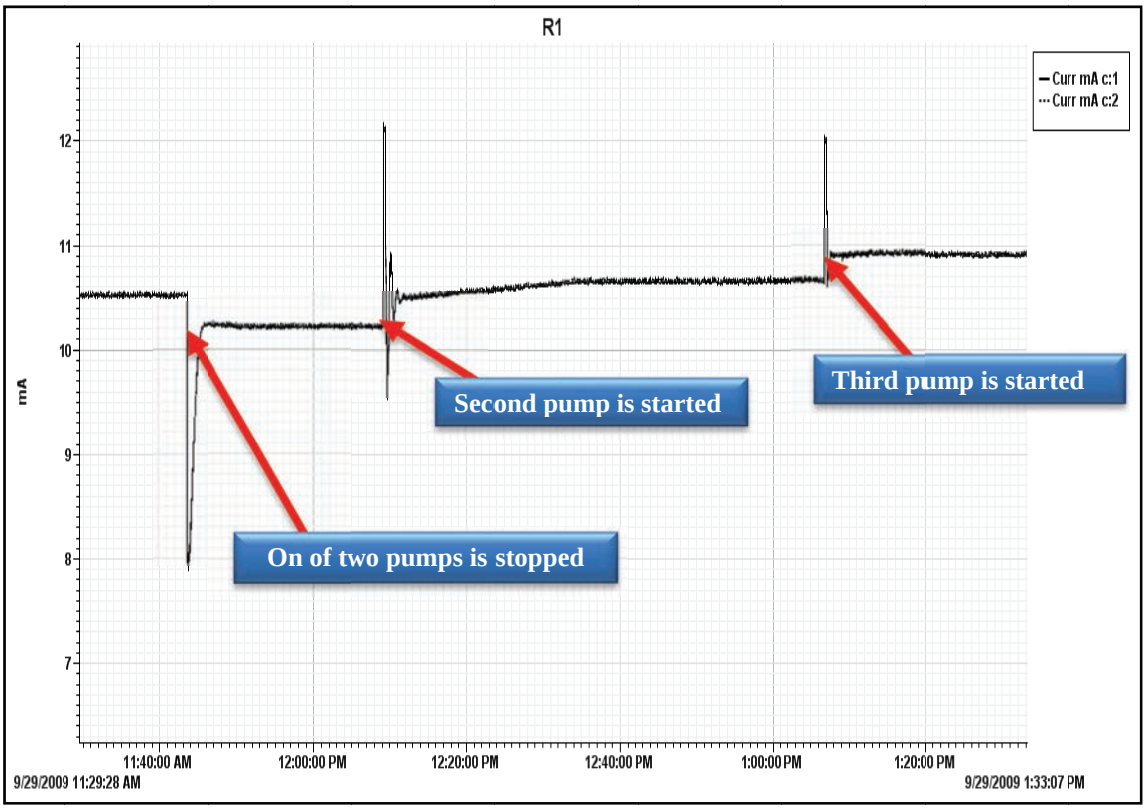

Figure 5.11: Value of the recorded pressure variation (in mAmp) at Station R1 for the operational change in the pumps on the section of the Rossing Pipeline between Booster 2 and Booster 3

Table 5.15 reflects the recorded pressures for the different steady state condition for flow rate F2.

Table 5.15: Value of the recorded pressure (in mAmp) for the F2 flow rate in a section of the Rossing Pipeline

Event/Channel	R1	R2	R3
Flow F2			
Time	**13h11**		
Ch 1 (mAmp)	10,910	9,478	12,234
Ch 2 (mAmp)	10,925	8,224	12,082

5.4.2 Steady state recorded pressures in a section of the Rossing Pipeline

Table 5.16 indicates the recorded steady state heads for the different flow scenarios.

Table 5.16: Recorded steady state grade lines for the different steady state conditions of a section of the Rossing Pipeline

Flow ID	Pressure recording position	Chainage (m)	Level of the Transducer (m)	HGL (m)
F1	R1	33 031,982	397,409	No data obtained at R3. Head difference low compromising accuracy of calculation
	R2	39 255,434	469,924	
	R3	40 392,709	487,652	
F2	R1	33 031,982	397,409	506,4195
	R2	39 255,434	469,924	504,0313
	R3	40 392,709	487,652	503,1170
F3	R1	33 031,982	397,409	Head difference low compromising accuracy of calculation
	R2	39 255,434	469,924	
	R3	40 392,709	487,652	

5.4.3 Calculation of the friction parameter for the different flow rates on a section of the Rossing Pipeline

The recorded flow and head data was used to back calculate the current roughness parameters on the section of the Rössing Pipeline for a section of the pipeline between Booster Stations 2 and 3 (Chainage 28 810 m to Chainage 41 651 m).

Table 5.17 reflects the calculated friction parameters and compares it to the manufacturer's suggested roughness parameter.

Table 5.17: Calculated roughness in a section of the Rössing Pipeline

Flow rate, F2 (m^3/s)	Section	Head loss (m)	Calculated k_s (mm)		Manufacturers' suggested roughness (mm)	V m/s)	Re
			Barr	Colebrook White			
0,274	R1 to R3	3,297	0,0802	0,0786	0,03 to 0,15 with the normal value of 0,06 (HR Wallingford and D.I.H Barr)	0,708	4,5001E+05

Figure 5.12 reflects the Hydraulic Grade Lines for the different flow rates, while results are also indicated on the Moody Diagram in **Figure 5.13.**

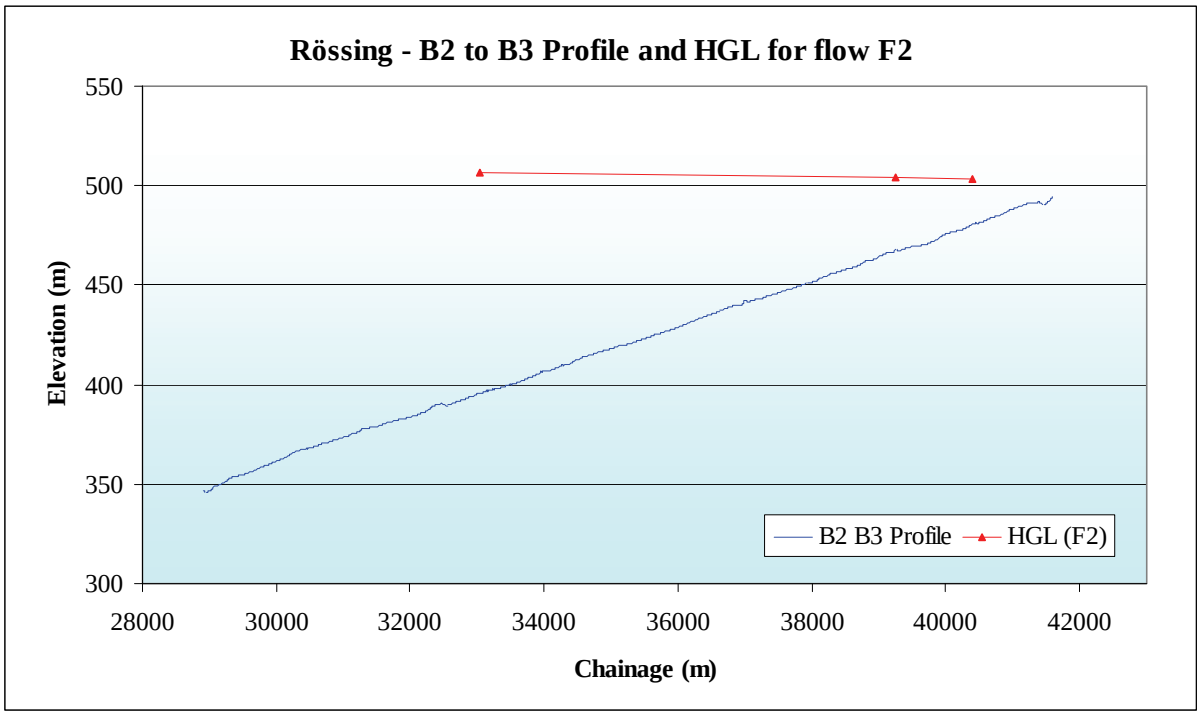

Figure 5.12: Hydraulic Grade Line for the flow rate, F2, in a section of the Rössing Pipeline

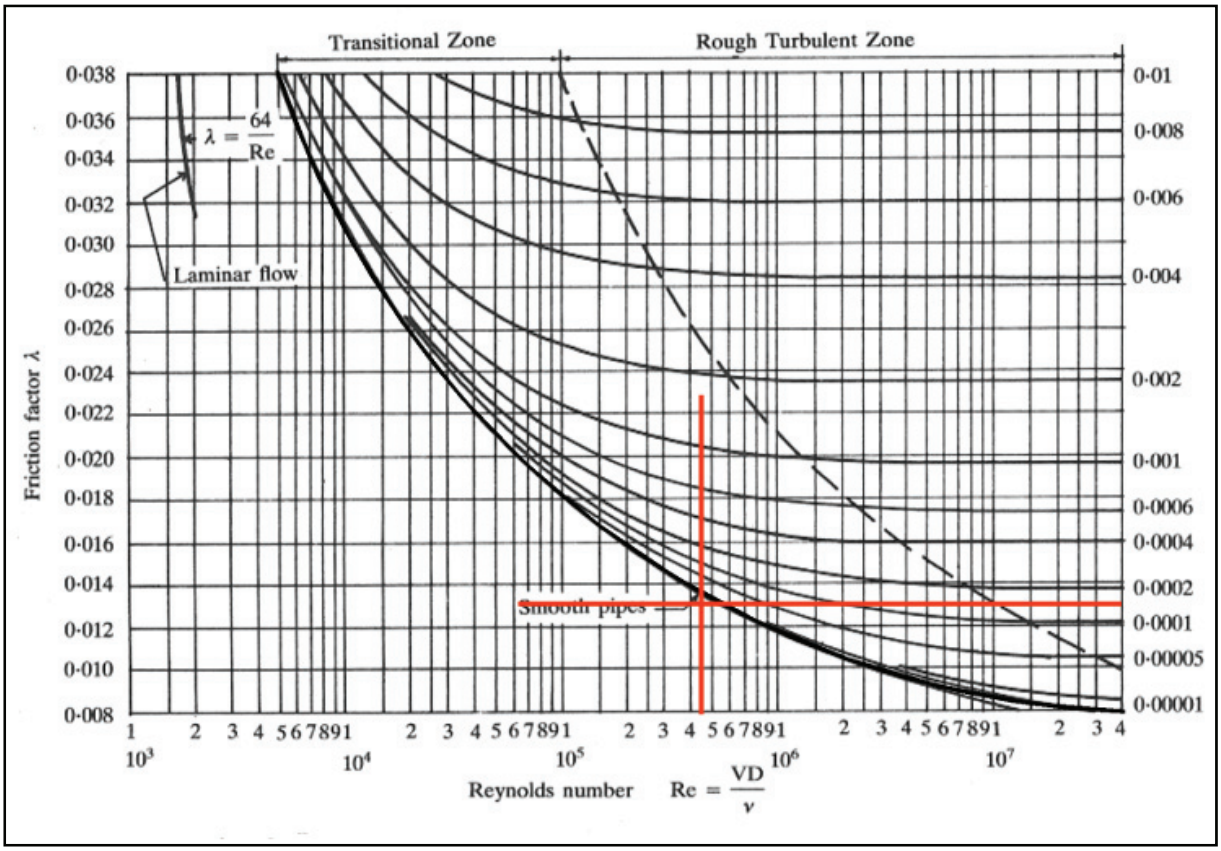

Figure 5.13: Moody diagram of the results obtained from the review of the Rössing Pipeline

The plotting position approaches the smooth boundary line for the pipes with the calculated roughness just higher than the prescribed "normal roughness" for these pipes.

Figure 5.14 reflects the influence of couplings on the lambda value, which was proposed in WRC TT 278/06 (2006). The procedure suggested, in that approach, was to calculate the value of Lambda for rough turbulent flow conditions and then to increase the value of Lambda by considering the dimensional details at the couplings. The relationship was experimentally determined.

Figure 5.15 reflects the typical coupling on the Rössing Pipeline.

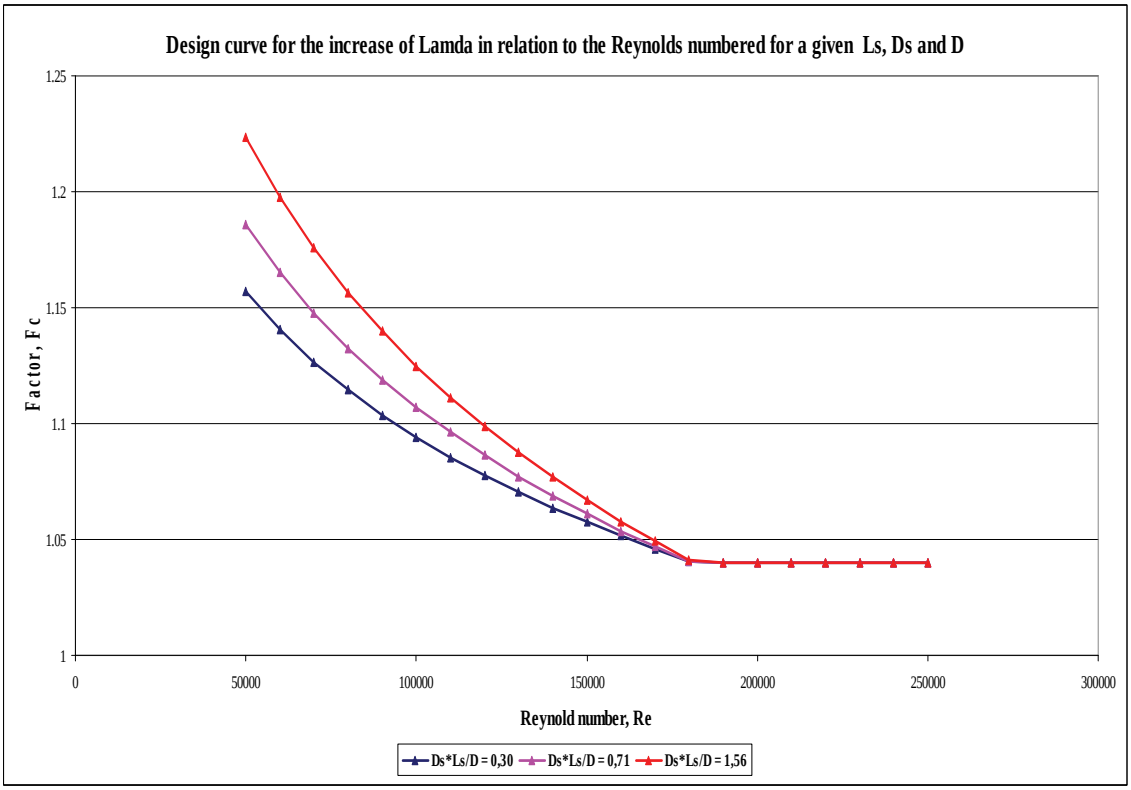

Figure 5.14: Alteration of the value of Lambda to compensate for the influence of the coupling losses (WRC TT 278/06)

Figure 5.15: Typical coupling on the Rössing Pipeline

Figure 5.16 reflects some of the dimensions of the coupling.

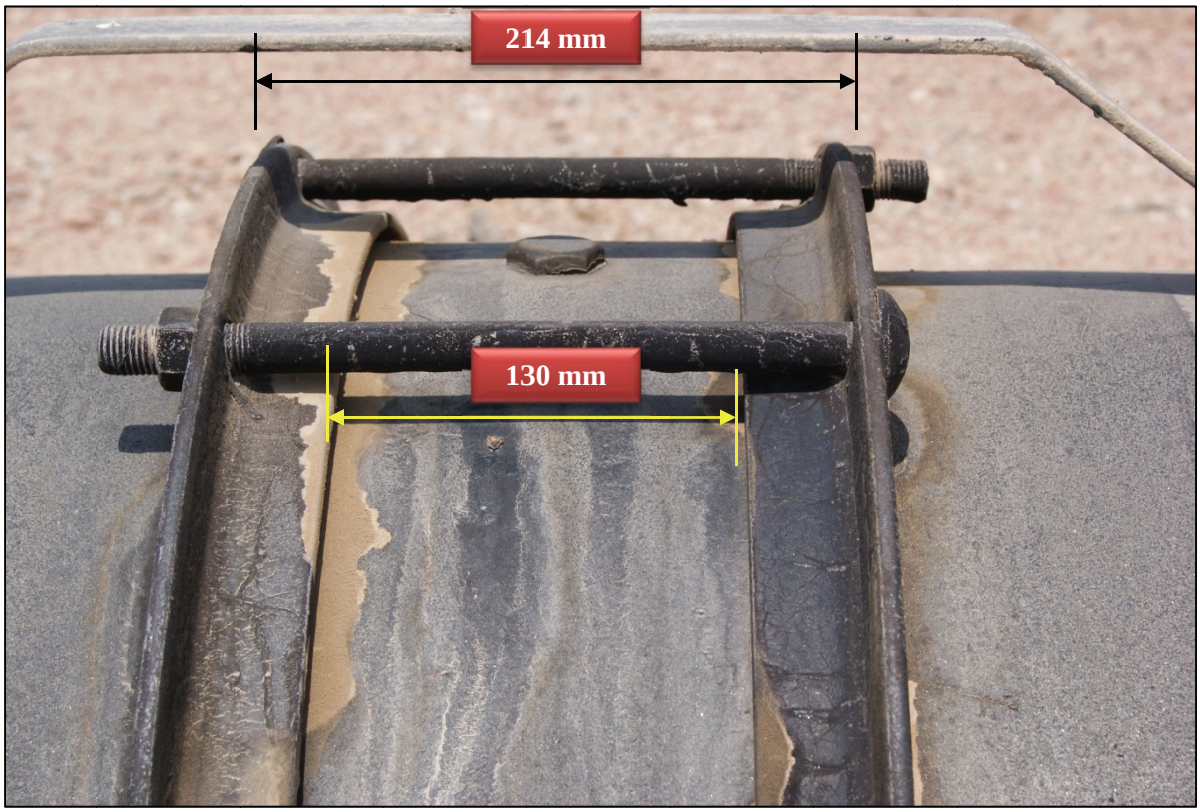

Figure 5.16: Some dimensions of the Viking Jonson Coupling on the Rössing Pipeline

Formulae 5.1 and 5.2 were used to back calculate the value of k_s for the Rössing Pipeline

Colebrook-White: $$\frac{1}{\sqrt{\lambda}} = -2\log\left(\frac{k_s}{3{,}7D} + \frac{2{,}51}{\mathrm{Re}\sqrt{\lambda}}\right) \quad \ldots(5.1)$$

Barr: $$\frac{1}{\sqrt{\lambda}} = -2\log\left(\frac{k_s}{3{,}7D} + \frac{5{,}1286}{\mathrm{Re}^{0{,}89}}\right) \quad \ldots(5.2)$$

The calculated values were reflected in **Table 5.17.**

Table 5.18 reflects the dimensions of the coupling for which the value of Ds*Ls/**D** was calculated.

Table 5.18: Dimensions of the coupling for which the value of Ds*Ls/D was calculated

Variable	Dimension	Units
D_s	8	mm
L_s	30	mm
D	701,5	mm
D_s*L_s/D	0,342124	mm

This indicates that the value of Lambda should be altered as shown in **Figure 5.14** with a factor of 1,04, since Re is more than 250 000.

Based on the alteration of Lambda the absolute roughness was recalculated and the results for the calculated roughness are shown in **Table 5.19.**

Table 5.19: Recalculated value of the absolute roughness for the Rössing Pipeline with the incorporation of the coupling losses

Flow rate (m^3/s)	Section	Head loss (m)	Calculated k_s (mm)		Manufacturers' suggested roughness (mm)	V m/s)	Re
			Barr	Colebrook White			
0,27372	R1 to R3	3,2965	0,06529	0,06371	0,03 to 0,15 with the normal value of 0,06 (WRC TT 278/06)	0,708	5,6637E+05

This result suggests that the roughness in the Rössing Pipeline is just above the "normal" manufacturer's suggested roughness [3] which could be indicating that some decay in the pipeline coating might be present.

With the current transfer rate between 500 and 800 m^3/h and a unit energy cost per kWh varying between 40 and 200 cents, the influence of the increased roughness can be calculated for different operating periods.

Assuming an efficiency of 70 % for the pumps, the additional discounted energy cost to overcome the additional roughness is reflected graphically in **Figure 5.17**. In this analysis a 15 year operating cycle was reviewed with a low increase in energy cost of 12 % and the time value of money (discount rate) of 6 % and the expected influence of the couplings have been compensated for. The discounted cost must hence be seen as a conservative low estimated of the additional energy costs.

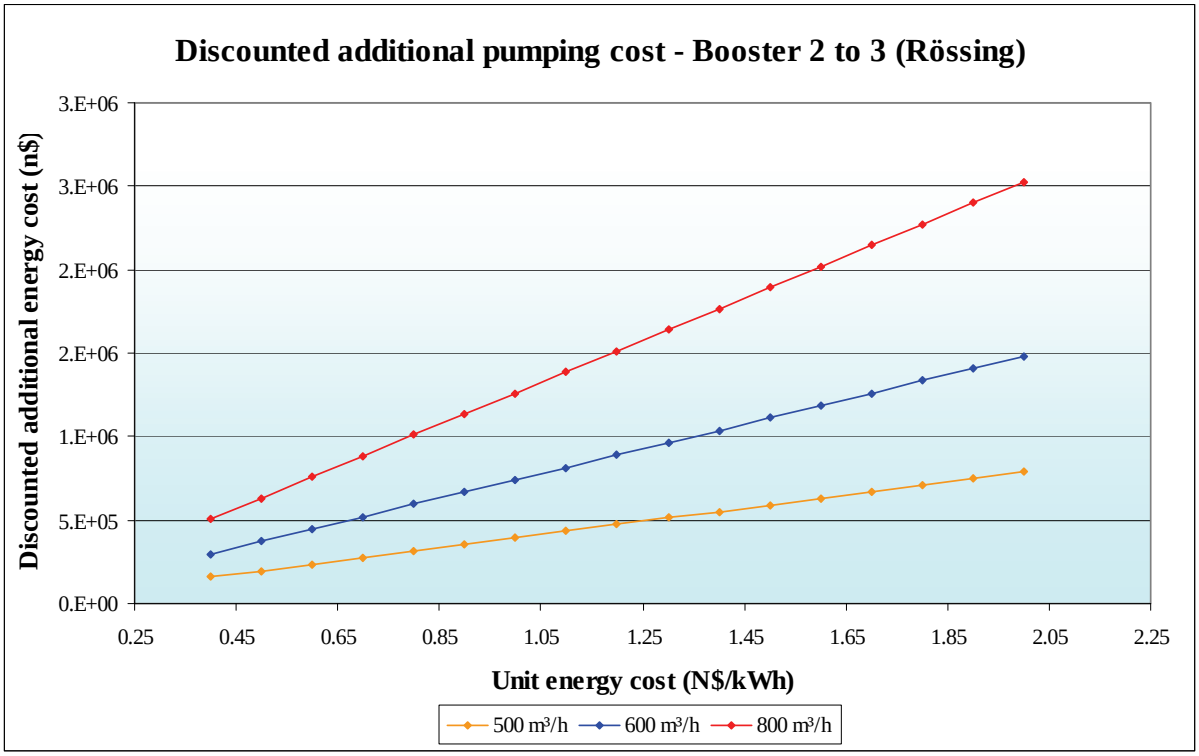

Figure 5.17: Graphical presentation of the additional energy cost used at Booster Station 2 on the Rössing Pipeline

The discounted increased additional energy cost is significant, reflecting the continuously review of the hydraulic characteristics of the pipelines.

5.5 Swartkopmund to Langer Heinrich Pipeline

5.5.1 Recorded data

On 28 September 2009 the pressure recordings were conducted on the Langer Heinrich Pipeline for a number of steady state conditions. **Figure 5.18** reflects the recorded incidences where steady state occurred. These steady state conditions were related to the number of pumps operational as is reflected in **Table 5.20**. The same reference is reflected in **Figure 5.18** to show the different steady state conditions at L1 (Air valve AV-16). **Figure 5.18** also reflects the discrete positions where the recorded data will be used to represent the pressures for the flow rate at that point in time.

Table 5.20: Details of the selected steady state conditions reviewed for the Langer Heinrich Pipeline

Flow ID	Number of pumps	Flow rate		Time when steady state conditions were reached
		(m^3/h)	(l/s)	
F1	2	58,0	16,1	11:47
F2	3	111,3	30,9	11:55
F3	4	158,12	43,9	12:47

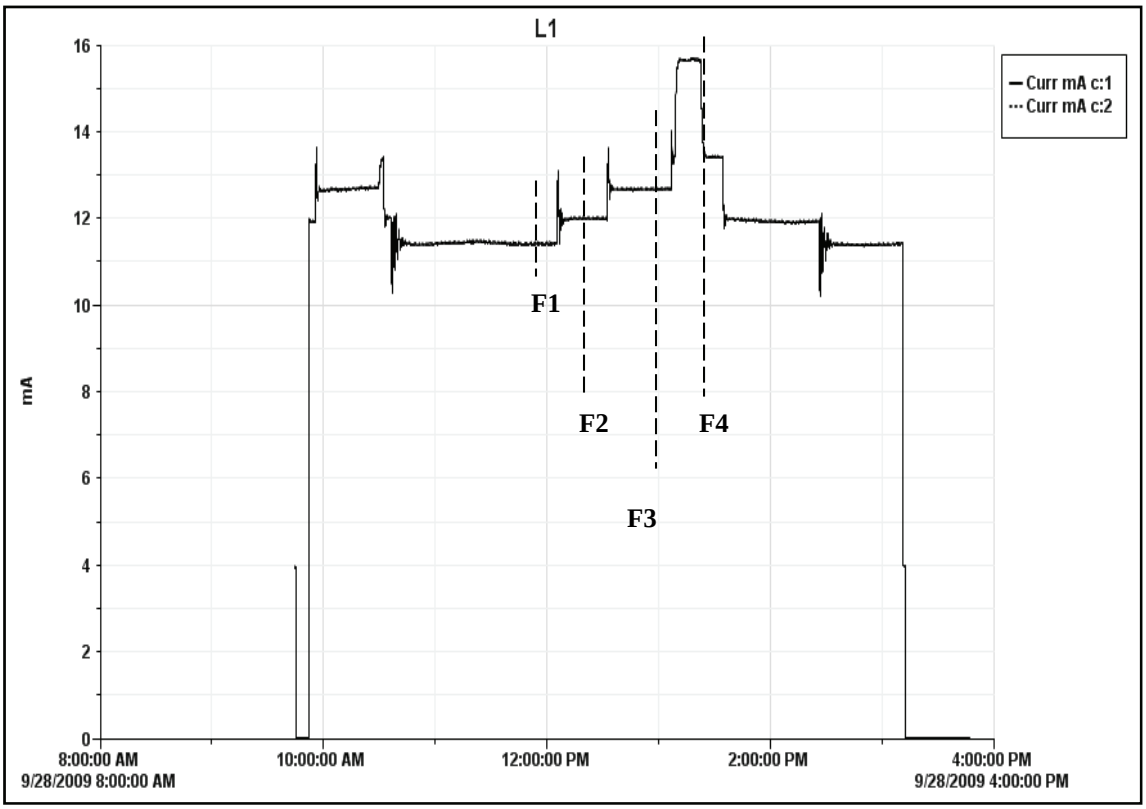

Figure 5.18: Pressure – time plot of the recorded pressures (in mAmp) at Station L1 for the different flow scenarios

Table 5.21 reflects the recorded heads graphically at the different recording positions for one of the flow rates (F2 = 30,9 l/s) which were reviewed.

Table 5.21: Graphical presentation of the recorded pressures at positions L1, L2 and L3 on the Langer Heinrich Pipeline

Recording position	Flow details	Graphical presentation of recorded data
L1	Flow ID F2 represented a flow arte of 30,9 l/s	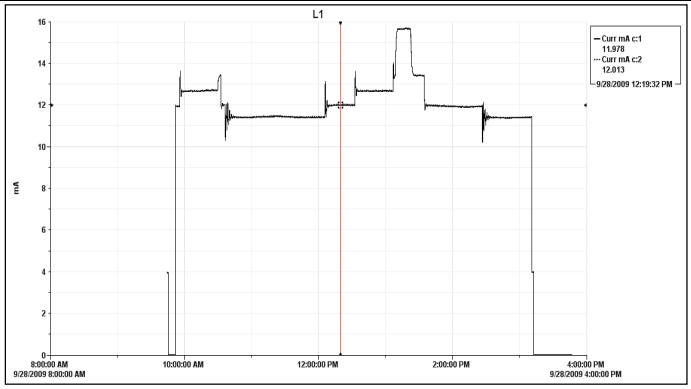
L2		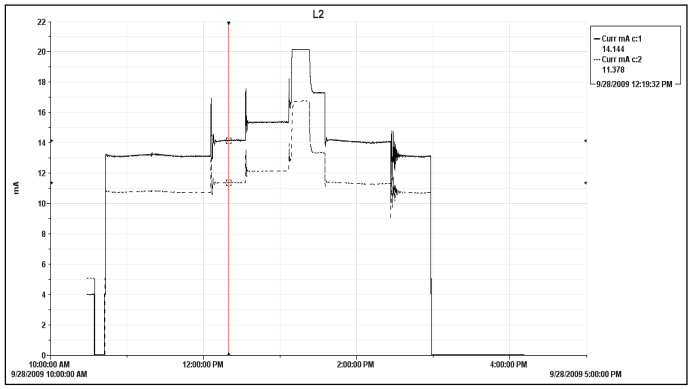
L3		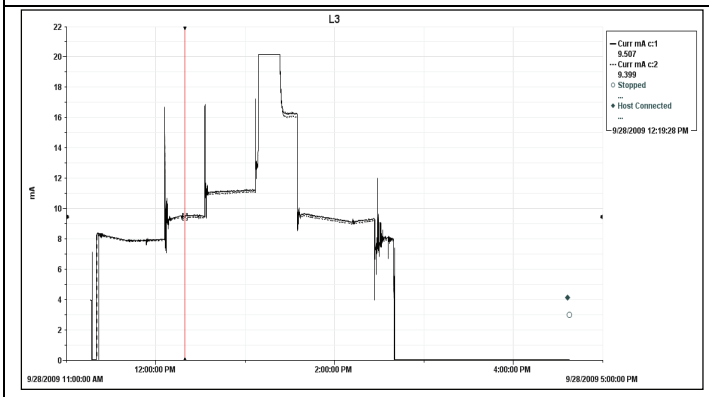

Figure 5.19 reflects that the pressure transducer exceeded the maximum output when 4 pumps were operated. It also indicates the pressure spike of more than 20 m, which is introduced during pump ramp-up.

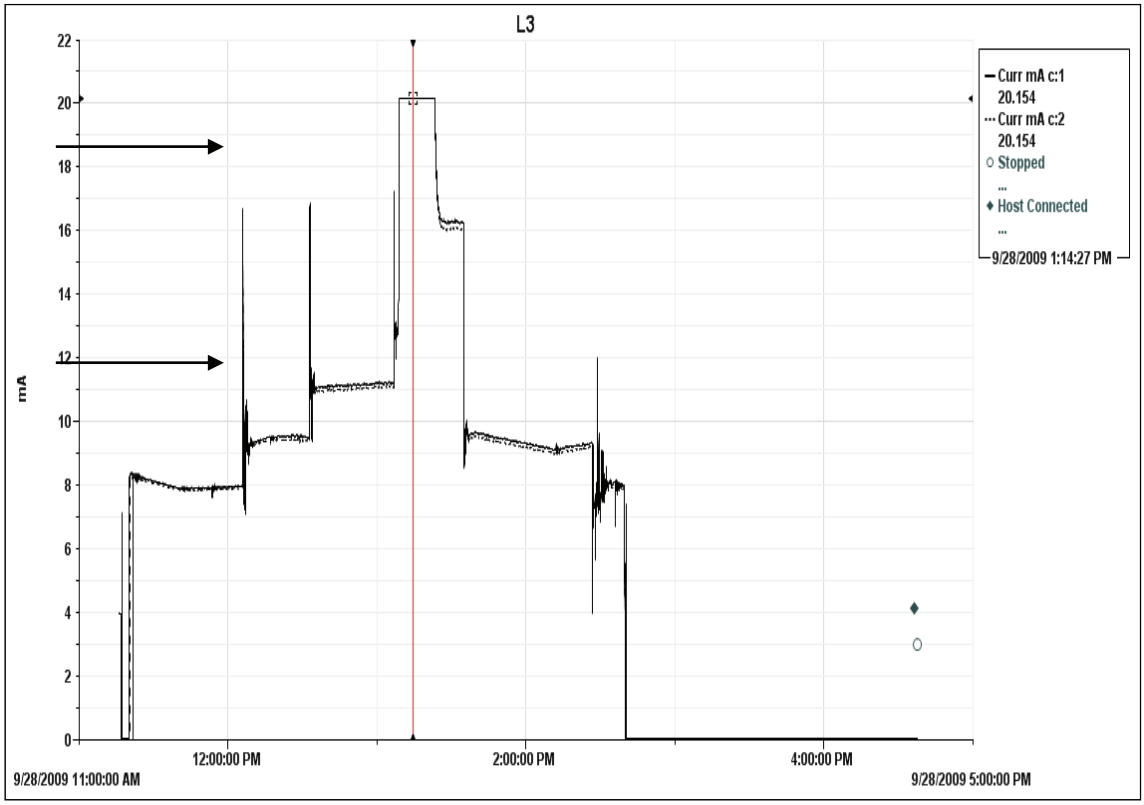

Figure 5.19: Value of the recorded pressure (in mAmp) at Station L3 for the flow rate F4

Steady state flow condition, F4, was not assessed due to a suspect value of the recorded flow rate during this condition. **Table 5.22** reflects the recorded pressures for the different steady state conditions.

Table 5.22: Value of the recorded pressure (in mAmp) for different operating conditions

Event/Channel	L1	L2	L3
Flow ID = F1 (16,1 l/s)			
Time			
Ch 1 (mAmp)	11,402	13,095	7,912
Ch 2 (mAmp)	11,432	10,718	7,844
Flow ID = F2 (30,9 l/s)			
Time	12:19:32	12:19:32	12:19:52
Ch 1 (mAmp)	11,978	14,144	9,497
Ch 2 (mAmp)	12,013	11,378	9,399
Flow ID = F3 (43,9 l/s)			
Time	12;51;14	12;51:22	12:51:10
Ch 1 (mAmp)	12,687	15,355	11,166
Ch 2 (mAmp)	12,704	12,131	11,048

5.5.2 Steady state recorded pressures

Table 5.23 indicates the recorded steady state heads for the different flow scenarios.

Table 5.23: Recorded steady state grade lines for the different steady state conditions

Flow ID	Pressure recording position	Chainage (m)	Level of the Transducer (m)	HGL
F1	L1	7490,648	119,045	235,333
	L2	13960,11	178,165	235,017
	L3	20715,52	225,258	235,094
F2	L1	7490,648	119,045	244,345
	L2	13960,11	178,165	241,604
	L3	20715,52	225,258	239,001
F3	L1	7490,648	119,045	255,250
	L2	13960,11	178,165	249,165
	L3	20715,52	225,258	243,129

5.5.3 Calculation of hydraulic roughness

The recorded flow and head data was used to back calculate the current roughness parameters on the section of the Lager Heinrich Pipeline between the Base Pump Station and Booster Station 1 (Chainage 7 490 m to Chainage 20 720 m).

Table 5.24 reflects the calculated friction parameters and compares it to the manufacturer's suggested roughness parameter.

Table 5.24: Calculated roughness in the pipeline for the section of the Langer Heinrich Pipeline

Flow rate (m^3/s)	**Section**	**Head loss (m)**	**Calculated Ks (mm)**		**Manufacturers' suggested roughness (mm)** (Rare Water (2010)	**V m/s)**	**Re**
			Barr	**Colebrook White**			
0,0161	L1 to L2	0,316	The flow rate is too low to back calculate the friction factor accurately		0,08 0,06 (HR Wallingford and D.I.H Barr)	0,223	6,12E+04
	L1 to L3	0,239					
0,0306	L1 to L2	2,740	0,0701	0,0672		0,422	1,16E+05
	L1 to L3	5,344	0,0557	0,0529			
0,0439	L1 to L2	6,085	0,0994	0,0973		0,607	1,67E+05
	L1 to L3	12,121	0,0881	0,0860			

Figure 5.20 reflects the Hydraulic Grade Lines for the different flow rates, while results are also indicated on the Moody Diagram in **Figure 5.21.**

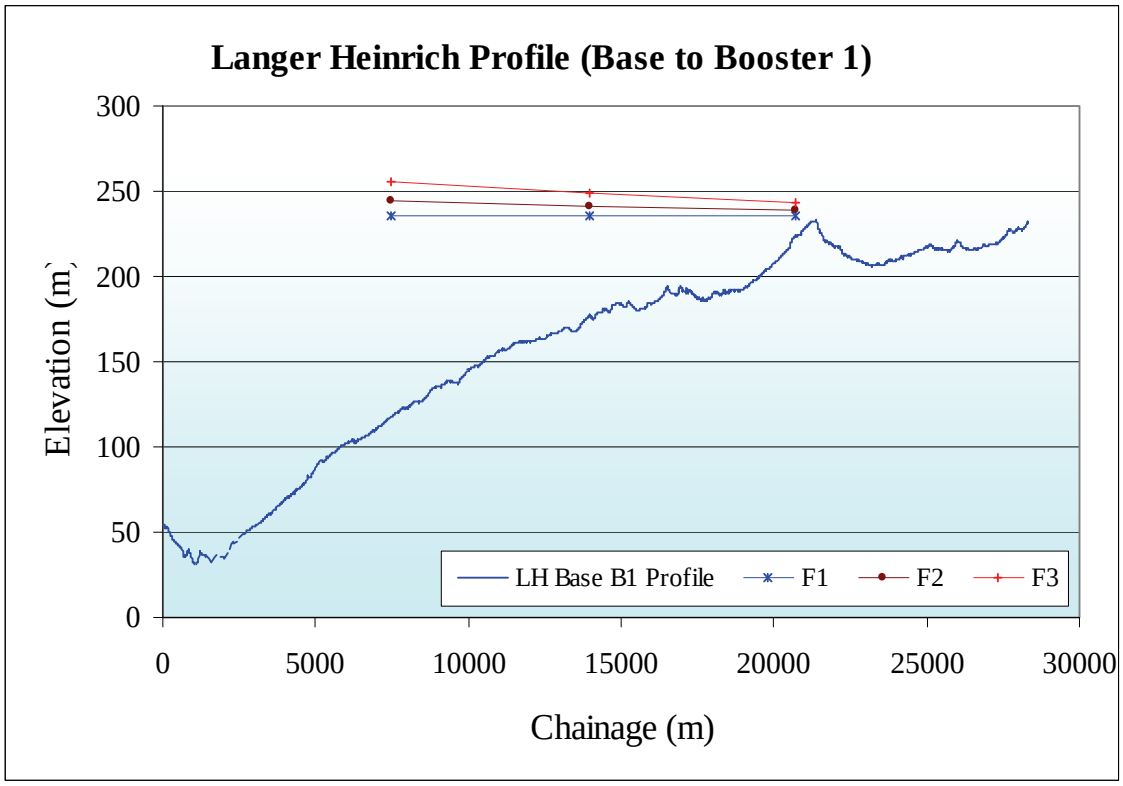

Figure 5.20: Hydraulic Grade Lines for the different flow rates in the tested section of the Langer Heinrich Pipeline

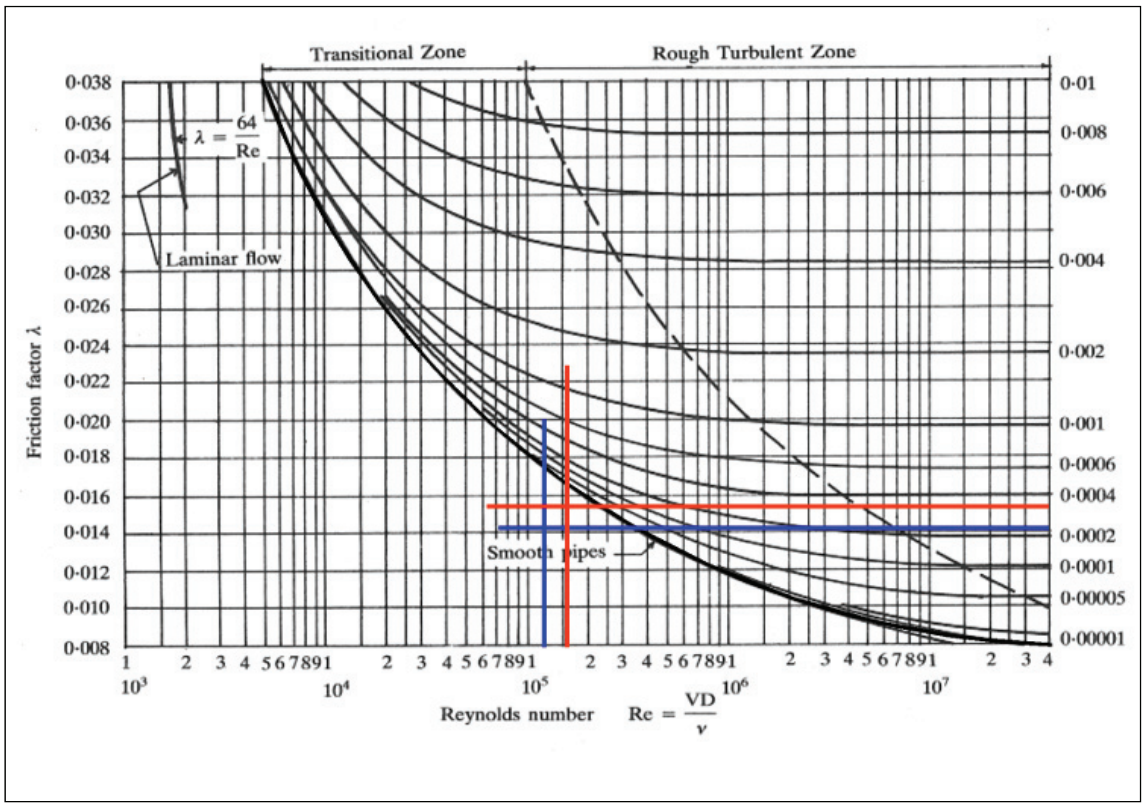

Figure 5.21: Moody diagram of the results obtained from the review of the Langer Heinrich Pipeline

5.5.4 Assessment of the pipe roughness of the Langer Heinrich Pipeline

Based on the recorded data for the Langer Heinrich Pipeline, it can be concluded that:

- The calculated roughness parameters of the pipeline is low (between 0,07 and 0,1 mm) and in accordance with the suggested roughness for a new CML lined ductile iron pipe;
- The roughness parameters results reflect that the pipeline lies in the smooth region;
- The recorder dynamic heads generated in the system by a pump start, could be reduced by changing the operational controls for the pump start up or shut down;
- The hydraulic performance of the other sections of the pipeline should be review to establish the base case; and
- The hydraulic performance of the pipeline should be reviewed frequently (once in 5 years).

5.6 Usutu State Water Scheme: Morgestond Dam to Jericho Dam Pipeline and Jericho Dam to Onverwaght Reservoir Pipeline

5.6.1 Recorded data obtained for the pipelines from Moregenstod Dam to Jericho Dam (M1-J and M2-J) and from Jericho Dam to Onverwaght Reservoir (J1-O and J2-O)

All the pressure data which were recorded for the pipelines from Moregenstod to Jericho Dam (M1-J and M2-J) and the pipelines from Jericho Dam to Onverwaght Reservoir (J1-O and J2-O) are graphically presented as referenced in **Table 5.25**.

Table 5.25: Reference to the graphical presentation of the pressure recordings (Raw data in mAmp)

Pipeline ID	Position	Chainage (m)	Pressure transducer		Table
			Range	ID	
M1-J (new pipeline)	**P1**	447,1	25 Bar G	Y096798	Table 5.26
	P2	4831	5 Bar G	Y125090 Y125091	
	P3	7498	4 Bar G	Y1021082	
M2-J (Old pipeline)	**P1**	947	10 Bar G	Y125088	Table 5.27
	P2	2749	4 Bar G	PT 2	
	P3	7493	4 Bar G	PT 3	
J1-O	**P1**	640	50 Bar G	PT 5	Table 5.28#
	P2	11000	40 Bar G	Y111336	
	P3	20523	25 Bar G	Y113023	
J2-O	**P1**	640	50 Bar G	PT 19	
	P2	11000	40 Bar G	Y111338	
	P3	20523	25 Bar G	Y096798	

Note:

The recordings on the pipelines from Jericho Dam to Onverwaght Reservoir (J1-O and J2-O) were recorded simultaneously on the same data recorder.

Table 5.26: Pressure recording on the Morgenstond to Jericho Dam pipeline M1-J, (new 2003)

Recording position	Description		Graphical presentation of recorded data
M1 P1	Chainage (m)	25 610,1	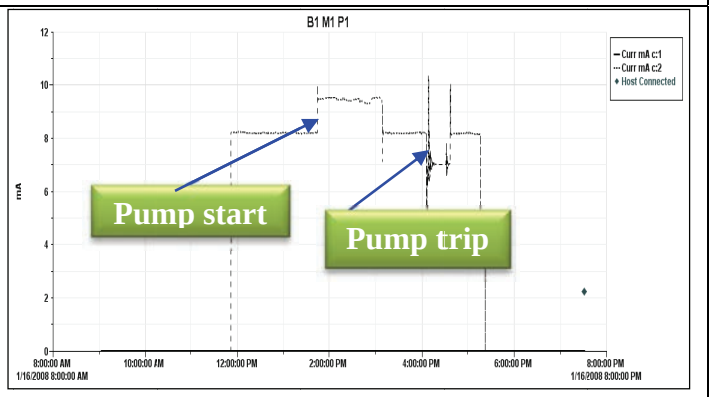
	Elevation (m)	1 452,64	
M1 P2	Chainage (m)	39 862,4	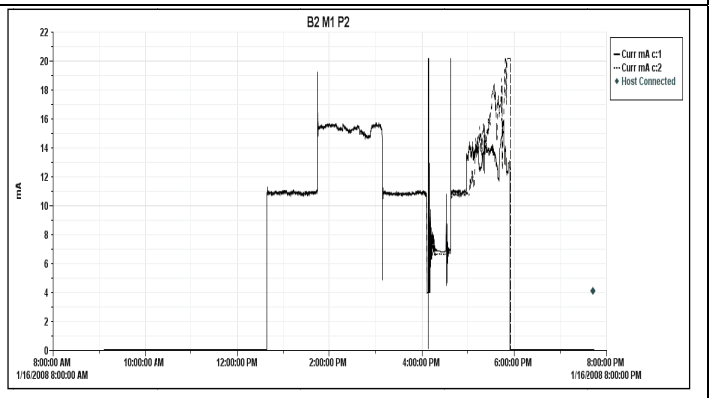
	Elevation (m)	1 418,65	
M1 P3	Chainage (m)	50 226,0	
	Elevation (m)	1 417,67	

Table 5.27: Pressure recording on the Morgenstond to Jericho Dam pipeline M2-J, (old 1964)

Recording position	Description		Graphical presentation of recorded data
M2 P1	**Chainage (m)**	25 610,1	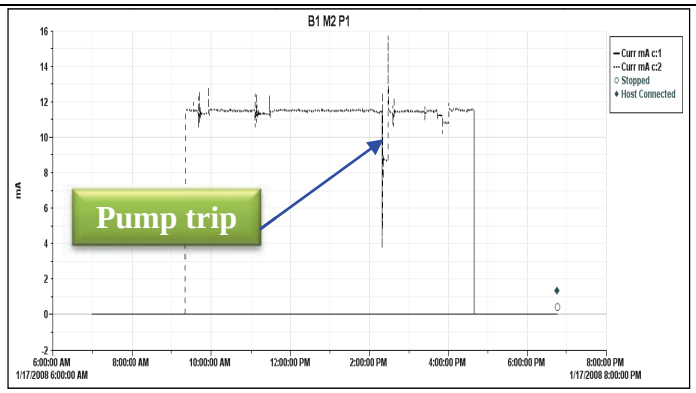
	Elevation (m)	1 452,639	
M2 P2	**Chainage (m)**	39 862,4	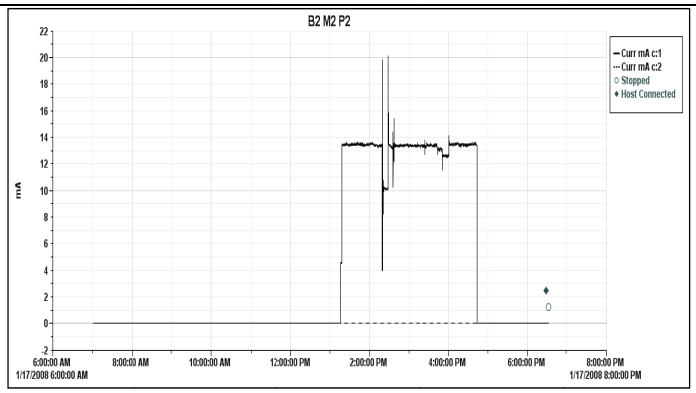
	Elevation (m)	1 418,646	
M2 P3	**Chainage (m)**	50 226,0	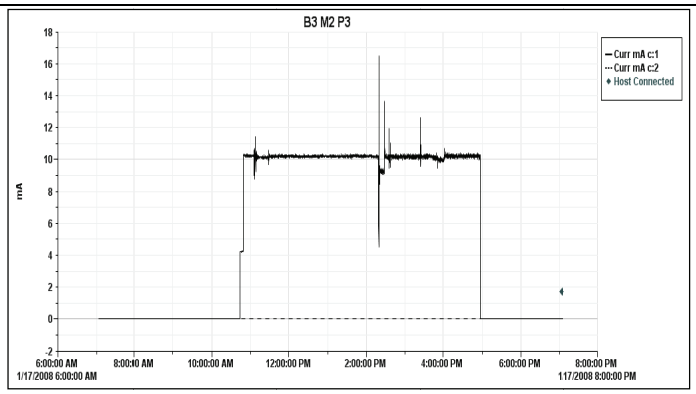
	Elevation (m)	1 417,665	

Table 5.28: Pressure recordings along the two pipelines between Jericho Dam and Onverwaght Reservoir (J1-O (Northen) Channel 2 and J2-O (Southern – new 2001) Channel 3)

Recording position	Description		Graphical presentation of recorded data
J1 J2 P1	**Chainage (m)**	25 610,1	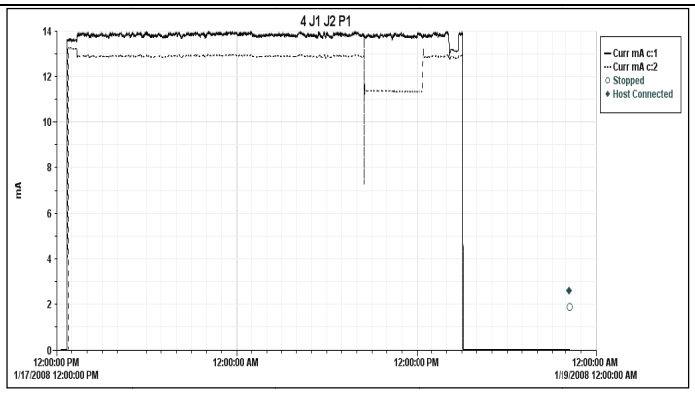
	Elevation (m)	1 452,639	
J1 J2 P2	**Chainage (m)**	39 862,4	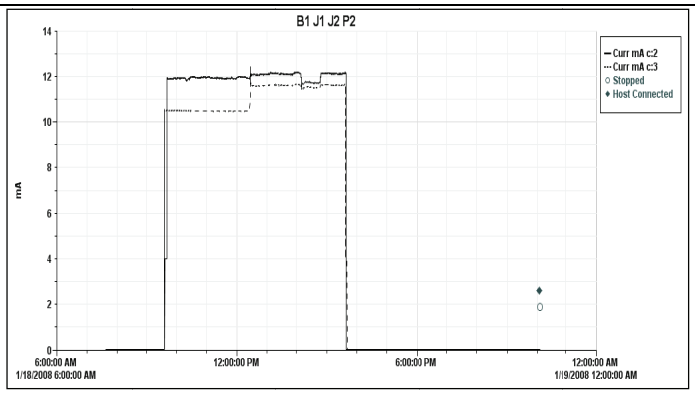
	Elevation (m)	1 418,646	
J1 J2 P3	**Chainage (m)**	50 226,0	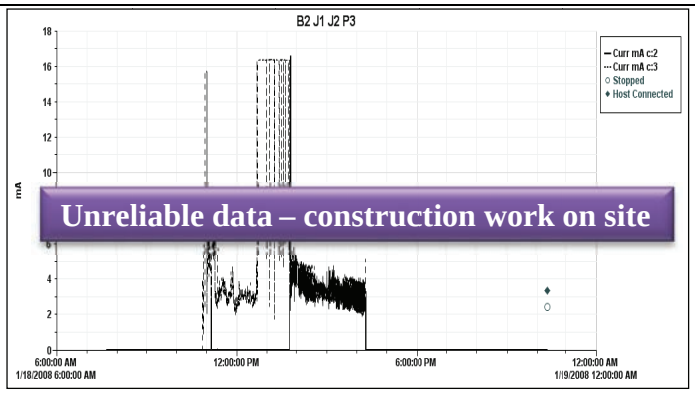
	Elevation (m)	1 417,665	

5.6.2 Calculation of the hydraulic roughness of the Morgenstond to Jericho and Jericho to Onverwacht pipelines

The recorded output from the transducers in mAmp was converted to meters of pressure head. The energy loss between the consecutive measuring locations was then determined by considering the installation elevation of the transducers and the chainage details. The total energy loss between the consecutive points was then calculated, and the energy slope determined based on the assumption that the secondary losses are insignificant.

During the recordings on the M1-J and M2-J pipelines, pump trips occurred leading to dynamic pressures that are graphically reflected in the appropriate figures indicated in Tables 5-1 and Table 5-2. This report does not review the dynamic pressure variation.

5.6.3 Results for pipeline Morgenstond to Jericho pipeline, M1-J (new Pipeline)

Table 5.29 reflects the data of the flow rates for the different tests that were conducted on the suction pipeline, M1-J.

Table 5.29: Recorded flow rate in the M1-J Pipeline

Data set	Flow (m^3/s)
1	1,3379
2	1,280

5.6.4 Hydraulic grade line in Morgenstond to Jericho pipeline, M1-J

Table 5.30 reflects the energy slope between the recorded positions for pipeline M1-J.

Table 5.30: Energy slope between the pressure gauging points (m/m), M1-J

		Energy slope (m/m)		
		Gauging chainage positions		
Data set	**Flow (m^3/s)**	**447,1 to 2749**	**2749 to 7498**	**447,1 to 7498**
1	1,3379	0,006954	0,003825	0,004847
2	1,280	0,004757	0,001368	0,002474

5.6.5 Results for the Morgenstond to Jericho pipeline M2-J (Old pipe)

The following three different flow rates were evaluated as is reflected in **Table 5.31**.

Table 5.31: Flow rates in the Morgenstond to Jericho pipeline M2-J (Old)

Flow set	Flow (m^3/s)
1	0,861
2	0,815
3	0,742

5.6.6 Hydraulic grade line in the Morgenstond to Jericho pipeline M2-J

The results obtained from the field work for the M2-J pipeline are reflected in **Table 5.32** and the energy slope is reflected in **Table 5.33**.

Table 5.32: Summary of the recorded pressures (mAmp) on the old Morgenstond to Jericho pipeline, M2-J

Chainage (m)	Box	Transducer	Channel	Recorded data					
				Time – 17/01/2008		Zero reading (mA)	Average pressure recording of Data Set (m)		
				Start	End		Flow set 1 0,861	Flow set 2 0,815	Flow set 3 0,742
P1/947	1	125088	2	9h21	16h30	4,093	46,36	44,80	42,23
P2/4831	2 #	PT 2	1	13h16	16h45	4,547	22,89	22,14	20,85
P3/7500	3	PT 3	1	10h49	16h58	4,228	15,12	14,92	14,56

Note:

Re-calibration of the equipment after the field tests were conducted, reflected that Box 2 give inconsistent readings

Table 5.33: Energy slope between the pressure gauging points (m/m), M2-J

		Energy slope (m/m)		
		Gauging chainage positions		
Flow set	**Flow (m^3/s)**	**947 to 4831**	**4831 to 7493**	**Average slope – 947 to 7493***
1	0,861	Box 2 gave inconclusive results #		0,002483
2	0,815			0,002274
3	0,742			0,001935

Notes:

* Close to air valve on new line

\# Data recorder (Box 2) gave inconsistent readings

5.6.7 Results for pipelines from Jericho Dam to Onverwacht reservoirs, J1-O and J2-O

Similar to the discussion above for the pipeline between Morgenstond Dam and Jericho Dam the pipelines (the J2-O pipeline and the J1-O pipeline) between the Jericho Dam and the Onverwaght Reservoir are discussed in this section.

5.6.8 Flow rate in the J1-O pipeline

The flow was recorded on the J1-O pipeline while the flow rate in the J2-O pipeline was obtained from the display in the control room at Jericho Dam, because it was impossible to obtain access on the J2-O pipeline and hence the flow rate displayed (2 decimals of m^3/s) had to be used.

Table 5.34 and **Table 5.35** reflect the hydraulic grade line and the energy slope in the J1-O pipeline.

Table 5.34: Hydraulic grade line based on average pressure heads for the different flow rates in the Jericho – Onverwacht pipeline, J1-O

		HGL for the different flow rates (m)		
		Chainage (m)		
		640	**11000**	**20523**
		Elevation (m)		
Data set	**Flow (m^3/s) #**	**1473,745**	**1537,545**	**1513,73 ##**
1	1,125	1776,584	1740,742	Unreliable
2	0,953	1752,821	1730,752	

Note:

\# The measured flow rate in the pipeline from Jericho Dam to Onverwacht Reservoir is suspect

\# \# Data from Box 2 at Chainage 20523 m was unreliable

Table 5.35: Energy slope between the pressure gauging points (m/m) on the Jericho – Onverwacht pipeline, J1-O

		Energy slope (m/m)		
		Gauging chainage positions		
Data set	**Flow (m^3/s) #**	**640 to 11000 #**	**11000 to 20523 ##**	**640 to 20523**
1	1,125	0,0034596	Unreliable	Not calculated
2	0,953	0,0021303		

Note:

The measured flow rate in the pipeline from Jericho Dam to Onverwacht Reservoir is suspect

Data from Box 2 at Chainage 20523 m was unreliable

5.6.9 Overview of the results of the Usutu State Water Scheme Pipelines

It has been indicated that the measurement of the flow in the Jericho-Onverwacht pipelines were suspect and therefore the analyses to determine the roughness parameter in these pipelines was not reviewed in detail.

In the case of the Morgenstond to Jericho pipelines, the flow and pressure recordings were used to determine the roughness parameter of the two pipelines. **Table 5.36** reflects the summary of the results for the Morgenstond to Jericho pipelines.

Table 5.36: Summary of the results for the tests that were conducted on the Morgenstond to Jericho Pipelines

Pipeline (sections)	**Constructed**	**Relined (CML)**	**Friction parameter calculated with the following relationships**			
			Colebrook-White, k_s (mm)	**Barr, k_s (mm)**	**Hazen Williams, C**	**Manning, n ($s/m^{0,333}$)**
M1-J (S1 and S2)	2003	-	0,533	0,522	117,971	0,012
M2-J (S1 and S2)	1964	1999	0,963	0,945	113,404	0,013

With the objective to compare the efficiency of the different pipelines an indicative parameter was defined. The minimum value of Sf/Q% for the comparative pipes will indicate the most effective pipe for a unit transfer rate.

Figure 5.22 and **Figure 5.23** reflect the relationships of the efficiency (parameters described below) of the pipelines M1-J and M2-J. M1-JS1 and M1-JS2 respectively refer to section S1 and section S2 of the Morgenstond-Jericho pipelines.

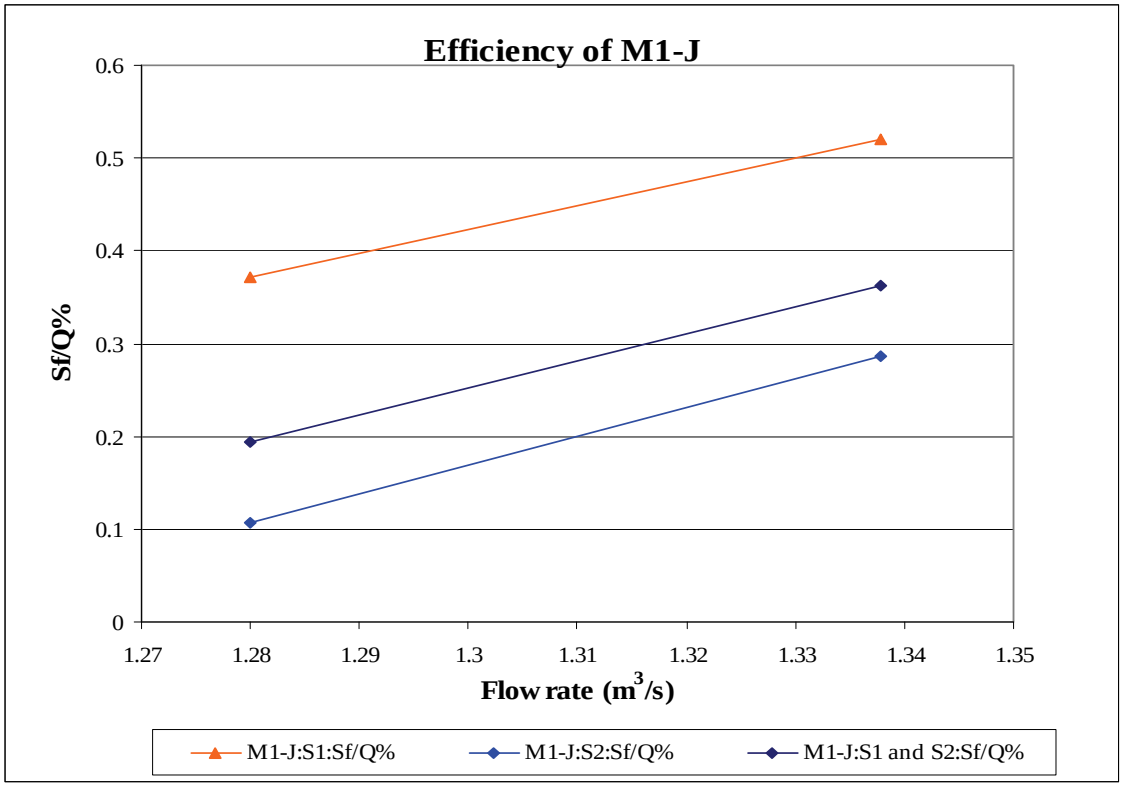

Figure 5.22: Graphical representation of the efficiency of pipeline M1-J

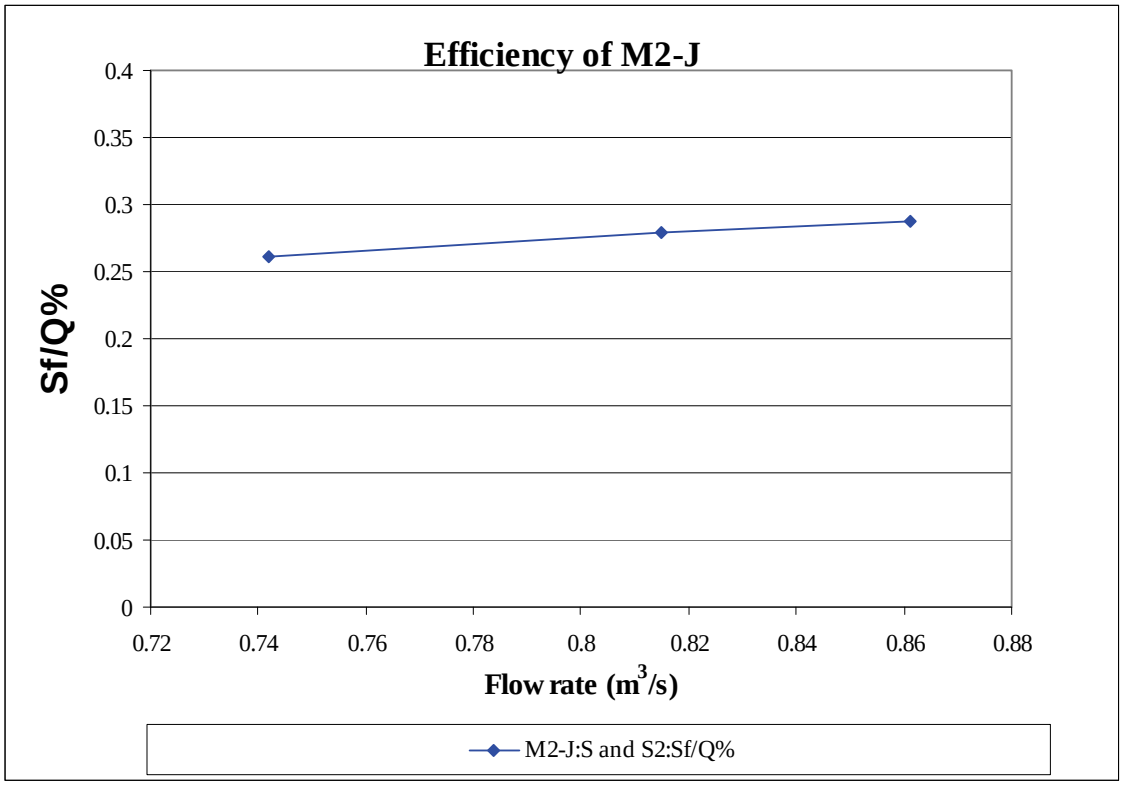

Figure 5.23: Graphical representation of the efficiency of pipeline M2-J

In **Figure 5.24** the efficiency of M1-J and M2-J is compared.

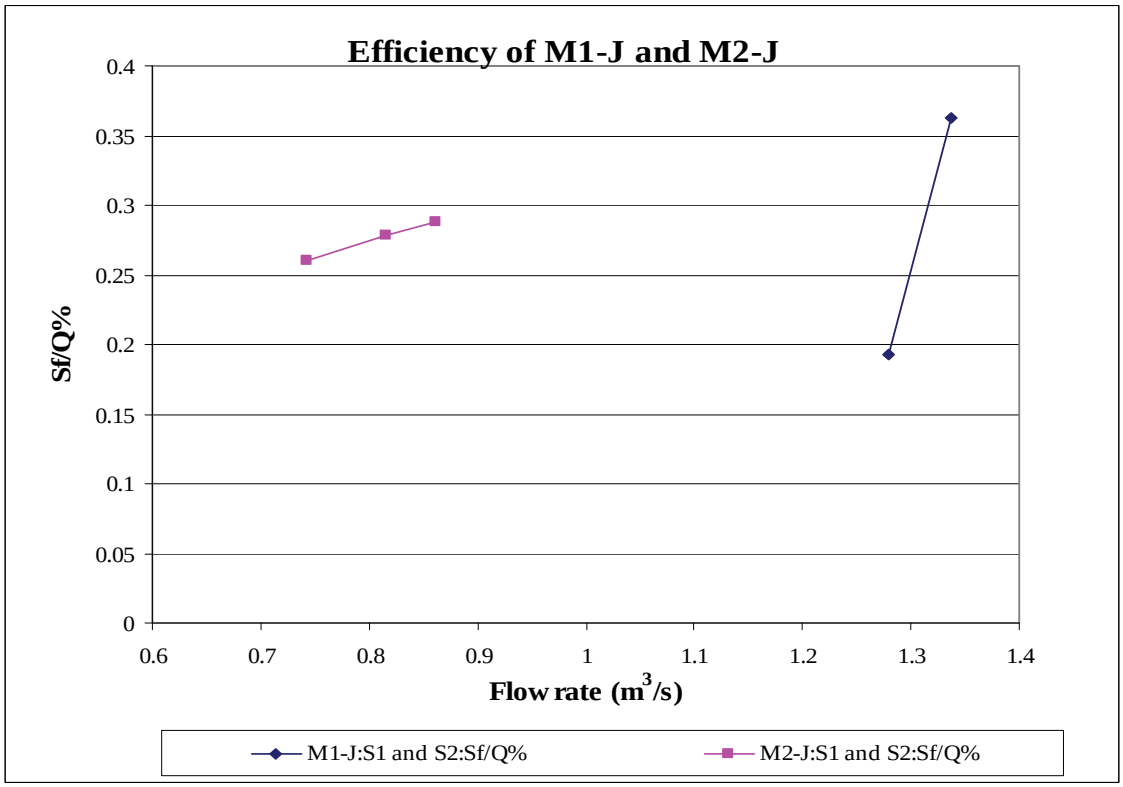

Figure 5.24: Graphical comparison of the efficiency of pipelines M1-J and M2-J

The comparison **of the two pipelines from Morgenstond Dam to Jericho dam (**Figure 5.22 and **Figure 5.24)** reveals that:

- The first section of the M1-J pipeline has a lower hydraulic capacity than the latter section of the pipeline (Change in roughness) and
- That the new pipeline (M1-J) is performing better than the old pipeline (M2-J) for the flow rate up to 1,3 m^3/s.

5.7 Pipeline from Hendrina to Duvha Power Station

5.7.1 Recorded data

As described earlier, most of the measuring points were equipped with two pressure transducers. Readings from both these pressure transducers were captured on a data logger. The logged data, measured in milliamps, were converted into pressure (based on the specific pressure transducers' range) when installed at the measuring point.

The recorded pressure difference between the two pressure transducers at each of the pressure recording nodes were determined for the whole data set and the average and maximum difference where calculated as shown in **Table 5.37**.

Table 5.37: Pressure transducer comparisons

		Recorded pressure variance between the two pressure transducers which were installed	
Measuring point	**Chainage (m)**	**Average pressure difference (m)**	**Maximum pressure difference (m)**
HD 1	30170	0,23	0,37
HD 2	23620	0,19	0,03
HD 3.1	17089[#]	0,37	0,57
HD 3.2	17078[#]	0,06	0,38
HD 4	8475	0,13	0,18
HD 5	2775	0,05	0,21
HD 6	1750[*]	n.a.	n.a.

Notes: * Only a single pressure transducer was connected at this measuring point

[#] Turbulence experienced at the line control valve.

The HGL is the sum of the recorded pressures at the measuring points, plus the surveyed elevation height obtained from the Surveyor, Mr Ian McIlrae. **Figure 5.25** depicts the calculated average hydraulic grade line (HGL) for a typical measuring point (HD 1) over the recording period undertaken on 8 February 2011 and 3 March 2011. The average HGL is based on the average pressure of the two pressure transducers, except for measuring points HD 6, where only one pressure transducer could be installed on 3 March 2011. These recording periods varies reflecting the time when the recording was started at the different recording positions.

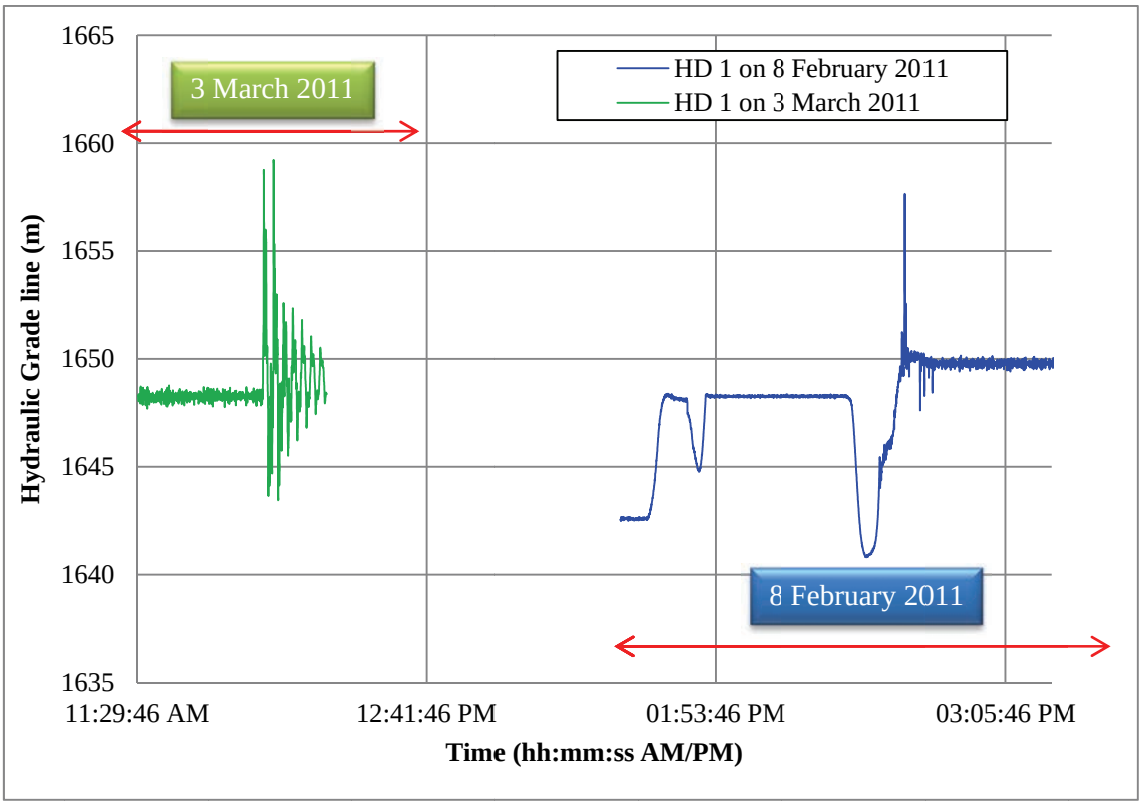

Figure 5.25: HD 1 – Recorded HGL (Chainage 30 170 m, Elevation 1625.321 m)

5.7.2 Flow recordings

Flow rate was recorded at a frequency of 0,2 Hz by ATLANTA INSTRUMENTS. The flow data from the MagFlow flow meter at the Hendrina Power Station was also electronically recorded by EKSOM's operational staff. Flow metering by ESKOM is undertaken according to ESKOM's described protocol for flow recordings. This protocol was not made available to the Research Team, although from the recorded data it is visible that ESKOM records flow rate at intervals varying between 19 sec and 20 sec with a maximum of 4 reading per minute if the first reading is taken within 3 seconds of the starting minute. These recorded flow data is indicated in **Figure 5.26**. The recorded flow measurements by ATLANTA INSTRUMENTS were approximately the same as that measured

by ESKOM. **Table 5.38** reflects the recorded flows at the times when the system was reflecting constant pressures at the pressure gauging positions.

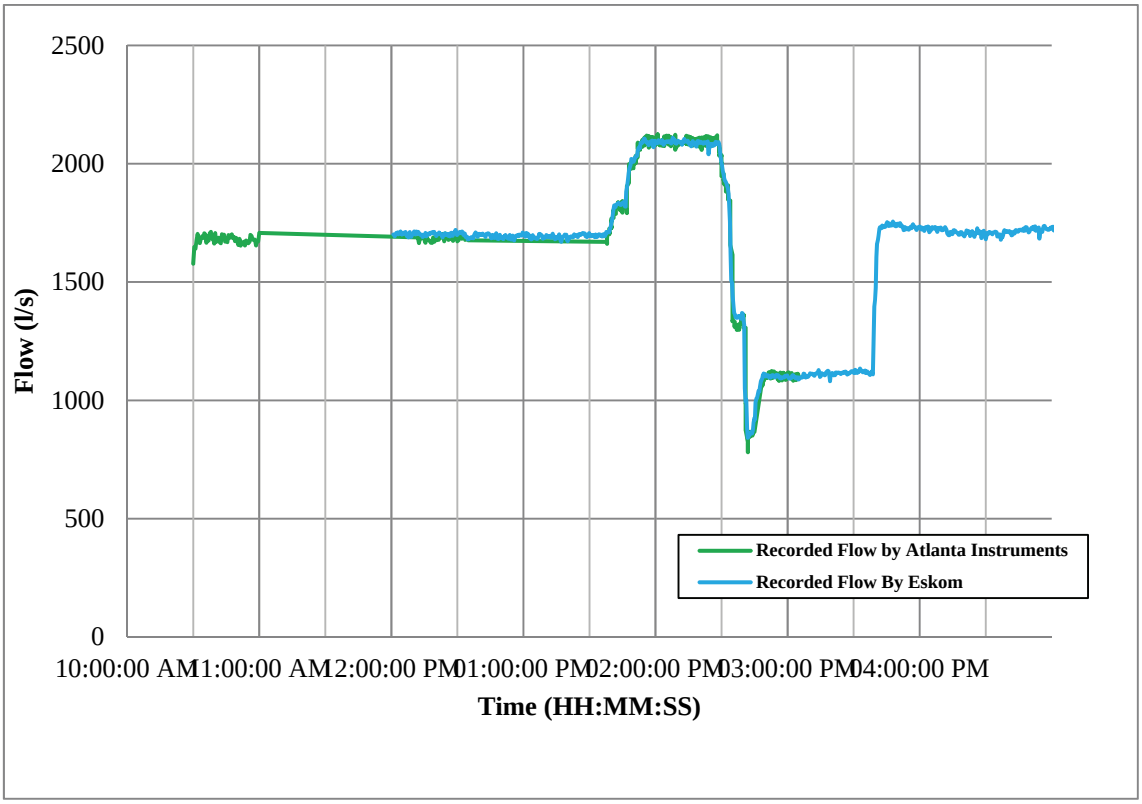

Figure 5.26: Recorded flow data by Atlanta Instruments and Eskom

Table 5.38: Flow rates in the Hendrina to Duvha Pipeline

Time	Flow (l/s)	Velocity (m/s)
12:00:58 PM	1700,81	1,14
12:01:38 PM	1692,66	1,14
01:42:58 PM	1829,53	1,23
01:43:10 PM	1834,03	1,23
02:07:54 PM	2109,56	1,42
02:08:04 PM	2109,56	1,42
02:36:18 PM	1362,47	0,91
02:36:20 PM	1362,47	0,91

The flow rate in the Hendrina to Duvha pipeline is influenced by the following factors:

- The recorded pressures in the pipeline just downstream from Hendrina, reflects that the energy is not controlled by the levels in the storage reservoir at Hendrina, elevation 1 644,10 m;

- High dynamic pressures occur due to the apparent manual controlling of flow at the Duvha Power Station;
- Workable recorded pressure data sets were obtained from all the pressure gauging positions except at HD 2 where data from 8 February 2011 was lost due to a surge in the pipeline that caused the air valve chamber to flood;
- High surge pressure waves are present on a daily basis in the Hendrina-Duvha Gravity main Pipeline. At HD 6 the pressure fluctuations increase to approximately +80 m and -40 m of the current operational pressure. Closer to Hendrina (HD1), these pressure fluctuations are decreasing. This dynamic pressure variation is caused by a disturbance at the Duvha Power Station due to the operation of the needle valve that regulates the flow to the power station (**Figure 5.27**). A graphical presentation of the surge waves of 8 February and 3 March 2011 are given in **Figure 5.28** and **Figure 5.29** respectively.

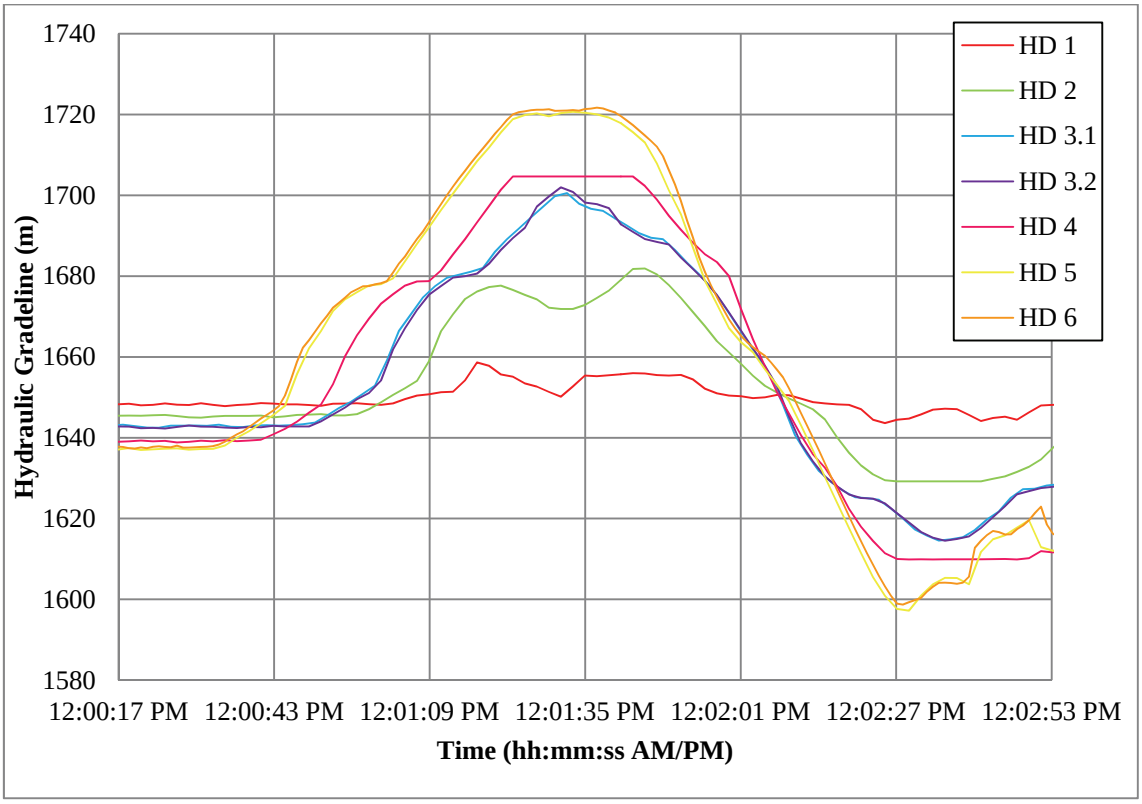

Figure 5.27: time snap of the dynamic pressure wave recorded on 3 March 2011

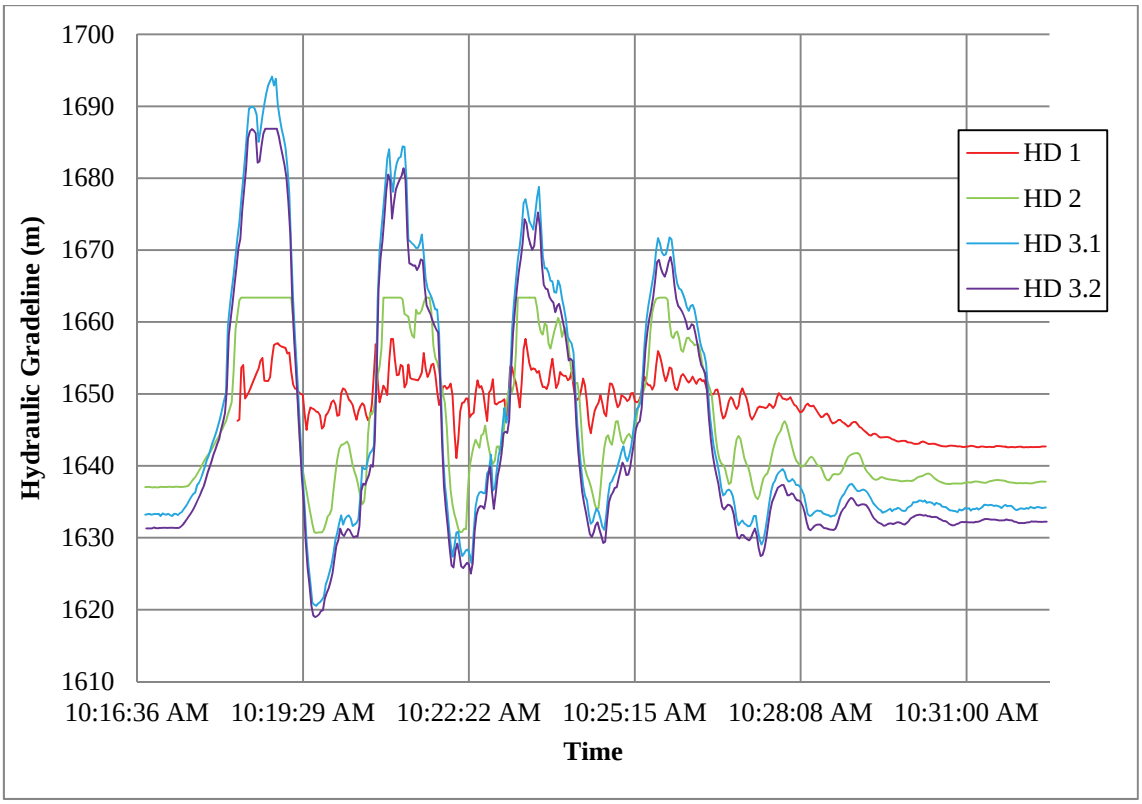

Figure 5.28: Dynamic pressure wave recorded on 8 February 2011

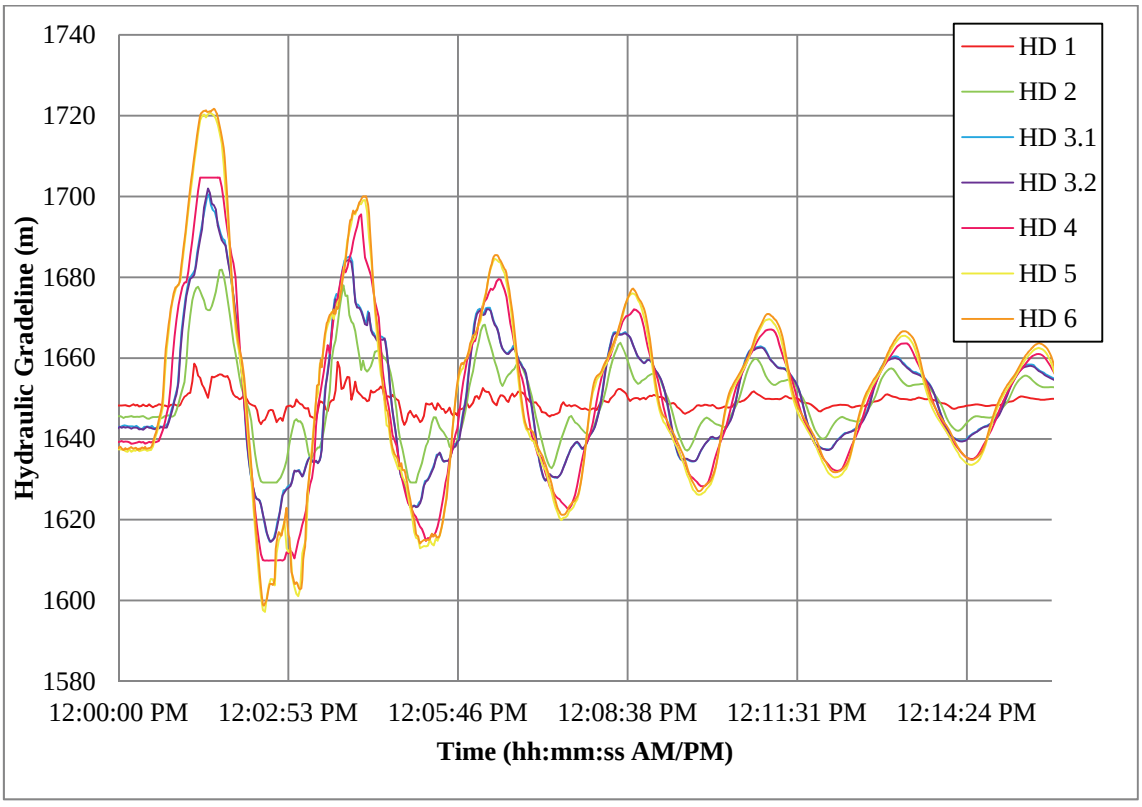

Figure 5.29: Dynamic pressure wave recorded on 3 March 2011

5.7.3 Summary of recordings conducted on the Hendrina to Duvha Pipeline

From the recorded flow and pressure recordings, 4 distinct time snap shots were selected with constant flow rates, to review the recorded pressures and flow at all the measuring points. These 4 time snap shots were selected as reflected in **Table 5.38** on 8 February 2011 (**Figure 5.30**).

Figure 5.30: Selected time snap shots for the calculation of the roughness parameter (λ)

Figure 5.31 depicts the HGLs for different flow rates. Although the HGL values were simply connected with straight lines in **Figure 5.31,** it is acknowledged that local losses occurring at the isolating valves are not reflected in **Figure 5.31.** These secondary losses are, however, incorporated in the recorded HGL values at each of the measuring points.

Secondary losses were incorporated for all horizontal and vertical bends, as wells as discontinuities at single small orifice air valves (SSA), single large orifice air valves (SLA), double air valves (DAV), farmers off takes (FOT), scoure valves (SV), bulk off takes (BOT) and access positions (AP) on the pipeline. The secondary loss coefficients used to calculate the secondary pressure head losses are reflected in **Table 5.39** for horizontal and vertical bends and in **Table 5.40** for all other irregularities.

The total secondary loss coefficient contributed only by the flied joints every 12 m equated to 4,57.

Table 5.39: Secondary loss coefficients assigned to horizontal and vertical plan bends (USBR, 1987)

Angle (degrees)	Secondary loss coefficient
0	0
22.5	0.05
45	0.09
67.5	0.11
90	0.13

Table 5.40: Secondary loss coefficients assigned to irregularities in pipeline

	Secondary loss coefficients due to change in									
	horizontal plane	vertical plane	SSA	SLA	DAV	FOT	SV	BOT	AP	Total K
Secondary loss coefficient (K)	**See US Bureau of Reclamation 1987**		**0.05**	**0.05**	**0.05**	**0.05**	**0.5**	**0.5**	**0.5**	
HD 1 to HD 3.1	0.69	0.51	0.35	0.70	0.60	0.55	4.00	0.50	2.50	10.40
HD 3.2 to HD 4	0.34	0.39	0.15	0.00	0.35	0.25	1.50	0.50	1.50	4.98
HD 4 to HD 5	0.26	0.26	0.20	0.25	0.25	0.10	1.00	0.50	1.50	4.31
HD 5 to HD 6	0.00	0.13	0.05	0.00	0.00	0.05	0.50	0.00	0.00	0.73

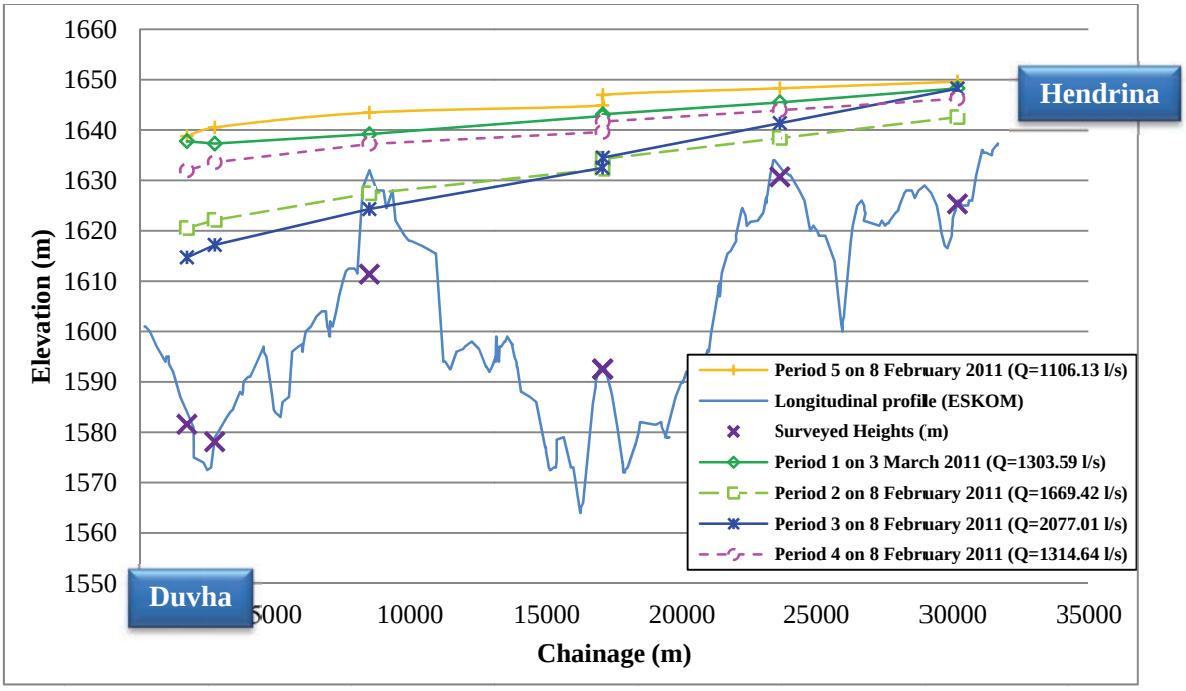

Figure 5.31: Combined graph with hydraulic grade lines

The variation in pressure recorded at position HD 6 reflects that the pressure transduces may have been faulty during the recording as the variation in pressure reflected in **Figure 5.31** is impossible. The HGL must always connect measuring positions with lines parallel to each other (lines with the same gradient). **Figure 5.32** reflects the HGL without the inclusion of the recorded data obtained from position HD 6.

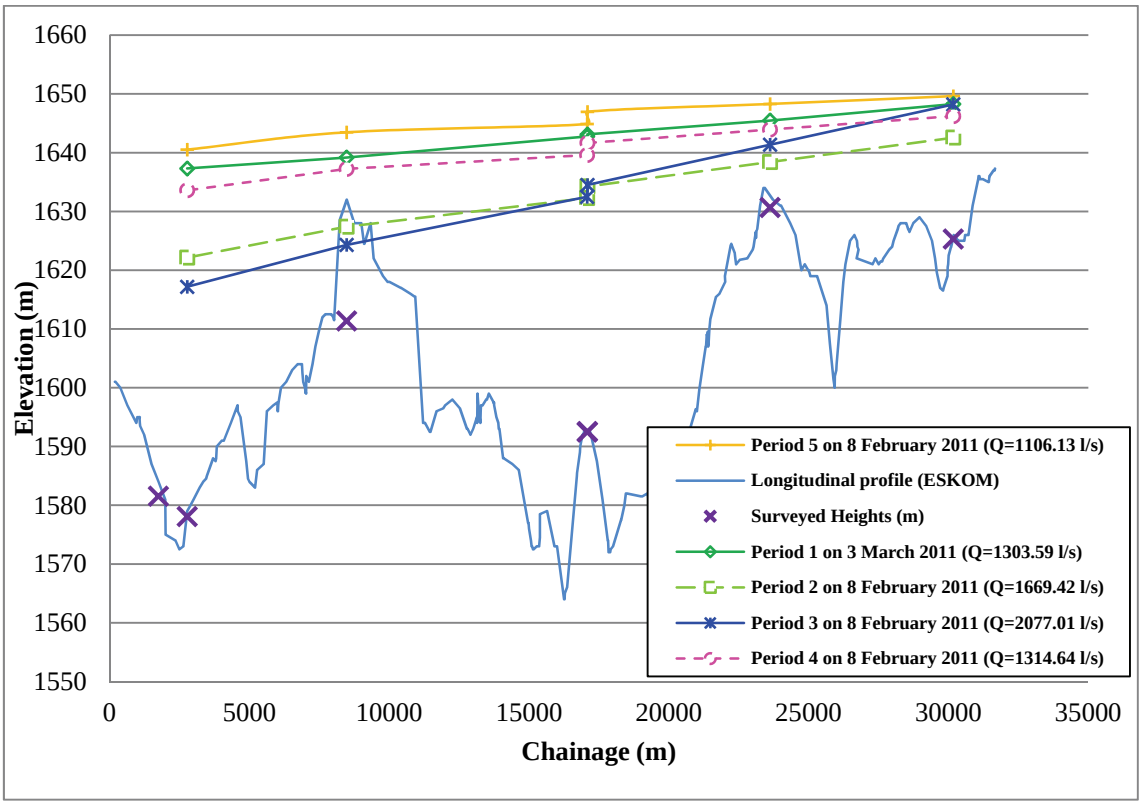

Figure 5.32: Hydraulic grade lines (discarding HD 6)

5.7.4 Calculation of hydraulic roughness in the Hendrina to Duvha Pipeline

As was indicated above it was established that in the continuous welded steel pipeline, supplying raw water from the Hendrina Power station to the Duvha power station, the secondary losses at the field joints (every 12 m) is significant and should be included in the determination of the assessment of the hydraulic capacity of pipelines.

Hendrina-Duvha Gravity Main was constructed as a continuous welded pipeline with field joints at all pipe connections. These joints tend to fail due to debonding of the field applied bitumen which then led to corrosion of the steel, unlike the factory installed lining. The process of field repairs at the joints also tend to cause a cold joint between the factory applied bitumen lining and the field placed

bitumen. An example of this on the Hendrina-Duvha Gravity Main where a cold joint is also visible is reflected in **Figure 5.33**.

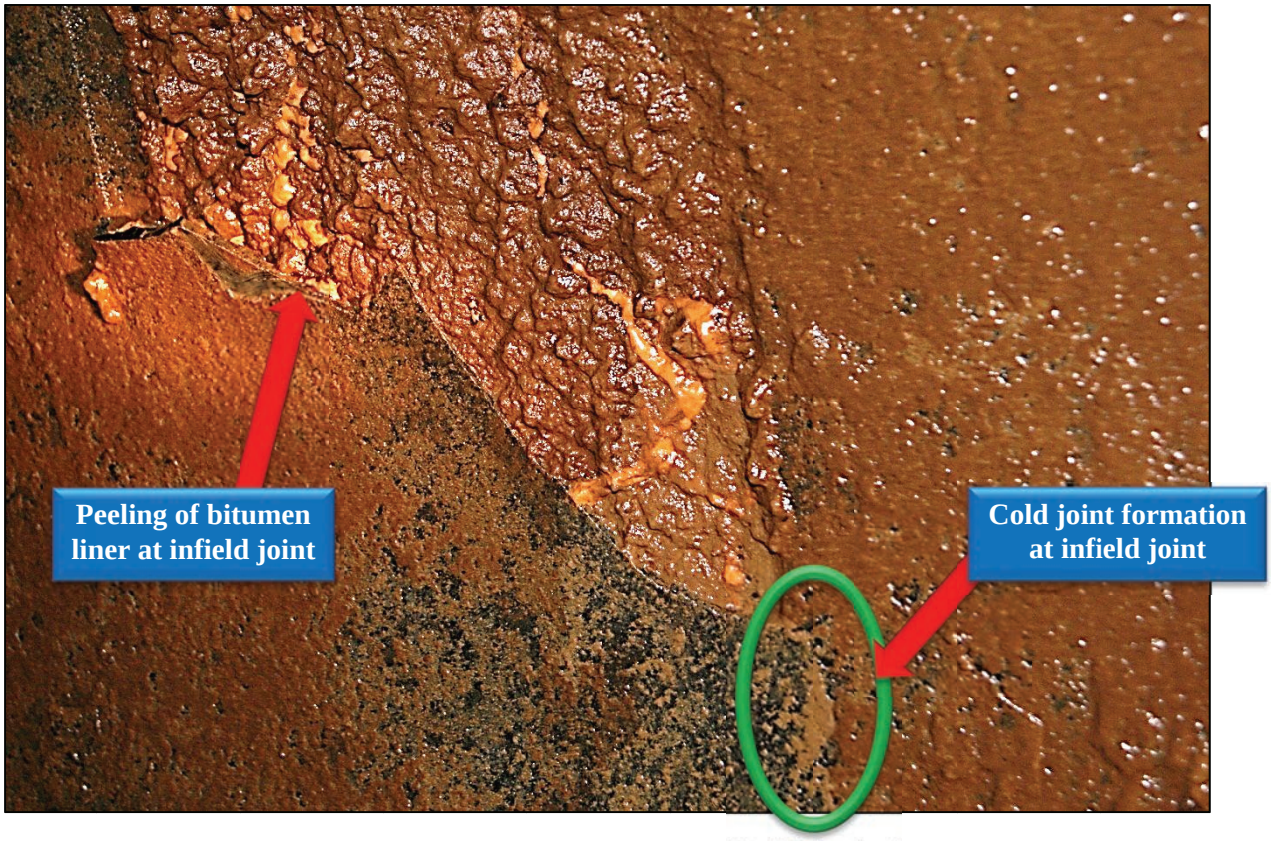

Figure 5.33: Infield joint taken at Hendrina-Duvha Gravity Main during a repair exercise on 26 May 2010

Figure 5.33 also indicates the peeling or debonding of the bitumen liner at the field joints. These debonded / peeled segments may tend to be lifted into the flow path of the transported raw water and increase the relative roughness of the pipe significantly when increased flow conditions occur. At these field joints there are also an increase in the absolute roughness of the pipe's internal wall. These field joints tend to be corroded where the bitumen liner has peeled away from the steel. Crustaceans and knobbles of rust, coated with biofilm are positioned at all these field joints. These Crustaceans or knobbles are up to a few millimetres high and will cause a significant contribution to the frictional pressure loss in the gravity main. **Figure 5.34** reflects the increase in absolute roughness at a typical field joint in the Hendrina-Duvha Gravity Main.

Figure 5.34 reflects the increase in absolute roughness at a typical field joint in the Hendrina-Duvha Gravity Main.

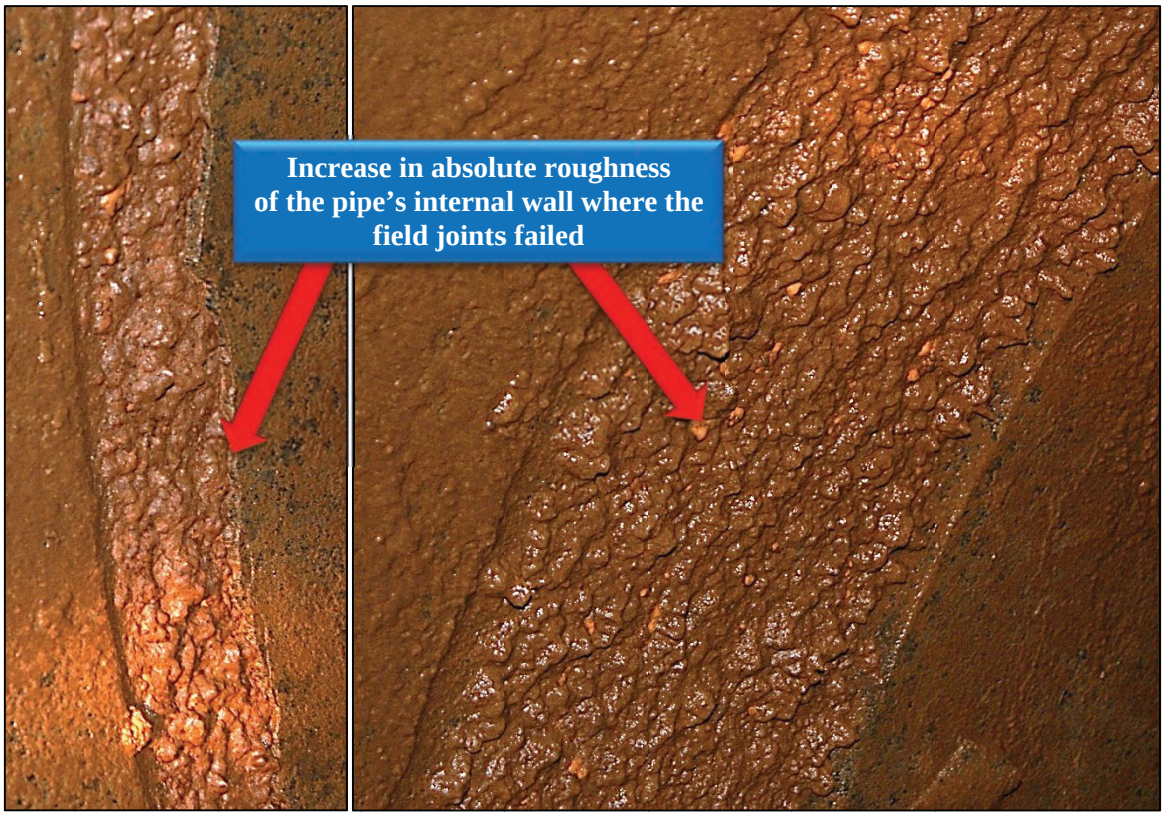

Figure 5.34: Increase in absolute roughness of the pipe's internal diameter at field joints

Without the inclusion of the secondary losses occurring at the couplings the absolute roughness calculations reflected the unexpected variation of the roughness parameter as a function of the velocity as indicated in **Figure 5.38**. From **Figure 5.38** the calculated roughness reflects that at higher flow rates the roughness seems to be higher than the calculated roughness at lower flow rates.

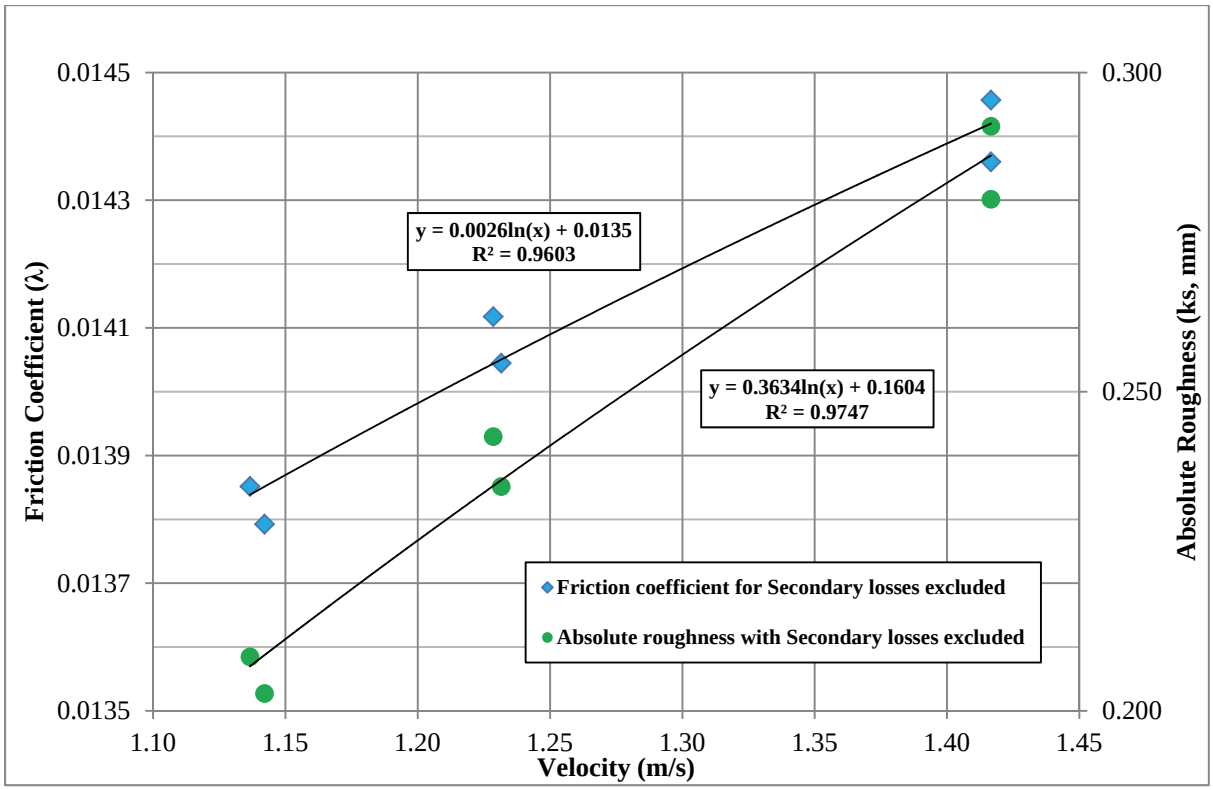

Figure 5.35: Unexpected variation in the calculated roughness of the Hendrina-Duvha pipeline when the secondary losses at the couplings were not considered

Since the full data sets of the recorded pressures at the different recording positions did not cover the pressures for the same time horizon and hence it was required to select time incidences when the flow was stable and for which the roughness could be determined. **Table 5.41** reflects the calculated roughness for the case where no provision was made for the pressure drop at the couplings or air valve discontinuities.

Table 5.41: Calculated roughness in the Hendrina Duvha Pipeline excluding the influence of the losses at the couplings.

Flow (l/s)	V (m/s)	Lambda (λ)	Reynolds number	CWT[#] (ks, mm)	Moody (ks, mm)
1700,81	1,14	0,0138	1379519	0,203	0,186
1692,66	1,14	0,0139	1372904	0,208	0,191
1829,53	1,23	0,0141	1483922	0,243	0,218
1834,03	1,23	0,0140	1487572	0,235	0,212
2109,56	1,42	0,0145	1711054	0,292	0,257
2109,56	1,42	0,0144	1711054	0,280	0,248

Note: [#] Colebrook-White Transition (CWT) equation

The roughness were recalculated with the incorporation of the losses at the couplings, air valves, access holes, bulk off takes and farmer supply lines. **Table 5.43** reflects the calculated roughness's and reflects the energy loss associated to the secondary losses at these positions. The results are also graphically presented in **Figure 5.41**.

Table 5.42: Absolute roughness for the Hendrina-Duvha Gravity Main including secondary losses

Flow (l/s)	V (m/s)	Lambda (λ)	Reynolds number	CWT# (ks, mm)	Moody (ks, mm)	Frictional Headloss	Secondary Headloss
1685,81	1,13	0,01287	1367353	0,117	0,115	13,23	1,58
1685,81	1,13	0,01288	1367353	0,118	0,116	13,24	1,58
1832,16	1,23	0,01287	1486051	0,123	0,119	15,03	1,87
1831,78	1,23	0,01291	1485747	0,127	0,122	15,28	1,87
2109,56	1,42	0,01320	1711054	0,162	0,149	20,97	2,48
2109,56	1,42	0,01314	1711054	0,156	0,144	20,87	2,48

Colebrook-White Transition (CWT) equation

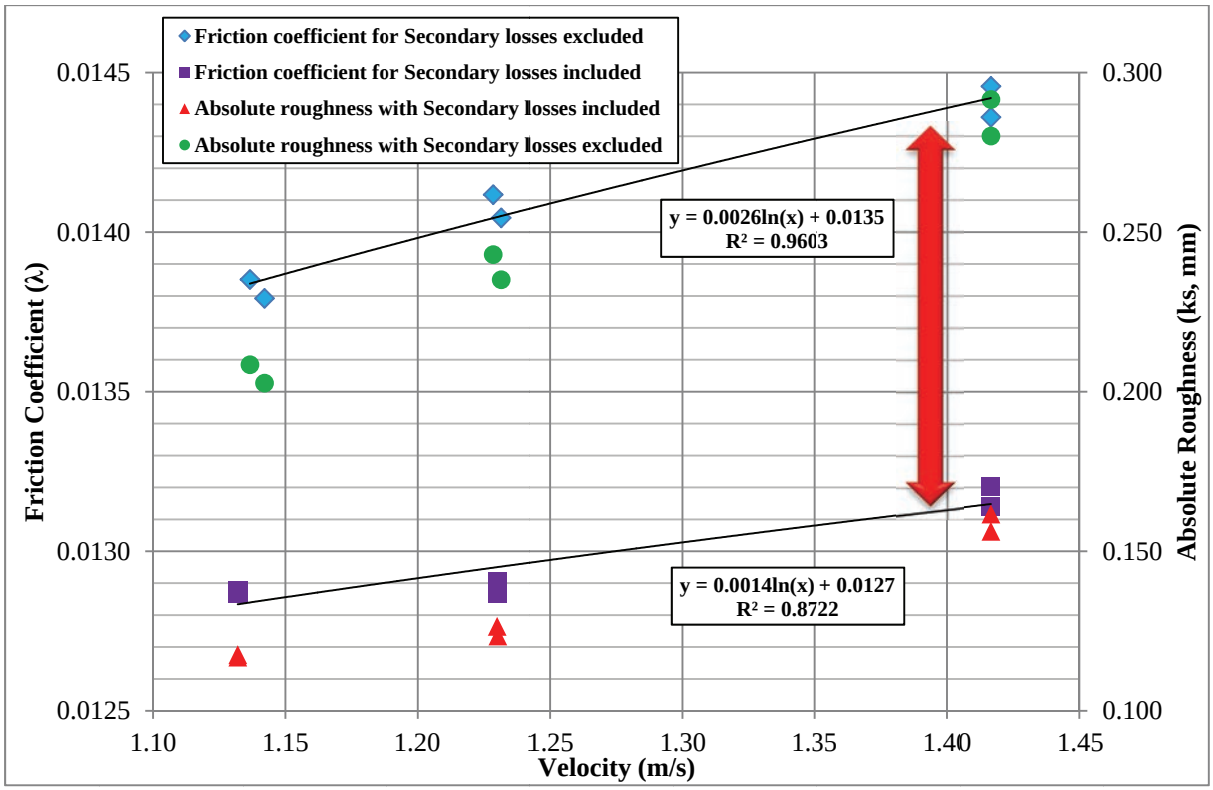

Figure 5.36: Comparison of absolute roughness of the Hendrina-Duvha Gravity Main

This case demonstrates the severity of the secondary losses associated with the failure of the field joints.

Roughness stay constant with increased flow rate; however, the contribution of pressure loss only by considering secondary pressure losses at all field joints **have a significant influence on the absolute roughness of the pipeline**. The contribution of secondary pressure losses to absolute roughness are reflected by the red arrow in **Figure 5.41**. The absolute roughness of the Hendrina-Duvha Gravity Main when considering a secondary pressure loss coefficient (k) at all field joints of 0.002 was calculated to be **0,15 mm** compared to 0,25 mm if secondary losses are ignored.

Common expectations that pipelines operate within the full-turbulent flow regime region rendering to the Moody-diagram was also investigated. According to the recorded data measurements of the Hendrina-Duvha Gravity Main it was found that operation of the pipeline in all cases are within the transition flow regime which necessitates the use of relationships which include the influence of the liquid's inherent resistance (Moody, Barr, and Colebrook-White) different to the renowned Karman-Prandtl relationship. Reference to these recorded measurements that fall within the transition flow regime reflected graphically on the Moody-diagram, is reflected in **Figure 5.37**.

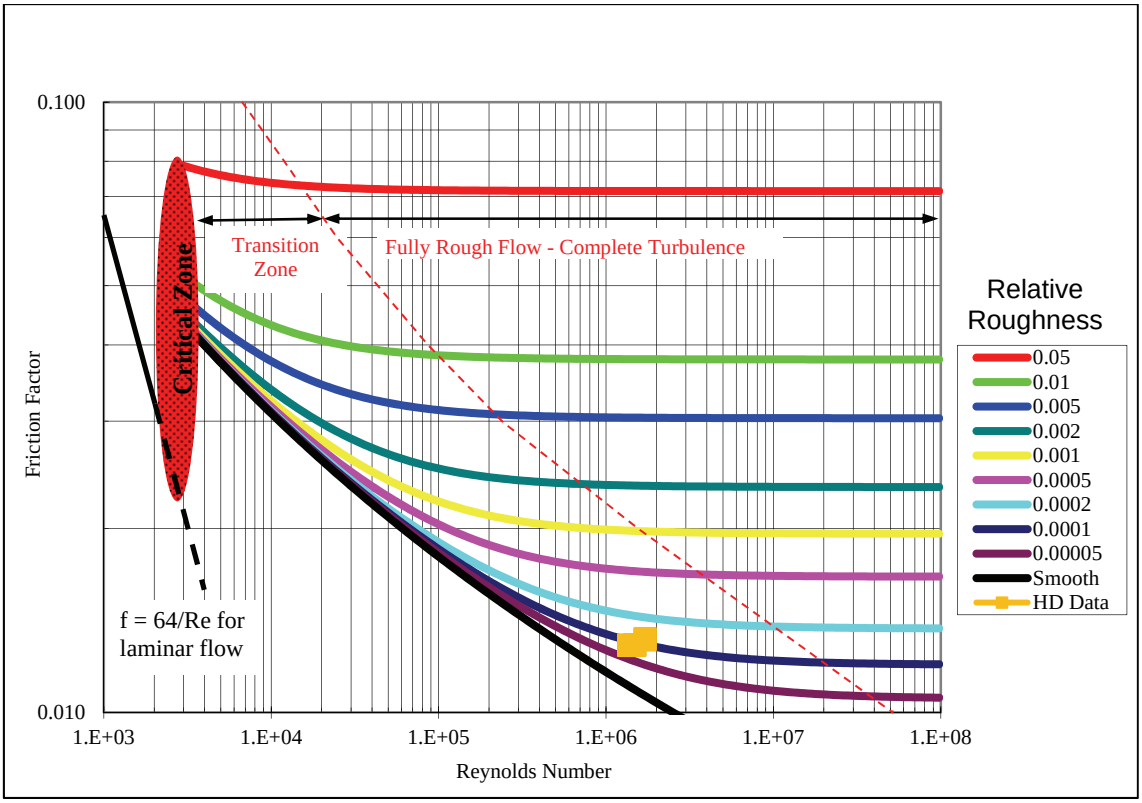

Figure 5.37: Recorded data observed for Hendrina-Duvha Gravity Main fall within the transition flow regime

5.7.5 Comparing the current absolute roughness to the initial absolute roughness of the Hendrina to Duvha Pipeline (assessment of the pipe aging)

It was indicated before that no historic assessment of the roughness was conducted and hence no decay of the roughness can be calculated. It is however, worth noticing that these values that were calculated indicated that the absolute roughness was much greater than when compared with a new bitumen lined pipe. A typical new bitumen coated pipeline has a claimed absolute roughness in the order of 0,1 mm *(EDSTech, Mecaflux, Simmons et al)*. Roughness values measured here were in some cases more than four times that of a new pipe which might be an indication that the current bitumen coating in the Hendrina-Duvha Gravity Main pipeline is cracking and pealing. This is causing a decrease in the hydraulic capacity of the pipeline and ultimately leading to inefficient operation and higher energy usage.

When comparing the current state of the Hendrina-Duvha Gravity Main's absolute roughness (k_s) to the typical design values as stated by *EDSTech, Mecaflux, and Simmons et al* there is a clear indication that aging of the bitumen lining has taken place. This aging effect can be illustrated by simulating the flow rate during time snap 3 and the current absolute roughness value, (which was the most severe in terms of headloss during time snap 3), with that of a new bitumen lining for the Hendrina-Duvha Gravity Main. From this simulation it is possible to calculate and compare the hydraulic grade lines for the different scenarios by considering the influence of the current absolute roughness with the absolute roughness of a newly bitumen lining. The simulated friction loss parameters and headloss in the system are reflected in **Table 5.43**. The hydraulic grade line values for the new bitumen lined pipeline are indicated in **Table 5.44**. **Figure 5.38** reflects the comparison between the current hydraulic grade line and that of a newly bitumen coated pipe's hydraulic grade line with simulated flow rate.

Table 5.43: Simulated headloss parameters for a flow of 2077 l/s

Measured flow (l/s)		2077,01		
Calculated velocity (m/s)		1,355		
Re		1 660 533		
H_L(m) – Total secondary losses		2,012		
Length between HD 1 and HD 5 (m)		27384	**Simulated head loss for new bitumen lined pipe**	
Absolute roughness – ks(mm)		0,01	**H_f (m)**	**S_f (m/m)**
Friction factor (λ)	**Kármán& Prandtl**	0,011253	20,643580	0,000754
	Colebrook-White transition	0,012440	22,821816	0,000833
	Barr	0,012540	23,003966	0,000840
	The Moody diagram	0,012468	22,873133	0,000835
	Colebrook-White combination	0,012440	22,821816	0,000833
Manning – n ($s/m^{1/3}$)		0,0105		
Hazen-Williams – C		143,8		

Table 5.44: Hydraulic grade line for simulated absolute roughness conditions

Measuring point	**Chainage (m)##**	**Hydraulic Grade line (m) calculated by:**				
		Kármán& Prandtl	**Colebrook-White transition**	**Barr**	**The Moody diagram**	**Colebrook-White combination**
HD 1	30170	1648,220	1648,220	1648,220	1648,220	1648,220
HD 2	23620	1643,282	1642,761	1642,718	1642,749	1642,761
HD 3.1	17089	1638,359	1637,318	1637,231	1637,294	1637,318
HD 3.2	17078	1636,339	1635,297	1635,210	1635,273	1635,297
HD 4	8475	1629,853	1628,128	1627,983	1628,087	1628,128
HD 5	2775	1625,556	1623,377	1623,195	1623,326	1623,377

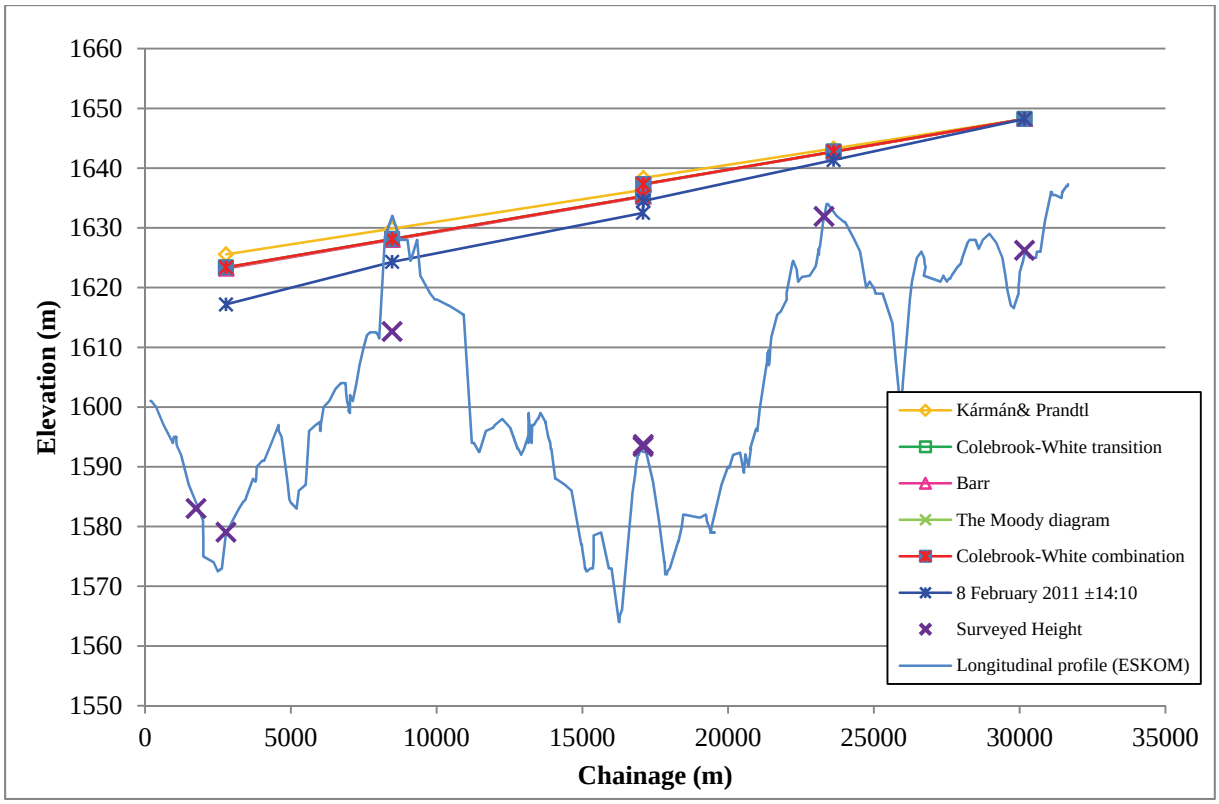

Figure 5.38: Hydraulic grade line for simulated new bitumen lining versus current bitumen lining during time snap 3

When comparing the new simulated bitumen liner to the current bitumen liner installed in the Hendrina-Duvha Gravity Main there is a clear indication that pressure head loss due to the absolute roughness have a significant influence on the hydraulic grade line. This is portrait by the fact that the excess pressure at Duvha-Power station could potentially be increased by ± 6.5 m should a new bitumen liner be considered. Raw water can thus be more efficiently transported from Hendrina Power Station to Duvha Power Station. However, because the Hendrina-Duvha Gravity Main was converted from a pumping main to a gravitating main the importance of conveying water efficiently is of lower importance, unless Duvha-Power Station requires inflow at a specific head or specific flow rate.

5.7.6 Biofilm growth in Hendrina0Duvha Gravity Main

In the above **Figure 5.33** and **Figure 5.38** visible biofilm growth on the bitumen lining, as well as the crustaceans or knobbles at the field joints can be noticed. The biofilm tend to form blobs of biofilm that are scattered at random positions in the pipeline. Scattered blobs of biofilm are reflected in **Figure 5.39**. The biofilm have a thickness of up to 2 mm in some cases and will significantly

contribute to the pipe's absolute roughness. The biofilm can easily be removed by hand and is reflected in **Figure 5.40**.

Figure 5.39: Blobs of biofilm scatted throughout the Hendrina-Duvha Gravity Main

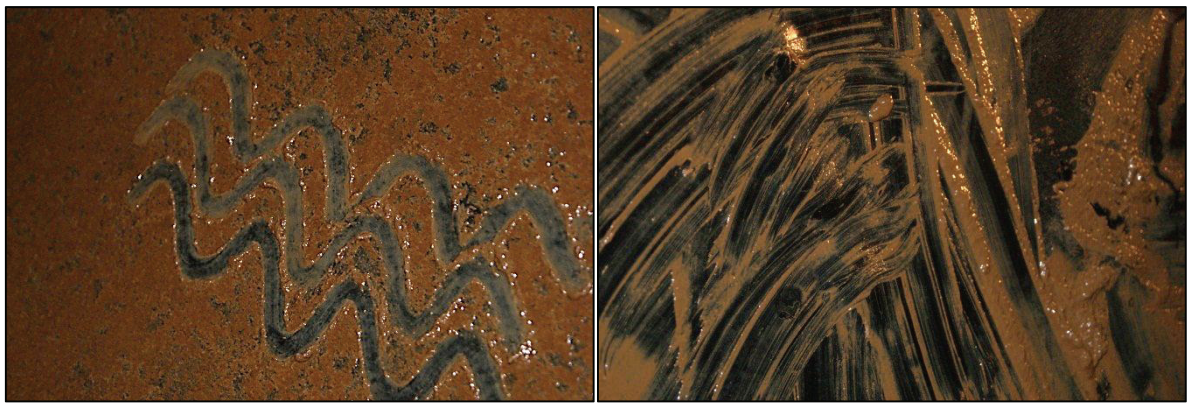

Figure 5.40: Biofilm thickness up to 2 mm in the Hendrina-Duvha gravity Main

The contribution of biofilm growth to pressure head loss was not included in the calculations of absolute roughness for the Hendrina-Duvha Gravity Main.

5.8 Lower Blyde River Irrigation System

5.8.1 Introduction

In the case of the Lower Blyde River Irrigation System it was reported by the operational staff that the hydraulic capacity of the gravity pipeline connecting the source (Blyderivierpoort Dam) with the Strainers was insufficient to provide the demand which was lower than the design capacity of the pipeline.

The first section of the pipeline was reviewed to quantify the hydraulic performance and then to identify the factors which contribute to the reduction of the hydraulic capacity.

During a field investigation it was discovered that the pipeline experienced excessive biofilm growth with residue material deposited in the biofilm. This aspect was investigated and the results are discussed below.

5.8.2 Assessment of the hydraulic roughness in the upper section of the Lower Blyde River Irrigation Scheme

The recorded pressure heads were plotted and a least square regression line was fitted through the recorded data point to smooth the hydraulic grade line. **Figure 5.41** reflects the different grade lines which represent different flow rates which were evaluated during the field tests.

The flow rate was recorded with the Portaflow flow rate meter and the pipe's internal diameter was measured to be 1.462 m.

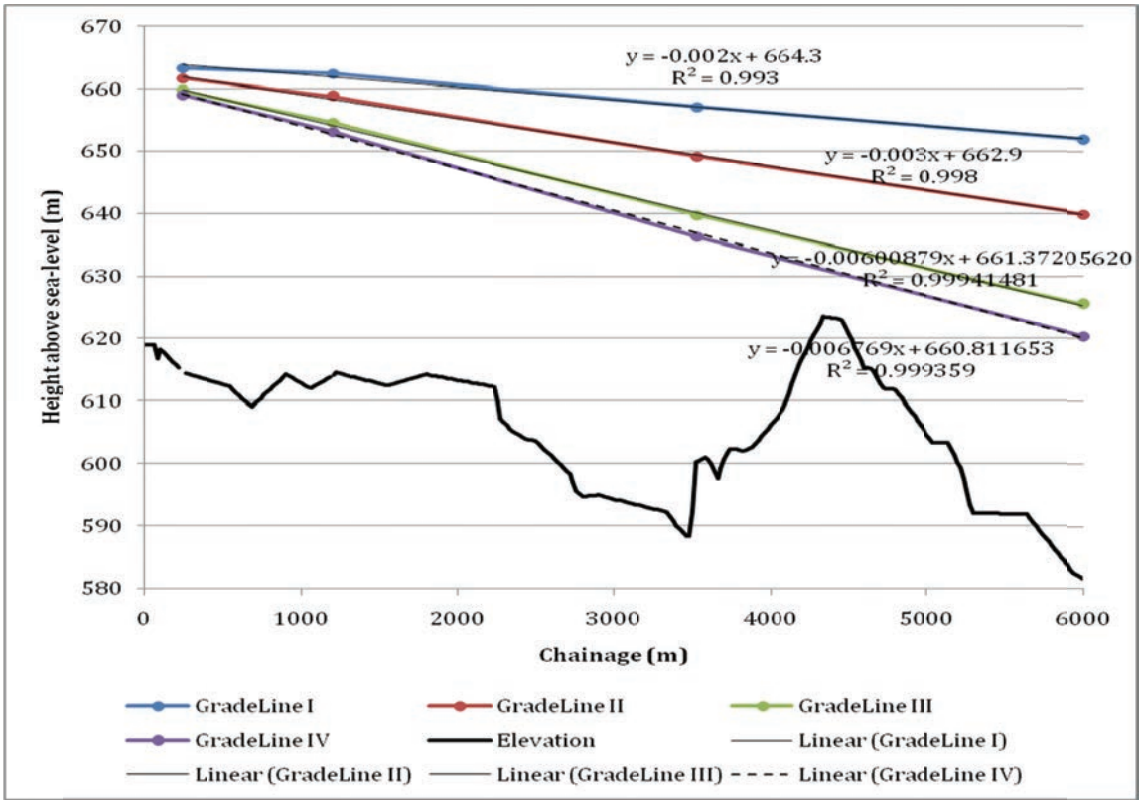

Figure 5.41: Plotted grade lines for different flow rates

5.8.3 Roughness assessment of the upper section of the Lower Blyde River Irrigation System

The gradient of each of the four grade lines were used to determine the corresponding roughness value (k_s). The roughness values were calculated with different relationships. Furthermore the deterioration of the roughness (α) was established in accordance to the linear relationship reflected in **Equation 5.3**, were determined. The roughness values, average roughness value en alpha factor are shown in **Table 5.44**.

$$k_\alpha = k_0 + \alpha t \quad \text{... (5.4)}$$

Where;

k_α = k-value after period 't' have elapsed (mm)

k_o = k-value at start of period 't', (0,5 mm used for an aged pipe)

α = growth rate per period (mm/a)

t = period [years]

Table 5.45: Roughness (k_s) values and roughness growth factors (α).

Formulation of friction parameter used	Measured flow rate (m^3/s)			
	2,85	**4,1**	**5,1**	**5,45**
	Grade line i	**Grade line ii**	**Grade line iii**	**Grade line iv**
Coolbrook C.F., and White C.M. (1939)	1.814	1.810	1.785	1.790
Barr D.I.H (1981)	1.819	1.815	1.789	1.794
Swamee P. K and Jain A. K. (1976)	1.797	1.797	1.773	1.779
Chen N. H. (1979)	1.815	1.812	1.787	1.791
Haaland S. E. (1983)	1.805	1.752	1.774	1.778
Romeo E., Royo C. and Mozon A. (2002)	1.777	1.813	1.797	1.793
Zigrang D. J. and Sylvester N.D. (1982)	1.814	1.810	1.785	1.790
Manadilli G. (1997)	1.797	1.797	1.799	1.779
Moody L.F. (1944)	1.549	1.545	1.522	1.526
Average (mm)	1.78	1.77	1.76	1.76
α (mm/a)	0.128	0.127	0.126	0.126

5.8.4 Review of the factors which could contribute to the biofilm growth in the Lower Blyde River Irrigation System

The hydrological and chemical characteristics of the inflow to the Blyderivierpoort Dam were reviewed and are discussed below.

5.8.4.1 Contributing catchments to the inflow into the Blyderivierpoort Dam

Department Water Affairs (DWA) water quality and hydraulic flow measurement structures records were used to review the LBIS background water quality. **Figure 5.42** gives an indication of the relative contribution of the three rivers flowing into the Blyderivierspoortdam. The legend in **Figure 5.42** indicated DWA code for the relevant flow measurement structure and the name of the river the

flow structure is built in. During the past eleven years the Blyde River contributed and average of 162 x 10^6 m^3/year, the Treur River 45 x 10^6 m^3/year and the Orighstad River 18 x 10^6 m^3/year.

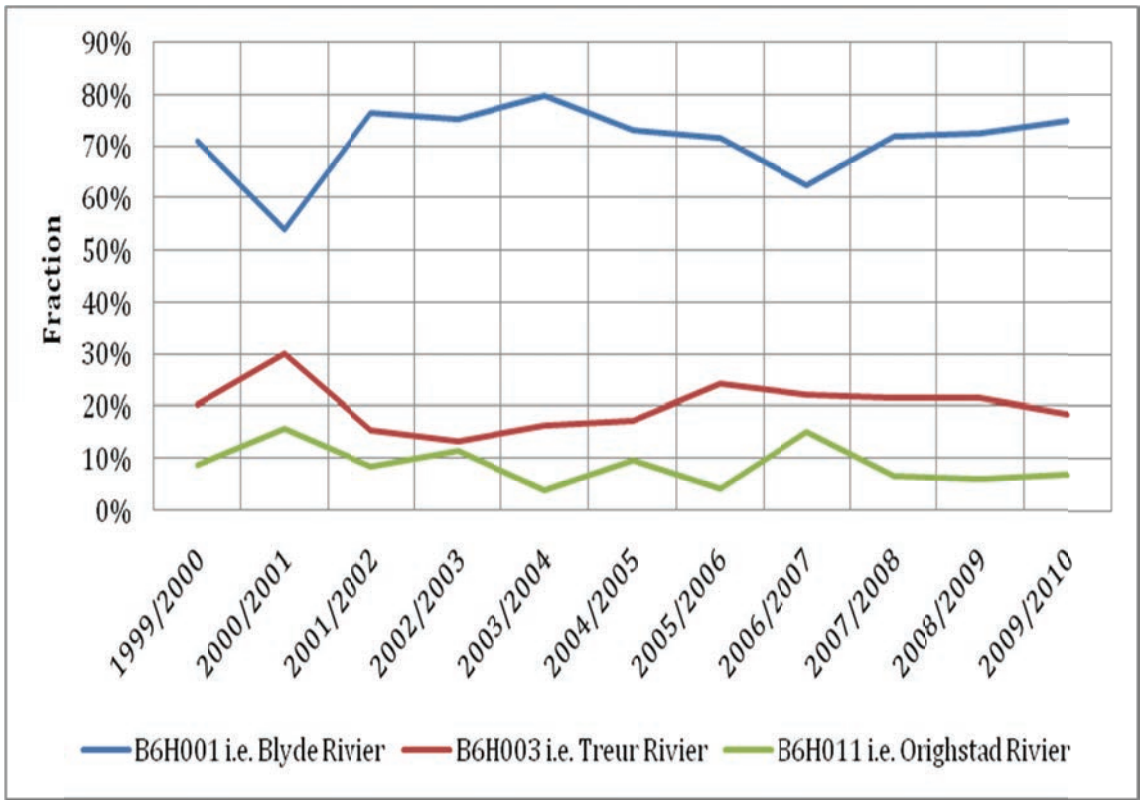

Figure 5.42: Relative flow contributions of rivers flowing into Blyderivierspoortdam

5.8.4.2 Water quality parameters of the inflow to Blyderivierpoort Dam

Water quality records were obtained from DWA. Water samples are taken at monitoring points in the Blyderivierspoortdam and in the Blyde-, Treur- and Orighstad Rivers. **Table 5.46** indicates details of the water quality monitoring points.

Table 5.46: Relevant DWA Hydrological gauging stations where the water quality is monitored

Hydrological Station	Description of the location of the Hydrological Station	River	Up or downstream of dam
B6R003Q01	Blyderivierpoort 595 Kt – on Blyde River: Near Dam Wall	Na	Near Dam Wall
B6H001Q01	Blyde River at Willemsoord	Blyde River	Upstream
B6H003Q01	Willemsoord on Treur River	Treur River	Upstream
B6H004Q01	Blyde River at Chester	Blyde River	Downstream

In order to review the background water quality a selection of water quality parameters must be made from the entire range received from DWA. The primary water quality parameters that are reported is

pH, Alkalinity and non-Calcium Magnesium hardness are reported. These three parameters play a significant role in the lifecycle and growth of the LBIS pipeline biofilm. The reported water quality graphs indicate the raw data (samples taken twice a month) and a moving average over 50 points (about two years moving average).

In the following figures the pH, Alkalinity and Non Ca-Mg Hardness are reflected for the period between 1977 and 2010 at the monitoring positions described in **Table 5.46**.

Figure 5.43 indicates the recorded pH at the monitoring points.

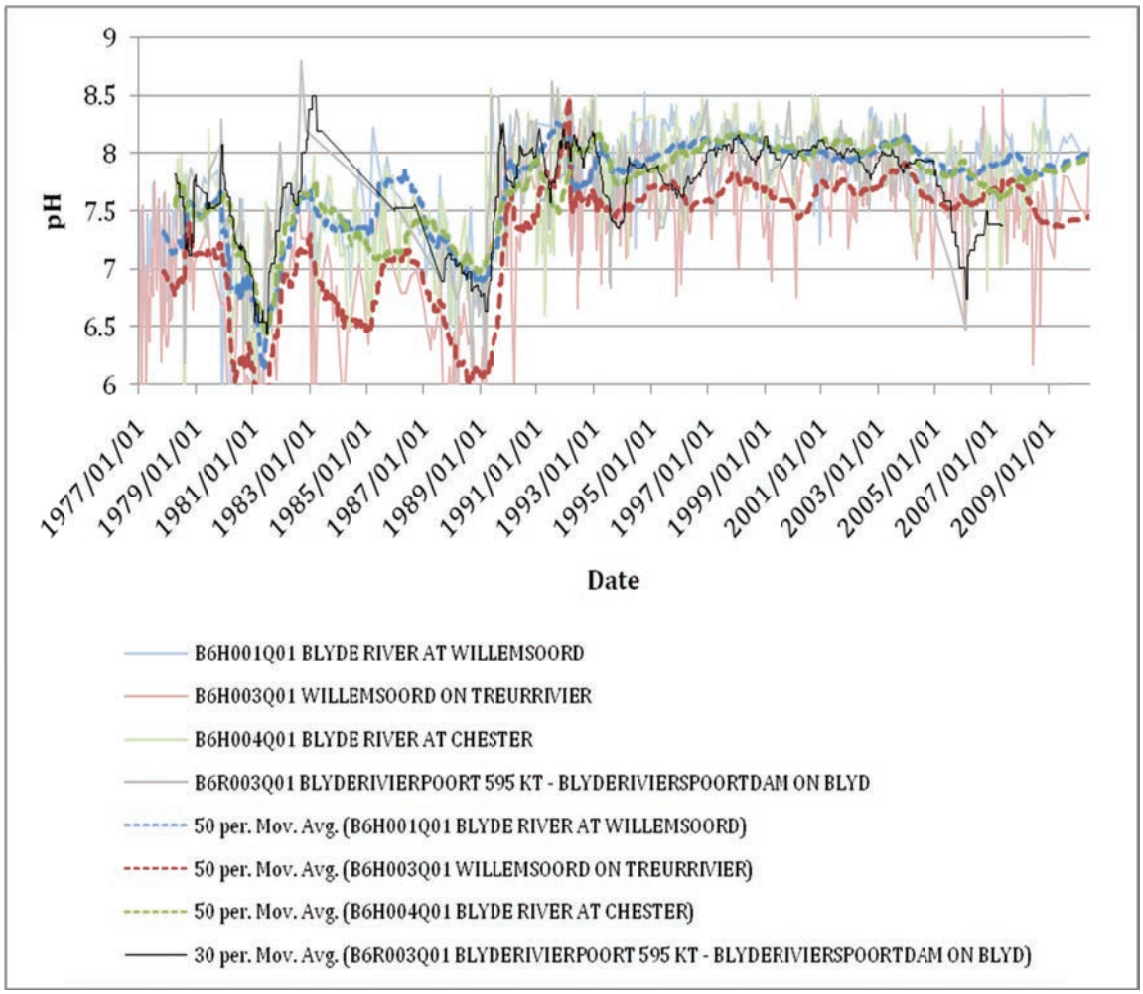

Figure 5.43: Background water quality of the LBIS: pH

Figure 5.44 indicates alkalinity at the monitoring points.

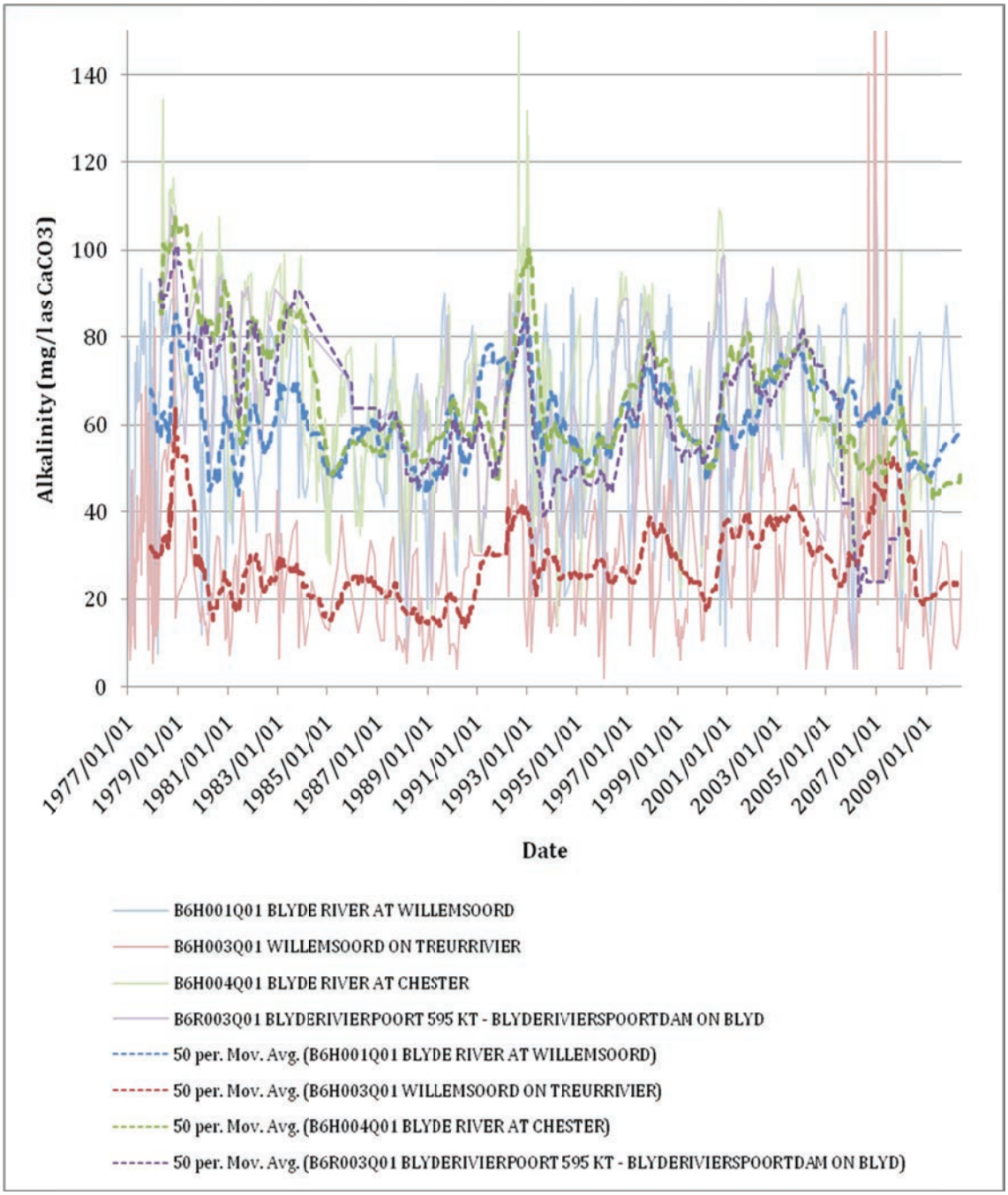

Figure 5.44: Background water quality of the LBIS: Alkalinity

Figure 5.45 indicates the non-Calcium-Magnesium Hardness for the review period.

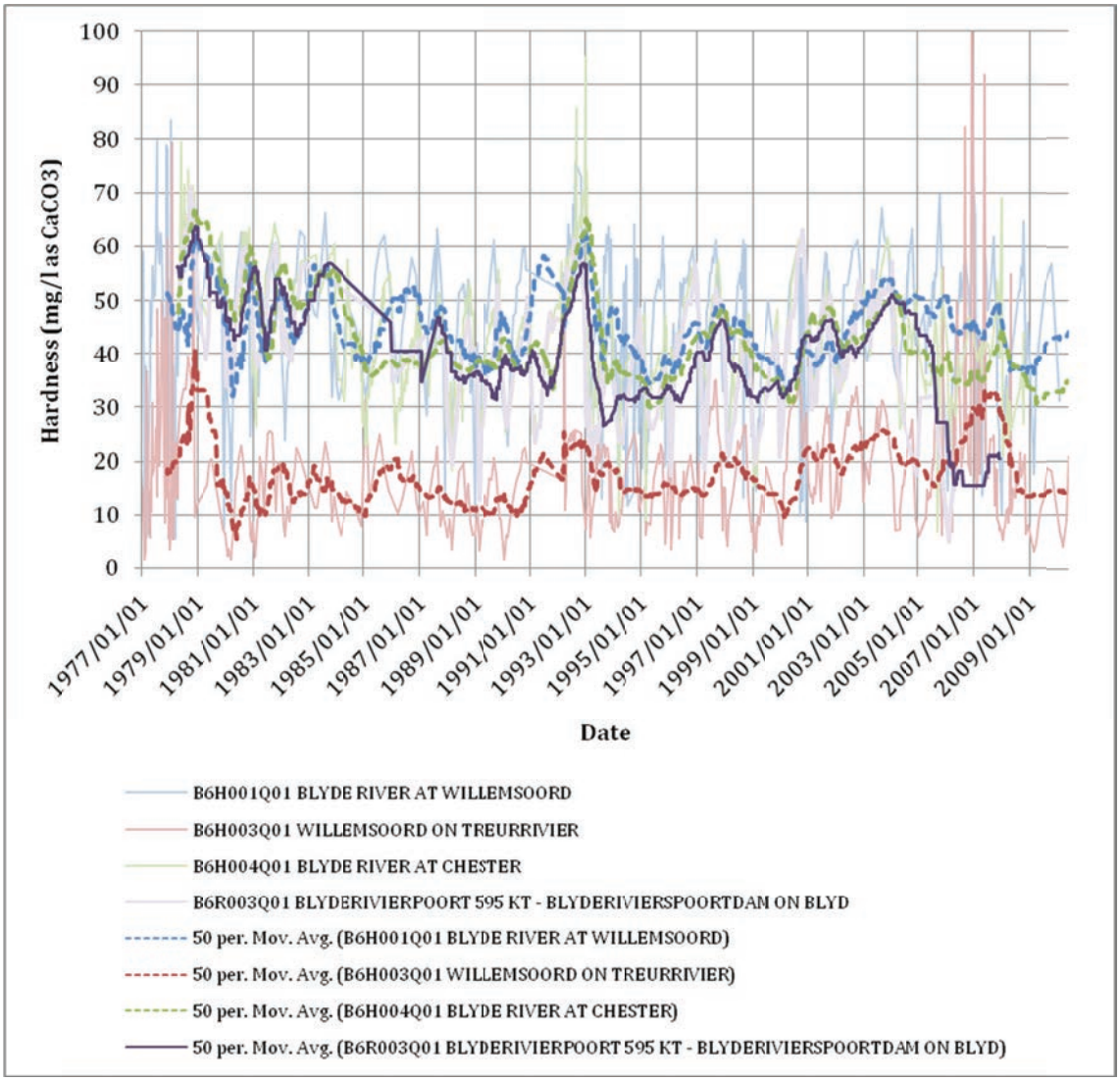

Figure 5.45: Background water quality of the LBIS: Non Ca-Mg Hardness

5.8.5 Biofilm analyses

5.8.5.1 Introduction

Samples of the biofilm was obtained from the pipeline and analysed. The analysis type, technique and equipment used to perform the biofilm analyses are summarized in **Table 5.47**. The results of these analyses are reported in the following paragraphs.

Table 5.47: Biofilm analyses performed

Analysis Type	Technique	Location
Drying	Reduce moisture content	University of Pretoria, Department Civil Engineering
Magnetic fraction	Magnet test	
Visual	Light microscopy	University of Pretoria, Department of Microscopy
Visual	Scanning electron microscopy	
Visual & Analytical	Energy dispersive spectroscopy	
Chemical	Chemical sludge analysis	ERWAT Laboratories
Microbiological	Microbiological analysis	

5.8.5.2 Drying of biofilm

As preparation for some of the more complex analyses techniques, a biofilm sample had to be dried resulting in biofilm residue. The appearances of the dried and 'in-situ' biofilm samples were completely different. An image taken of the 'in-situ' biofilm in the pipeline and not in contact with water for approximately 1 hour is shown in **Figure 5.46**. An image of the biofilm residue (sampled dried in air for 2 days) is shown in **Figure 5.47**. The difference in appearance is manly to the complete loss of 'slime' or exo-polymeric substances. The particle sizes in the dried biofilm are insignificant, as drying and abrasions resulted in breakup and crumbling. If particles were rubbed between fingers, a fine brown powder resulted.

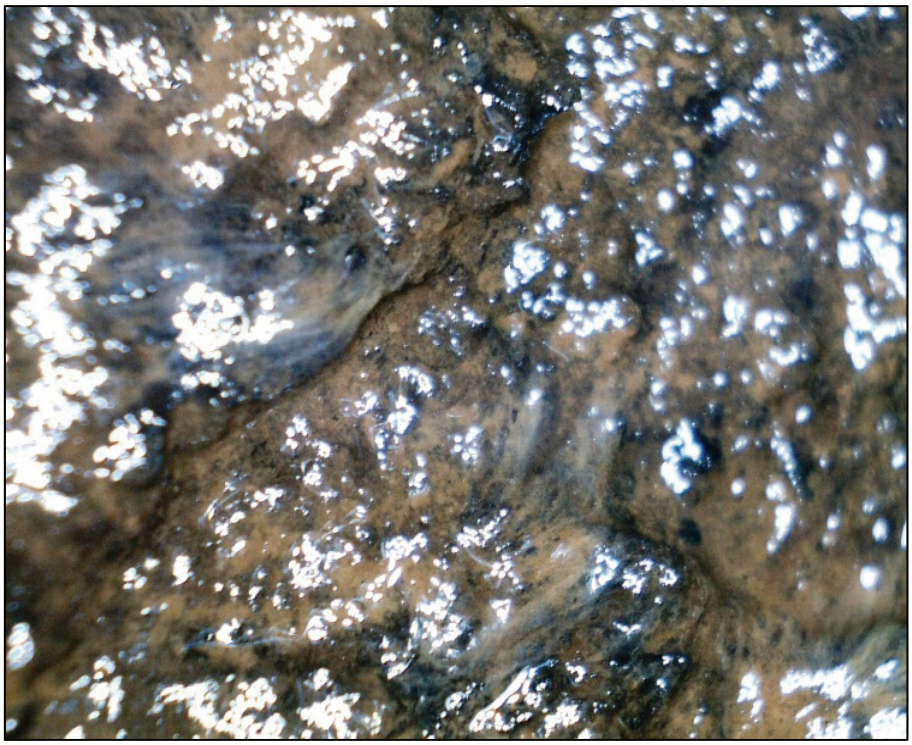

Figure 5.46: 'In-situ' biofilm

Figure 5.47: Biofilm residue

5.8.5.3 Magnetic fraction of biofilm residue

Biofilm residue was manipulated in order to break up the large particles. Five random samples were placed on a small piece of pre-cut paper that acted as a holding surface. The piece of paper was weighed before a sample of biofilm residue was placed on the paper. The paper with the biofilm was then weighed before exposure to a magnet. After the magnet exposure the paper and biofilm residue left on the paper were weighed again. **Table 5.48** lists the masses of the samples at the various stages of the test.

Table 5.48: Magnetic fraction of biofilm residue results

Sample number	Sample holding paper mass (g)	Sample & paper mass before magnet exposure (g)	Sample mass before magnet exposure (g)	Sample & paper mass after magnet exposure (g)	Sample mass after magnet exposure (g)	Sample mass removed by magnet (g)	Magnetic fraction (%)
1	0.4900	0.5120	0.0220	0.5090	0.0190	0.0030	13.6%
2	0.4920	0.5250	0.0330	0.5210	0.0290	0.0040	12.1%
3	0.4890	0.5175	0.0285	0.5135	0.0245	0.0040	14.0%
4	0.4970	0.5165	0.0195	0.5138	0.0168	0.0027	13.8%
5	0.4920	0.5201	0.0281	0.5166	0.0246	0.0035	12.5%
						Average	*13.2%*

The average magnetic mass fraction of the dried biofilm was 13.2%.

5.8.5.4 Chemical analysis of the biofilm obtained from the Lower Blyde River Irrigation System

5.8.5.5 Light microscopy

A wet biofilm specimen was studied under a light microscope. The following imagery was recorded. **Figure 5.48** at an amplification of 50 X, indicates grainy clumpy structures. **Figure 5.49** focused on one of the lumps and revealed small particles with a filamentous extrusion.

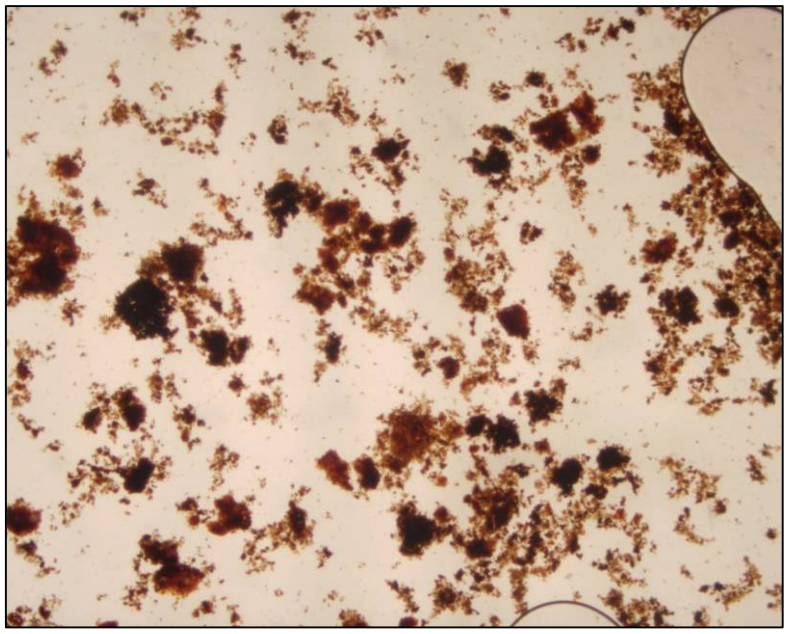

Figure 5.48: Light microscope image of Biofilm at 50x enlargement

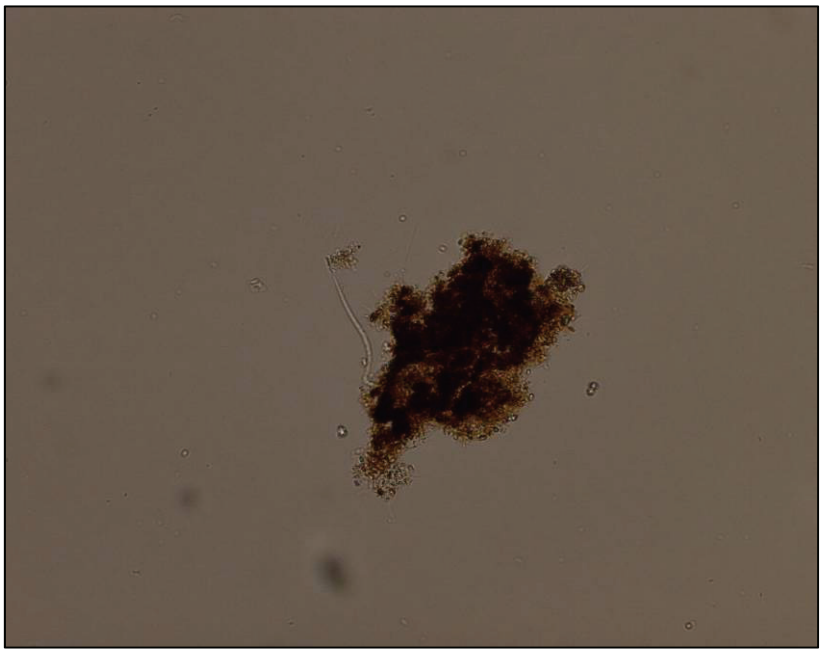

Figure 5.49: Light microscope image of Biofilm at 200x enlargement

Further viewing of the sample revealed numerous filamentous structures with grainy particles on and in close proximity to the filaments.

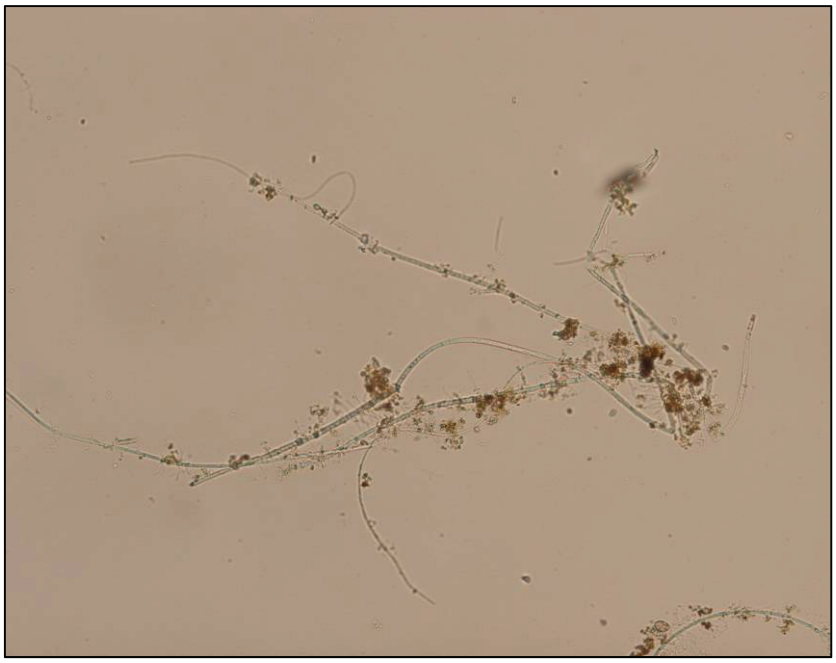

Figure 5.50: Light microscope image of Biofilm at 200x enlargement

5.8.5.6 Scanning electron microscopy

The scanning electron microscope (SEM) is a type of electron microscope that images the sample surface by scanning it with a high-energy beam of electrons in a raster scan pattern. The electrons interact with the atoms that make up the sample producing signals that contain information about the sample's surface topography and other characteristics. The specimen placed in the SEM is dried and coated with a layer of gold particles. Reporting are done on a per image bases, starting at low magnification ending at a high enlargement.

Figure 5.51 characterizes a microscopic 'overview' of random dried biofilm specimen from the LBIS pipeline biofilm. The dark grey backdrop represents a coupon (copper plate) that is used to found the sample inside the SEM apparatus. First impressions are the presence of a variation in the size of the particles. This is probably due to the specimen preparation, and not significant. Furthermore an impression of porosity is evident in the larger particles. Subsequent images will explore these first impressions and in more detail, by exploring the structure of one of the particles.

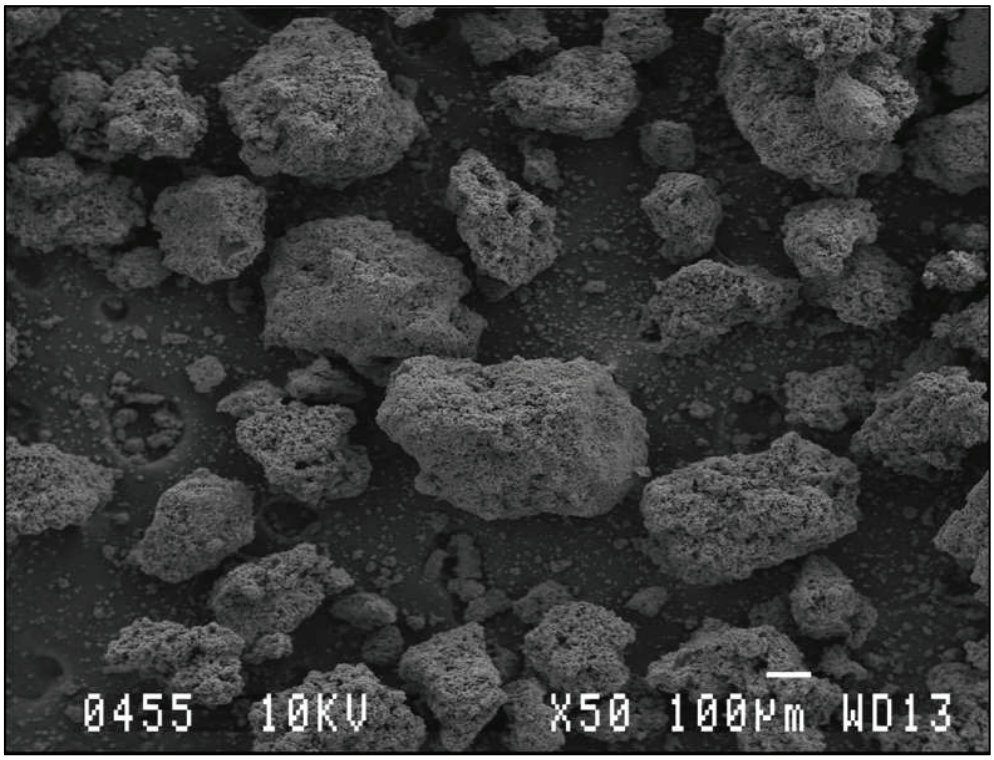

Figure 5.51: Microscopic 'overview' of random dried biofilm specimen

Figure 5.52 shows one of the particles at a 1500 times magnification. A hollow amorphous structure with small spherical elements draped with a dense almost spider web-like coat is visible.

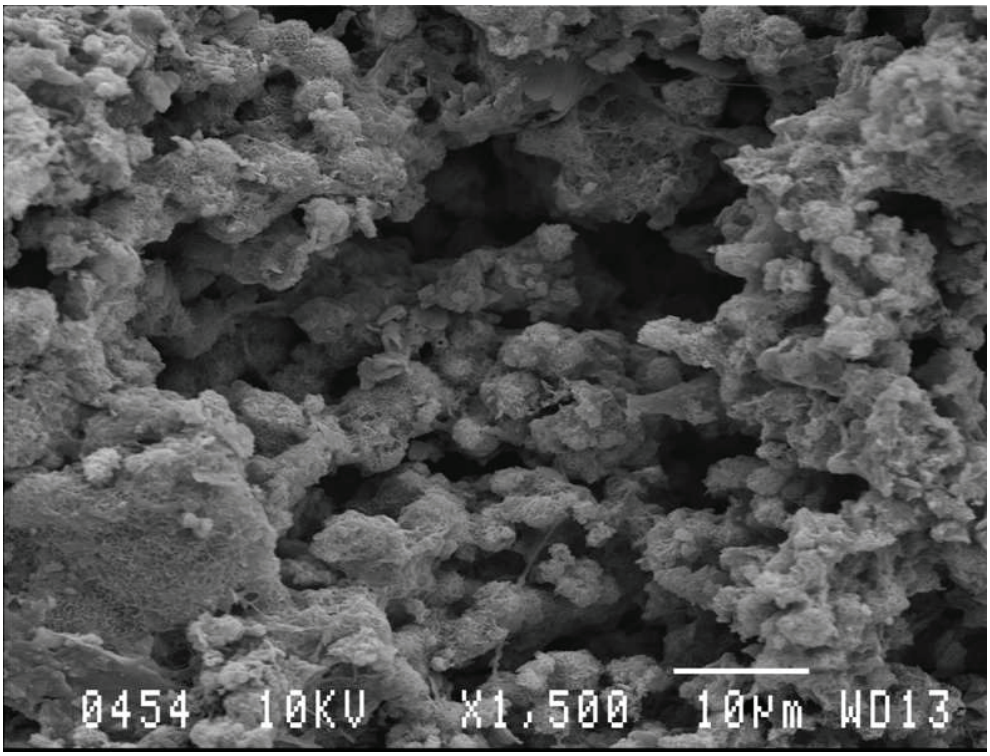

Figure 5.52: SEM image of dried biofilm at 1500 magnification

Figure 5.53 indicated a continuation of the fine amorphous structure with small flat surface embedded in the sample.

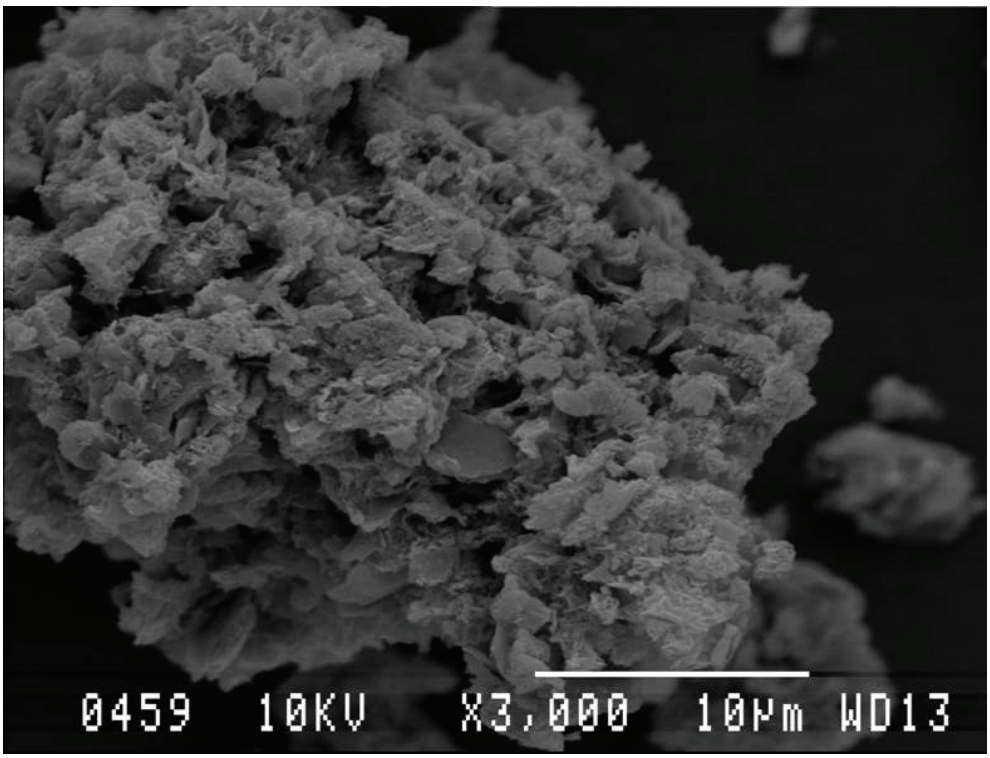

Figure 5.53: SEM image of dried biofilm at 3000 magnification

Figure 5.54 is zoomed in on one of the smaller particles in the 'overview' image, indicating the same fine amorphous structure.

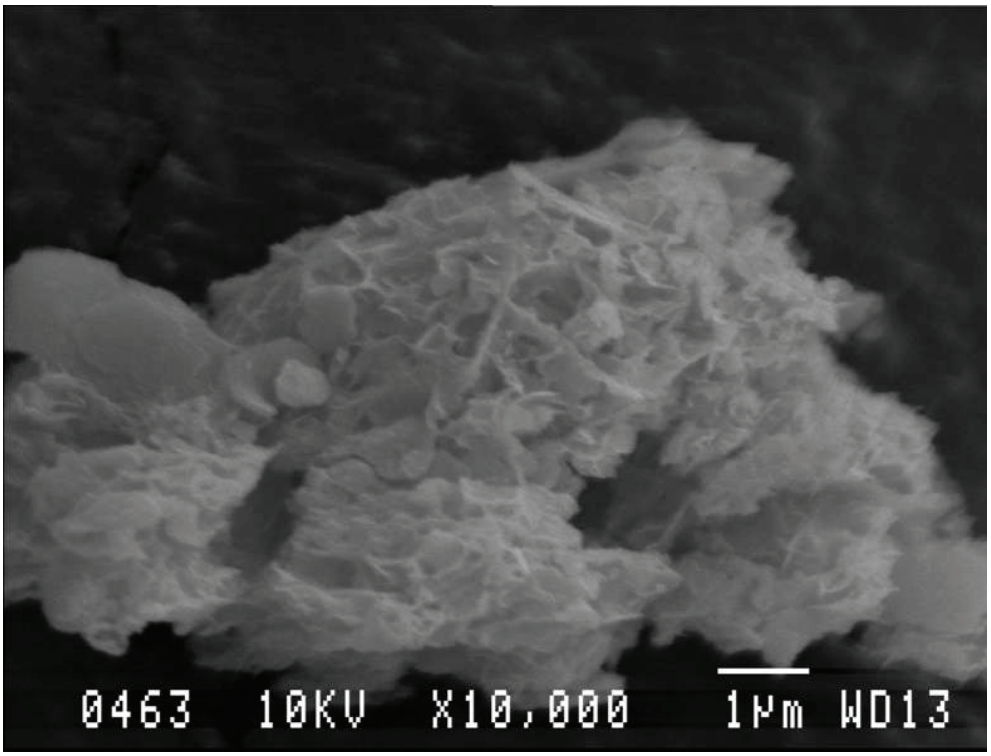

Figure 5.54: SEM image of dried biofilm at 10 000 magnification

Figure 5.55 is zoomed in on one of the smallest particles in the 'overview' image. The SEM microscope is nearing the limit of magnification, hence the out-of-focus appearance.

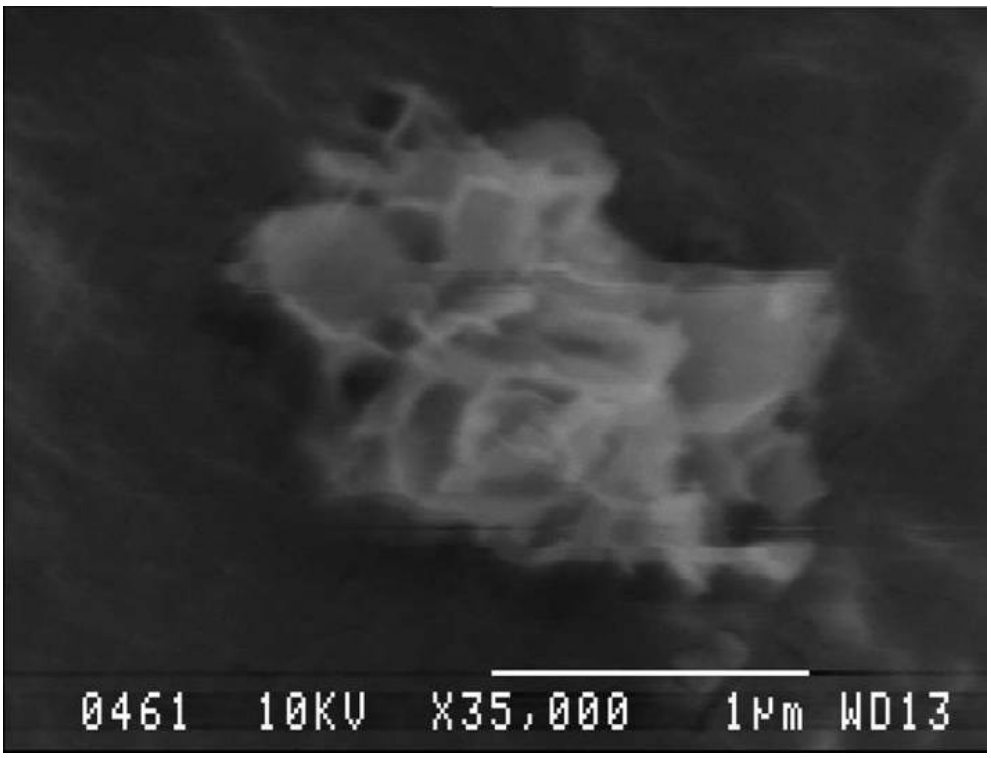

Figure 5.55: SEM image of dried biofilm at 35 000 magnification

The criteria for deciding when a solid becomes dissolved are set at 0.45 microns. If solids are larger than 0.45 microns they become particulate. The particle represented in **Figure 5.55** is just over one micron in size, and probably represent an early stage of the development of the 'building blocks' of the particle embedded in the biofilm.

5.8.5.7 Energy-dispersive X-ray spectroscopy

Energy-dispersive X-ray spectroscopy (EDS) is performed on a specimen by means of a scanning electron microscope with analytical functionality. An electron beam is aimed at a sample that results in a backscattered electron image. This image display compositional contrast due to different atomic number elements and their distribution. EDS allows for the identification of the presence of any element and their relative proportions. The biofilm specimen preparation includes drying, embedment in a resin, polishing and coating with carbon. A photo of the prepared specimen is shown in **Figure 5.56**.

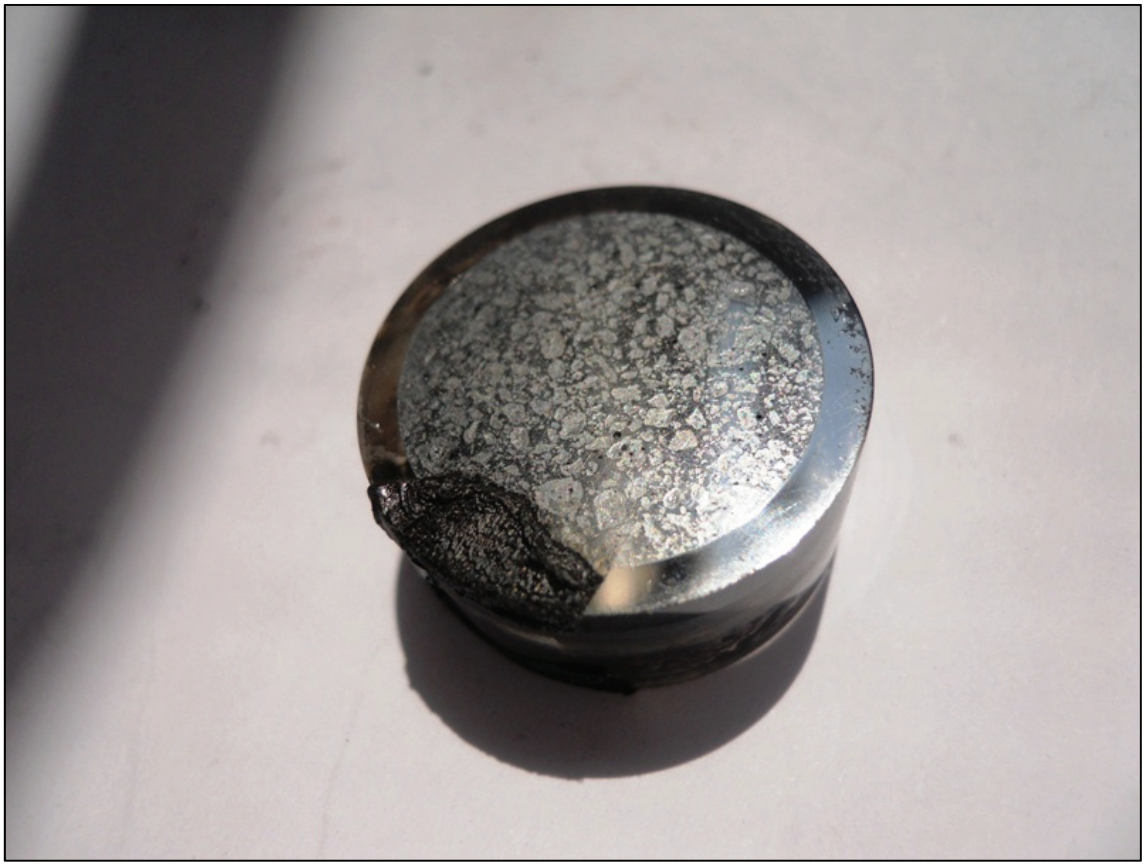

Figure 5.56: EDS biofilm specimen

EDS is reliable in reporting the presence and mass fraction of an element within a specimen. The EDS sample depth is 8 microns measured from the surface. It is, however important to keep in mind that the reported mass fractions are for the lower third of volume under the SEM, resulting in actual mass fractions being as much as much as 2 to 3 times higher.

EDS results are represented as a secondary electron image or backscatter imagery of a specimen. Each image has user defined sub-areas, which are analysed individually for each element on the periodic table. Three backscatter biofilm images (**Figure 5.57** to **Figure 5.61**) are shown below, each at a different magnification factor. Within each image the sub-areas for energy dispersive spectroscopy are highlighted and reported. The reporting is done in table format, indicating the sub-area number within the image and the mass percentage of a specific element. Graphs of each sub-area where the Y-axis shows the counts (number of X-rays received and processed by the EDS detector) and the X-axis shows the energy level of those counts in terms of kilo electron volts (keV).

Three images represented their names, magnification factors and number of sub-areas as shown in **Table 5.49**.

Table 5.49: EDS image summary

Image name	Magnification	Number of sub-areas
NR2A(1)	330	6
NR3A(1)	600	7
NR4A(1)	6000	3

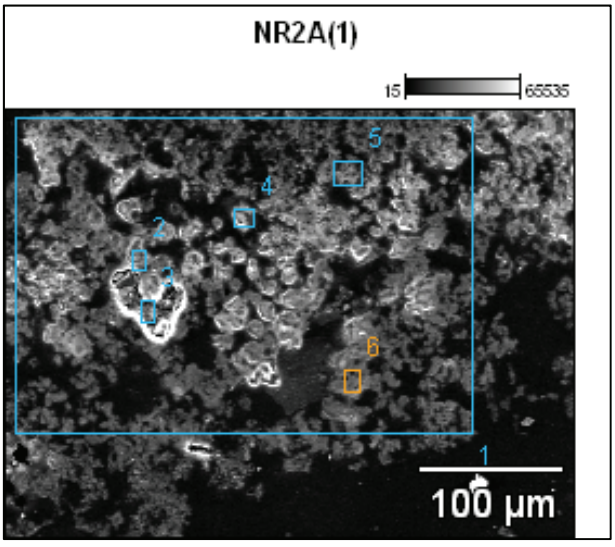

Figure 5.57: Backscatter biofilm image number NR2A(1)

The mass fractions of each identified element in each sub-area are shown in **Table 5.50** and **Figure 5.58** below.

Table 5.50: Mass fractions of each identified element

	Sub-area number in image NR2A(1)					
Element	1	2	3	4	5	6
C	58.12	46.65	65.17	53.48	49.33	44.3
O	29.47	30.63	18.71	26.95	29.49	34
F		0	0.48			
Na		0.12	0.13			
Mg	0.16	0.26	0.16	0.25	0.27	0.36
Al	0.3		0.52	0.46	1.25	0.34
Si	0.49	0.32	0.61	0.55	1.37	0.32
P					0.04	
S	0.05	0.1	0.26			
Cl	0.08	0.05	0.09	0.04	0.06	0.09
K	0.52	1.2	0.69	1.17	1.13	0.46
Ca	0.54	0.72	0.78	0.67	0.75	1.2
Ti		0.04	0.34		0.07	
Cr			0.05			
Mn	10.28	19.13	12	16.05	16.23	18.6
Br		0.45				
Mo				0.14		
Ba		0.32		0.23		0.37

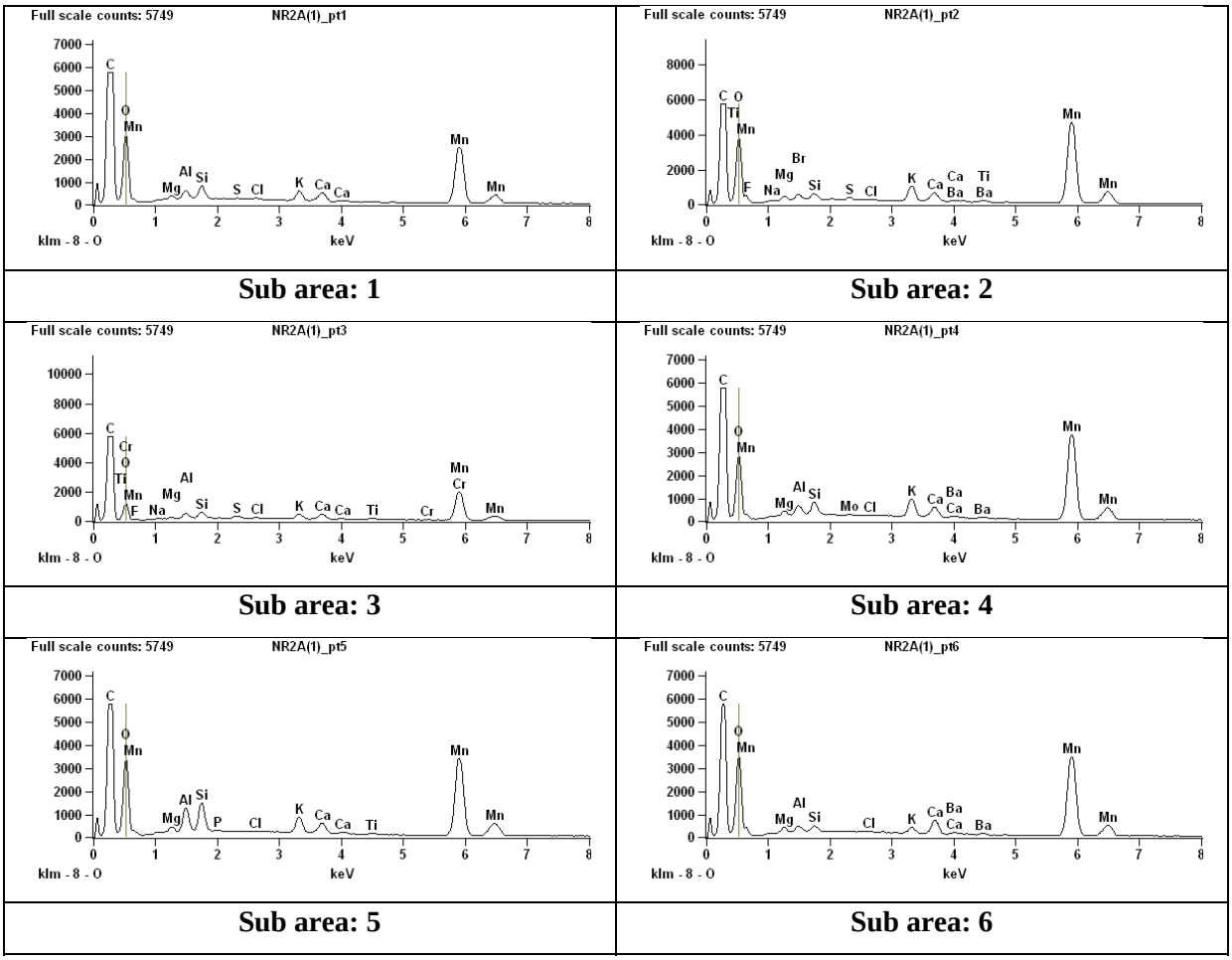

Figure 5.58: Biofilm residue EDS graphs of image NR2A(1)

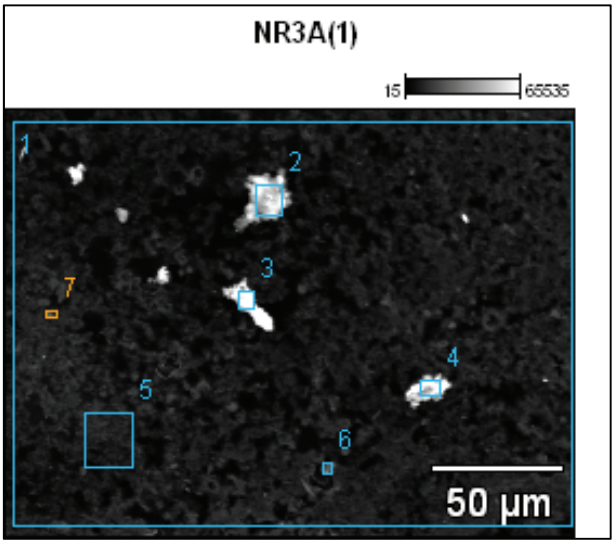

Figure 5.59: Backscatter biofilm image number NR3A(1)

The mass fractions of each identified element in each sub-area are shown in **Table 5.51** and **Figure** 5.60 below.

Table 5.51: Mass fractions of each identified element

	Sub-area number in Image NR3A(1)						
Element	**1**	**2**	**3**	**4**	**5**	**6**	**7**
C	53.16	55.07	51.07	35.86	45.08	44	46
O	32.3	30.97	35.71	40.91	33.74	26	32.3
Na			0.45	0.24	0.14		
Mg	0.24	0.33	0.46	0.4	0.28	0.11	0.24
Al	2.03	1.92	1.59	4.56	4.1	0.95	3.64
Si	2.76	2.67	4.15	5.68	5.2	1.08	4.07
P			0.15				
S		0.17	0.34			0.09	
Cl	0.06	0.16	0.27	0.09	0.1	0.04	0.14
K	0.37	0.44	0.28	0.28	0.7	0.37	0.54
Ca	0.45	0.71	1.32	0.39	0.55	0.25	0.44
Ti	0.14	0.13	0.16	0.21	0.22	9.86	2.96
Mn	5.92	5.43	2.27	1.7	6.68	3.52	5.05
Fe	2.44	2	1.78	9.5	3.21	13.8	4.52
Mo	0.12			0.18			0.12

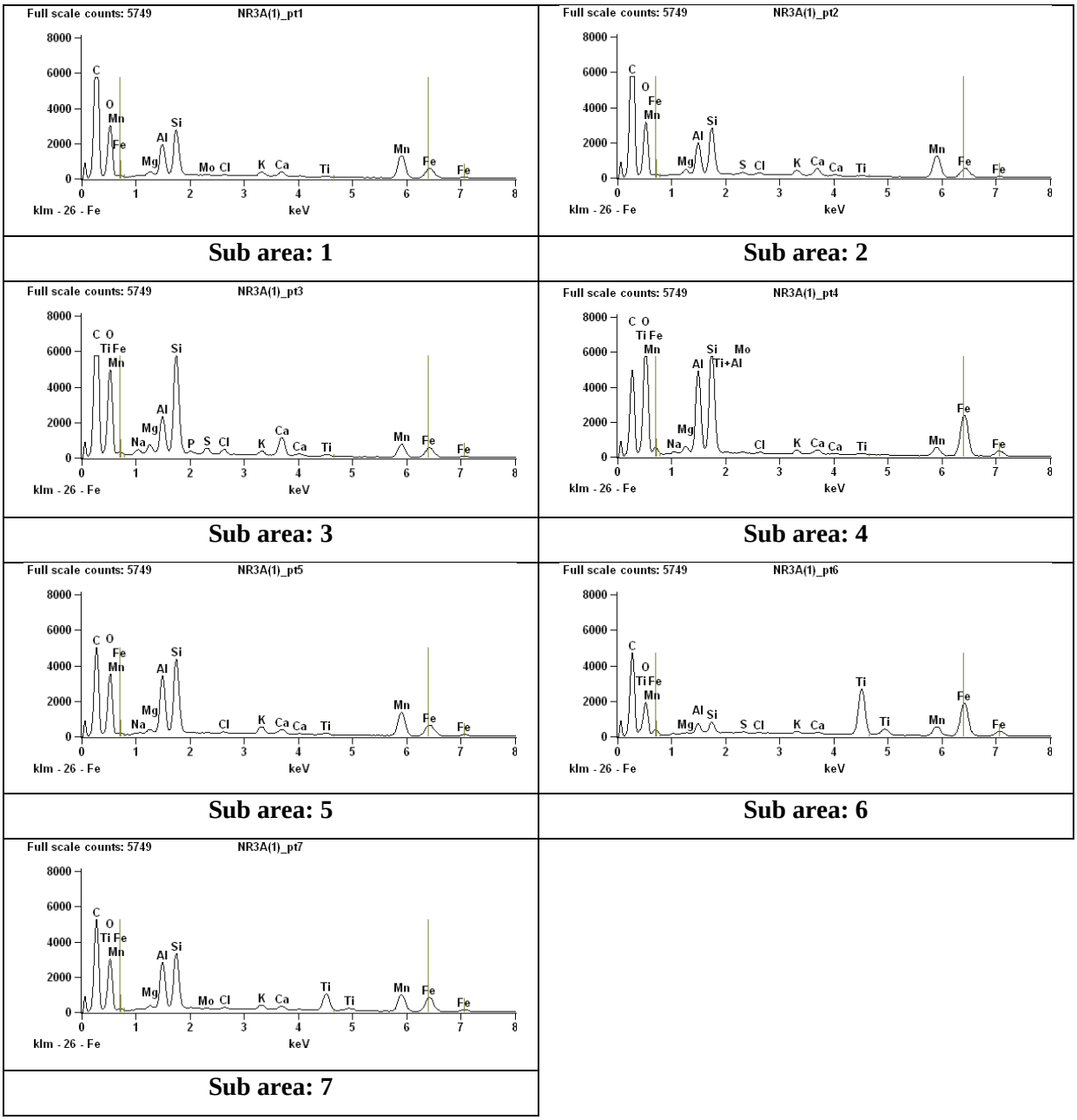

Figure 5.60: Biofilm residue EDS graphs of image NR3A(1)

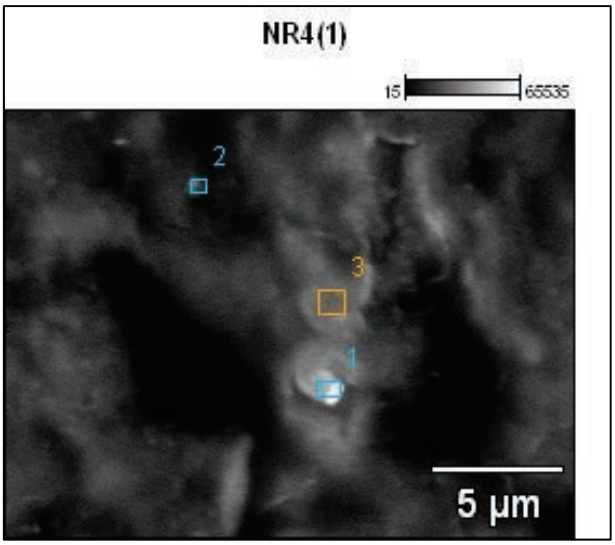

Figure 5.61: Backscatter biofilm image number NR4A(1)

The mass fractions of each identified element in each sub-area are shown in **Table 5.52** and **Figure 5.62** below.

Table 5.52: Mass fractions of each identified element

	Sub-area number in image NR4(1)		
Element	**1**	**2**	**3**
C	43.64	59.94	46.56
O	30.64	26.67	32.62
Mg	0.59	0.18	0.34
Al	0.4	0.61	1.34
Si	0.72	0.67	1.47
S	0.06		0.05
Cl	0.04	0.13	0.06
K	0.71	0.14	0.62
Ca	1.14	0.76	0.99
Mn	21.64	8.13	15.63
Fe		2.76	
Ba	0.43		0.31

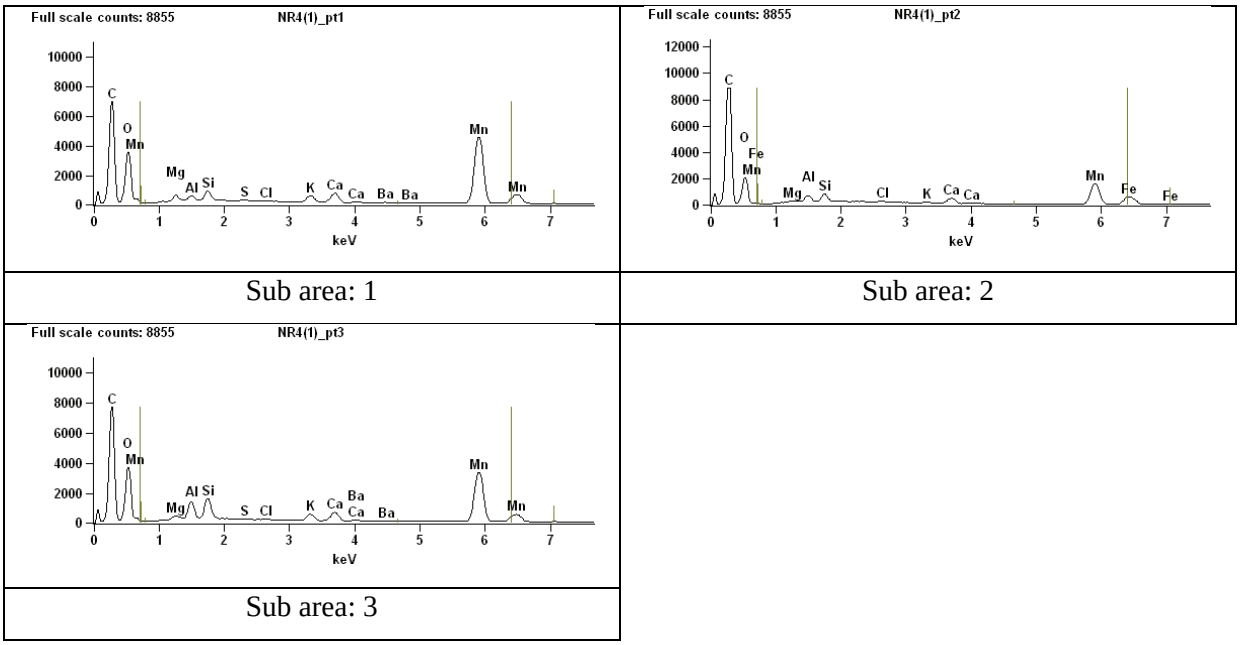

Figure 5.62: Biofilm residue EDS graphs of image NR4A(1)

5.8.5.8 Biofilm thickness measurements

Biofilm thickness measurement was taken at chainage 4340 m, in three different locations (i.e. -1.09 m, -2.09 m and 3.86 m measured as a positive distance in the flow direction) with the Biofilm Gauge. An angular reference system was used, i.e. facing in the direction of flow 0 degrees are on the base of the pipeline, measured anti-clockwise positive, as illustrated in **Figure 5.63**. The results of the thickness measurements are shown in **Figure 5.64**.

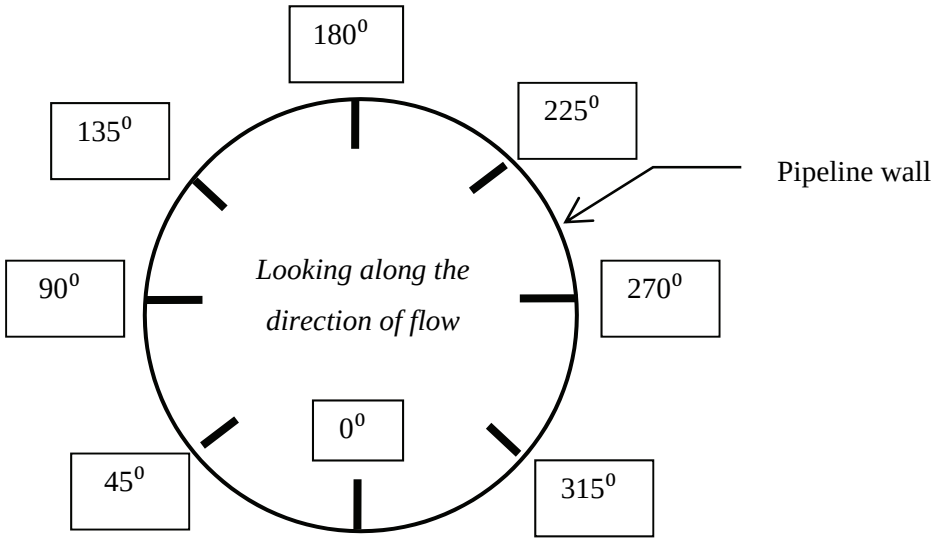

Figure 5.63: Biofilm measurements, circular referencing system

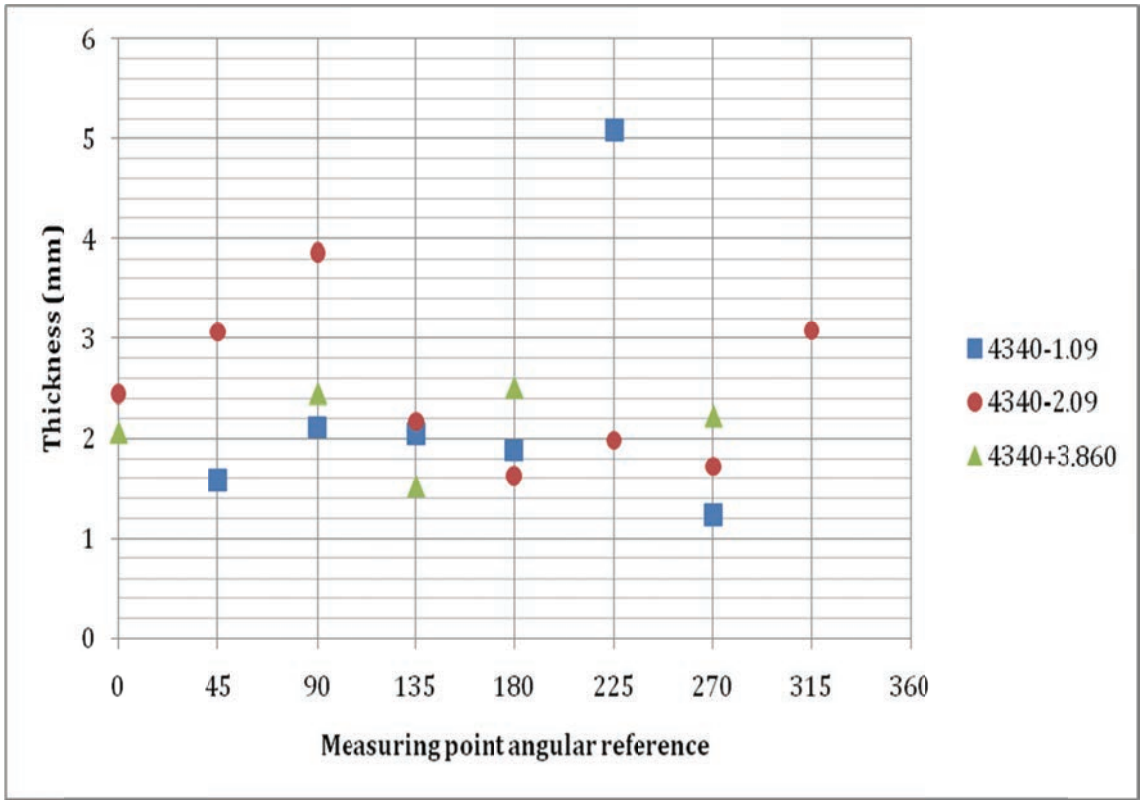

Figure 5.64: Biofilm thickness measurements near Chainage 4340 m

5.8.6 Discussion

The pressure grade line assessment indicates that the roughness of the pipe has increased significantly since it was commissioned. The maximum design roughness value used for the aged pipeline of 0.5 mm and it has increased to 1.76 mm. This is a 12% change per year over the last ten years. This is even a more dramatic rise in the roughness when compared with the roughness of the new Copon lined pipe of 0.08 to 0.15 mm.

The increase in roughness is due to biological fouling, i.e. biofilm growth, on the pipeline wall. The biofilm has a thickness of between 2 and 4 mm and results in an increase in the surface friction. The presence of biofilm in water transmitting pipelines is well established, as reviewed in the current projects literature review.

The composition and visco-elastic nature of the biofilm in the LBIS pipeline however are distinctive due to the strong presence of what appears to be Manganese Oxidising Bacteria. The chemical composition of biomass is C_5H_7ON [10]. In this context the presence and extent of carbon and oxygen in the EDS results can be expected. The presence of the quantities of Manganese, Iron and Aluminium are more challenging to interpret. The quantities of manganese in the biofilm residue

suggest and active source of manganese, and is probably symptomatic of a processes that have been going in for a while. Evidence suggests that manganese oxidising bacteria are responsible for the oxidation of Mn(II), resulting particulate deposition of Mn(III)-forms [11] [12] [13] [14] [15] [16]. The particulates are typically thermodynamically stable as a carbonate, hydroxide or oxide [17]. The water quality parameters of the rivers flowing into the Blyderivierspoortdam are of such nature that it is unlikely that the biofilm growth will be inhibited in any way. Al indications are that biofilm growth will continue, and to what extent is unknown.

It was mentioned prior that the Portaflow Ultrasonic flow meter readings indicated abrupt changes in flow rate data. It is possible that this is due to the metal content in embedded in the biofilm that intervene with the Portaflow signal, resulting in errors in the recordings.

5.8.7 Conclusion

Hydraulic capacity of a portion of the Lower Blyde Irrigation System pipeline has reduced during the last ten years. The reduction is due to an increase in the pipeline surface roughness from a designed value of 0.5 mm to 1.76 mm. Surface roughness increase is not due to degradation of the pipeline material, but due to biological fouling or biofilm growth in the pipeline. The presence of high quantities of manganese in the biofilm residue, suggests the presence of manganese oxidising bacteria.

The extent of the biofilm makes the removal impractical. The implications are two-fold;

- reduction in hydraulic capacity; and
- *serious* operation control risks.

5.9 Summary of the research findings on the pipelines which were field tested

5.9.1 Introduction

In the preceding paragraphs the results obtained from the field studies were discussed for the pipelines which were investigated during this research project. The pipelines which have been investigated included clean water pipelines as well as pipelines which transferred raw water.

The following pipelines conveying treated water were reviewed:

- De Hoek to Uitkijk pipeline (BloemWater);

- Uitkijk to Brandkop pipeline (BloemWater);
- Swakopmund to Rossing Pipeline (Namwater); and
- Swakopmund to Langer Heinrich Pipeline (Namwater).

The following raw water pipelines were reviewed:

- Morgestond Dam to Jericho Dam;
- Jericho Dam to Onverwacht reservoir;
- Hendrina to Duvha Power Station; and
- Lower Blyde River Irrigation System.

In the following paragraph the results obtained are summarized.

5.9.2 Summary of the findings

The absolute roughness's were calculated for all the pipes which were investigated. Although the results obtained from the Lower Blyde River Irrigation System indicated the severe influence which the biofilm could have on the hydraulic resistance, this aspect still has to be investigated further. Disregarding the influence of the biofilm and by assuming the relative contribution of the secondary losses were identified scientifically, the results for the calculated roughness's in all the pipelines are provided in **Table 5.53**.

Table 5.53: Comparison of the recorded and reference roughness for different pipe material and liner systems

Country	Pipe ID	Pipe diameter (mm)/Installation date	Pipe material/liner	Water quality #	Roughness parameter				
					Reference roughness new pipe (mm)			Calculated roughness	
					smooth	rough	Reference	Barr (mm)	Colebrook-White (mm)
South-Africa	Bloemwater: De Hoek to Uitkijk	1168/1971	PCP/none	T	0,06	0,6	Wallingford and Barr (2006)	0,167	0,176
	Bloemwater: Uitkijk to Brandkop							0,091	0,098
	Hendrina-Duvha *	1400/1974	Steel/Bitumen	R	0,04	1	Mecaflux (2009)	0,292	0,302
	Kuthala Kendal **	650/1986	Steel/Bitumen	R	0,06	1	Bhave (1991)	0,624 to 1,599	0,622 to 1,597
	Morgenstond Dam to Jericho Dam M1-J	1500/2003	Steel/CML	R	0,06	1,5	Bhave (1991) & Barr et al (2006)	0,533	Not determined
	Morgenstond Dam to Jericho Dam M2-J	1500/1964 (relined 2008)	Steel/CML (replaced)	R	0,06	1,5	EDSTech & Bhave (1991)	0,963	Not determined
	Lower Blyde Irrigation System Pipeline	1500/2000	Steel/Copon	R	0,02	Not defined	EDSTech	1,76	
	Baviaanspoort – Kameelfontein	250/Unknown	Steel/Bitumen	T	0,015	0,3	Bhave (1991)	Not determined	1,327
Namibia	Rössing Pipeline	600/1979	Ductile Iron/CML	T	0,02	Not defined	EDSTech	0,080	0,079
	Langer Heinrigh Mine	325/2004	Steel/CML	T	0,06	1,5	EDSTech & Bhave (1991)	0,088	0,086

Notes:

\# "R" reflects raw water and "T" reflects treated water; * In this case it was established that the secondary losses at the couplings are significant;

** The profile allows sections of the pipeline to drain, resulting in the variance of the absolute roughness values.

6 Influence of high energy cost on the optimal diameter of pumping mains

6.1 Introduction

The South African energy crisis contributed another reality, complexity and uncertainty to the optimal design of pumping systems. The contribution of energy cost during the life cycle outweighs the capital cost of most pumping systems (OIT, 2001), requiring thorough analyses of the optimal component design by minimizing the life cycle cost (especially the energy cost) of the pump system. **Figure 6.1** indicates the life cycle cost breakdown for typical pump installation.

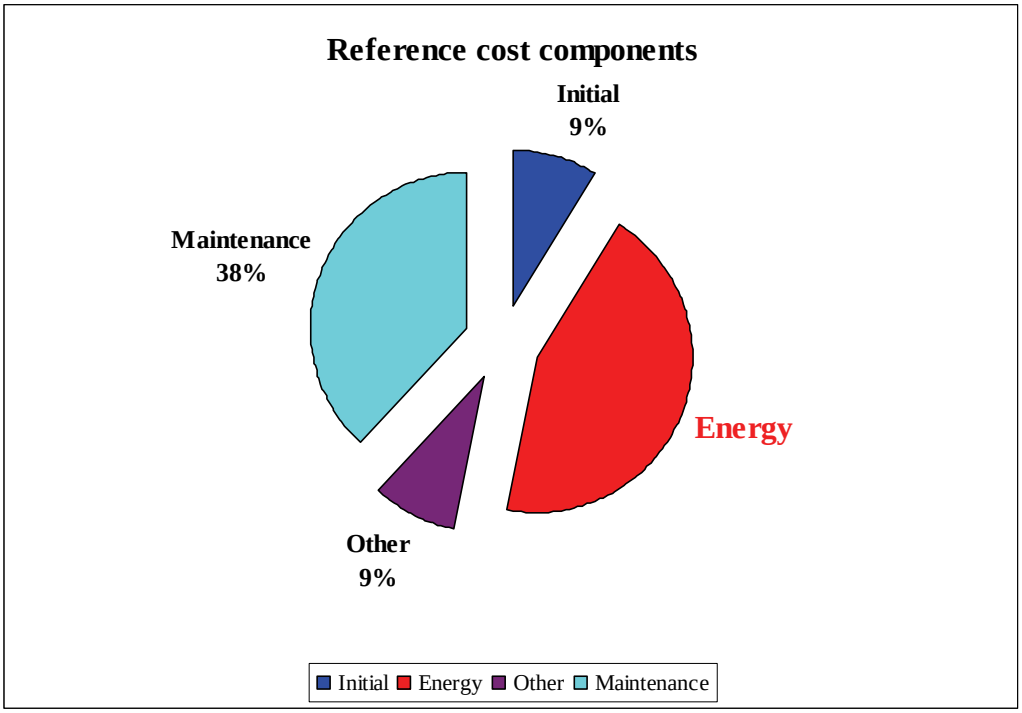

Figure 6.1: Typical life cycle cost breakdown of a pumping main

In an attempt to mobilize the required capital for the extensions of the generating capacity in South Africa and to control the demand for energy, the energy regulator, NERSA agreed rates increases to be implemented in South Africa as indicated in **Table 6.1**.

Table 6.1: Agreed energy tariff for the period 2010 to 2012

Year	Agreed energy tariff increases (%)
2010	24,8
2011	25,7
2012	25,8

6.2 Expected influence of the energy cost on pumping systems

It was well understood that the increase in the energy tariffs will have an effect on the cost of water supply. Based on the agreed tariffs a number of scenarios were investigated based on an assumption of the expected CPIX. The following scenarious were evaluated:

- Scenario 1 – Expected CPIX = 8 %
- Scenario 2 – Expected CPIX = 9 %
- Scenario 3 – Expected energy cost increase = CPIX +1%
- Scenario 4 – Expected energy cost increase = CPIX +2%

The results obtained from an analyses period of 25 years, reflected that in the case of scenarios 3 and 4 that the energy component of the LCC could increase to **46** and **52,5 %** of the total LCC of the pumping system. This is disturbing in the South African context where water has to be pumped over high static heads and long distances between the resource and the users.

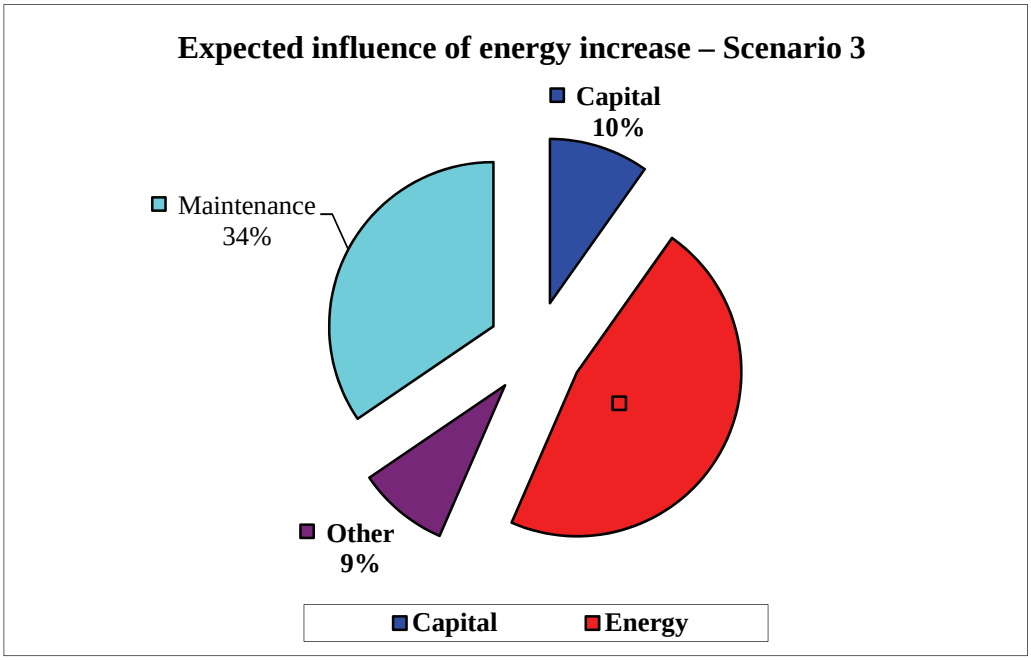

Figure 6.2: LCC breakdown for scenario 3

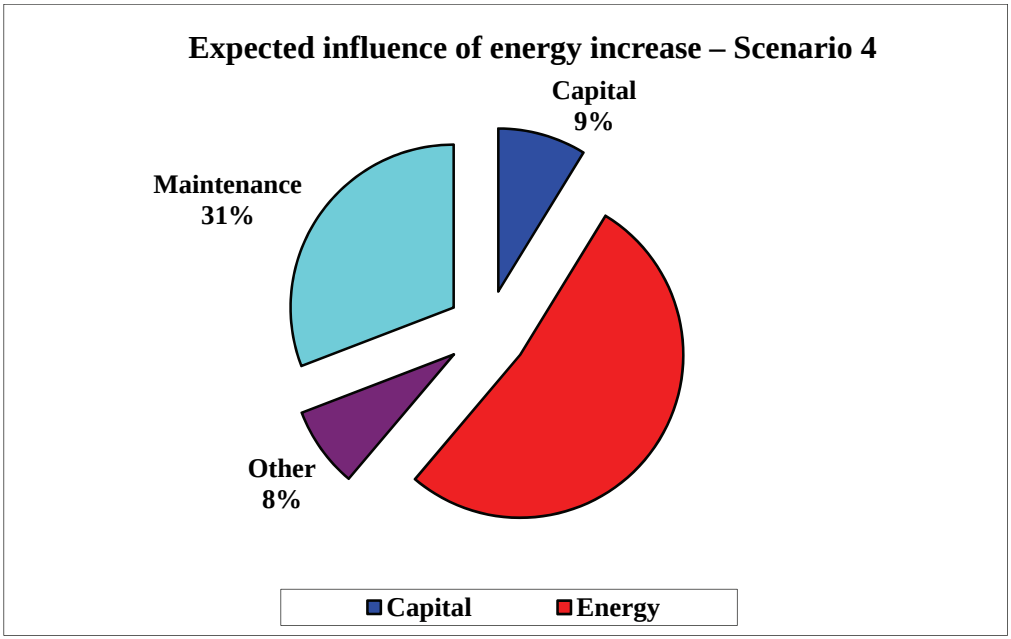

Figure 6.3: LCC breakdown for scenario 3

This led to the question: Which of the pumping systems (and more specifically the pumping mains) should be reviewed for upgrade, refurbishment or replacement to ensure the maximum benefit on the investment in terms of the reduction in the energy cost.

6.3 Pumping lines reviewed

An investigation of a number of pumping systems was undertaken in the Tshwane Metropolitan Council's clean water infrastructure. The comparison of these systems was done on the following conceptual parameters:

- Ratio of energy loss to static head (hf/Hs); and
- The static head, Hs.

Frictional head loss, hf was selected as it is directly related to the diameter and energy cost associated with the non-optimal diameter. The static head, Hs in a sense defines the required pressure class for the installation (capital cost of the installation). **Figure 6.4** reflects a number blocks (9) defined by decision lines (D1 and D2) on the horizontal axis (indicating the pressure class range) and two lines on the vertical axis, indicating the replacement or the upgrade (parallel section) of the pipeline.

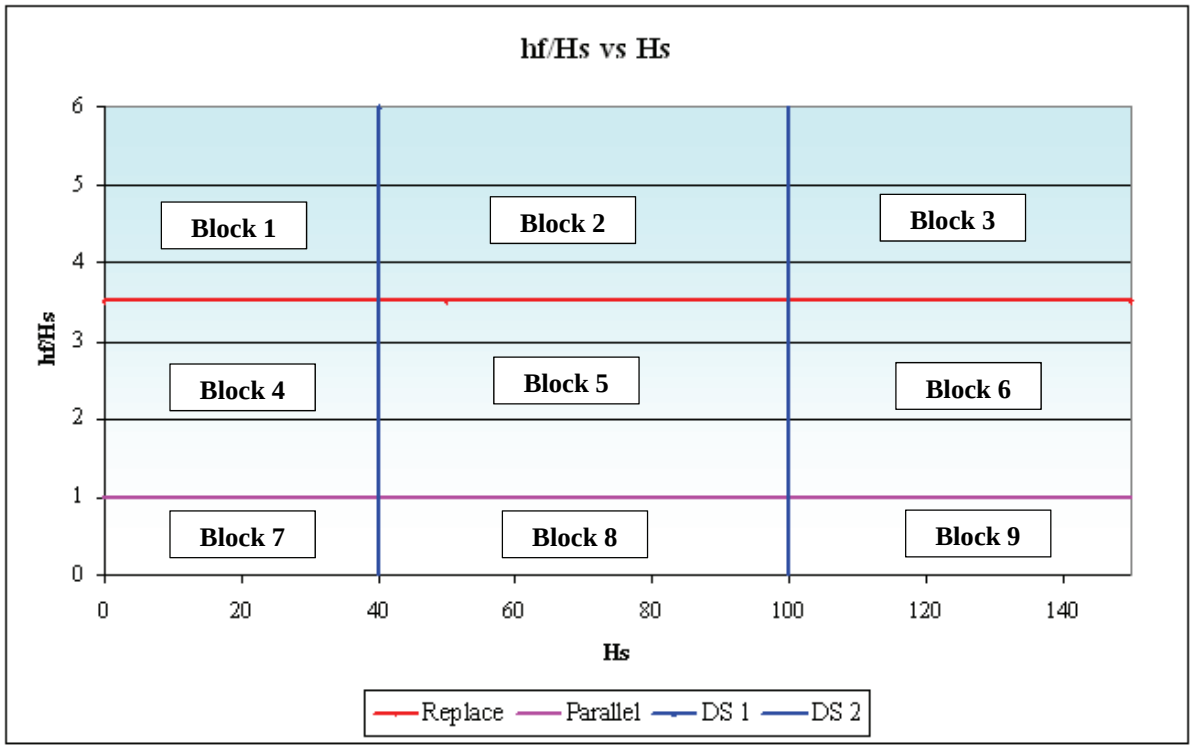

Figure 6.4: Guidance on the options to improve the operation of pumping systems

It can now be argued that if two systems are assessed and compared, and say the one plot in Block 1 while the other plot in Block 9, the best investment of capital will be to invest in the system that plots in Block 1. The reason for this is that lower pressure class pipes will be required and the biggest advantage in terms of the reduction of the friction loss, hf will be experienced.

This could be developed further to define a decision matrix which will indicate where improvements should be implemented as illustrated in **Figure 6.5**.

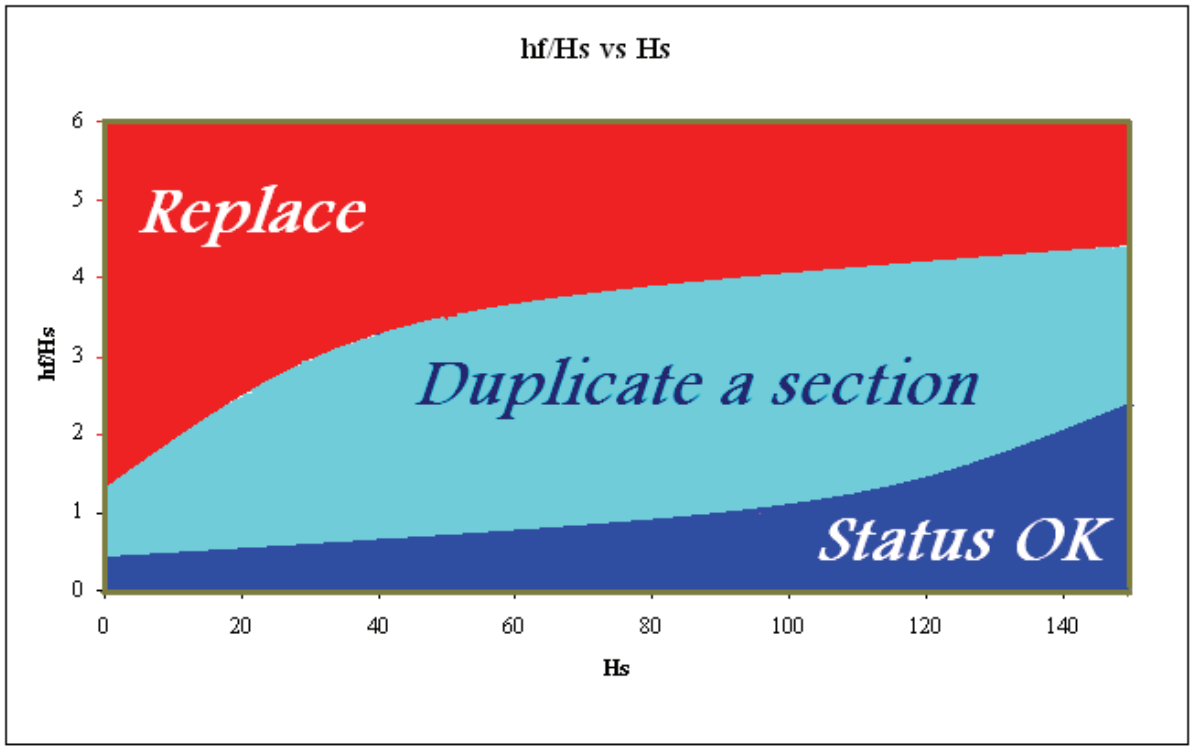

Figure 6.5: Decision matrix indicating the options to improve pumping mains

6.4 Results obtained from the pumping mains assessed in the Tshwane Metropolitan Council's water distribution network

The 11 pumping systems which have been reviewed (Scenario 3) are reflected in **Table 6.2** while the results are graphically shown in **Figure 6.6**.

Table 6.2: Pumping systems reviewed

Pipeline	Pumpstation (reservoir)
BH	Babelegi (Hammanskraal)
BC	Brickfields (Constantia Park)
BE	Brickfields (Erasmusrand)
D	Dorinkloof (Dorinkloof)
FS	Fountain (Salvokop)
GE	Garsfontein (Elarduspark)
KC	Klapperkop (Carina Street)
KB	Klipdrift (Babelegi)
PVR	Pierre van Ryneveld (Pierre van Ryneveld)
RG1	Rietvlei (Garsfontein)
RG2	Rietvlei borehole (Garsfontein)
RM	Roodeplaat (Montana)
VKF	Vader Kestell (Florauna)

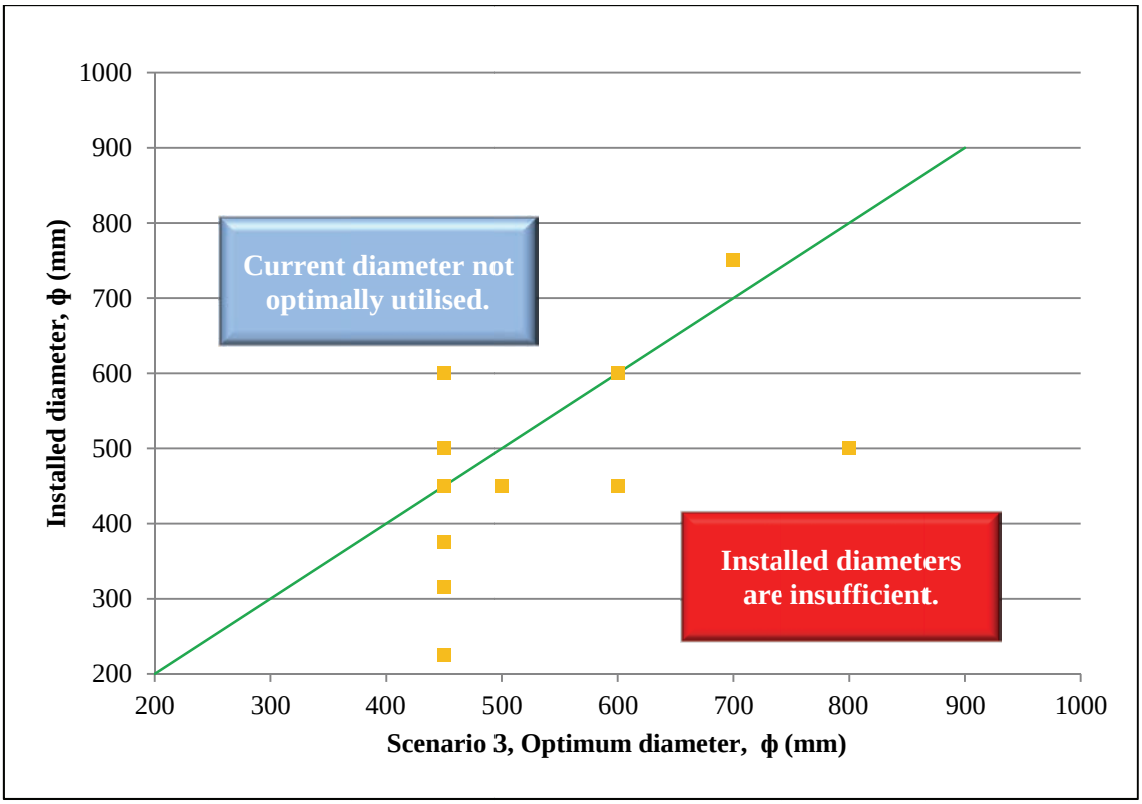

Figure 6.6: Review of 11 pumping systems (Tshwane)

Based on the results, the different systems were compared indicating that the highest priority for upgrading is to replace the Babelegi to Hammanskraal pipeline.

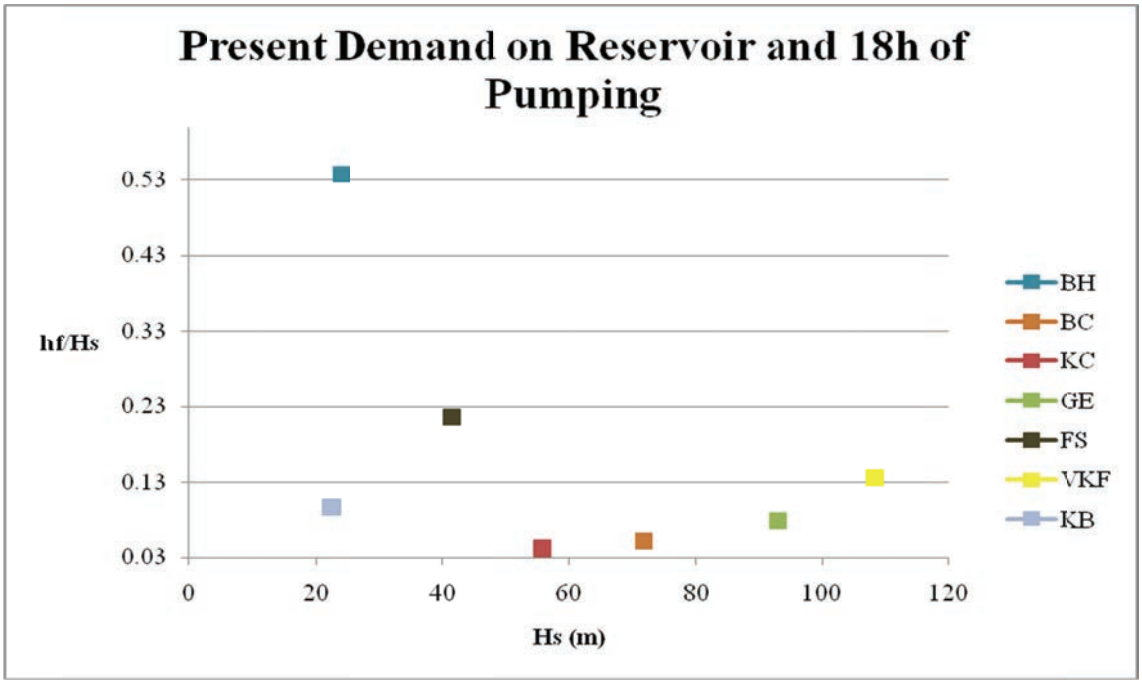

Figure 6.7: Comparison of different which were assessed

7 Conclusions and Recommendations

7.1 Introduction

The focus of this research was to investigate a number of pipelines by conducting field measurements of the energy loss in the system from which the roughness of the pipelines was calculated. The calculated roughness was compared with the reference roughness for the type of pipe material from which it was possible to determine the yearly decay of the roughness.

In the case of the Lower Blyde River Irrigation System (LBIS) excessive biofilm residue (Mn the by-product of MOB) was found resulting in a roughness of 1,75 mm. This led the inclusion of some research on the parameters in the Blyderiver contribution to the high activity of MOB.

The uncertainty of the biofilm thickness in pipelines led to the development of a biofilm thickness meter which requires further refinement.

During the contract period of this research, South Africa experienced power shortages which led to the escalation of the energy cost well above normal escalation. This sparked the review of the optimal diameter for pumping systems. The results of a number of pumping lines which were reviewed reflected that on a life cycle cost bases these pipe diameters not optimal and too small.

The intention was also to construct a database to be used as a reference for designers and managers of pipelines.

The research also highlighted that:

- Insufficient accurate physical data of the pipeline material, installation details and data and status description of the hydraulic capacity of the pipeline infrastructure in South Africa is available;
- There is a lack of periodic review of the performance of pipelines,
- There is a lack of a description/definition or understanding of the influence of Biofilm on the hydraulic capacity of the pipelines, and
- That uncertainty still exists with regard to the prediction of the aging of the pipeline and the prediction of the remaining operational life.

7.2 Recommendation

It is recommended that the following aspects be researched in more detail:

- Assess the influence of energy cost on the optimization of pumping mains and to develop a decision matrix for the upgrade, refurbishment or replacement of system components;
- Develop a method to monitor the biofilm growth in pipelines;
- Define influence of biofilm on the hydraulic capacity of pipelines and develop a relationship to be able to determine the need for pigging pipelines; and
- The database of pipeline performance be further populated to provide design guidance for new installations.

8 References

Barr, D.I.H. Solutions of the Colebrook-White functions for resistance to uniform turbulant flows. 1981, Proc.Inst.Civil.Engrs. Part2, Vol. 71.

Barton, A.F., et al. Hydraulic Roughness of Biofouled Pipes, Biofilm Character, and Measured Improvements from Cleaning. June 2008, JOURNAL OF HYDRAULIC ENGINEERING, pp. 852-857. 10.1061/(ASCE)0733-9429(2008)134:6(852)

Bentley, L.D. and Whitten, J.L. (2007). *Systems Analysis and Design for the Global Enterprise.* 7th ed. McGraw-Hill Irwin, New York.

Boogerd, F.C. and de Vrind, J.P.M. Manganese Oxidation by Leptothrix discophora. 1987, Journal of Bacteriology, Vol. 169(2), pp. 489-494.

Colerbrook, C.F. and C.M., White. Experiments with Fluid friction in artificaily roughned pipes. 1937, Proc. R.Soc.(A), Vol. 161.

Chen, N.H. An Explicit Equation for Friction factor in Pipe. 1979, Ind.Eng.Chem.Fundam., Vol. 18(3), p. 296.

Haaland, S.E. Simple and Explicit formulas for friction factor in turbulant pipe flow. s.l. : JFE, 1983, Trans.ASME, Vol. 105

Hydraulic Research (HR) Wallingford and Barr D.I.H, Tables for the hydraulic design of pipes, sewers and channels, 8th edition, pp 56-57.

Leslie-Grady, C.P., Diagger, G.T. and H.C., Lim. Biological Wastewater Treatmant. 2. New York : Marcel Dekker, Inc., 1999. p. 63

Manadilli, G. Replace implicit equations with sigmoidal fucntions. 1997, Chem.Eng.J., Vol. 104(8).

Moody, L.F. Friction factors for pipe flows. 1944, Trans.ASME, Vol. 66, p. 641

Nealson, K.H. The Manganese-Oxidizing Bacteria. [book auth.] S. Falkow, E. Rosenberg, K. Schleifer, E. Stackebrandt M. Dworkin. The Prokaryotes: A Handbook on the Biology of Bacteria : Proteobacteria: Alpha and Beta Subclasses. 3. s.l. : Springer, 2006, Vol. 5, 3.1.10, pp. 222-231.

OIT, Pump Life Cycle Cost, A Guide to LCC Analysis for Pumping Systems, www.oit.doe.gov, 2001.

Polastre, J.R. (2003). *Design and Implementation of Wireless Sensor Networks for Habitat Monitoring.* Department of Electrical Engineering and Computer Science, University of California at Berkeley.

Rare Water (2010), South Africa. Verbal communication.

Romeo, E., Royo, C. and Mozon, A. Improved explcit equations for estimation of the friction factor in rough amd smooth pipes. 2002, Chem.Eng.J., Vol. 86, p. 369
Swamee, P.K. and Jain, A.K. Explicit equation for pipeflow proeblems. s.l. : ASCE, 1976, J.Hydr.Div., Vol. 102(5), p. 657.

Slya, L.I., Hodgkindonb, M.C. and Arunpairojana, V. Effect of water velocity on the early development of manganese-depositing biofilm in a drinking-water distribution system. 1988, FEMS Microbiology Ecology, Vol. 53, pp. 175-186.

Stumm W., Morgan J.J. Aquatic Chemistry: Chemical Equilibria and Rates in Natural Waters. 3. New York : John Wiley & Sons, Inc., 1996.

Tyler, P.A. and Marshall, K.C. Microbial oxidation of manganese in hydro-electric pipelines. 1967, Antonie van Leeuwenhoek, Vol. 33, pp. 171-183.

Tyler, P.A. Hyphomicrobia and the oxidation of manganese in aquatic ecosystems. 1970, Antonie van Leeuwenhoek, Vol. 36, pp. 567-577.

van Wyk, C., Effect of energy cost on the optimum selection of pumping mains. Unpublished report compiled under supervision of Professor S J van Vuuren, in partial fulfilment of the requirements for the degree o of Engineering, University of Pretoria, 2010.

WRC, 2006. Project title: K5-1269: Review of the factors that influence the energy loss in pipelines and procedures to evaluate the hydraulic performance for different internal conditions, TT 278/06, 2006.

WRC, “Life Cycle Costing Analysis for Pipeline Design and Supporting Software”. Van Vuuren S J and van Dijk M; TT 278/06, 2006.

Zigrang, D.J. and Sylvester, N.D. AICHE J. Explicit approximations to the Colebrook’s friction factor. 1982, , Vol. 28(3), p. 514.

The User Manual and supporting software Hydraulic Performance DBV1 mentioned in this report can be obtained at www.wrc.org.za/software/.